Integration of Organic Rankine Cycles in Process Sites for Waste Heat Recovery

A thesis submitted to The University of Manchester for the degree of Doctor of Philosophy in the Faculty of Science and Engineering

2022

Zheng Chu

The Faculty of Science and Engineering, School of Engineering, Department of Chemical Engineering & Analytical Science

Table of Contents

Table of Contents

List of Figures

List of Figures

List of Tables

Nomenclature

Abbreviations

ORC	Organic Rankine Cycle
UNFCCC	United Nations Framework Convention on Climate Change
IPCC	Intergovernmental Panel on Climate Change
PI	Process Integration
GCC	Grand Composite Curve
TSA	Total Site Analysis
HEN	Heat Exchanger Network
MINLP	Mixed-Integer Non-Linear Programming
MILP	Mixed-Integer Linear Programming
NLP	Non-Linear Programming
LP	Linear Programming
COP	Coefficient of Performance
SSSP	Site Source-Sink Profile
SUGCC	Site Utility Grand Composite Curve

Abstract

Integration of Organic Rankine Cycles in process sites for waste heat recovery
Zheng Chu
The University of Manchester
2022
PhD Thesis

With more and more stringent policies on reducing greenhouse gas emissions, for the industries, the improvement on energy efficiency to reduce the consumption of fossil fuels should be an essential matter to be considered. It is pointed out that the exploitation of industrial waste heat could increase energy efficiency in process sites, achieving considerable economic and environmental benefits (Oluleye 2016). When considering recovering industrial waste heat, there are diverse commercialized technologies such as Compression Heat Pumps, Absorption Heat Transformers, Absorption Heat Pumps, Absorption Chillers and Organic Rankine Cycles (ORC)) available. Amongst the technologies, ORC is becoming a promising one for recovering the waste heat in industrial fields.

For the practical applications of ORCs in industrial sites, there could be multiple waste heat sources geographically dispersed with different temperature levels and heat duties; and correspond to different operating conditions, the implemented ORCs could have various architecture selections and working fluids selections. In this case, in order to achieve a maximum power output or minimum total marginal cost, how to design an effective network for extracting waste heat and how to optimally configure and operate the implemented ORCs are the questions that should be dealt with. These questions lead to a systematic analysis problem, namely an ORC integration problem.

This thesis proposes several methodologies (which are separately presented in the three appended papers), aiming to address the integration problems of ORCs. For extracting waste heat, two strategic options, i.e., transferring heat in a direct way or through intermediate heat carriers (in an indirect way), are considered. While for implementing ORCs, the proposed methodologies allow for integrating more than one ORC unit, and the optimal working fluid selection for each ORC can be determined.

Technically, the proposed methods are based on mathematical-programming process integration technologies, which normally consists of procedures of model establishment and optimization. For model establishment, two different superstructures are developed, representing the direct and indirect integration of ORCs, respectively. The corresponding models lead to mixed-integer non-liner programming. For optimization, an iterative procedure is developed, which is used for determining the optimal unit number of the ORCs to be integrated. Besides, for determining the optimal working fluid of each ORC, a bi-level decomposition optimization strategy is proposed, which is illustrated in the third appended paper.

The methodologies are applied to industrial case studies. Results indicate that integrating ORCs for waste heat recovery could yield additional increases in overall energy efficiencies and reductions in the total annualized cost for dealing with waste heat. The case studies also demonstrate that, for some cases, the integration of multiple ORCs could gain more extra benefits than the integration of a single ORC.

Declaration

No portion of the work referred to in the thesis has been submitted in support of an application for another degree or qualification of this or any other university or other institute of learning.

Zheng Chu

Copyright Statement

Acknowledgement

I would like to express my deepest gratitude to everyone who contributed to the completion of this thesis. First and foremost, I am extremely grateful to my supervisors Dr Nan Zhang and Professor Robin Smith. Their constant support, inspiring views, wisdom and feedback made this thesis a reality. I would also like to thank Dr Igor Bulatov, Dr Jie Li, Dr Dongda Zhang and Steve Doyle for their kind support from the onset and sharing their experiences.

Thanks also to all the staff and colleagues from the Centre for Process Integration for their friendship and the good times. A big massive shout out to every remarkable and exceptional researcher in B14.

Finally, I would love to appreciate my family for their understanding, support and prayers. Especially to my parents who taught me to always make excellence my lifestyle, and to my girlfriend for her accompany and encourage.

Chapter 1: Introduction

1.1 Research Background

1.1.1 Net-zero Emissions by 2050

It is pointed out that, with current policies on energy utilization, the global primary energy requirement could expand by over a quarter between 2017 to 2040 (International Energy Agency, 2018). Despite the fact that most countries have paid attention to exploiting sustainable energy since 2010, fossil fuels could still share about an 80% proportion in global primary energy consumption by 2030 (International Energy Agency, 2019). It can be estimated that the yearly consumption of coal, oil, and natural gas in 2030 would be 4154 Mtoe, 5174 Mtoe, and 4070 Mtoe, about 9%, 15%, and 24% higher than the data in 2018 (International Energy Agency, 2021). With current energy conservation policies, the increasing trend of fossil fuel consumption could be reversed until the 2050s (International Energy Agency, 2021).

One main issue brought up by fossil fuel utilization is the emissions of CO_2 — one kind of global warming gas. The combustion of fossil fuels is regarded as the primary contributor to the rise of CO_2 concentration in the atmosphere, which could be responsible for over 70% of the total emissions of human activities (Andres et al., 2011). It is predicted that, with the current state of fossil fuel consumption, the global energy-related CO_2 emissions could rise to about 36 gigatons in 2030 (International Energy Agency, 2021).

It is all well known that a high concentration of greenhouse gases in the atmosphere will result in global warming and a series of global climate changes. A detailed analysis has been carried out to assess the climate change induced by greenhouse gas emissions, of which the result shows that the global average surface temperature rise would exceed 1.5 degree Celsius (°C)

in the 2030s (International Energy Agency, 2021). It is also pointed out that if keeping the current trend of greenhouse gas emission, the temperature rise could be about 2.6 °C by the 22nd century, leading to a series of catastrophic climates such as extreme heat, drought, flooding, and crop failures (International Energy Agency, 2021). In current years, with an average temperature rise of 1.1 °C above the pre-industrial level, extreme heat events occurred almost three times more frequently than in pre-industrial times.

With increasing pressure on the ecosystem, more and more stringent schemes and policies have been stated to reduce fossil fuel utilization and the corresponding greenhouse gas emissions. Science 2005, the Kyoto Protocol and the European Union Emission Trading Scheme have been proposed, which clarified the obligations for industrialized countries to diminish greenhouse gas emissions. At the European Council of March 2007, the EU committed to achieving greenhouse gas emissions at least 20% less than the 1990 level by 2030. To achieve this target, the binding legislation, known as the 'climate and energy package', was proposed in 2008 and became law in 2009. In 2015, at the 21st conference of the Parties to the United Nations Framework Convention on Climate Change (UNFCCC), the Paris Agreement (which establishes a goal of ensuring less than 2°C increase in global average temperature) was emphasized, urging the Parties to peak their greenhouse gas emission and to achieve net-zero emissions as soon as possible. In 2018, a scientific report proposed by the Intergovernmental Panel on Climate Change (IPCC) warned that the ambition in dealing with global climate change should be reinforced, or global average temperature rise could still reach 2°C soon after 2060, approaching the critical bound of mass extinction of species. At the Katowice UNFCCC conference held in 2018, Parties reaffirmed their increasing ambitions to eliminate greenhouse gas emissions. The European Parliament was considering updating the previous target of reducing greenhouse gas emissions from 20% to 55% below the 1990 level. In 2020, the Chinese government announced that China aimed to peak CO_2 emissions before 2030 and to achieve carbon neutrality before 2060. In 2021, the 26th Conference of the Parties to the UNFCCC took place in Glasgow, of which the main purpose

is to keep strengthening the ambitions of global countries dealing with climate change. At the conference, more stringent emission reduction pledges were required to be declared by the participants, and the goal of achieving net-zero emissions by 2050 was reaffirmed.

1.1.2 Energy Efficiency Enhancement

In order to accomplish net-zero emissions for global countries by 2050, except developing renewable energy such as wind, solar, hydro, etc., the improvement on energy efficiency, especially for the energy-intensive industrial sector, is an essential factor to be considered. In 2020, it was estimated that the industrial sector, including agriculture, iron and steel, refining and petrochemicals, and nonmetals, occupies about 40% of the world's final energy consumption (including fuels used for electricity, district heating, space heating, and transportation fuels and industrial processing fuels) (International Energy Agency, 2021). An average 0.9% annual increase in energy consumption has been observed for the industrial sector since 2010. With the large proportion of energy consumption, it is pointed out that the industrial sector could be responsible for over 30% of global greenhouse gas emissions (Oluleye, 2016), which is the second-largest emitting sector after the power generation sector (International Energy Agency, 2021). However, with a large proportion of global total energy consumption, the industrial sector has relatively low energy efficiency. Globally, the sectors include industry, building and transporting can only transform 67% of total energy inputs into useful forms for final consumption (International Energy Agency, 2012). Compared with other sectors, the industrial sector could have the biggest implementation gap of efficiency improvement between the current state and the announced pledges that fulfil 2050 carbon neutralization (International Energy Agency, 2021). If excavating the potential of energy efficiency enhancement, the growth of energy demand in the industry could be reduced by 0.4% per year on average, achieving a total energy saving amount of 326 Mtoe in 2035 (Kesicki and Yanagisawa, 2014).

To improve industrial energy efficiency and reduce greenhouse gas emissions, except enhancing the performances of processing facilities by advanced designs or materials, a family of systematic-analysis methodologies, namely process integration (PI), have been proposed, which can design industrial sites in a holistic way, considering the optimal operations of processing units, the cooperation between manufacturing processes, and the cogeneration of utility systems. An accurate definition of PI, as adopted by the International Energy Agency (2020), reads as: 'systematic and general methods for designing integrated production systems ranging from Individual processes to total sites, with special emphasis on the efficient use of energy and reducing environmental effects.'

Basically, the PI techniques can be classified into two, i.e., graphical-based techniques and mathematical programming-based techniques. The following context introduces the most representative techniques, aiming to give a basic understanding of the PI techniques.

- **graphical-based techniques**

In 1983, the 'Pinch Analysis' technique was proposed as a tool for analyzing and developing efficient industrial processes (especially for the chemical and petrochemical industries) (Linnhoff and Hindmarsh, 1983). By applying the technique, one can target the maximum amount of heat recovery between process hot streams that should be cooled down and process cold streams that should be heated up, offering guidelines for the followed specific designs to improve energy efficiency.

A concept of 'Pinch Point' came up with the technique. Principles of applying the 'Pinch Point' concept can be summarized as: 1. heat transfer across a pinch point incurs the double penalty of hot and cold utility requirement; 2. to the terms of energy conservation, cooling utility consumption is not encouraged above a pinch point, while hot utility consumption is not encouraged below.

As part of the 'Pinch Analysis', a method of 'Composite Curve' was also adopted by Linnhoff and Hindmarsh (1983) as a graphical tool to cooperate with the concept of 'Pinch Point', which provides an intuitive way to target the maximum heat recovery under given minimum approach temperatures. The illustrative schematic is shown in Figure 1.1. The red line represents the composite curve of hot streams of a process, while the blue dashed line represents the composite curve of the corresponding cold process streams. The narrowest point(s) between the two curves locates the pinch point(s), where the temperature difference(s) between hot and cold sides defines the approach temperature (ΔT). The overlapped region between the composite curves indicates the heat recovery potential with current approach temperature. The heat recovery potential can be maximized by minimizing the approach temperature (ΔT_{min}) at the pinch point(s).

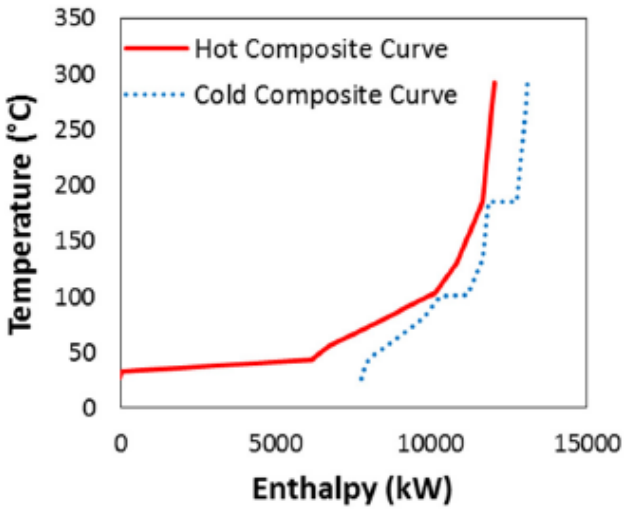

Figure 1.1 An illustrative schematic of a process composite curve (Oluleye, 2016)

Besides the 'Composite Curve', another method derived from the 'Pinch Analysis', namely 'Grand Composite Curve' (GCC), is worth to be mentioned. It is conceived that the 'Composite Curve' can only determine the quantity of utility usage, but is not a suitable tool for determining the temperatures of implementing utilities. In practice, there could be multiple utilities with different supply temperatures and quantities. The most economical strategy is selecting the most suitable utility to heat up or cool down a process stream. As such, the GCC was

developed as a tool for utility selection (Linnhoff et al., 1982). An illustrative schematic of a GCC is shown in Figure 1.2.

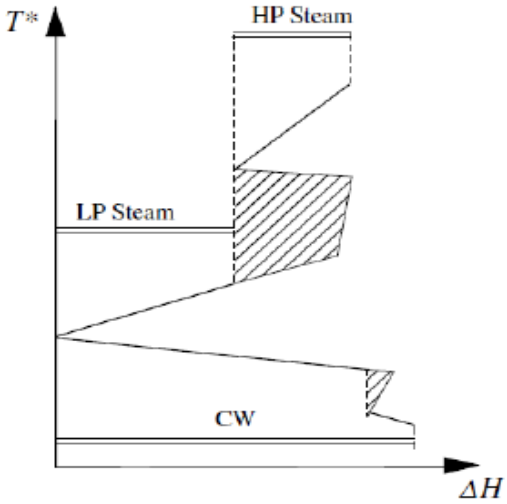

Figure 1.2 An illustrative schematic of a GCC (Smith, 2005)

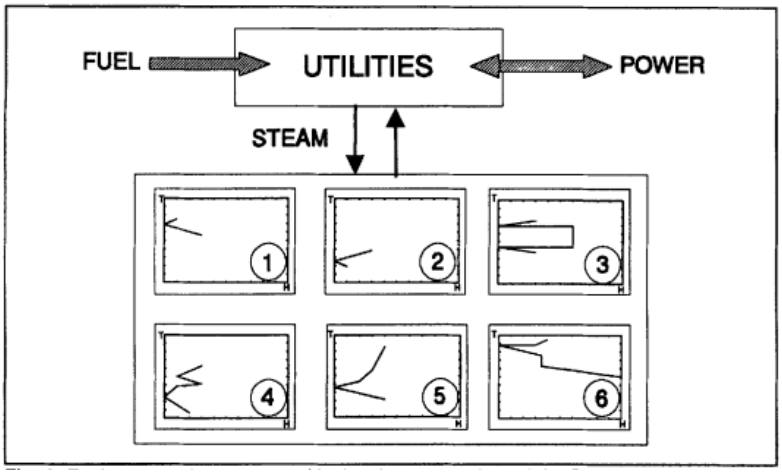

Figure 1.3 An illustrative schematic of TSA (Dhole and Linnhoff, 1993)

The 'Pinch Analysis' technique was wildly applied with huge success (Smith, 2005). However, it is realized that the technique is developed to optimize an individual process, which failed to explore the energy conservation potentials in the context of a total site. In the view of total site, the potential of heat integration amongst different processes exists. To this perspective, a technique, namely 'Total Site Analysis' (TSA), has been introduced as an extension of the

Pinch Analysis technique to consider heat integration in a total site context (Dhole and Linnhoff, 1993), as shown in Figure 1.3. According to the TSA, Pinch Analysis is firstly carried out within each process, through which the heat deficient and heat surplus zones of each process can be identified. Then, through the steam network of the utility system, heat integration amongst different processes can be achieved.

- **Mathematical programming-based techniques**

The main idea of mathematical programming-based techniques can be concluded as: through using mechanism or surrogate models to formulate the correlations of the decision variables of the research object, and through applying mathematical programming techniques to determine the optimal value of the variables. Compared with the graphical-based techniques, one advantage of mathematical programming-based techniques is that they are capable of pursuing global optimum solutions on the synthesizes and operations of processing plants and site utility systems. However, the solution quality of programming-based techniques depends on the accuracy of the established models and the robustness of the selected solvers. Besides, the solving processes of some large-scale problems could be time-consuming.

One of the representative techniques is developed by Yee and Grossman (1990), which is wildly applied for dealing with heat integration problems. In the technique, a stage-wise superstructure is proposed, providing a general but straightforward representation of the heat exchanger network (HEN) between hot and cold process streams. The mathematical model of the superstructure leads to a mixed-integer non-linear programming (MINLP) problem, through solving which the optimal HEN synthesis can be carried out. Case studies show that, by applying the techniques, the industrial sites with heat integration can achieve less energy consumption and lower total annualized cost. Based on the proposed superstructure, the followed works such as Shang and Kokossis (2004), Varbanov et al. (2004), Micheletto et al. (2008), Luo et al. (2011), Zhao et al. (2015), developed different models for dealing with heat integration or process synthesis problems, leading to MINLP, MILP (mixed-integer linear

programming), or NLP (non-linear programming) optimization problems.

In summary, based on physical insights, the graphical-based techniques can provide guiding principles for arranging heat recovery and minimizing utility consumptions, which are easily understandable for engineers on the ground. The optimality of graphical-based techniques could be near-optimum, which could be dependent on the experiences of designers. While the mathematical programming-based methods can simultaneously optimize a large number of decision variables, obtaining global optimum solutions. However, it is professional-required to establish accurate models of which the predictions can be highly consistent with the practical working conditions and to guarantee the quality of the optimization results.

The methodologies of PI have been extensively applied in the process industries (such as chemical, petrochemical, pulp and paper, food and drinks, steel making) over the last 40 years, leading to more effective and efficient site energy systems. However, it is pointed out that, even to a fully integrated site, there is still a large quantity of residual heat that cannot be utilized, which has to be discharged into the environment as waste heat. This is because: 1. the total site has reached its limit for further heat recovery; 2. the residual heat has a low temperature (no higher than 200 °C (Ammar et al., 2012)), which is too low to be used by conventional steam-based technologies such as turbines.

In 2016, as for the process industries in the UK, at least 40% of the energy content of fuel was wasted. (Oluleye et al., 2016). An investment proposed by the US Department of Energy revealed that, in the US's energy-intensive industrial sectors including glass, cement, iron/steel, aluminium, metal casting and chemical, there is still about 1.56 EJ/year residual energy dissipated as waste heat, accounting for about 18% of the total energy consumption (8.86 EJ/year) (Johnson et al., 2008). As for the energy-intensive sectors in China, the waste heat takes part about 15–40% of the total energy input (Lu et al., 2016). In the 28 countries in European Union, the total waste heat potential in the industries is estimated to be

300 TWh/year (Papapetrou et al., 2018).

It is logical to expect that if the industrial waste heat can be exploited, the energy efficiency could be further improved, and the primary energy consumption could be further saved, leading to fewer greenhouse gas emissions. On the other hand, it is also proved that waste heat recovery could have economic potential, leading to considerable annualized profit for the industries (Bruckner et al., 2015; Oluleye et al., 2016).

1.1.3 Industrial Waste Heat Recovery

Industrial waste heat recovery has drawn global attention in recent years. The European waste heat recovery market is estimated to expand to exceed €45 billion in 2018 (Jouhara and Olabi, 2018). While the global waste heat recovery market is expected to surpass $65 billion by the end of 2021, of which the corresponding compound annual growth rate is estimated to be 6.9% (Markets, 2018). For the Asian, in the past decades, China and India have been experiencing the highest growth rates (about 10% per annum) on the installations of waste heat recovery units (Bianchi et al., 2019). In industrial scenarios, the most common approaches for waste heat recovery are the ones that can be integrated with utility systems for steam generation, feed material preheating, and power generation (Bianchi et al., 2019). It is estimated that about 300-350TWh/year waste heat in the EU industries is potentially recoverable (Bianchi et al., 2019). In 2019, a project, namely I-THERM Horizon 2020, is proposed in the EU 28, declaring a 25% extra cost saving over the conventional technologies for energy conservation by applying waste heat recovery technologies (Agathokleous et al., 2019).

1.1.3.1 Definition of Industrial Waste Heat

To discuss industrial waste heat recovery, we need to specify the definition of industrial waste heat. Bending et al. (2013) defined industrial waste heat as the residual heat after heat

recovery within a process. However, this definition ignores the site-wide heat recovery potential between different processes. Similar definitions were proposed by Morandin et al. (2014), who defined industrial waste heat as “the heat at medium to low temperatures not used in industrial processes”; Viklund and Johansson (2014), who defined waste heat as a by-product of industrial processes; and Viklund and Karlsson (2015), who defined waste heat as the excess heat exchanged to a medium such as water, air and flue gas. Such definitions neglect the potential of applying PI techniques to reduce the creation of waste heat.

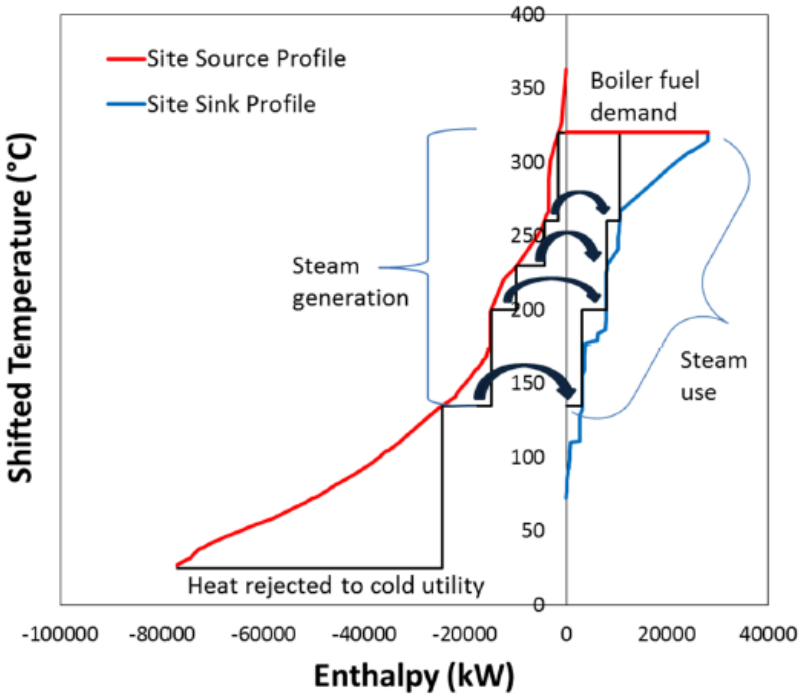

Figure 1.4 A total site profile of heat integration (Oluleye, 2016)

To this end, Oluleye (2016) made a progression on defining industrial waste heat by considering the potential of process heat integration. A premise, i.e., the total site has to reach its limit for heat recovery, was pointed out for defining industrial waste heat. The maximum heat recovery can be targeted by the Pinch Analysis and TSA techniques, as represented by Figure 1.4. The red and blue curves represent the hot and cold composite curves of a total site. According to Oluleye (2016), only when the two curves are fully integrated, the

corresponding residual heat (heat rejected to cold utility) can be defined as waste heat.

However, the definition proposed by Oluleye (2016) still has deficiencies. In practice, it is unreasonable for plants to merely consider achieving the maximum heat recovery, as the trade-off between energy recovery and the related costs should be taken into account. For most cases, the optimization objective could be to gain the maximum annualized profit rather than energy recovery. On the other hand, a specified temperature range should be given for defining waste heat, as high-temperature heat could still have the potentials to be used by conventional steam-based technologies. A common cognition of the temperature range of industrial waste heat is between the ambient temperature to 200℃ (Ammar et al., 2012). From these perspectives, this work defines industrial waste heat as the residual heat with a temperature range between the ambient temperature to 200℃ when a total site has reached its best economic performance (without considering waste heat recovery).

1.1.3.2 Feasible Technologies

There are diverse technologies feasible for recovering energy in the form of upgraded heat, cooling and power from waste heat sources. For providing upgraded heat, examples of technologies are mechanical heat pumps, absorption heat pumps, and absorption heat transformers. For providing cooling demand, examples of developed technologies are absorption chillers and adsorption chillers. For generating power, technologies such as Organic Rankine Cycles (ORCs) and Kalina cycles could be feasible. The working principles of these technologies are briefly introduced by the following.

- **Mechanical Heat Pumps**

A mechanical heat pump contains four main components, i.e., an evaporator, a compressor, a condenser, and an expansion valve. The working principle is illustrated in Figure 1.5. From Point 4 to 1, a strand of working fluid is evaporated by an evaporator, extracting waste heat;

From Point 1 to 2, The vaporized stream is compressed by a compressor, increasing the temperature; From Point 2 to 3, the vaporized stream is condensed in a condenser, supplying heat to heat sinks; From point 3 to 4, the condensed stream releases its residual pressure through an expansion valve, preparing for repeat the cycle.

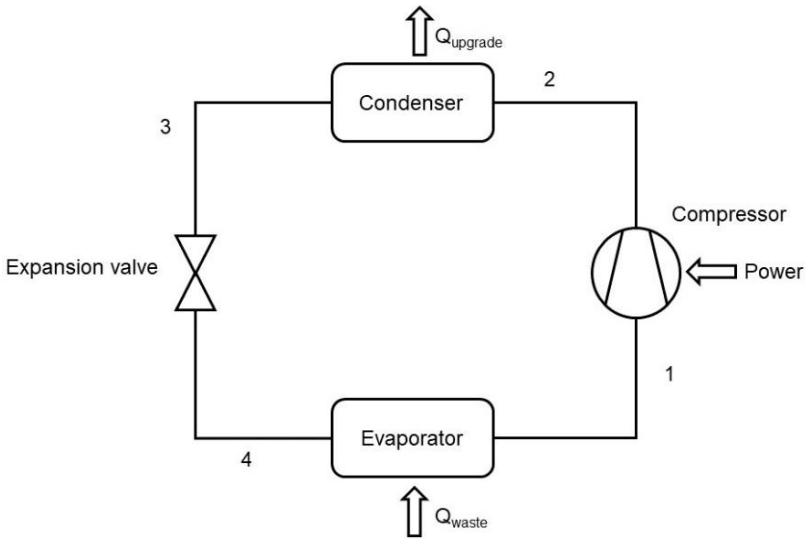

Figure 1.5 The illustrative schematic diagram of Mechanical Heat Pumps

- **Absorption Heat Pumps**

Compared with mechanical heat pumps, absorption heat pumps use thermal energy instead of electrical power to raise working fluid temperature. Commonly used working fluids are binary mixtures such as ammonia-water and water-lithium bromide. We take an ammonia-water mixture system as an example to explain the working principle of absorption heat pumps. The schematic diagram is shown in Figure 1.6. During operation, a generator is used to separate the working fluid into two sub-flows, i.e., a rich absorbent (water) with low ammonia concentration and a vaporized flow of pure ammonia. The vaporized pure ammonia is sent to a condenser, transferring heat to the outside. While the rich absorbent is refluxed to an absorber, preparing for receipting the cycled pure ammonia flow. After condensation, the pure ammonia flow goes through an expansion valve, releasing its residual pressure; and is then vaporized by an evaporator so that the absorbent can absorb it. Finally, the pure ammonia

flow is absorbed by the rich absorbent, and the cycle repeats. The generator and condenser are operated at higher pressure, assuring a high-enough condensation temperature provided to outside users. In contrast, the evaporator and absorber are operated at relatively low pressure so that the evaporation process can be driven by low-temperature waste heat sources.

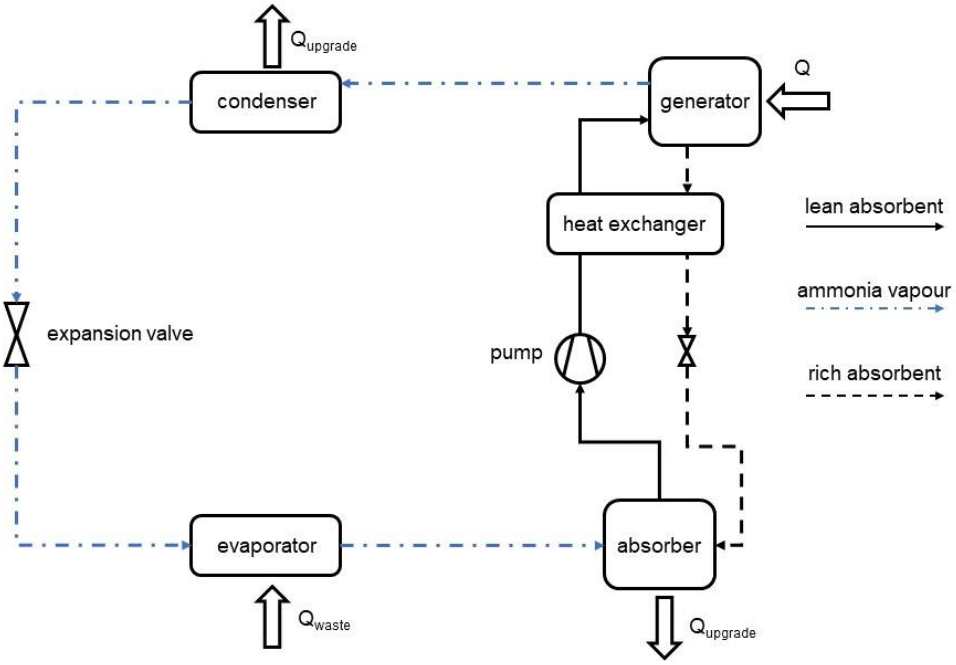

Figure 1.6 The illustrative schematic diagram of Absorption Heat Pumps

- **Absorption Heat Transformers**

Absorption heat pumps can convert low-temperature waste heat into medium-temperature heat by using high-temperature heat, as illustrated by Figure 1.7(a). While absorption heat transformers can convert medium-temperature waste heat into high-temperature heat and low-temperature heat, as illustrated by Figure 1.7(b). Absorption heat transformers can be regarded as having reverse operations as absorption heat pumps. Figure 1.8 shows the illustrative diagram of an absorption heat transformer. In an absorption heat transformer, the evaporator and absorber operate at a higher pressure than the condenser and generator. In the generator, waste heat sources at medium temperatures are responsible for separating the refrigerant (using ammonia as an example) from the absorbent (water). The refrigerant vapour

is condensed in the condenser, discharging its latent heat to the environment. The condenser outlet is pumped to a higher pressure; and is evaporated to saturated vapour, extracting heat from waste heat sources. The high-pressure saturated ammonia vapour is then sent to the absorber, in which the absorbing process can release heat at a high temperature, fulfilling users' demands.

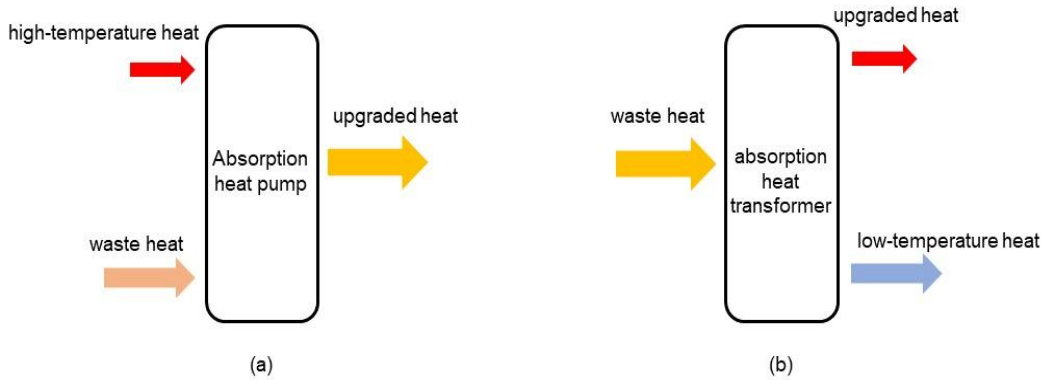

Figure 1.7 Difference between Absorption Heat Pumps and Absorption Heat Transformers

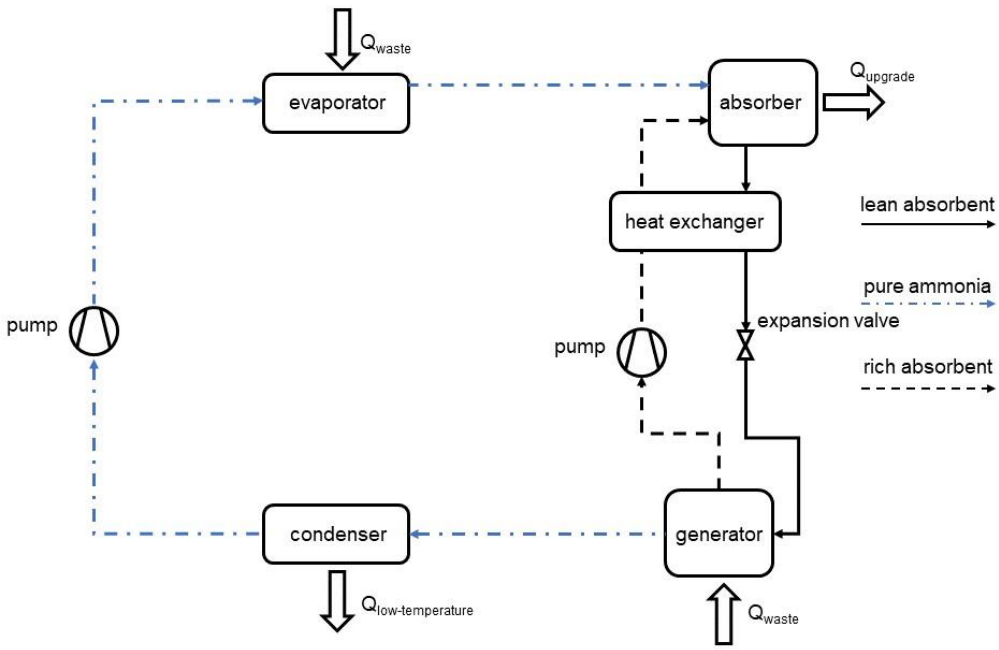

Figure 1.8 The illustrative schematic diagram of Absorption Heat Transformers

- **Absorption Chillers**

Absorption chillers use the same working component and working fluids as absorption heat

pumps but provide chilling rather than heat upgrading. The working principle is illustrated in Figure 1.9. In the cycle, chilling is provided by the evaporator. Waste heat is supplied to the generator to separate the refringent-absorbent pair. After the separation, the rich absorbent flows back to the absorber, while the separated refrigerant is sequentially sent to the condenser and the expansion valve and is finally recycled to the evaporator.

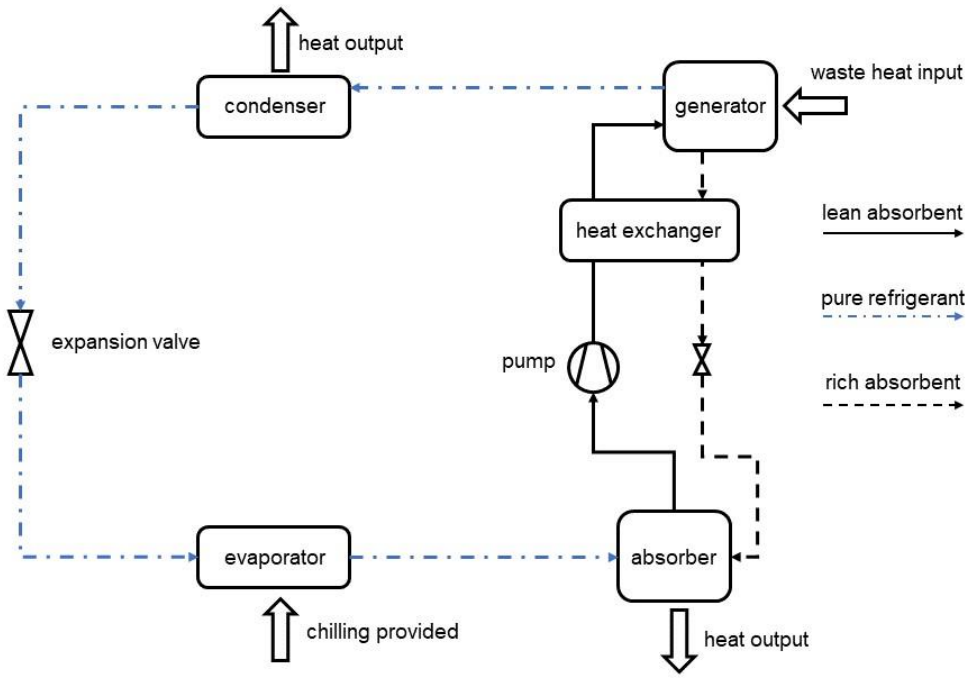

Figure 1.9 The illustrative schematic diagram of Absorption Chillers

- **Adsorption Chillers**

Adsorption Chillers adopt solid materials (such as silica gel) instead of liquid solution as absorbent and commonly use water as the corresponding refrigerant. A typical Adsorption Chiller consists of four main parts, i.e., an evaporation chamber, a condensation chamber, and two adsorption chambers, as shown in Figure 1.10. In each cycle, one of the adsorption chambers will be an adsorber while the other will be a desorber. In Figure 1.10, adsorption chamber 1 firstly works as an absorber, connecting to the evaporation chamber. Due to the existent of dry absorbent (silica gel) in chamber 1, the refrigerant (water) in the evaporation chamber can be vaporized, absorbing heat from the external cooling load so that chilling is

produced. Note that the dry absorbent will absorb the water vapour. As soon as chamber 1 is saturated with water, it will cut off the connection with the evaporation chamber and begins to desorb itself. The desorption process is driven by external thermal energy (waste heat). Meanwhile, adsorption chamber 2 should have finished its desorption, which will connect to the evaporation chamber to take over the adsorption chamber 1. As such, a continued provision of chilling can be assured.

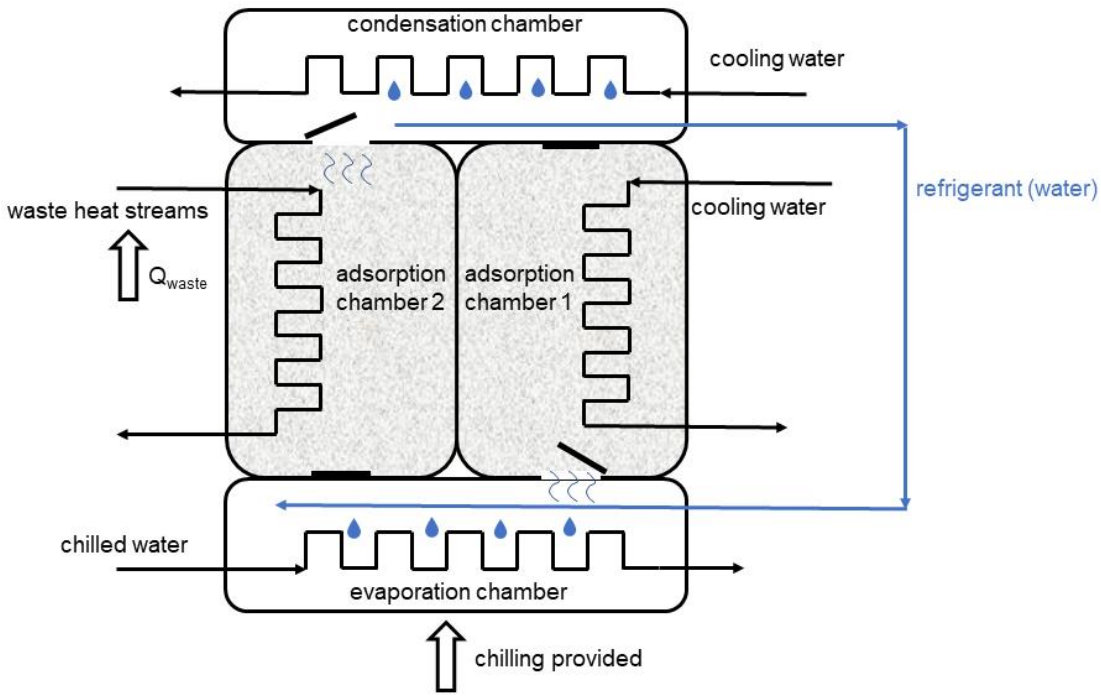

Figure 1.10 The illustrative schematic diagram of Adsorption Chillers

- **Organic Rankine Cycles**

Derived from conventional steam-based Rankine Cycles, Organic Rankine Cycles (ORCs) use organic compounds instead of water as working fluid, which is feasible to generate power from low-temperature heat sources. A typical ORC consists of four main components, i.e., an evaporator, a turbine, a condenser and a working fluid pump, as shown in Figure 1.11. In the evaporator, external waste heat sources provide thermal energy to vaporize the working fluid. The vaporized working fluid expands in the turbine, transforming its thermal energy to work

and then to power. The condenser and pump are responsible for liquifying and pressuring the turbine exhaust so that the cycle repeats.

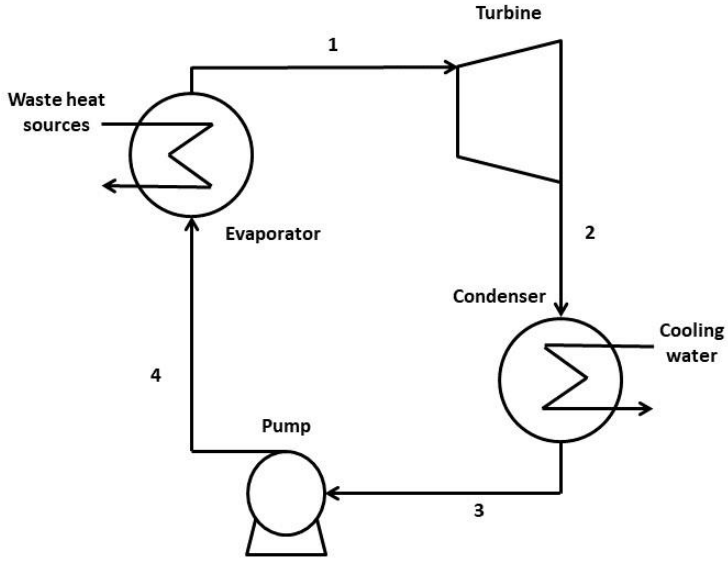

Figure 1.11 The illustrative schematic diagram of Organic Rankine Cycles

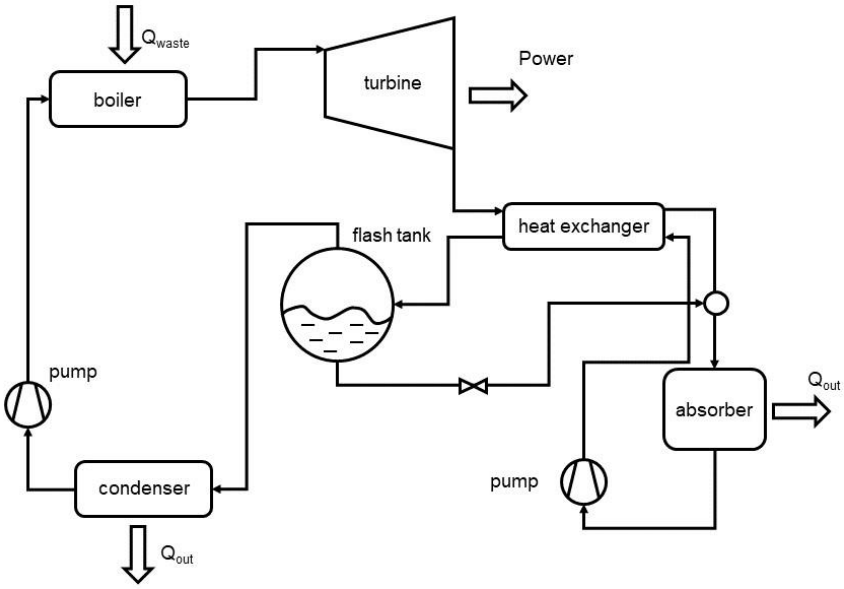

Figure 1.12 The illustrative schematic diagram of Kalina Cycles

- **Kalina Cycles**

Typical Kalina Cycles, firstly proposed by Kalina (1984), use ammonia-water as the working fluid, which is feasible for generating power from low-temperature waste heat sources. The

working principle is illustrated in Figure 1.12. In the boiler, after receiving thermal energy from waste heat sources, a high-concentrated ammonia-water mixture is superheated and is sent to the turbine for power generation. After expansion, the high-concentrated mixture is diluted with a lean absorbent in the absorber. Heated up by the residual heat from the turbine exhaust, the diluted liquid becomes saturated and is sent to the flash tank. Due to the significant volatility difference, a strand of rich-ammonia vapour is separated from the diluted liquid. The separated rich-ammonia vapour sequentially flows to the condenser for liquifying and to the boiler for reheating. While the lean absorbent left in the flash tank is sent back to the absorber so that the cycle repeats.

Applications of heat pump technologies include Mechanical Heat Pumps, Absorption Heat Pumps, and Absorption Heat Transformers are widely spread all over the world, while particular attention has been drawn in Sweden, USA, Japan, Germany, Austria, Denmark, etc. (Carmo et al., 2014). It is reported an increase of 7.2% by volume of the world's heat pump market in 2013 (Grassi, 2018). In industrial processes, heat pump technologies can be applied for drying, evaporation, distillation or can be directly integrated with utility systems. It is reported that distillation systems assisted with Absorption Heat Pumps or Absorption Heat Transformers can achieve up to 45% saving on primary energy usages (Wang and Lior (2011); Wu et al. (2014)). Compared with Absorption Heat Pumps, Absorption Heat Transformers are more popular in the industries for waste heat recovery due to their ability for temperature raising. Cortés and Rivera (2010) integrated an Absorption Heat Transformer for industrial waste heat recovery. From about 70℃ waste heat sources, 90-120℃ hot water is obtained. It was assessed that the applying of the absorption heat pump could save about 25% primary fuel consumption. Compared with absorption Heat Transformers, Absorption Heat Pumps are more commonly used for drying or civil heating, as they can achieve larger thermal energy output but with lower temperatures (Wu et al., 2014). The coefficient of performance (COP) is an indicator that can evaluate the rate of the useful energy output of heat pumps. The typical COP of Absorption Heat Pumps with respect to industrial waste heat recovery ranges from 13

to 1.6, while that of Absorption Heat Transformers ranges from 0.4 to 0.6.

Absorption Chillers and Adsorption Chillers are feasible technologies for chilling provision. In Adsorption Chillers, due to the large superficial area and porosity of the solid absorbents, it is capable of cycling large quantities of refrigerant, providing relatively large cooling capacities (Best and Rivera, 2015). Adsorption Chillers are normally operated with 65℃ to 100℃ heat sources and can provide chilling around 5 to 7℃. The most common absorbent-refrigerant pairs of Adsorption Chillers are silica gel/water and zeolite/water. Compared with Absorption Chillers, Adsorption Chillers have no corrosion and crystallization problems, leading to low maintenance requirements. However, it is also pointed out that Absorption Chillers could achieve higher coefficients of performance than Adsorption Chillers. In practice, Absorption Chillers are more mature and further developed (Chan et al., 2013).

Adopting mixtures of two fluids with different boiling points as working fluids, Kalina Cycles can obtain better thermal matches with background heat sources, leading to more heat extraction and higher exergy efficiency (Matsuda, 2014). It is declared that, for recovering industrial waste heat, Kalina Cycles can offer up to 32% more power generation than conventional steam-based Rankine Cycles (Zhang et al., 2012). Compared with Organic Rankine Cycles, Kalina Cycles could provide about 3% more power output (Law et al., 2013). However, due to the adoption of ammonia-water mixtures, the practical applications of Kalina Cycles always require non-corrosion materials as well as leakage prevention facilities, leading to relatively high capital costs (Zhang et al., 2012). On the other hand, Kalina Cycles also need more heat exchanger area and high operating pressure due to the superheating process (Oluleye, 2016). In contrast, Organic Rankine Cycles normally have high-dependent and essay operation, which makes them the most mature and tested technology when compared to the other power generation technologies for waste heat recovery.

1.1.4 ORC -- A Promising Technology

Amongst the mentioned feasible technologies, Organic Rankine Cycle (ORC) could be one of the most promising techniques for recovering low-grade heat due to its high reliability and low maintenance. In 2017, it was estimated that the ORC-related technology represents a total installed capacity of around 2.7 GW, corresponding to which there are about 700 commercialized projects and 1754 implemented ORC units (Tartière and Astolfi, 2017). At the end of 2020, it was reported that the cumulated ORC installed capacity expanded to about 4.07 GW (Wieland et al., 2021). It can be observed that the overall ORC market increased by 40 % in terms of installed capacity and by 46 % in terms of installed units since 2016. Except for generating power from geothermal energy, industrial waste heat recovery is the second main field of ORC applications. From 2016 to 2020, the installed ORC plants for recovering low-grade waste heat have increased by about 207% (Wieland et al., 2021).

In practice, the feasible heat source temperature for operating ORCs is ranged from 40℃ to 250℃. The capacity of a single ORC unit can be sized from 3kW to 18 MW, whilst the thermal efficiency can be up to 20% (Mahmoudi et al., 2018). The performance of an ORC is highly dependent on its architecture and working fluid.

1.1.4.1 Different Architectures of ORC

Several architectures of ORC have been derived from a basic cycle, aiming to improve the thermal efficiency of an ORC when facing different application scenarios. This thesis gives a brief introduction of each type:

1. **Basic Cycles.** The simplest architecture, which have been illustrated in Figure 1.11. The corresponding temperature-entropy (T-S) diagram is depicted in Figure 1.13 (a).
2. **Superheated Cycles.** The working fluid is superheated in the evaporator, obtaining a higher temperature. This type of cycle could avoid the creation of droplets at the turbine

outlet, preventing the corrosion of turbine blades. To another aspect, the superheating process could result in a better thermal match with heat sources, increasing the thermal efficiency to some extend (Hung et al., 1997). However, a larger heat exchanger area will cost. The corresponding T-S diagram is exhibited in Figure 1.13 (b).

3. **Cycles with Recuperators.** An internal heat exchanger (i.e., recuperator) is placed between the turbine exhaust and the inlet of the evaporator, heating the working fluid after pumping. By such configuration, for some cases the thermal match with background heat sources could be enhanced, leading to more power generation (Desai and Bandyopadhyay, 2009). The corresponding T-S diagram is shown in Figure 1.13 (c). Note that this type of cycles is named 'regenerative cycles' by (Kermani et al., 2018), but according to Lecompte et al. (2015), the most precise name should be 'ORCs with recuperator'.
4. **Reheating Cycles.** At an intermediate point of the turbine, part of the working fluid is separated from the main flow and is re-heated by heat sources. The re-heated partial flow is then re-injected into the turbine. This type of cycle could lead to a better thermal match with heat sources, reducing the exergy losses and increasing the evaporation temperature of the working fluid. The corresponding T-S diagram is presented in Figure 1.13(d).
5. **Supercritical Cycles.** The working fluid is heated up to its supercritical thermodynamic states before being sent to the turbine for expansion. This type of cycle is not always recommended, as its high operating pressures and temperatures may lead to higher capital and operating costs but not always better thermal efficiencies. Figure 1.13(e) shows the corresponding T-S diagram.
6. **Turbine Bleeding Cycles.** Part of the working fluid is extracted from the turbine at an intermediate pressure, which will be used to pre-heat the inlet flow of the evaporator by either direct mixing or an internal heat exchanger. The T-S diagrams of the direct mixing way and the applying of an internal heat exchanger are depicted in Figure 1.13(f) and (g), respectively.
7. **Cascaded Cycles.** Several ORCs are implemented in cascade, sequentially operating at

high to low pressures. Results have shown that cascaded cycles could achieve higher thermal efficiencies than basic cycles (Li et al., 2013). However, high enough temperatures of waste heat sources are necessary to drive the multi-cascaded ORCs, and more investment costs will be consumed. The related T-S diagram is shown in Figure 1.13(h).

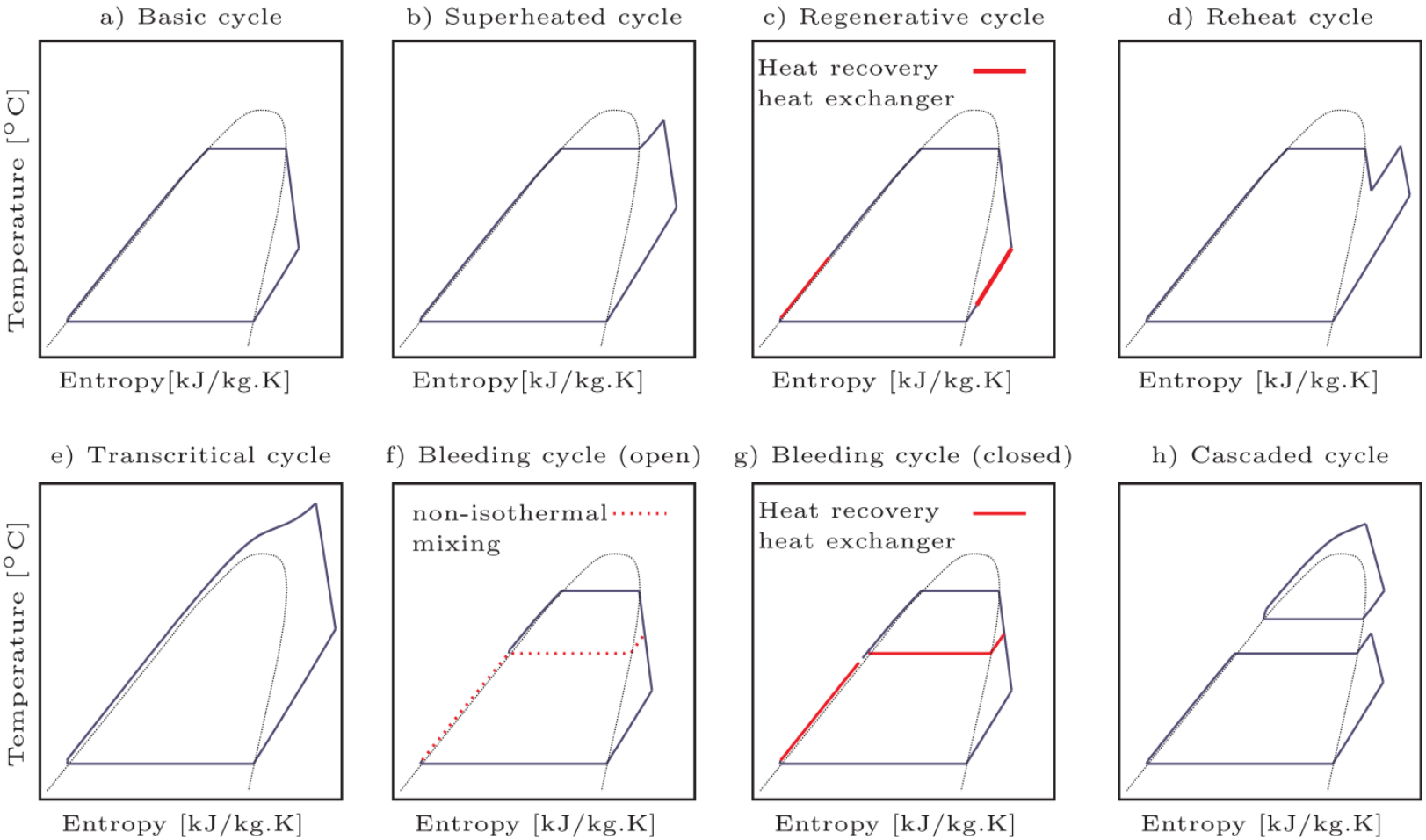

Figure 1.13 The T-S diagrams of different ORC architectures (Kermani et al., 2018)

1.1.4.2 Different Working Fluids of ORC

Organic compounds are normally considered as the feasible working fluids of ORCs. The advantages include low boiling point temperatures, medium vapour pressures at moderate temperatures, low specific volume and low isentropic turbine enthalpy drop (Hipolito-Valencia et al., 2013).

When implementing ORC systems, there are numerous candidates of organic working fluids to be selected: hydrocarbons, aromatic hydrocarbons, perfluorocarbons, alcohols and siloxanes (Oluleye 2016). In recent years, zeotropic mixtures are also considered, as their non-isothermal evaporating processes could improve the thermal match with heat sources, leading to higher evaporation temperatures with fewer exergy losses (Dong et al., 2020a). Different selections of working fluid could result in different thermal efficiency, economic viability, and security and environmental issues (Wang et al., 2020). Therefore, working fluid selection is one of the vital factors that should be considered when applying ORCs.

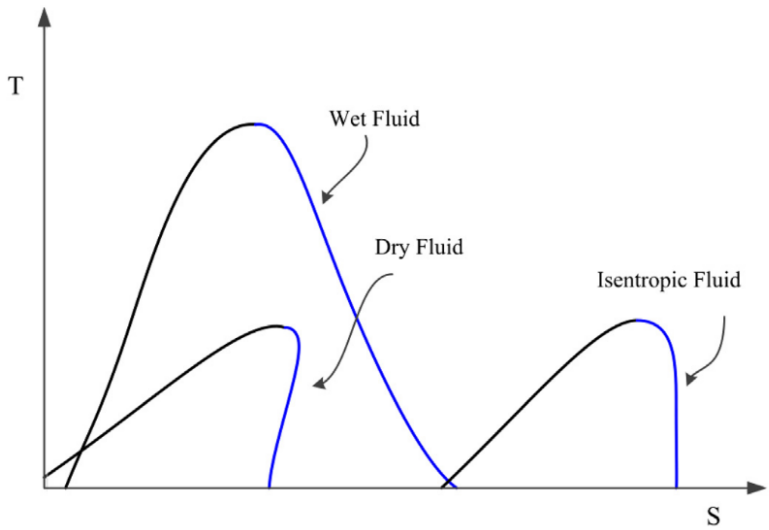

Figure 1.14 The T-S diagrams of wet, dry, and isentropic working fluids (Yu et al., 2015)

To select proper working fluids, both the thermodynamic properties (such as heat transfer coefficient, specific volume, boiling temperature, critical pressure/temperature, etc.), security,

and environmental protection of working fluids should be taken into account. According to the slopes of the saturated vapour curves in T-S diagrams, Huang et al. (1997) classified the ORC working fluids into three categories, i.e., wet, dry, or isentropic. The dry working fluids present positive slopes, whereas the wet working fluids exhibit negative slopes, and the isentropic ones typically have infinitely large slopes, as exhibited in Figure1.14. It is argued that the dry or isentropic working fluids are more favourable in practical applications as they are more operatable to avoid condensation at turbine outlets (Yu et al., 2015). Besides, feasible ORC working fluids should be non-toxic, low-corrosion, flammability-controllable, zero ozone depletion potential, and low global warming potential (Chen et al., 2010). The details of ORC working fluid selection will be further introduced in Literature Review.

1.1.4.3 Challenges Related to ORCs for Waste Heat Recovery

When applying ORCs for recovering industrial waste heat, challenges are associated, which can be concluded into three main aspects, i.e., how to extract waste heat effectively, how to generate power efficiently, and how to simultaneously consider waste heat extraction and power generation.

- **how to extract waste heat effectively**

Waste heat sources in industrial sites could be geographically dispersed with different supply temperatures, heat duties, and cleanliness (Oluleye 2016). Different selections and integrations of waste heat sources correspond to different capital and operating costs. Besides, different way of waste heat extraction may lead to different thermal match with ORCs, influencing the overall thermal efficiency of the ORCs. Some of the previous research works, such as Kapil et al. (2011), Garimella (2012), and Miro et al. (2015), discussed industrial waste heat recovery problems ignoring the diversity of industrial waste heat sources. However, in practice, representing waste heat sources systematically and determining how to transport the waste heat from sources to sinks optimally are essential matters that should be taken into

account.

- **how to generate power efficiently**

The thermal efficiency of an ORC could be affected by its architecture selections, working fluid selections, and operation conditions.

There are multiple architectures available for an ORC. It should be realized that each type of architecture has its advantages and drawbacks, suitable for different application scenarios. It is case-sensitive to determine adopting which type of ORC architecture to get better system performances. Moreover, as different architecture selections could bring up different investment costs, the trade-off between the related cost and the bonus on power generation should be considered.

Besides architecture selections, working fluid selections also exert considerable influences on the performances of ORCs. On the one hand, for an ORC itself, the different architectures and operating conditions could correspond to different optimal working fluids, leading to different thermal efficiencies. To another aspect, working fluid selections also affects the thermal match with background heat sources. It is realized that the isothermal boiling process of ORC working fluids in evaporators could create Pinch points on composite curves, limiting the further improvement of evaporating temperatures or the recovery rate of waste heat sources, as illustrated in Figure 1.15. Different working fluids could exhibit different latent and sensible heat ratios, performing diverse composite curves and obtaining different thermal matches with background heat sources. Furthermore, the factors of different heat transfer coefficients, the corrosiveness, and the specific volume of working fluids could respectively decide the heat transfer area usages, the consumptions of corrosion-resistance materials, and the designs of turbines, to some extent, resulting in different trade-offs between costs and profits. Some of the previous researchers have provided heuristical principles for selecting proper working fluids depending on some given working conditions (Saleh et al., 2007; Xu and Yu, 2014;

Wang et al., 2020); however, there are no universal principles suitable for all the cases considering all the above factors. It is pointed out that the selections of optimal working fluids are case-sensitive, which should be carried out in systematic ways (Dong et al., 2020b).

- **how to simultaneously consider waste heat extraction and power generation**

Some previous research works sequentially consider the problems of heat extraction and power generation (Desai and Bandyopadhyay, 2009; Song et al., 2014; Yu et al., 2017a). In the works, the power generation of ORC(s) is firstly maximized by optimizing the architectures, working fluids and operations, then the optimal strategy for extracting waste heat is determined, aiming to minimize the related capital and operating costs. Though such sequential-based methodologies could simplify the solving process of the problems, it is realized that the corresponding solution could be sub-optimal rather than optimum. In some cases, pursuing the maximum power generation could lead to more extra capital cost, overcoming the bonus brought up by power generation and decreasing the gained profit. To this end, it is necessary to consider waste heat extraction and power generation in a holistic way, fully considering the trade-off between costs and profits.

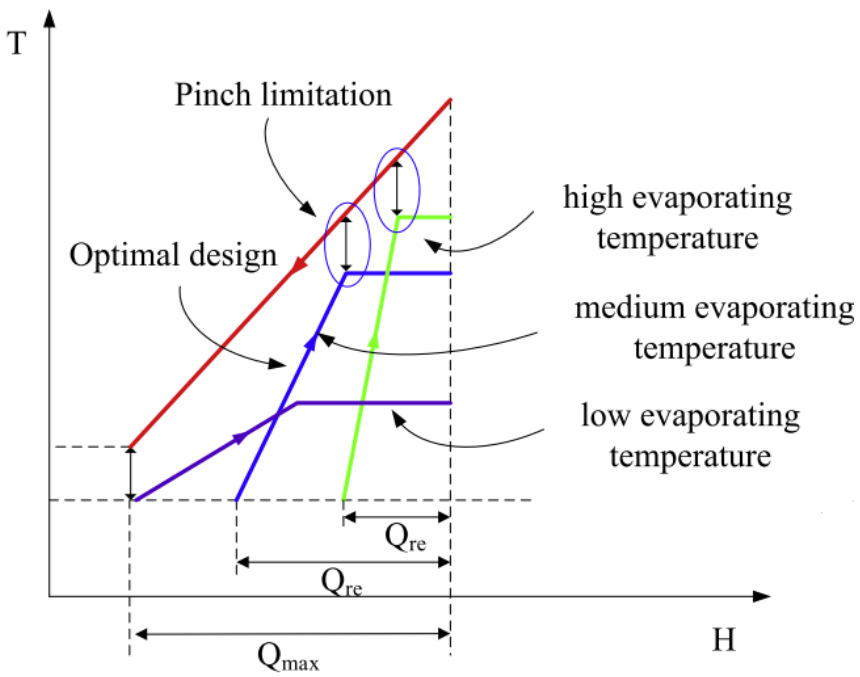

Figure 1.15 The Pinch points created by isothermal boiling processes (Yu et al., 2018)

1.1.4.4 Process Integration of ORCs

To effectively address the related challenges of applying ORCs for recovering industrial waste heat, a concept, namely process integration of ORCs (or ORC integrations), is proposed, of which the objective is: through considering both the aspects of waste heat extraction and ORC power generation, achieving the best trade-off between capital costs, operating costs, and the profit gained from power generation. Based on such objective, for waste heat extraction, ORC integrations can advise the specific strategies and the corresponding designs; for power generation, the optimal operations, architecture sections, and working fluid selections of ORC(s) can be carried out.

Technically, the process integration of ORCs can be achieved by extending the existed PI techniques (either graphical-based or mathematical programming-based). Some representative PI techniques have been briefly introduced in the previous sections of this chapter, while the others will be reviewed in Literature Review.

When dealing with ORC integration problems, no matter developing which type of PI-based techniques, a general strategy of waste heat extraction and power generation should be given in advance so that the graphical representations or the mathematical models can be accordingly established.

In terms of heat extraction, this thesis conceives three different strategic options, i.e., direct heat transfer, indirect heat transfer, and the combination of direct and indirect heat transfers. In the direct heat transfer strategic option, waste heat is directly transferred from its sources to the integrated ORC(s) without using any intermate heat carriers. The illustrative diagram is shown in Figure 1.16. The option of indirect heat transfer regulates that waste heat must be first transferred to intermediate heat carriers (normally hot water) before being transferred to ORC working fluids. The illustrative diagram is exhibited in Figure 1.17. Compared with indirect heat transfer, the main advantage of direct heat transfer is that it can achieve less

approach temperature differences between heat sources and sinks, achieving more power generation with a relatively small heat exchanger area. However, it is pointed out that indirect heat transfer may be preferred in practice due to safety and controllability considerations (Yu et al., 2017b). Except for adopting a single strategy to extract waste heat, the combination of both direct and indirect heat transfer strategies could be more intelligent, of which the diagram is illustrated in Figure 1.18. In modern industrial sites, waste heat sources could be geographically dispersed with different temperatures and supply quantities (Lu et al., 2016); and can be carried by different kinds of heat carriers such as exhausted gas, steam, hot water, process stream, etc., leading to different rates of cleanness. In this case, it is logical to deduce that some industrial waste heat sources may be more suitable to be recovered directly, while others can be gathered by intermediate heat carriers. However, this thesis still cannot provide clarified principles or comprehensive methodologies for applying the combination strategy. This part of work (applying the combination strategy) is left as future work.

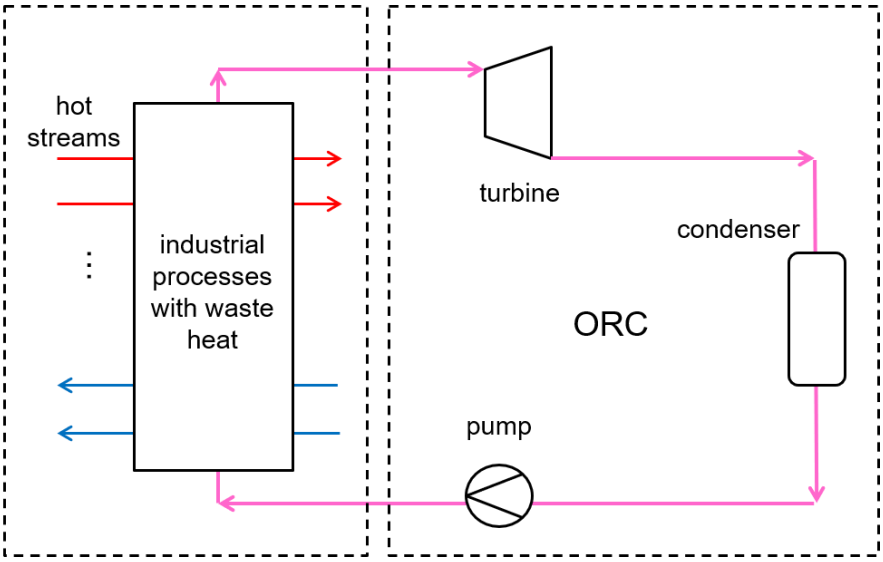

Figure 1.16 The direct heat transfer strategic option

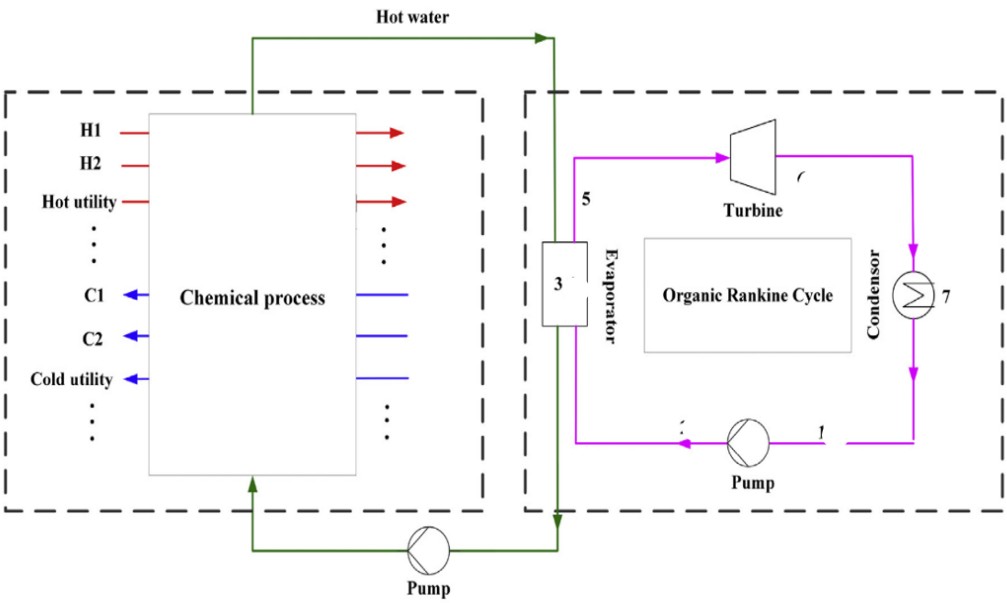

Figure 1.17 The indirect heat transfer strategic option (Yu et al., 2017b)

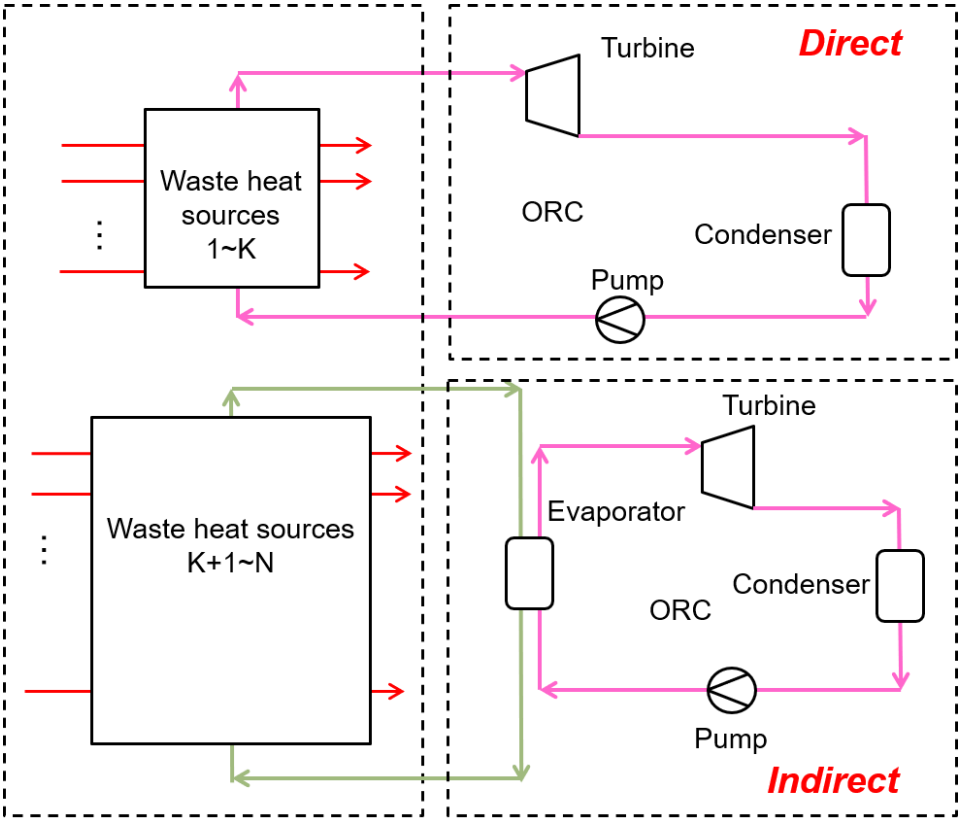

Figure 1.18 The combination of direct and indirect heat transfer

In terms of power generation, one can choose whether to implement a single ORC or multiple ORCs to generate power. Compared with a single ORC, multiple ORCs could have better operating flexibility coping with fluctuated conditions of waste heat sources. For geographically dispersed projects, implementing only a single ORC unit could lead to long-distance pipe construction and more heat losses during the transportations of heat carrier streams (Chen et al., 2016). From the thermodynamic perspective, applying only a single ORC could have a weak thermal match with background heat sources due to the pinch point caused by the isothermal boiling process (Yu et al., 2018), while multiple ORCs could debottleneck the pinch, leading to more power generation. However, it should be realized that applying a multiple-ORCs system could bring more capital costs. The trade-off between costs and profits should be carried out.

Once a general strategy has been determined, it is meaningful to discuss the specific design problems. Depending on the problems, suitable PI-based techniques can then be developed, through which the optimum solutions can be given out.

1.2 Research Problem

With more and more stringent global-wide policies on reducing greenhouse gas emissions, the industry, as one of the major consumers of fossil fuels, has been focusing on improving energy efficiency, expecting to decrease its primary energy consumption and greenhouse gas emissions. From the view of systematic analysis, a proper site-wide integration, including different manufacturing processes as well as the utility systems, could lead to higher overall energy efficiency. However, it is observed that even with a fully integrated industrial site, there are still lots of waste heat worth being exploited to improve the overall energy efficiency further.

When considering recovering industrial waste heat, ORC could be one of the most promising technologies. To implement ORCs in practical fields, a proper integration between ORCs and

background processes should be considered by the project managers so that the best trade-off between capital costs, operating costs, and the profit gained from power generation can be achieved. Through the introductions of the previous sections, it can be realized that the related challenges of ORC integrations include how to generate power efficiently, how to extract waste heat effectively, and how to consider the system in a holistic way.

In terms of power generation, there are different architectures as well as multiple working fluid candidates that can be selected. The selections of ORC architectures and working fluids are case-dependent, which could lead to different energy efficiencies and investment costs. The related challenge is how to select the proper ORC architectures and working fluids for a given project to increase the gained profit. Besides the selections of architectures and working fluids, the operating conditions of ORCs also exert influences on system performance. For most cases, increasing evaporating temperatures or decreasing condensing temperatures could improve the energy efficiencies of ORCs (Yu et al., 2015). However, with the increase (decrease) in evaporating (condensing) temperatures, the approach temperature differences with heat sources (sinks) are decreased, leading to larger heat transfer areas and the corresponding capital costs. To another aspect, with the same working fluid, high evaporating temperatures correspond to high evaporating pressures, which could increase the relevant costs on leakage prevention. Therefore, the related challenge is how to determine the optimal operating conditions of ORCs, gaining the best trade-off between profits and expenses. The two challenges on power generation are correlated with each other. Lots of the previous research efforts (Hipólito-Valencia et al. 2013; Chen et al., 2014; Chen et al., 2016; Dong et al., 2020a) provide methods for integrating ORCs focusing on optimizing the operating conditions, while the multiple choices of working fluids and architectures are neglected. Besides, some previous works (Desai and Bandyopadhyay, 2009; Xi et al., 2013; Chen et al., 2014; Toffolo, 2014; Song et al., 2014; Yu et al., 2017a; Stijepovic et al. 2017) set their goals as to maximize the power generations of ORCs, ignoring the trade-offs between energy and capital costs. In such cases, the calculated optimal working conditions of ORCs could be

deviated, leading to sub-optimal solutions.

In terms of heat extraction, an industrial site could have multiple waste heat sources with different temperatures, heat duties, thermodynamic properties, etc. The related challenge is how to determine which heat sources are worth to be recovered and how to construct the heat exchanger network (HEN) for extracting heat from sources to sinks. Some previous works (Quoilin et al., 2011; Guo et al., 2014; Li et al., 2015; Huang et al., 2010) discuss ORC applications by assuming a homogeneous background heat source, i.e., the heat is available from a single source with a single temperature level.

As different HEN synthesizes could not only result in different capital costs but also influence the working conditions of the downstream ORCs, another challenge is to consider the waste heat extraction and power generation simultaneously. Some previous researchers (Yu et al., 2017a; Yu et al., 2017b; Kermani et al., 2018) address ORC integration problems in sequential ways. They first maximize the power generation of ORCs to determine the optimal working fluids, architectures, and operations, according to which the corresponding HEN synthesizes are then be determined. Furthermore, it is mentioned that there could be different strategic options on waste heat extraction (i.e., direct or indirect heat transfer) and power generation (i.e., single or multiple ORCs), leading to different strategic combinations. It is case-sensitive to determine adopting which type of strategic combination. Most of the previous research discuss ORC integration problems merely considering the strategic combination of direct heat transfer and single ORC, while the feasibilities of applying the other combinations are ignored.

Some of the representative work in the research field of ORC integration is summarized in Table 1.1, which provides an intuitive insight into the progressiveness and insufficient of the proposed methodologies for integrating ORCs.

Table 1.1 The previous work on ORC integration

Articles	Heat extraction strategy	Power generation strategy	HEN synthesis	Auto-architecture selection	Auto-working fluid selection	Solution strategy	Mathematical programming	Objective(s)
Desai and Bandyopadhyay (2009)	Direct	Single ORC	N	N	N	Heuristically	/	Max. power output
Hipólito-Valencia et al. (2013)	Direct	Single ORC	Y	N	N	Model-based	MINLP (simultaneously)	Min. total cost
Chen et al. (2014)	Direct	Single ORC	Y	N	N	Model-based	MINLP (sequentially)	Max. power output
Song et al. (2014)	Direct	Double ORCs	N	N	N	Model-based	/	Max. power output
Yu et al. (2017a)	Indirect	Single ORC	Y	N	N	Model-based	NLP+MILP (sequentially)	Min. total cost
Yu et al. (2017b)	Direct	Single ORC	Y	N	N	Model-based	NLP (sequentially)	Min. total cost
Kermani et al. (2018)	Direct	Single ORC	Y	N	Y	Model-based	GA+MILP (simultaneously)	Min. total cost
Elsido et al. (2019)	Direct	Single ORC	Y	N	N	Model-based	MILP+NLP (sequentially)	Min. total cost
Dong et al. (2020)	Direct	Single ORC	N	N	Y	Model-based	NLP (simultaneously)	Min. total cost
Huang et al. (2020)	Direct	Single ORC	Y	N	N	Model-based	MINLP	Min. total cost

From Table 1.1, it can be found that in the field of ORC integration, some insufficiencies still exist, which are:

1. The automatic selection of the optimal working fluids for the integrated ORCs is rarely discussed.
2. The automatic selection of the optimal architectures for the integrated ORCs is not fully addressed.
3. Even though there are several advanced methodologies developed for network synthesis of waste heat extraction, setting the optimization objective as minimizing total annualized cost rather than maximizing power generation could be more practical.
4. The strategic options of implementing more than one ORC working unit and/or adopting intermediate heat carriers to transport waste heat are rarely discussed.

1.3 Research Objective

This work aims to develop a series of methodologies of ORC integration, addressing the open problems mentioned in the last section. To this end, the main contribution of this work will be:

1. Develop a methodology to discuss the techno-economic feasibility of integrating more than one ORC into an industrial site for waste heat recovery.
2. Develop methodologies to address different strategic options (i.e., direct and indirect) of waste heat extraction.
3. Develop a methodology to achieve the optimal working fluid selection for each integrated ORC.
4. The methodologies should set minimizing total annualized cost rather than maximizing power output as the optimization goal.

The methodologies are mainly based on mathematical programming-based PI techniques, while some graphical-based analyses are also adopted. To achieve such goal, a series of sub-objectives are targeted, corresponding to the milestones of this PhD project, which can be

specified as follows:

1. Establish the mathematical model of an ORC, which can accurately evaluate the amount of generated power of ORC(s) and allow for selecting different working fluids. The possibility of adopting more than one ORC unit (i.e., multiple ORCs) to improve total power generation will be considered.
2. Develop mathematical optimization frameworks to represent the extraction of waste heat. Note that the different heat extraction strategic options (i.e., indirect and direct heat transfer) will be considered.
3. Integrate the ORC model into the developed frameworks to capture overall capital-energy trade-offs.
4. Develop effective optimization procedures, which could include both deterministic algorithms and stochastic algorithms, to solve the developed models.

1.4 Thesis Outline

This thesis contains seven chapters with sections and subsections providing a consistent orientation for integrating ORCs into process sites. The “Alternative format” of the University of Manchester is used, incorporating papers to be published. A list of appended papers is provided in Section 1.5. The outline is summarized in Table 1.2.

Table 1.2 Thesis outline

Chapter	Description
Chapter 2: Literature Review	The previous work related to PI techniques as well as ORCs for industrial waste heat recovery is reviewed — this literature review supplements the reviews provided in the appended papers.

Chapter 3: Indirect integration of ORCs	Chapter 3 contains one journal paper, which provides a novel systematic analysis method for integrating ORCs (single and multiple) into total sites, where an indirect heat transfer strategy is adopted.
Chapter 4: Direct integration of ORCs	Chapter 4 contains one journal paper, which provides a novel systematic analysis method for integrating ORCs (single and multiple) into total sites, where a direct heat transfer strategy is adopted.
Chapter 5: Working fluid selections for integrating ORCs	A journal paper is appended in Chapter 5, which provides a method that can simultaneously consider the optimal working fluid selection of each ORC unit when integrating ORCs.
Chapter 6: Conclusions and future work	Chapter 6 presents key findings, limitations of the present work and recommendations for future work

1.5 Appended Papers

This thesis is based on the work contained in the following papers (all the papers have been submitted or prepared to be submitted for publication in peer-reviewed journals):

Publication 1. Chu Z., Zhang N., Smith R., Modelling and Integration of Multi-Parallel Organic Rankine Cycles into total site, Energy (under review)

Publication 2. Chu Z., Zhang N., Smith R., The Opportunities of Integrating Multi-parallel

ORCs into Total Site for Waste Heat Recovery, Applied Thermal Energy (ready for submitting)

Publication 3. Chu Z., Zhang N., Smith R., Automatic Working Fluid Selection for Integrating Multi-Parallel ORCs into Total Site, Industrial & Engineering Chemical Research (under review)

Chapter 2: Literature Review

This chapter contains a review of pertinent literature relating to the PI technologies for energy efficiency improvement and the ORC applications for waste heat recovery, aiming to supplement the reviews provided in the publications presented in Chapter 3, 4, and 5.

2.1 Overview on PI Technologies

PI technologies have been raised from the early 1970s, of which the purposes are mainly for process heat integration. The development of PI technologies has accelerated over the years, owing to which the applications of PI technologies have been extended from heat integration to water integration, hydrogen integration, process optimization, etc. Note that this chapter will mainly review the PI technologies related to heat integration, as they are the most relevant to the integration of ORCs for waste heat recovery. As for the other developments of PI technologies, readers are referred to Smith (2005) if interested.

It has been introduced that the existing PI technologies could be classified into two categories, i.e., graphical (heuristical)-based technologies and mathematical programming-based technologies, of which the related literature will be reviewed separately.

2.1.1 Graphical (Heuristical)-Based Technologies

One of the first works addressing process heat integration could be proposed by Hohmann (1971) in his PhD thesis at the University of Southern California, USA. In the thesis, a method of Feasibility Table is developed, which is regarded as the first rigorous way to target the minimum utility consumption ahead of design (Gundepsen and Naess, 1988). Hohmann (1971)

also proposed an ‘N-1’ principle, which can target the minimum number of heat exchangers for synthesizing a HEN. Besides, for targeting the minimum heat transfer area, guidance to the splitting and mixing of streams was provided. Ponton and Donaldson (1974) came up with a heuristical principle for matching the heat transfers between hot and cold process streams. It was advised that the hot stream with the highest supply temperature should be matched with the cold stream with the highest target temperature. Huang and Elshout (1976) were regarded as the first ones who invented and applied the ‘Composite Curves’ to represent the potential of heat recovery between hot and cold process streams. Wells and Hodgkinson (1977) considered general situations of process synthesizes and presented a list of heuristic rules as the guideline of grassroots designs. In 1978, Linnhoff and Flower (1978) presented a thermodynamic-oriented method to synthesize HENs. In the method, a concept, namely Temperature Intervals, is proposed, according to which a HEN synthesis can be carried out sequentially from high to low temperatures. Another useful tool, namely ‘Problem Table’, is adopted in the method, which gives a fast way to calculate the minimum usage of cold and hot utilities.

In the end of the 1970s, a concept of ‘Heat Recovery Pinch’ was proposed by researchers, representing the bottlenecks for further heat integrations and thus energy savings (Huang and Elshout, 1976; Umeda et al. 1979; Linnhoff et al. 1979). Based on the ‘Heat Recovery Pinch’, Linnhoff found that the excess utility consumption of industrial processes can be related to the cross-pinch heat flows, such as process to process heat transfers, heating below and cooling above the pinch. In the early 1980s, Linnhoff and coworkers have further developed the ‘Heat Recovery Pinch’ concept into a complete methodology, i.e., the well-known ‘Pinch Analysis’, which has been wildly applied for addressing several aspects of process design problems (Gundepsen and Naess, 1988).

In the "User Guide" drafted by Linnhoff et al. (1982), an approach, namely the ‘Grand Composite Curve’, is introduced, which offers intuitive graphical representations of heat flows

vs temperatures. The applications of the 'Grand Composite Curve' include utility targeting, the optimal selection of utilities, process cogeneration, etc. Based on 'Pinch Analysis', Linnhoff and Hindmarsh (1983) developed a novel method for the design of HENs. The method starts the design of a HEN at its pinch location, separating a HEN synthesis problem into two or more remaining sub-problems. Compared with the designs started at the hot sides (such as the method proposed by Linnhoff and Flower (1978)), the pinch-located designs can avoid cross-pinch heat transfers. However, the method cannot offer a comprehensive consideration of the trade-off between energy and capital costs.

When considering process heat integration problems, heat transfer area and the unit number of heat exchangers could be the main factors related to capital costs. Several pieces of literature (Nishida et al., 1981; Townsend and Linnhoff, 1983) have indicated that, for most cases, arranging vertical heat transfers between hot and cold composite curves could lead to near-minimum heat transfer area. Nishida et al. (1981) assumed that the heat transfer coefficients of all process streams are equal, while in Townsend and Linnhoff (1984), the individual film transfer coefficients of process streams are considered. Adopting the strategy of vertical heat transfers means that the stream splitting and mixing in each interval should be considered, of which the corresponding network may involve a large number of splits and heat exchangers (Gundepsen and Naess, 1988). Such kind of strategies of HEN synthesis was named 'Spaghetti Design'. However, even though it is proved that vertical heat transfers can usually lead to a minimum or near-minimum total heat transfer area, as explained by Ahmad (1985) and Tjoe and Linnhoff (1986), there are some special cases in which the minimum heat transfer area could be gained by criss-cross heat transfers, as illustrated in Figure 2.1.

With similar total heat transfer area, the network design with fewer units of heat exchangers could be preferred. One of the first targeting methods for minimizing the unit number of heat exchangers is the 'N-1' rule introduced by Hohmann (1971), where N indicates the total number of process and utility streams. Later, Linnhoff et al. (1979) extended the 'N-1' rule by

proposing an 'N-S+L' rule to target the minimum unit number, which takes the number of subsystems (S) and loops (L) of a network into account. Wood et al. (1985) discussed the necessities of importing stream splitting, mixing and bypassing for network designs to reduce the number of units. Based on the concept of 'Heat Recovery Pinch', Linnhoff and Turner (1981) considered minimizing the number of units in the cases of maximum energy recovery. Ahmad (1985), Ahmad et al. (1988) emphasized that the minimum number of heat exchanger units should be considered as a part of the trade-offs between energy and capital costs.

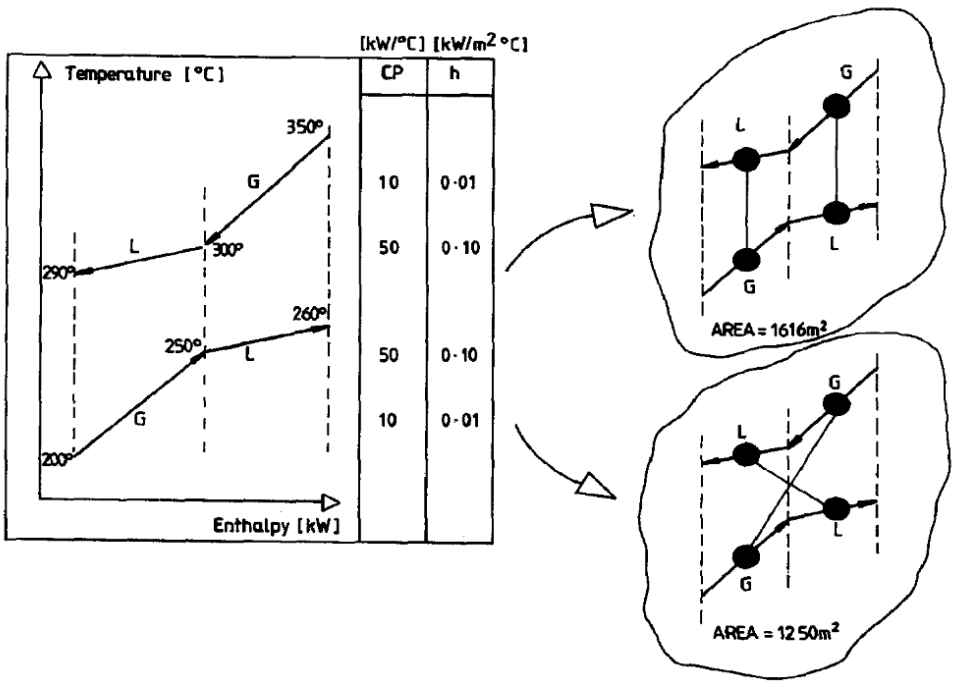

Figure 2.1 Vertical heat transfer vs criss-cross arrangement (Linnhoff and Ahmad, 1990)

In the late 1980s and early 1990s, researchers have realized the importance of simultaneously considering the targets of energy conservation and the related capital costs. Ahmad (1985), conceived that the minimum approach temperature could be a significant indicator that reflects the total cost of HENs. They developed methods or principles to pre-determine the optimal values of minimum approach temperatures, leading to near-minimum cost networks. Linnhoff and Ahmad (1990) declared that the sequential ways of process heat integration, in which a minimum-energy network is first identified, then to minimize the relevant costs, could always

lead to near-optimal solutions rather than global optimists. From this perspective, they developed a procedure for targeting and design of HENs with objectives of optimum total annual cost, which simultaneously considered the factors of energy conservation, heat transfer area, and unit number.

Besides considering the heat integration within a stand-alone manufacturing process, some researchers have paid attention to a site-wide context. For a site-wide heat integration, the utility system could be an essential intermediate responsible for transferring the heat between processes. One of the first strategies for site-wide heat integration, namely the 'Heat Path Diagram', was proposed by Westerberg (1983). In the strategy, each site process is divided by its pinch point into a sink and source part. The divided sinks and sources, as well as the site utility system, are positioned according to their temperatures, through which further integration between the processes can be considered. Steinmetz and Chaney (1985) proposed a 'Heat and Power Distribution Diagram', which can provide an intuitive understanding of the interconnections between site processes and the utility system, as shown in Figure 2.2. As a screening tool, the diagram can incorporate with the 'Pinch Analysis' method, establishing reduction goals for every single process so that the minimum utility consumption of each steam distribution level can be targeted. Linnhoff and Eastwood (1987) confirmed the effectiveness of the diagram in achieving utility savings. However, it was also pointed out by Raissi (1994) that the representation of the diagram is limited to existing configurations, lack of flexibility, and the optimal pressures of the stream mains are not addressed. In Dhole and Linnhoff (1993), a graphical-based tool named 'Site Source-Sink Profile (SSSP)' is developed, which can determine the targets of steam/power generations and fuel consumptions of site utility systems, as shown in Figure 2.3. In the figure, the potential of steam generation from site manufacturing processes can be graphically targeted. The process-generated steam is sent to the site utility system (i.e., steam means), compensating the boiler-generated steam, and is used for process heating.

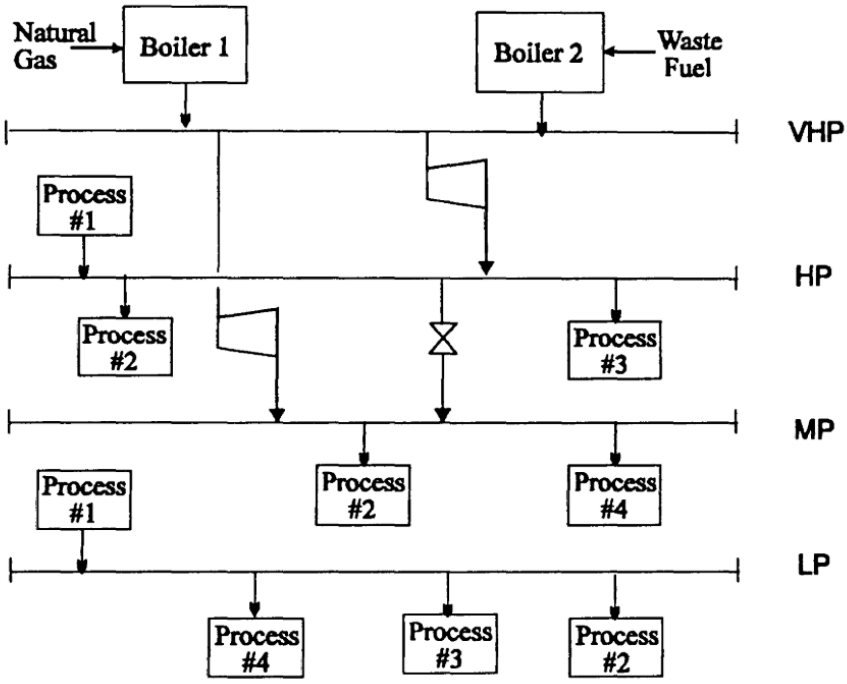

Figure 2.2 The heat and power distribution diagram (Steinmetz and Chaney, 1985)

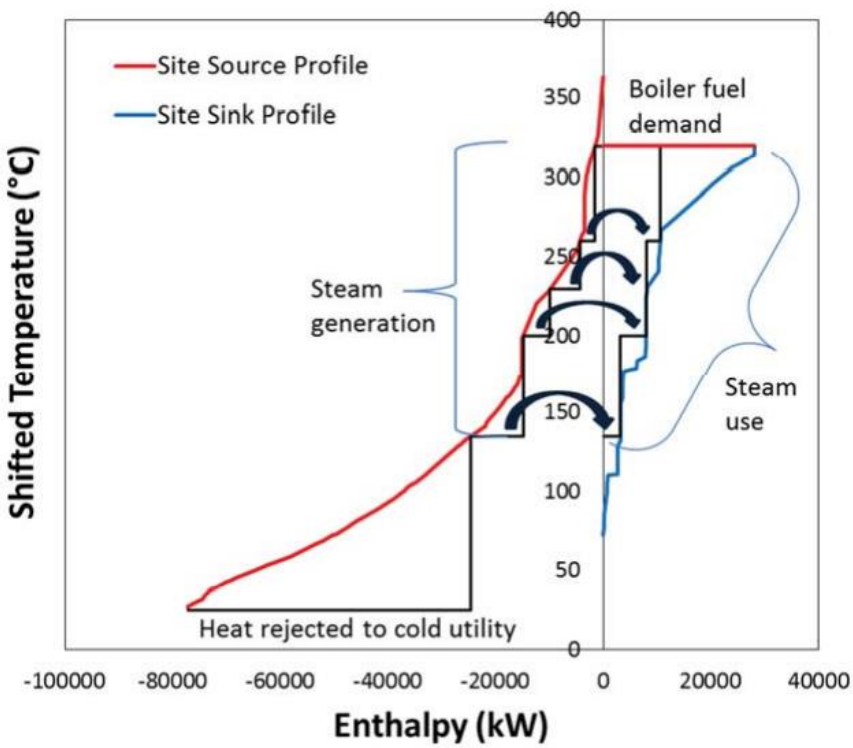

Figure 2.3 A site source-sink profile (Oluleye, 2016)

The followed works, such as Raissi (1994) and Klemes et al. (1997), further extended the work of Dhole and Linnhoff (1993) by proposing a graphical-based tool named the 'Site Utility Grand Composite Curve (SUGCC)', as shown in Figure 2.4. The SUGCC gives a clear representation of site steam expansion levels.

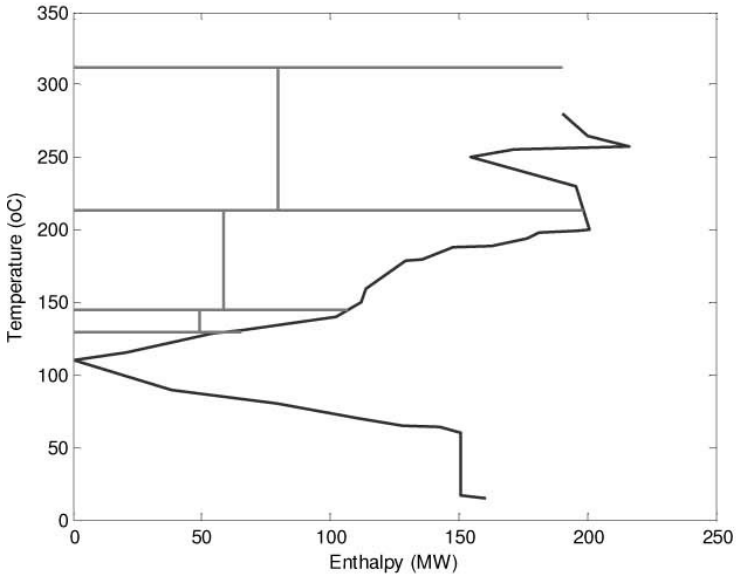

Figure 2.4 A Site Utility Grand Composite Curve (SUGCC) (Kapil et al., 2011)

2.1.2 Mathematical Programming-Based Technologies

Graphical-based tools can provide physical insights for understanding the nature of heat integration. However, Grossmann and Papoulias (1983) conceived that graphical-based tools could not guarantee optimality, as their applications are constrained by human experiences. Therefore, besides the development of graphical (or heuristical)-based technologies, mathematical programming-based technologies were also proposed, in which heat integration problems are transformed to mathematical models and are solved by diverse mathematical programming methods. The established mathematical models can be subject to deserve objective functions such as maximum energy conservation, minimum greenhouse gases emissions, minimum total annualized cost, etc., or using multiple objectives (Varbanov et al.,

2004).

It can be realized that there are two main parts of applying mathematical programming-based technologies, i.e., modelling and optimization. This review section will mainly introduce the proposed methods for establishing models, while the development of optimization algorithms is omitted. If interested, readers can find more details in Furman and Sahinidis (2002), Klemes et al. (2013), and Smith (2015).

One of the first mathematical programming-based methods is proposed by Kesler and Parker (1969), who divided each process hot/cold streams into several heat duty elements with equal quantities and arranged the matches between hot and cold elements, leading to a combinatorial problem. Kobayashi et al. (1971) and Cena et al. (1977) followed this technique route of model establishment but gave their own contributions. Kobayashi et al. (1971) extended the previous work by considering stream splitting and looping, while Cena et al. (1977) allowed for constraints and multiple utilities.

Cerda et al. (1983) introduced an analytical representation for dealing with HEN synthesis problems, which can consider network configurations include not only parallel splitting and cyclic but also constrained matches. In their work, first, the minimum utility consumption is targeted; then, all the process streams are partitioned into several temperature intervals, and the corresponding HEN synthesis problem is modelled as a transportation problem. Such a transportation problem considers all possible routes for transporting heat from hot streams to cold streams, leading to a linear programming (LP) problem. It was pointed out that the minimum unit number of heat exchangers can be involved by reformulating the LP problem as a mixed-integer linear programming (MILP) problem. Papoulias and Grossmann (1983a) formulated HEN synthesis problems by adopting transshipment models, which is a variation of the transportation problem mentioned above. The main difference between transshipment and transportation models is that a transportation model seeks to determine the optimum

network where commodities (i.e., heat) are directly transported from suppliers (i.e., heat sources) to destinations (i.e., heat sinks), while a transshipment model considers using warehouses (i.e., temperature intervals) as intermediates for shipping commodities. Compared with transportation model-based methods, transshipment model-based methods also allow for targeting the minimum utility cost and the minimum number of units; besides, they can be incorporated with process models so that heat integration can be performed simultaneously with process optimization (Papoulias and Grossmann,1983b). However, it can be realized that the capital cost of heat exchangers is not taken into account in both of the methods of model establishment, which could lead to sub-optimal solutions of HEN synthesis.

Duran and Grossmann (1986) proposed a method for handling the heat integration of a manufacturing process, which allow for considering process streams as variables rather than constant. The advantage of this method is that it allows for the simultaneous optimization and heat integration of process flow sheets, offering the optimal operating conditions (e.g., mass flowrate, supply and target temperatures) of process streams. The main idea of this method is to establish a mathematical model which can automatically locate the pinch points for given minimum approach temperatures (even with variable temperatures and mass flowrates of process streams). As soon as pinch points are located, the corresponding minimum utility consumptions can be determined. The established model leads to non-linear programming (NLP). This method has been successfully applied for decades (Klemeš and Kravanja, 2013); however, it considers process heat integrations only in the aspect of energy conservation, while the related capital costs are not taken into account.

In the early 1980s, attempts in mathematical programming-based heat integrations were more about developing models for predicting the minimum consumption of utilities and the minimum number of units (Klemeš and Kravanja, 2013). For more advanced achievements, Floudas et al. (1986) developed a method that can automatically generate the optimal structure of a HEN, featuring the minimum total investment cost. The method consists of several sequential steps.

In the first step, the LP-transshipment model proposed by Papoulias and Grossmann (1983b) is firstly applied to target the minimum utility consumption. In the second step, according to the minimum utility consumption, the MILP-transshipment model (Papoulias and Grossmann,1983b) is adopted to determine the corresponding minimum number of units. In the third step, a superstructure, which can represent many different configurations of possible network structure, is established. In the next step, based on the superstructure, the corresponding mathematical model can be established, leading to non-linear programming (NLP). At last, through solving the NLP, the final network configuration that is subjected to the minimum investment cost can be determined. The illustrative diagram of this sequential method is shown in Figure 2.5.

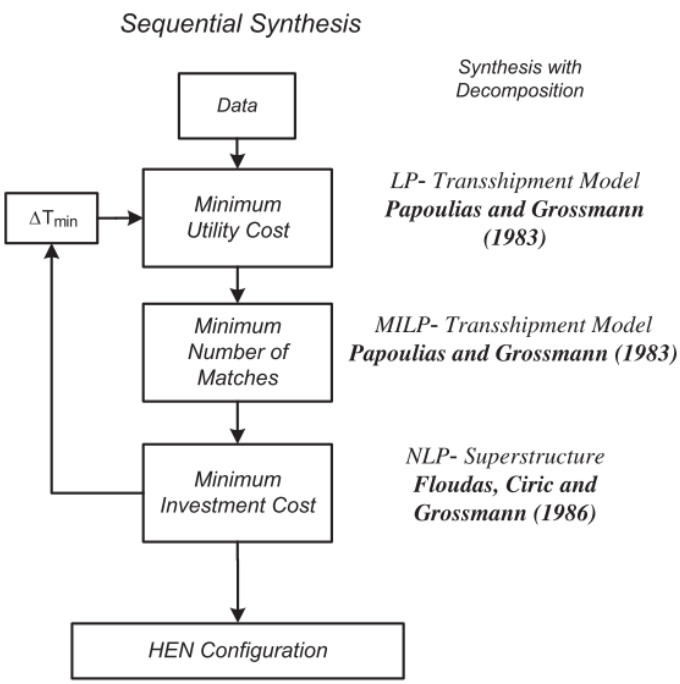

Figure 2.5 The illustrative diagram of the proposed sequential method (Escobar and Trierweiler, 2013)

The main advantage of the sequential method for HEN synthesis is that they separate the original single-task problem (i.e., minimum total cost) into several sub-problems that can be treated by much easier approaches (Escobar and Trierweiler, 2013). However, it is also

pointed out that the sequential methods could lead to sub-optimal solutions since the trade-offs amongst the utility consumption, the number of units, and the minimum investment cost may not be taken into account appropriately (Escobar and Trierweiler, 2013). From this perspective, researchers in the late 1980s and early 1990s paid attention to simultaneous methods.

The most representative simultaneous approaches for process heat integration could be Yee and Grossmann (1990) and Ciric and Floudas (1991). Yee and Grossmann (1990) proposed a general superstructure to represent the possibilities of the selections and matches of heat transfers between hot and cold process streams. It was declared by Yee and Grossmann (1990) that the proposed representation enables simultaneous considerations of multiple design factors, avoiding the limitations of sequential analysis methods. The establishment of the superstructure is illustrated in Figure 2.6. In the figure, there are two cold streams and two hot streams. The overall superstructure is divided into stages, of which the number is normally the same as the maximum number of the cold or hot streams (in this example, two stages are divided). For each stage, each of the participated streams is split into paralleled sub-streams, of which the number should be equal to the number of the streams on the opposite side. Each sub-stream is directed to a heat exchanger so that each potential match of heat transfer can be represented. At each stage, the split sub-streams are iso-thermally mixed at the end, but the corresponding outlet temperatures are treated as variables. Based on such representation, the established mathematical model could lead to mixed-integer non-linear programming (MINLP), through solving which the objective of minimum total annualized cost can be addressed in one step. Ciric and Floudas (1991) presented another simultaneous method for dealing with HEN synthesis problems. The method adopted the hyperstructure proposed by Floudas and Ciric (1989) to optimize the configuration of HEN, and a modified version of the transshipment model of Papoulias and Grossmann (1983a, b) to select heat loads. Compared with the superstructure-based model proposed by Yee and Grossmann (1990), this hyperstructure-based model allows for not only stream splitting and mixing but also bypassing,

leading to a more complex but comprehensive configuration of HEN.

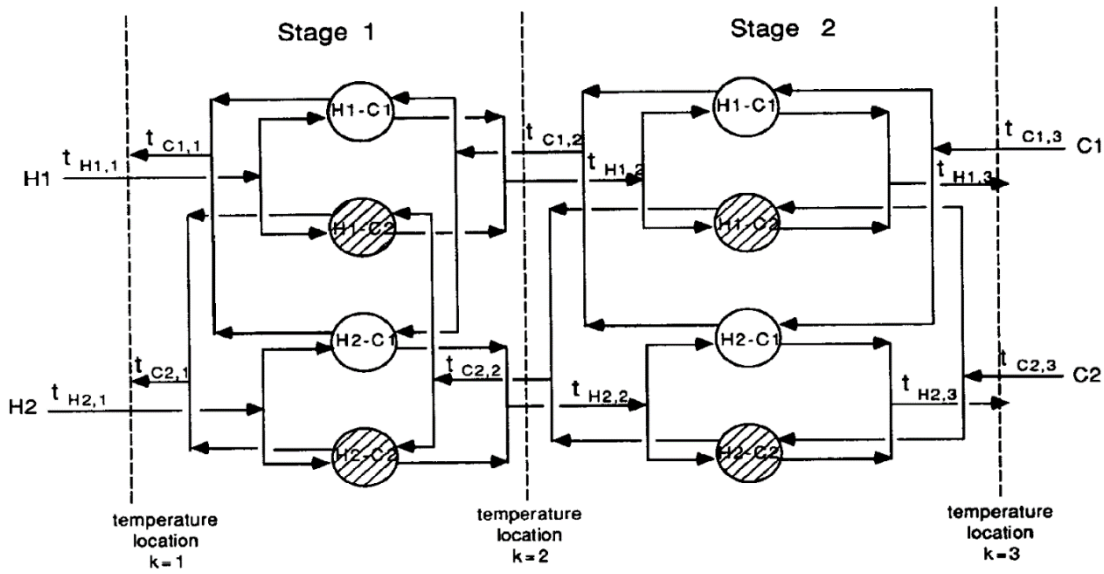

Figure 2.6 The representation of the proposed superstructure (Yee and Grossmann, 1990)

Extended from Yee and Grossmann (1990), Soršak and Kravanja (1999) merged a detailed design model of heat exchangers into the superstructure-based model of Yee and Grossmann (1990) in order to accurately evaluate the pressure drops and heat transfer coefficients. Their work aims to obtain feasible networks that have the optimal trade-offs between energy conservation, capital investment, and the power consumption of pumps. Similarly, Mizutani et al. (2003) included a rigorous model of shell-and-tube heat exchangers into the HEN synthesis model of Yee and Grossmann (1990). Besides considering network configuration, heat exchanger area, heat duties, pumping and utility expenses, their optimization model also takes into account several detailed design variables of heat exchangers, including the number of tubes and passes, internal and external tube diameters, tube arrangement pattern, the number of baffles, head type, and fluid allocation. Nemet et al. (2012) emphasized that the full lifetime of HENs and future utility prices should be considered for process heat integration. Thus, they developed deterministic and stochastic MINLP models for multi-period HEN synthesizes, where utility prices are forecasted as a function of the project's lifetime.

Except for dealing with the heat integration within a manufacturing process, some mathematical programming-based methods were also developed for the heat integration of a total site. Shang and Kokossis (2004) presented a mathematical programming-based approach to optimize the steam levels of a total site utility system. They developed a transshipment network to represent the heat flows of a total site., of which the corresponding model leads to an MINLP problem. The major decision variables are temperatures of steam levels, overall fuel requirement, the cogeneration potential and cooling utility demand. Zhao et al. (2015) pointed out that a typical refinery consists of a manufacturing system and the utility system, and the conventional optimization procedure of a total site is to consider each of the systems hierarchically. To meet the demand for higher profit and energy utilization, it is important to integrate the two systems simultaneously. However, they observed that adopting mathematical programming-based methods to solve a total site integration could be imperative but challenging, as the corresponding models could lead to MINLP problems with a large number of discrete variables, resulting in inconsistency between solution quality and time. To this point, they developed a solution strategy based on heuristics, in which the overall model is decomposed into a MILP and an NLP model, and the two models are then solved iteratively. They used a case study from a real refinery plant to demonstrate the effectiveness of the strategy. Martelli et al. (2017) proposed a novel approach for simultaneously addressing the synthesis of a site-wide HEN and the optimization of the utility system. For an industrial site, there could be a set of providers of the utility demand and multiple hot/cold streams to be cooled down/heated up. Their goal is to determine the optimal selection, arrangement, and design of a HEN and the corresponding utility providers, leading to the minimum total annualized cost. For representing a HEN, the superstructure proposed by Yee and Grossmann (1990) is adopted; as for the utility system, a novel superstructure, namely the 'Ad Hoc Superstructure', is developed. An MINLP model is established to formulate the superstructures, and a sequential optimization algorithm is specifically developed for solving the MINLP model.

2.2 Overview on ORCs for Waste Heat Recovery

When considering applying ORCs, there are multiple architectures to be selected, leading to different thermal efficiencies; besides the architecture selections, different working fluids could also exert significant influences on thermal efficiencies. Due to the multiple choices of architectures and working fluids and the designs of HENs for extracting waste heat, there are complexities and challenges of implementing ORCs into industrial sites, which have been introduced in the previous chapter. In this section, the previous publications addressing the architecture selections, working fluid selections, and integration of ORCs for recovering industrial waste heat are overviewed, aiming to provide insights into the progressions of current research.

2.2.1 Architecture Selections of ORCs

According to the previous introductions, except for the basic architecture, normally, there could be six different designs of ORCs, including Superheated Cycles, Regenerative Cycles, Reheat Cycles, Transcritical Cycles, Bleeding Cycles, and Cascaded Cycles.

- **Superheated Cycles**

Hung et al. (1997) found out that the thermal efficiencies of ORCs increase nearly linearly with the turbine-inlet temperature for wet working fluids like water, ammonia, etc. However, unlike wet working fluids, dry fluids could present decreased trends in ORC thermal efficiency at their superheated regions. According to such results, they advised that dry working fluids may be better to be operated along the saturation curve rather than superheated. Yu et al. (2015) also did not recommend the superheating of dry working fluids. They declared that the superheating of dry working fluids may not obviously increase the thermal efficiency of an ORC but could lead to increases in the investment costs of heat exchangers. Other research efforts such as Hu et al. (2017) investigated the effects of superheating working fluids on the

stability of an ORC system with different types of heat exchangers. According to the test results, they confirmed the correlations between superheating operations and the operation stability of ORC systems. When using R245fa as the working fluid, with a superheat of (or below)1.8℃, they found that instability could be occurred in plate evaporators due to liquid entrainment. As for shell-and-tube evaporators, the superheat could be as low as 0.2℃ without unstable oscillations.

- **Cycles with Recuperators**

Several authors (Saleh et al., 2007; Chen et al., 2010) have suggested the implementation of an internal heat exchanger to reuse the heat of turbine exhaust gas to preheat the evaporating working fluid. Saleh et al. (2007) declared that, without considering the thermal match with background heat sources, implementing an internal heat exchanger could essentially increase the thermal efficiency of an ORC. Lecompte et al. (2015) illustrated that, in order to implement an internal heat exchanger, a superheated state is necessary at the turbine outlet.

If considering the thermal match with heat sources, Dai et al. (2009) argued that if the target temperatures of heat sources are not limited (i.e., can be as low as the ambient temperature), the net power output of an ORC may not be increased by adding an internal heat exchanger. Zhang et al. (2018) investigated the effects of adopting an internal heat exchanger on the thermo-economic performance of an ORC. In their report, the working fluid candidates considered are R161, R1234ze, R152a, cyclopentane, cyclopropane, butane, R123, heptane, and cyclohexane. They found out that, under a lower heat source temperature and load, the implementation of an internal heat exchanger cannot guarantee a higher power generation but always a worse economic performance than a basic ORC. However, they also indicated that, with the increases of heat source temperatures, the ORC with an internal heat exchanger could have a possibility to achieve better thermo-economic performance. In summary, the feasibility of adopting an internal heat exchanger strongly depends on the type of working fluid and the profile of heat sources.

- **Reheat Cycles**

DiGenova et al. (2013) realized that a total processing site could normally have multiple waste heat sources with different temperature levels and duties, resulting in a composite heat source with a complex temperature-enthalpy profile. Therefore, they emphasized the necessity of considering different types of ORC architectures to obtain the best thermal match with heat sources. One of the architectures they customized is the 'Reheat Cycles'. They adopted the waste heat sources from a Fischer Tropsch reactor and its associated processes as the demonstration case. The results showed that a reheat cycle could have a better thermal match with the heat sources, leading to higher energy conversion. However, it was also pointed out that the low heat transfer coefficient caused by the vapour phase of a reheating process could lead to a larger heat transfer area. In their work, the trade-off between capital cost and energy conservation is not discussed. Hemadri and Subbarao (2021) integrated a reheat ORC into a gas turbine cycle to recover the low-temperature exhaust heat from the gas turbine. They considered cyclopentane, hexane, and benzene as the working fluid candidates and found that a reheat ORC could achieve an increased net power output than a basic ORC. They also optimized the operating conditions (such as reheat pressure ratio, evaporating temperature/pressure, and condensing temperature/pressure) of a reheat ORC integrated with different gas turbine cycles subjected to the maximum power output.

Even though several studies have proved that reheat cycles can achieve higher power generations than the basic ones, it should be noticed that the implementation of reheat cycles is case-dependent. On the one hand, the performances of reheat cycles are highly dependent on the temperature-enthalpy profiles of heat sources; on the other hand, the trade-off between extra capital cost and power generation should be considered.

- **Transcritical Cycles**

In terms of net power output, Schuster and Karellas (2010) compared the difference between a basic ORC and an ORC with supercritical working conditions. According to their

demonstrations, for an ORC itself, the supercritical working conditions do not always lead to a higher thermal efficiency, which is dependent on the working fluid selections; however, when considering the integration with heat sources, the supercritical working conditions of working fluids could achieve better temperature matches with heat sources, leading to higher rates of heat recovery. The extra investment costs brought up by transcritical operations are not discussed in their work. Xu et al. (2016) compared the net power outputs of a basic (subcritical) ORC and a transcritical ORC for recovering the waste heat from flue gas with inlet temperatures of 150-250℃. They found that if the heat source temperature is about 25-40℃ higher than the working fluid's critical temperature, adopting supercritical working conditions instead of subcritical working conditions could achieve the maximum power output. However, again, the trade-off between capital cost and power generation is not addressed in their work.

- **Bleeding Cycles**

Desai and Bandyopadhyay (2009) integrated an ORC with multiple heat sources, considering multiple choices of working fluids and different ORC architectures. They illustrated that the choice of working fluid and architecture for appropriate integration depends on the heat rejection profile of the background heat sources. According to the results of the integration, they concluded that when background heat sources end up with high temperatures, it is possible to implement different cycle modifications like turbine bleeding to improve the power generation of ORC; otherwise, if the target temperatures of background heat sources are close to the ambient temperature, different modifications are not recommended, as they could finally lead to higher heat rejection and thereby, do not improve the power output. Desai and Bandyopadhyay (2009) have provided selection criteria on two modified ORC architectures (the Bleeding Cycles and Cycles with Recuperators) subjected to the maximum power output, while the economic performances of the different architectures were not discussed. Meinel et al. (2014) compared the thermodynamic and economic performances of a basic ORC, a bleeding ORC and an ORC with a recuperator. The heat source is configured as the waste heat from an internal combustion engine of an existing biomass digestion plant, of which the

minimum target temperature is regulated to be above 180℃. It is found that, due to the high temperature of heat sources, the bleeding ORC can achieve both a better thermodynamic (higher power output, better match of the temperature profiles) and economic (lower specific investment costs, higher sales) performance.

- **Cascaded cycles**

In a cascaded configuration, several ORCs are operated in series with multiple evaporation temperatures. The benefit of arranging the cascaded configurations is that it allows different working fluid selection and mass flowrate for each ORC, which could lead to a better thermal match with the temperature-enthalpy profile of the background heat sources. Li et al. (2015) used the first and second law of thermodynamic to analyze the thermal and exergy efficiency of a two-cascaded ORC. The corresponding background heat source is configured as a strand of hot water with several temperature levels (from 95℃ to 150℃). The analysis results showed that the two-cascaded ORC could obtain higher power output than a basic ORC for all the temperature levels. For an ORC itself, the basic ORC was observed to have the highest thermal efficiency (i.e., the highest rate of power generation from the heat absorbed); however, if accounting for the rate of heat recovery from the background heat source, the basic ORC has a higher ratio of exergy loss due to the weak thermal match.

In summary, the primary purposes of developing different architectures of ORCs are to improve the thermal efficiencies of ORC units or enhance the thermal matches with heat sources. It should be realized that the selections of ORC architectures are case-dependent, which could be affected by the temperature-enthalpy profile of background heat sources, and the trade-offs between the extra investments and the profits brought up by power generation should be considered.

2.2.2 Working Fluid Selections of ORCs

There are thousands of pure substances that can be selected as the working fluids of ORCs, which include hydrocarbons, aromatic hydrocarbons, perfluorocarbons, alcohols and siloxanes (Oluleye, 2016). Besides, zeotropic mixtures can also be used as working fluids. Different selections of working fluids could not only exert different influences on the thermal efficiencies of ORCs, thermal match with heat sources, leading to different power generations, but also have impacts on operating costs, investment costs, and the environment.

For selecting pure working fluids, He et al. (2012) developed a mathematical model to determine the optimal evaporation temperatures of 22 different organic compounds when operating with a basic ORC, aiming to achieve the maximum power output. A single strand of waste heat stream with an inlet temperature of 150℃ and an unlimited outlet temperature is configured as the heat source. The results showed that the working fluids whose critical temperatures approach the supply temperature of the heat source (150℃) could produce larger net power outputs. Under the given conditions of the background heat source, they recommended selecting R114, R245fa, R123, R601a, n-pentane, R141b and R113 as the potential candidates of ORC working fluids. Long et al. (2014) proposed two concepts, namely 'internal exergy efficiency' and 'external exergy efficiency', to evaluate the exergy efficiency of a stand-alone ORC and an ORC integrated with heat sources, respectively. The two concepts were then adopted to analyze the impacts of working fluids on the performances of ORCs. The results indicated that with the same evaporating temperature, different working fluids could exhibit little impact on the internal exergy efficiency of an ORC. However, it was also emphasized that the working fluid selection could play a significant role in determining the external exergy efficiency. They concluded that the working fluids with lower critical temperatures could lead to higher evaporation temperatures, implying not only better temperature matches with the background heat source (higher external exergy efficiency) but also higher internal exergy efficiency of the ORC.

For selecting mixture working fluids, Victor et al. (2013) developed a mathematical programming-based method for determining the optimal composition of mixed working fluids for ORCs subjected to the maximum thermal efficiency of the cycle. In the method, the evaporation temperature of the cycle was directly configured, which could be ranged from 100℃ to 250℃, and the corresponding heat duty was set as 1MW. The optimization procedure was carried out by the Simulated Annealing technique. According to the optimization results, it could be concluded that, for a stand-along ORC (i.e., neglect the thermal match with background heat sources), the pure component organic fluids are more energy-efficient than mixed organic fluids. Andreasen et al. (2014) proposed another mathematical programming-based method to find the most promising working fluid (pure or mixture) that could lead to the maximum net power output of an ORC system. The work considered the thermal match with background heat sources by configuring a strand of hot fluid with inlet temperatures at 120℃ and 90℃. Based on such configuration, the optimization results indicated that mixed working fluids could exhibit more potentials on increasing the net power output than pure working fluids. Ethane is found to obtain a large net power output increase when used in mixtures, and the mixture of ethane and propane with an optimized mixing ratio is recommended.

Except for investigating the thermodynamic performances of different working fluids, some researchers focused on the environmental impacts. Hickenbottom et al. (2018) performed a comparative life-cycle assessment to evaluate the environmental impacts of an ORC. They related the environmental issues not only to the construction and transportation of ORCs but also to the operation periods. The promising working fluids of ORCs should be non-toxic and low-flammable and should have zero ozone depletion potential.

Wang et al. (2020) proposed the optimal selection principle for 14 different ORC working fluids, of which the selection criteria are based on environmental and economic performances. They configured a single waste heat source with a temperature range from 90 to 230℃ and set the electricity production cost and the reduction of greenhouse gas emissions of an ORC as their

optimization objective. Their calculation indicated that if based on the maximum emission reductions, the optimal working fluid could be R601 operated from 363 to 384 K and from 481 to 503 K. While regarding the economic performance, they recommended R245fa working with 363-468 K as the best choice.

The literature review shows that there is no single “winner” for the working fluid selections of ORCs. For a stand-alone ORC, most of the previous research works considered critical temperature as the most significant criteria for selecting promising working fluids. The objective is typically set to maximize the thermal efficiency of an ORC. However, in practice, the thermal match with background heat sources should be considered. To this perspective, some researchers set the maximum power output as their goal, while some other researchers discussed the economic performance of an ORC system by considering the trade-offs between capital cost and the profit gained by power generation. In summary, the analysis results of the previous researchers indicated that the selections of working fluids are case-dependent. This point was emphasized by Dong et al. (2020b), who declared ‘no fluid is suitable for all ORC systems’.

2.2.3 Process Integrations of ORCs

As the previous literature on ORC integration for recovering industrial waste heat has been fully reviewed by the appended papers in the following chapters, this section will only give a general summarization of the previous research without detailed introductions.

It has been introduced that the main purpose of ORC integration is to minimize the total annualized cost for dealing with waste heat, considering optimizing both waste heat extraction and ORC power generation. One of the first research dealing with ORC integration problems could be Desai and Bandyopadhyay (2009), who developed a graphical-based method based on the ‘Pinch Analysis’ technique. By applying the method, one can heuristically determine the

optimal operating condition, architecture selection, and working fluid selection of a single ORC, leading to the maximum net power output. One limitation of the graphical-based method is that the quality of its optimization solution could be highly dependent on the experiences of designers. To this point, Hipólito-Valencia et al. (2013), Chen et al. (2014), Chen et al. (2016), Yu et al. (2017a), Yu et al. (2017b), and Dong et al. (2020a) tried to adopt the mathematical programming-based PI techniques for dealing with ORC integration problems. The main idea of mathematical programming-based methods is to imbed the thermodynamic equations of an ORC into the network model of waste heat extraction to formulate an overall model. The objective function of the overall model can be subjected to the maximum power generation or the minimum total annualized cost so that the integration problem can be transformed into an NLP, MINLP, NLP+MILP, or NLP+MINLP optimization problem.

It can be noticed that all of the previous works mentioned above adopt deterministic algorithms to solve the formulated optimization problems. More recently, some researchers tried to import stochastic algorithms as their solvers. Kermani et al. (2018) and Dong et al. (2020b) developed a bi-level decomposition optimization strategy for solving ORC integration problems, in which the Genetic Algorithm is adopted.

Except for integrating ORCs with process flows, Elsido et al. (2019) and Huang et al. (2020) considered integrating ORCs into utility systems. In their work, the correlations between a total site utility system and the downstream ORCs were discussed, and mathematical programming-based methods were proposed for simultaneously addressing the optimal configurations of a utility system and its corresponding ORCs.

Chapter 3: Indirect Integration of ORCs

This chapter contains one journal-format paper, providing a mathematical programming-based method that adopts the indirect-heat-transfer strategic option for ORC integration problems. The method also allows for integrating more than one ORC unit, leading to an arrangement of multi-parallel ORCs.

3.1 Introduction to Publication 1

The paper presented in this chapter contributed a mathematical programming-based method for solving the ORC integration problems with an indirect heat transfer strategy.

For establishing the mathematical model, first, a modified stage-wise superstructure, namely 'Modified-IBMS', is proposed to synthesize the network of waste heat extraction. It is proved that the 'Modified-IBMS' can decrease the number of the divided stages, leading to less continuous and discrete variables than the previous superstructures, so that the computational time of the corresponding optimization process can be reduced. For comparison purpose, this study adopted the same Equation of State (i.e., the Peng-Robinson Equation of State) with Yu et al. (2017a) to formulate the thermodynamic properties of ORC working fluids so that the optimization consequences of this study can be compared with those of the previous literature. The established mathematical model leads to an MINLP optimization problem, which can be implemented into the GAMS® platform and is solved by the Baron solver. For optimization, the paper develops an iterative procedure, which can simultaneously determine the optimal unit number of ORCs, the optimal working conditions of each ORC, and the optimal HEN synthesis.

The case studies validate the feasibility of the proposed method. The results indicate that, for some cases, implementing multi-parallel ORCs could achieve less total annualized costs than

a single ORC.

3.2 Publication 1

Chu Z., Nan Z., Smith R., Modelling and Integration of Multi-Parallel Organic Rankine Cycles into Total Site, Energy (under review)

Modelling and Integration of Multi-Parallel Organic Rankine Cycles into Total Site

Zheng Chu, Nan Zhang*, Robin Smith

Centre for Process Integration, Department of Chemical Engineering and Analytical Science, the University of Manchester, M13 9PL, Manchester, United Kingdom

nan.zhang@manchester.ac.uk

Abstract

Organic Rankine Cycle (ORC) is a promising technology for exploiting the industrial low-grade waste heat. When trying to implement ORCs, proper integration with background waste heat sources is one of the crucial matters that should be considered. Research on ORC integration has been carried out during the last few decades. However, it is observed that the existing methodologies for integrating ORCs into industrial sites are still insufficient. Lots of the research efforts deal with ORC integration problem assuming only one single ORC participates, while the options of applying multi-parallel ORCs are rarely taken into account. Besides, existing research mainly focuses on direct integration of ORC(s) (i.e., waste heat is transferred directly from heat sources to ORC working fluids), whereas the option of utilizing intermediate heat carriers indirectly is neglected. As such, this study proposes a model-based methodology for indirect integration of multi-parallel ORCs. The overall model covers both waste heat extraction and ORC power generation. For heat extraction modelling, a modified superstructure based on Isafiade and Fraser (2008) is proposed, which simplifies the construction of a heat extraction network (HEN) and reduces computational time. For thermodynamics, the Peng-Robinson Equation of State is adopted. The overall model leads to a mixed-integer nonlinear programming (MINLP) problem and can be solved by a General Algebraic Modelling System, e.g., the GAMS software. Two case studies are performed in this work to validate and illustrate the application of the proposed method, the results of which show that applying multi-parallels ORCs instead of using a single ORC can decrease the overall annualized cost effectively.

Nomenclature

Variables		***Subscripts***	
A	heat exchanger area (m^2)	c	critical state
Capital	total capital cost ($)	con	condenser
FC	heat capacity flowrate (kW/K)	cu	cold utility
FIX	fixed charge ($)	cw	cooling water
h	enthalpy (kJ/kg)	eva	evaporator
LMDT	logarithm approach temperature	extraction	heat extraction section
m	mass flowrate (kg/s)	generation	power generation section
NORC	number of ORCs	in	inlet
Obj	objective variable	is	isentropic state point
OP	operating cost ($/year)	l	liquid
Operating	total operating cost ($/year)	latent	latent heat
P	pressure (kpa)	min	the minimum value
PC	purchase cost ($)	out	outlet
PO	power output	pump	pump
Profit	profit ($/year)	r	residual
q	heat amount (kJ)	sensible	sensible heat
T	temperature (K)	sl	saturated liquid
W	shaft work output (kW)	tb	turbine
Z	binary variable	wf	ORC working fluid
ρ	density (kg/m^3)	1, 2, 3, …6	state points
v	molar volume (cm^3/mol)		
Parameters		***Superscripts***	
AF	annualized factor	s	supply
AOH	annual operating hours	t	target
L	a constant with large value		
Price	marketing price		
U	heat transfer coefficient		
η	efficiency		
Sets			
hc	elements in the set of heat carrier streams HC= {hc1, 2 ... n}	orc	elements in the set of ORCs ORC= {orc|1, 2 ... n}
ti	elements in the set of temperature intervals TI= {ti|1, 2 ... TI}	ws	elements in the set of waste heat streams WS= {ws|1, 2 ... n}

1. Introduction

Organic Rankine Cycle (ORC), which can generate electricity from waste heat sources, is becoming a promising technology for exploiting waste heat in industrial fields. Derived from the conventional steam-based Rankine Cycle, ORC uses organic compounds instead of water as working fluid, ensuring operational feasibility when coping with low-grade heat sources. The schematic diagram and the corresponding thermodynamic T-S diagram of a typical ORC can be seen in Figure 1. As shown in Figure 1, a typical ORC consists of four main working components: a turbine, a condenser, a pump, and an evaporator. During operation, sub-cooled organic liquid is evaporated to saturated vapor in the evaporator, absorbing waste heat (5-6-1). And then, the saturated vapor is sent to the generator-connected turbine to generate power (1-2). The exhaust gas of the turbine is condensed in the condenser (2-3-4), and is recycled by the pump (4-5).

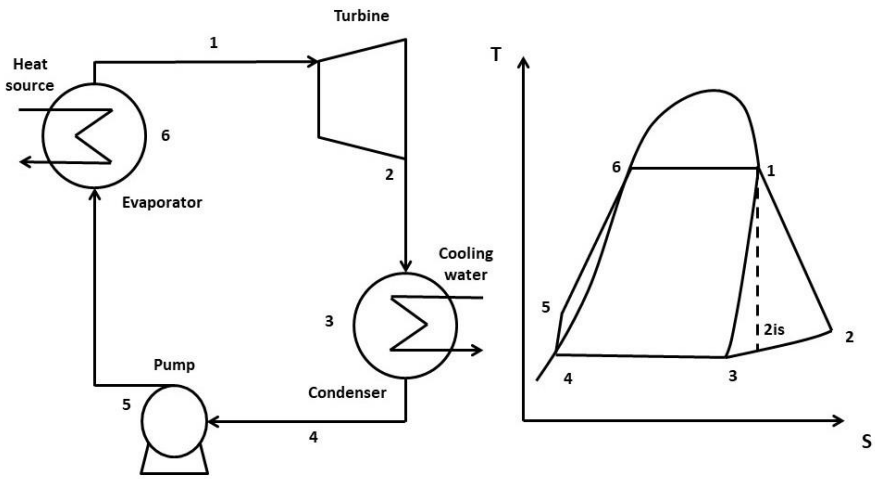

Figure 1. The schematic diagram and T-S diagram of a basic ORC configuration

When applying ORCs to exploit waste heat in an industrial site, an appropriate general strategy, including how to extract waste heat and generate power, should be determined. For heat extraction, waste heat can be directly transferred from heat sources to ORC(s) or indirectly transferred through intermediate heat carriers. The advantage of direct heat transfer is that it can achieve more power generation with less heat transfer area, leading to a higher

annual profit. However, it is pointed out that indirect heat transfer may be preferable in practical operations due to safety and controllability considerations (Yu et al., 2017a). As for power generation, it will be case-dependent to choose whether to use a single ORC or multi-parallel ORCs. The multi-parallel configuration could have better operating flexibility to cope with fluctuated conditions of heat sources. From the thermodynamic perspective, a single ORC could have a weak thermal match with background heat sources due to the 'pinch limitation' (shown in Figure 2) caused by the isothermal boiling process of ORC working fluid (Yu et al., 2018). Applying multi-parallel ORCs could debottleneck the 'pinch limitation' and improve the thermal match with heat sources, leading to more power generation (Stijepovic et al., 2017). However, more capital costs may be needed for implementing the extra ORC parallels. The trade-off between the capital cost and the power generation should be considered.

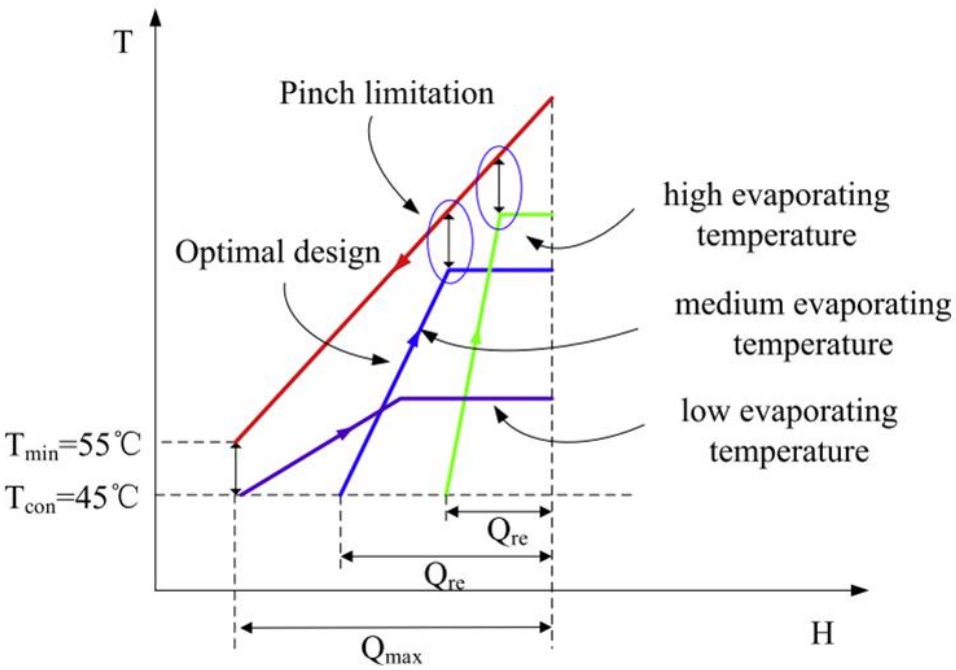

Figure 2. The 'pinch limitation' caused by a single ORC (Yu et al., 2018)

In general, considering both heat extraction and power generation, there will be four general strategic options, which are listed in Table 1. Developed methods dealing with these options

will be reviewed below, through which the improvements and deficiencies of the previous research can be concluded.

Table 1. Strategic options for integrating ORCs

Heat extraction / Power generation	Direct	Indirect
Single ORC	Direct & Single	Indirect & Single
Multi-parallel ORCs	Direct & Multi-parallel	Indirect & Multi-parallel

- **Direct heat transfer & Single ORC**

The direct integration of a single ORC could be the most common topic in the research field of ORC integration. Desai and Bandyopadhyay (2009) integrated a single ORC by using a graphical-aided method. In the method, through incorporating the heat absorption profiles of an ORC into the grand composite curve of background processes, near-maximum power output can be graphically determined. Hipólito-Valencia et al. (2013) developed a model-based method for integrating a single ORC. The overall model is generated by embedding a simplified ORC model into a superstructure-based model of HEN synthesis, leading to mixed-integer non-linear programming (MINLP). Another model-based methodology was proposed by Chen et al. (2014). In the method, first, a stage-wise superstructure model is adopted to identify the heat surplus zone of the given background processes. Second, a rigorous ORC model is incorporated into the superstructure model, formulating an ORC-imbedded superstructure model, which is then used to integrate a single ORC into the heat surplus zone. Yu et al. (2017b) solved single ORC integration problems with a two-step model-based method. In the first step, the Duran-Grossman NLP model (Duran and Grossmann, 1986) is applied to determine the best trade-off between utility consumption and ORC power generation. In the second step, the transhipment MILP model proposed by Papoulias and Grossmann (1983) is adopted to carry out the HEN synthesis. Huang et al. (2020) established an MINLP model, which can not only optimize the operations of a utility plant and an ORC, but also carry out the corresponding HEN synthesis.

Some other recent works tried to deal with single ORC integration problems considering the working fluid selection and architecture selection are to be considered. Kermani et al. (2018) developed a comprehensive bi-level approach for solving a single ORC integration problem. The bi-level approach adopts the Genetic Algorithm (GA) in a master level and mixed-integer linear programming (MILP) in a sub level. The master level can determine the optimal operation and the best working fluid selection of the ORC. And the sub level is responsible for optimizing the rest design variables. Dong et al. (2020) proposed another bi-level method for integrating a single ORC. The bi-level method consists of the GA in a master lever and non-linear programming (NLP) in a sub level. The method can determine the optimal working conditions of the ORC simultaneously with working fluid selection. However, the HEN synthesis is excluded.

- **Indirect heat transfer & Single ORC**

Yu et al. (2017a) realized that using an intermediate heat carrier (e.g., hot water) to transfer heat from heat sources to an ORC system may be preferable in practice due to safety and controllability considerations. They developed a sequential method for solving indirect ORC integration problems. Based on a given minimum approach temperature, the first step determines the optimal working conditions of the heat carrier stream and ORC, in which the Duran-Grossman NLP model is adopted (Duran and Grossmann, 1986). The HEN synthesis can then be carried out in the second step.

- **Direct heat transfer & Multi-parallel ORCs**

There are a few works focused on the integration of multi-parallel ORCs. Stijepovic et al. (2017) observed that more power generation could be achieved by applying a multi-parallel ORCs system. They proposed an MINLP model for integrating a multi-parallel ORCs system. In the model, simplified thermodynamic correlations are imported. Besides, the ‘temperature-interval (T-I)’ concept proposed by Linhoffand and Flower (1978) and the transhipment model

proposed by Papoulias and Grossmann (1983) are adopted. The results indicate that the multi-parallel ORCs could have advantages on power generation compared with a single-ORC.

- **Indirect heat transfer & Multi-parallel ORCs**

Up to now, the relevant research on integrating multi-parallel ORCs with an indirect heat transfer strategy is still unavailable in the open literature. As introduced earlier, the indirect heat transfer strategy can avoid safety and controllability issues in practice (Yu et al., 2016). And the multi-parallel configuration could achieve a higher power generation (Stijepovic et al., 2017). On the premise of ensuring safety and controllability operations, the indirect integration of multi-parallel ORCs may be preferable. Therefore, it is worth investigating this strategic option.

This paper aims to fill the gap in the field of the indirect integration of multi-parallel ORCs. A detailed model-based methodology will be developed to optmise the configuration of a multi-parallel system, HEN synthesis and operating conditions simultaneously.

2. Problem Statement

The illustrative diagram of the 'indirect heat extraction & multi-parallel ORCs' strategic option is shown in Figure 3. The whole system can be decomposed into a heat extraction section and a power generation section. In the heat extraction section, a set of waste heat streams, WS= {ws|1, 2 ... n}, are identified, with which the working conditions (including supply temperatures, target temperatures, and heat capacity flowrates, etc.) are known. A set of intermediate heat carriers (typically hot water), HC= {hc|1, 2 ... n}, are customized for extracting the waste heat, of which the working conditions are variables. In the power generation section, there is a set of ORC parallels, ORC = {orc|1, 2 ... n}. Each of the ORC parallels is coupled with an intermediate heat carrier stream. The operating conditions of the ORCs, including the evaporating temperatures/pressures, the condensing temperatures/pressures, and the working fluid mass flowrate, are variables to be optimized.

In addition, cold utilities with inlet and outlet temperatures are provided. The objective is to minimize the total annualized cost, considering the trade-off between the capital/operating costs and the profit brought up by power generation, which can be achieved by solving the following problems: 1. find the optimal number of parallel ORC trains; 2. determine the optimal working conditions of the heat carrier streams and ORCs; 3. determine the optimal HEN synthesis.

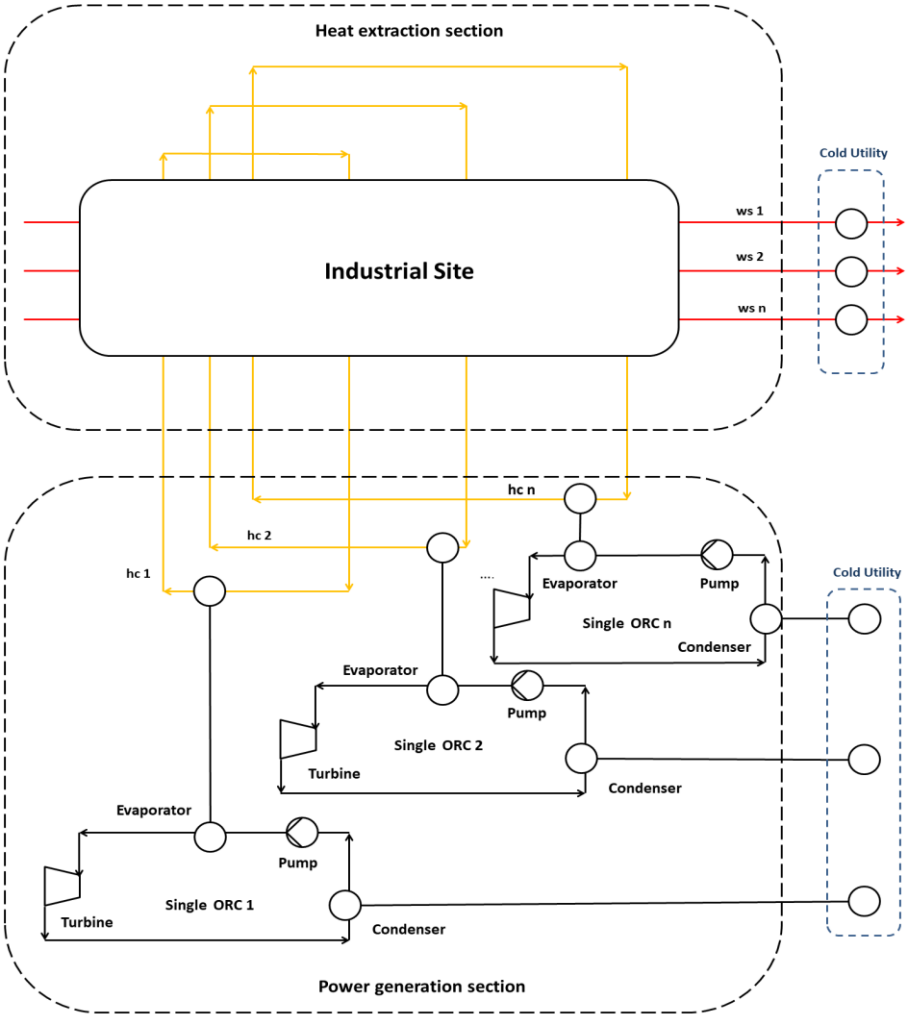

Figure 3. The graphical illustration of a multi-parallel ORCs system

3. Model establishment

The overall model for the integration problem can be separated into a heat extraction module and a power generation module. The heat extraction module is formulated by a superstructure-based technology. The power generation module represents the thermodynamic performance of each ORC in parallel, where rigorous thermodynamic correlations (i.e., the Peng-Robinson Equation of State) are adopted.

3.1. Heat extraction module

Several superstructure-based technologies such as the hyperstructure model (Ciric and Floudas, 1991), the Synheat model (Yee and Grossman, 1990), and the IBMS model (Isafiade and Fraser, 2008) are feasible candidates for establishing the heat extraction module. However, due to the combinatorial nature of HEN synthesis problems, the technologies mentioned above are MINLP in nature, which face computational difficulties in solving the corresponding optimization problem (Martelli et al., 2017). In this study, the heat extraction module will be simultaneously optimized with the power generation module, which could make the computational process even more challenging. As such, it is desirable to improve the computational efficiency.

It is observed that, with the same or fewer intervals, the IBMS model could have less computational time than the Syntheat or the hyperstructure model. However, in most cases, the IBMS model could generate much more intervals than the other superstructure-based approach, leading to more computational time. It is logical to assume that the decrease in the interval number of the IBMS model could reduce the computational time. Therefore, this study proposed a modified-IBMS model, which is derived from the IBMS model but with fewer intervals. In the modified-IBMS model, a concept of ‘narrow interval’ is proposed, which will be illustrated in the following context. Through eliminating the ‘narrow intervals’, the total interval number can be decreased, and the computational time is expected to be decreased. The assumption is verified by several case

studies (presented in supplementary materials). Comparison results show that the modified-IBMS model can reduce the number of continuous and discrete variables as well as the computational time.

The procedure for establishing a modified-IBMS model is introduced as below:

Step 1: As for given sets of process hot streams and heat carrier streams, establish an IBMS superstructure (Isafiade and Fraser, 2008). Note that cold utilities are placed at the end of each hot streams, and there is no hot utility usage. An example is given in Figure 4(a).

Step 2: Identify the 'narrow intervals' in the established IBMS superstructure.

The 'narrow intervals' are defined as the intervals of which the heat duty is less than X kW. The value of the X is heuristically determined, normally between 100 ~ 500 kW. One can case-dependently adjust the X value. With a proper X value, inspired by the 'block decomposition' concept (Zhu, 1995), it is assumed that the 'narrow intervals' can be merged into their adjacent interval without any strong impacts on the final optimization consequences. This assumption has been verified by several case studies (presented in supplementary materials), in which the relative deviations of the optimization results applying the modified-IBMS are found less than 1% to the literature results. Note that if there are no 'narrow intervals' found, the following steps can be skipped, and the modified-IBMS superstructure is equivalent to an IBMS superstructure. In this example, we can regard the 'ti 3' and 'ti 5' in Figure 4(a) as the 'narrow intervals'.

Step 3: Merge the 'narrow intervals' into their adjacent intervals according to the following rules:

1. The merging should be carried out from the high-temperature intervals to the low-temperature ones.
2. As for the 'narrow interval' bounded by a pair of supply temperatures, it should be merged into the subsequent interval rather than the preceding one, as illustrated in Figure 5-(a).
3. As for the 'narrow interval' bounded by a pair of target temperatures, it should be merged into the preceding interval rather than the subsequent one, as illustrated in Figure 5-(b).

4. As for the 'narrow interval' bounded by a target temperature and a supply temperature, its merging rule is case-dependent. If the target temperature is higher than the supply temperature, the narrow interval should be merged into the preceding interval (Fig 5-(c)); if the supply temperature is higher, then the narrow interval should be merged into the subsequent interval (Fig 5-(d)).

5. After each incorporation, check if the newly formed interval is a narrow interval or not. If the newly formed interval is still a narrow interval, merge it before moving to the next interval.

Step 4: Once all the narrow intervals are merged, a modified-IBMS is established (shown in Figure 4(b)). The corresponding mathematical model can then be formulated.

The formulation of the modified-IBMS model is similar to that of the IBMS model, which includes heat balance, temperature assignment, thermodynamic feasibility, logical constraints and heat exchanger area calculations. The formulas can be found in Appendix A.

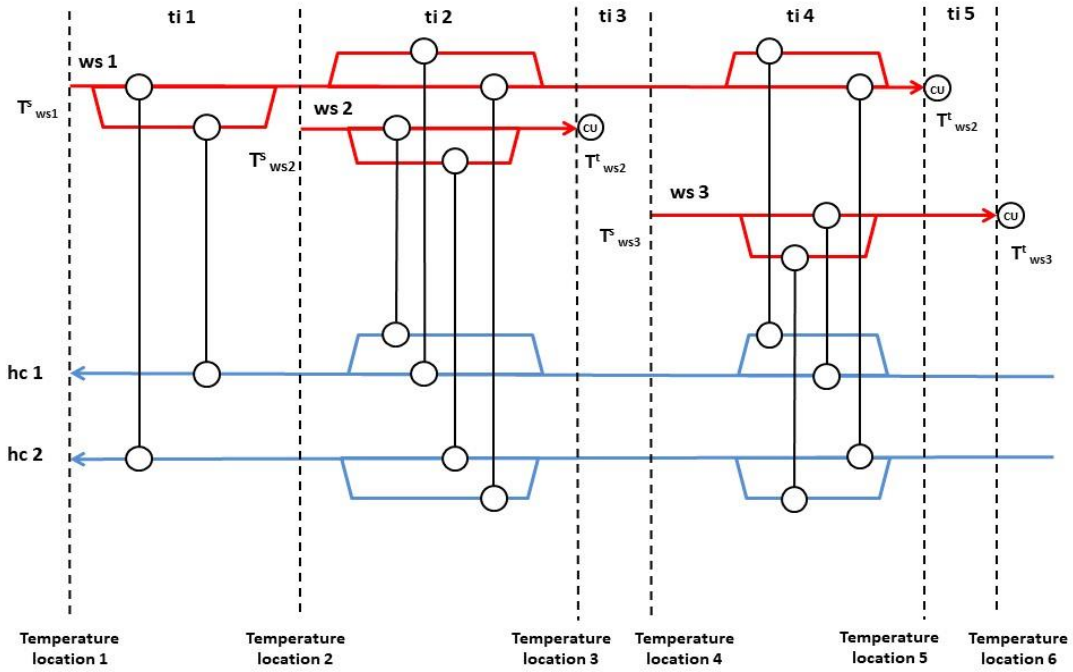

Figure 4(a). The graphical illustration of an IBMS

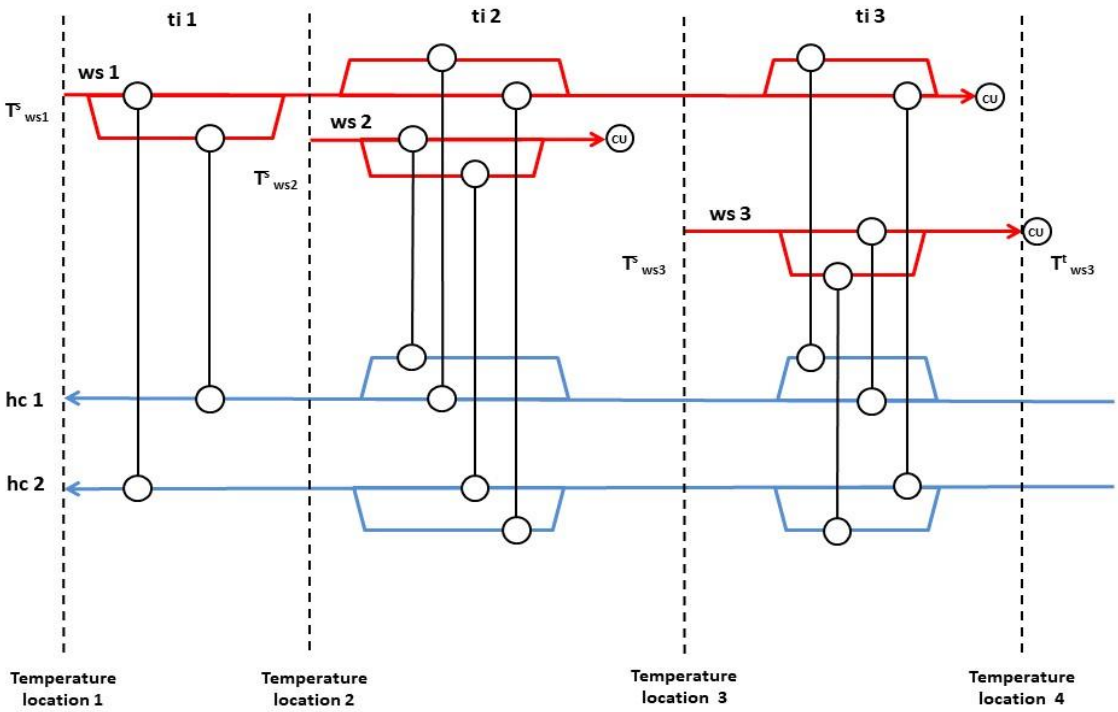

Figure 4(b). The graphical illustration of a modified-IBMS

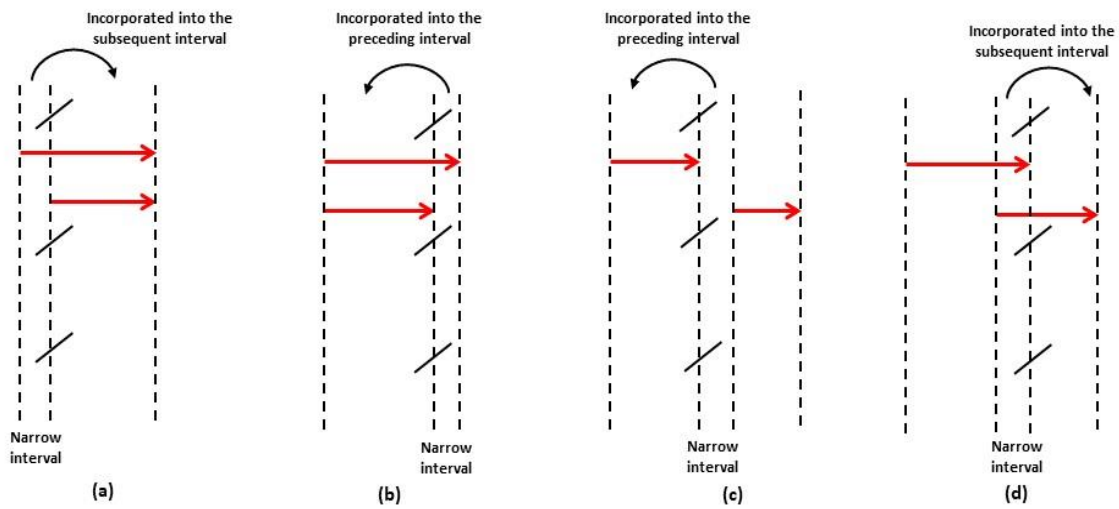

Figure 5. The incorportations of narrow intervals: (a) bounded by a pair of supply temperatures; (b) bounded by a pair of target temperatures; (c) & (d) bounded by a target temperature and a supply temperature

3.2. Power generation module

A power generation section consists of several stand-alone single ORCs. The model of a power generation section is actually a combination of several single ORC models. As for modelling every single ORC, the concept of thermodynamic state points can be used. As shown in Figure 6, there are several thermodynamic state points marked on an ORC T-S diagram. Through calculating the thermodynamic properties (flowrate, temperature, pressure, enthalpy, entropy, etc.) of the state points, the performance of each working component (evaporator, condenser, turbine, and pump) can be evaluated, and an ORC system can then be modelled. In this work, the thermodynamic properties of the state points are formulated by the Peng-Robinson equation of state (P-R EoS) and the Extended Antonie equation, of which the detailed formulations are given in Appendix B. Once the thermodynamic properties of each state point are formulated, the performance of each working component can be calculated as follows.

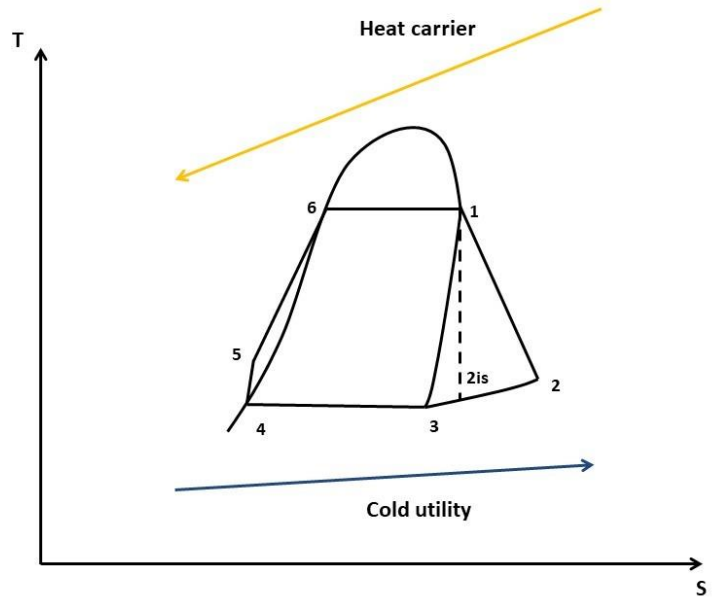

Figure 6. T-S diagram of a typical ORC with thermodynamic state points

- ***Turbines***

$$W_{tb}^{orc} = m_{wf}^{orc} \cdot (h_1^{orc} - h_2^{orc}) = m_{wf}^{orc} \cdot \eta_{tb}^{orc} (h_1^{orc} - h_{2is}^{orc}), \quad orc \in ORC \tag{1}$$

Note that the superscript 'orc' indicates the elements in the set ORC= {ORC |1, 2 ... n}; η_{tb}^{orc} represents the turbine isentropic efficiency; W_{tb}^{orc} represents the shaft work output of an ORC in parallel.

- ***Condensers***

The sensible heat transferred between the state points 2 and 3 is calculated by Equation (2). The latent heat transferred between the state points 3 and 4 is calculated by Equation (3).

$$q_{con,sensible}^{orc} = m_{wf}^{orc} \cdot (h_3^{orc} - h_2^{orc}), \quad orc \in ORC \tag{2}$$

$$q_{con,latent}^{orc} = m_{wf}^{orc} \cdot (h_4^{orc} - h_3^{orc}), \quad orc \in ORC \tag{3}$$

If assuming that a number of cold utility streams with given inlet and outlet temperatures are used in the condensers, the heat exchanger area of the sensible and latent heat transfers can be calculated as:

$$A_{con,sensible}^{orc} = \frac{q_{con,sensible}^{orc}}{U_{sensible} \cdot LMDT_{con,sensible}^{orc}}, \quad orc \in ORC \tag{4}$$

$$A_{con,latent}^{orc} = \frac{q_{con,latnet}^{orc}}{U_{latent} \cdot LMDT_{con,latent}^{orc}}, \quad orc \in ORC \tag{5}$$

$$LMDT_{con,sensible}^{orc} = \left[\frac{(T_2^{orc} - T_{cw,out}^{orc})(T_3^{orc} - T_{cw,int}^{orc})(T_2^{orc} - T_{cw,out}^{orc} + T_3^{orc} - T_{cw,int}^{orc})}{2} \right]^{1/3}, \quad orc \in ORC \tag{6}$$

$$LMDT_{con,latent}^{orc} = \left[\frac{(T_3^{orc} - T_{cw,int}^{orc})(T_4^{orc} - T_{cw,in}^{orc})(T_3^{orc} - T_{cw,int}^{orc} + T_4^{orc} - T_{cw,in}^{orc})}{2} \right]^{1/3}, \quad orc \in ORC \tag{7}$$

Where $U_{sensible}$ and U_{latent} are the sensible/latent heat transfer coefficients; $LMDT_{con,sensible}^{orc}$ and $LMDT_{con,latent}^{orc}$ are the logarithm temperature differences for the sensible/latent heat transfers; $T_{cw,int}^{orc}$ is an intermediate temperature of the cooling water, which can be calculated by Equation (8).

$$\frac{(T_{cw,int}^{orc} - T_{cw,in}^{orc})}{(T_{cw,out}^{orc} - T_{cw,int}^{orc})} = \frac{q_{con,latent}^{orc}}{q_{con,sensible}^{orc}}, \quad orc \in ORC \tag{8}$$

- ***Working fluid pumps***

The power consumption of the working fluid pumps is calculated as:

$$W_{pump}^{orc} = \frac{m_{wf}^{orc}}{\eta_{pump}^{orc} \cdot \rho_{wf}^{orc}} (P_5^{orc} - P_4^{orc}), \quad orc \in ORC \tag{9}$$

Where η_{pump}^{orc} is set as a constant parameter, indicating the isentropic efficiency of the pump. The density of working fluid ρ_{wf}^{orc} can be calculated by the Extended Rackeet Equation (Kyle, 1992):

$$v_l^{orc} \approx v_{sl}^{orc} = (R \cdot T_c / P_c)(RA^{orc})^{1+(1-T_r^{orc})^{2/7}}, \quad orc \in ORC \tag{10}$$

$$RA^{orc} = \alpha + \beta(1 - T_r^{orc}), \quad orc \in ORC \tag{11}$$

$$T_r^{orc} = T_4^{orc} / T_c, \quad orc \in ORC \tag{12}$$

Where v_L^{orc} represents the actual liquid molar volume; α and β are two regression parameters, whose values depend on the type of working fluid.

- ***Evaporators***

There are two thermodynamic processes occurred in the evaporators, i.e. a heating process (from state point 1 to 2) and an evaporation process (from state point 2 to 3). The energy balances for the two processes are formulated as follows:

$$q_{eva,sensible}^{orc} = m_{wf}^{orc} \cdot (h_6^{orc} - h_5^{orc}), \quad orc \in ORC \tag{13}$$

$$q_{eva,latent}^{orc} = m_{wf}^{orc} \cdot (h_1^{orc} - h_6^{orc}), \quad orc \in ORC \tag{14}$$

As the supply and target temperatures of the heat carrier streams are pre-calculated in the heat extraction module (Appendix A), the logarithm temperature differences in the evaporator can be calculated as follows:

$$T_{in}^{hc} = T_t^{hc}, \quad hc \in HC \tag{15}$$

$$T_{out}^{hc} = T_s^{hc}, \quad hc \in HC \tag{16}$$

$$LMDT_{eva,sensible}^{orc} = \left[\frac{(T_{out}^{hc} - T_5^{orc})(T_{int}^{hc} - T_6^{orc})(T_{out}^{hc} - T_5^{orc} + T_{int}^{hc} - T_6^{orc})}{2} \right]^{1/3}, \quad orc \in ORC, hc \in HC \tag{17}$$

$$LMDT_{eva,latent}^{orc} = \left[\frac{(T_{int}^{hc} - T_6^{orc})(T_{in}^{hc} - T_1^{orc})(T_{int}^{hc} - T_6^{orc} + T_{in}^{hc} - T_1^{orc})}{2} \right]^{1/3}, \quad orc \in ORC, hc \in HC \tag{18}$$

Where $LMDT_{eva,sensible}^{orc}$ and $LMDT_{eva,latent}^{orc}$ are logarithm temperature differences for sensible and latent heat transfer separately; T_{int}^{hc} is an intermediate temperature of a heat carrier, which is given by Equation (19).

$$(T_{int}^{hc} - T_{out}^{hc}) \cdot FC_{hc} = q_{eva,sensible}^{orc}, \quad orc \in ORC, hc \in HC \tag{19}$$

The approach temperature feasibility is considered in Equations (20) - (22):

$$T_{out}^{hc} - T_5^{orc} \geq DT_{min}, \quad orc \in ORC, hc \in HC \tag{20}$$

$$T_{int}^{hc} - T_6^{orc} \geq DT_{min}, \quad orc \in ORC, hc \in HC \tag{21}$$

$$T_{in}^{hc} - T_1^{orc} \geq DT_{min}, \quad orc \in ORC, hc \in HC \tag{22}$$

So that the heat exchanger area of the evaporator can be calculated as:

$$A_{eva,sensible}^{orc} = \frac{q_{eva,sensible}^{orc}}{U_{eva,sensible} \cdot LMDT_{eva,sensible}^{orc}}, \quad orc \in ORC \tag{23}$$

$$A_{eva,latent}^{orc} = \frac{q_{eva,latent}^{orc}}{U_{eva,latent} \cdot LMDT_{eva,latent}^{orc}}, \quad orc \in ORC \tag{24}$$

3.3. Combination of the modules

The interaction between the heat extraction section and the power generation section can be represented by energy balance. Equation (25) defines the overall energy balance. The energy balance of each ORC train is given by Equations (26) and (27).

$$\sum_{hc \in HC} \left[(T_{in}^{hc} - T_{out}^{hc}) FC^{hc} \right] = \sum_{orc \in ORC} (q_{eva,sensible}^{orc} + q_{eva,latent}^{orc}) \tag{25}$$

$$q_{eva,sensible}^{orc=1,2..n} + q_{eva,latent}^{orc=1,2..n} = (T_{in}^{hc=1,2..n} - T_{out}^{hc=1,2..n}) FC^{hc=1,2..n}, \quad orc \in ORC, hc \in HC \tag{26}$$

$$q_{con,sensible}^{orc} + q_{con,latent}^{orc} = q_{cu}^{orc}, \quad orc \in ORC \tag{27}$$

3.4. Cost function

To evaluate the annualized profit of an integrated multi-parallel ORCs system, the capital cost,

operating cost, and the profit brought by power generation should be calculated.

- ***Capital cost***

The capital cost of heat extraction section is mainly contributed by heat exchangers and heat carrier pumps. The capital cost of heat exchangers is calculated by Equation (28), which is referred from Yu et al. (2017a).

$$\mathrm{Capital}_{\mathrm{extraction,he}} = 10000 + 800 \cdot \mathrm{A}_{\mathrm{extraction}}{}^{0.7} \tag{28}$$

Where $\mathrm{A}_{\mathrm{extraction}}$ indicates the total heat exchanger area of the heat extraction section. Note that the coefficient of '10000' and '800' should be case dependent, rather than fixed. They can be correlated if relevant cost data are available.

To calculate the capital cost of heat carrier pumps, the power consumption of the pumps must be first evaluated. In this work, we applied a simplified equation (Poling et al., 2001) to evaluate the pressure drop of heat carrier streams, as shown in Equation (29). Then the corresponding power consumption can be calculated by Equation (30).

$$\Delta \mathrm{P}_{\mathrm{pump}} = -0.0023\mathrm{FC}_{\mathrm{hc}} + 9.0925, \quad \mathrm{hc} \in \mathrm{HC} \tag{29}$$

$$\mathrm{W}_{\mathrm{pump}}^{\mathrm{hc}} = \frac{-0.0023\mathrm{FC}_{\mathrm{hc}}{}^{2}}{\rho_{\mathrm{hc}}\mathrm{Cp}_{\mathrm{hc}}} + \frac{9.0925\mathrm{FC}_{\mathrm{hc}}}{\rho_{\mathrm{hc}}\mathrm{Cp}_{\mathrm{hc}}}, \quad \mathrm{hc} \in \mathrm{HC} \tag{30}$$

The capital cost of each heat carrier pump is given by Equation (31):

$$\mathrm{Capital}_{\mathrm{pump}}^{\mathrm{hc}} = 500 \cdot \left(\frac{\mathrm{W}_{\mathrm{pump}}^{\mathrm{hc}} \cdot 1000}{300}\right)^{0.25}, \quad \mathrm{hc} \in \mathrm{HC} \tag{31}$$

As for the power generation section, the capital cost contains the investment of ORC components, the installation fee, and the cost brought up by auxiliary facilities. The investment of each ORC component can be calculated by Equations (32), (33), (34), and (35) respectively, which are also adopted by Yu et al. (2017a). The installation fee and auxiliary cost are regarded as a fixed charge, which depends on the number of ORC parallel, as calculated in Equation (36).

$$\mathrm{PC}_{\mathrm{turbine}}^{\mathrm{orc}} = 1.5 \cdot (225 + 170 \cdot \mathrm{V}_{2}^{\mathrm{orc}}), \quad \mathrm{orc} \in \mathrm{ORC} \tag{32}$$

$$PC_{eva}^{orc} = 190 + 310 \cdot (A_{eva,sensible}^{orc} + A_{eva,latent}^{orc}), \quad orc \in ORC \tag{33}$$

$$PC_{con}^{orc} = 190 + 310 \cdot (A_{con,sensible}^{orc} + A_{con,latent}^{orc}), \quad orc \in ORC \tag{34}$$

$$PC_{pump}^{orc} = 900 \cdot (\frac{W_{pump}^{orc} \cdot 1000}{300})^{0.25}, \quad orc \in ORC \tag{35}$$

$$FIX_{generation} = \xi \cdot (NORC) \tag{36}$$

The total capital cost of the power generation section is:

$$Capital_{generation} = \sum_{orc \in ORC} (PC_{tb}^{orc} + PC_{eva}^{orc} + PC_{con}^{orc} + PC_{pump}^{orc}) + FIX_{genertaion} \tag{37}$$

- ***Operating cost***

The operating cost mainly consists of the cold utility costs of the heat extraction section (calculated by Equation (38)) and the power generation section (calculated by Equation (39)).

$$Op_{extraction} = Price_{cu} \cdot q_{cu} \tag{38}$$

$$Op_{generation} = Price_{cu} \cdot \sum_{orc \in ORC} q_{cu}^{orc} \tag{39}$$

- ***Profit***

The profit is determined by the net power generation of multi-parallel ORCs. The net power generation is evaluated by Equation (40). And the total annual profit is calculated by Equation (41).

$$PO_{net}^{orc} = W_{tb}^{orc} - W_{pump}^{orc}, \quad orc \in ORC \tag{40}$$

$$Profit = AOH \cdot Price_{electric} \cdot \sum_{orc \in ORC} PO_{net}^{orc} \tag{41}$$

Where $Price_{electric}$ is electricity price; AOH is annual operating hours.

3.5. Objective function

The objective is to minimize the total annualized cost, which takes into account the annualized capital cost of the heat extraction section and the power generation section, the annualized investment of ORC components, the annual operating cost, as well as the profit from power

generation.

$$\text{obj}=\text{AF}\cdot(\text{Capital}_{\text{extraction}}+\text{Capital}_{\text{generation}})+\text{Operating}-\text{Profit} \tag{42}$$

4. Solution Strategy

The integration problem is to determine: (1) the optimum number of the parallel ORC trains; (2) the optimal structure of the NEN; (3) the optimal working conditions of each heat carrier stream; (4) the optimum operation of each ORC train. Based on the established model, an MINLP problem, namely **'PM'**, is formulated, where the points (2), (3), and (4) can be simultaneously addressed. As shown below, the symbol 'a' denotes a set of free variables to be optimized, $\alpha(\mathrm{a})$ represents the feasible search space defined by the constraints.

$$\text{Min: obj}=\text{AF}\cdot(\text{Capital}_{\text{extraction}}+\text{Capital}_{\text{generation}})+\text{Operating}-\text{Profit}$$

(PM)

$$\text{s.t.}\quad \alpha(\mathrm{a})=\left\{\mathrm{a}\left|\begin{array}{l}\text{heat extraction module (Modifie-IBMS)}\\ \text{power generation module Eqs. (1)}\sim\text{(27)}\\ \text{objective function Eqs. (28)}\sim\text{(42)}\end{array}\right.\right\}$$

To determine the optimal number of ORC trains in parallel (problem (1)), an iterative method is applied. First, set a reference case by integrating a single ORC system. Then, create a double-parallel ORCs system by adding one more parallel train into the single system. If the objective function (total annualized cost) of the double-parallel system is lower than that of the single one, the double-parallel system is set as the reference case; if not, the search is terminated, outputting the single system as the optimum solution. When the double-parallel ORCs system is selected as the reference case, a triple-parallel one can be further assessed, and a similar comparison procedure can be carried out. The search process can be repeated until the optimal number of the parallels is identified. The iterative search procedure is summarized in Figure 7.

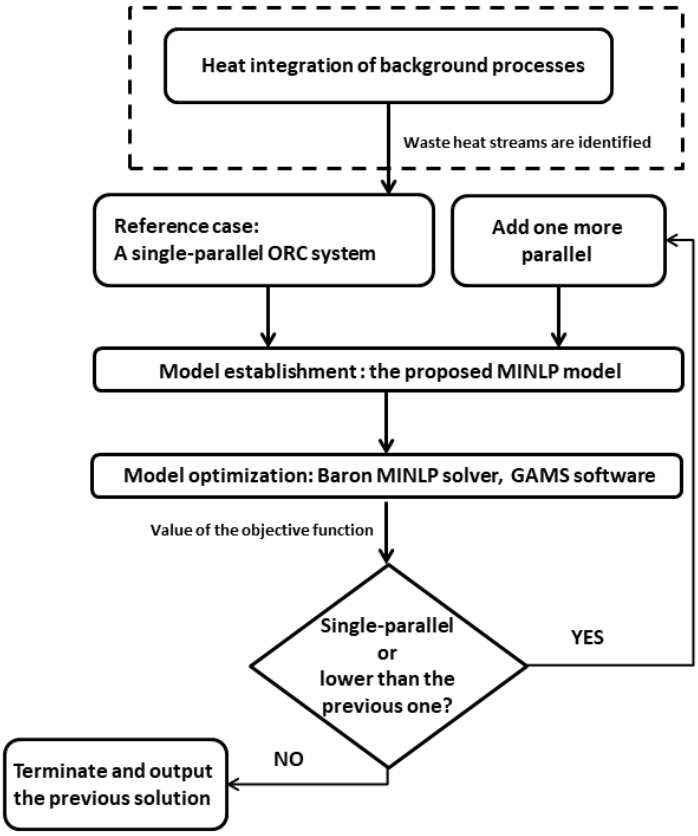

Figure7. The searching procedures of the trial-and-error method

5. Case Studies

In this chapter, two case studies are presented to illustrate the application of the proposed method for integrating multi-parallel ORCs. In the case studies, the following parameters are defined:

- The cold utility cost is 20 $\$/(\mathrm{kW}\cdot\mathrm{year})$
- The hot utility cost of the background processes is 100 $\$/(\mathrm{kW}\cdot\mathrm{year})$
- The electricity price is 0.10 $\$/(\mathrm{kW}\cdot\mathrm{year})$
- The AOH (annual operating hours) is assumed to be 8000 hours per year
- The isentropic efficiency $\eta_{\mathrm{tb}}^{\mathrm{orc}}$ of each turbine is assumed as 80%
- The isentropic efficiency $\eta_{\mathrm{pump}}^{\mathrm{orc}}$ of each pump is assumed as 95%
- The AF (annualized factor) is assumed as 0.18/year, corresponding to a 6-year project with 3% interest rate

- The working fluid of the multi-parallels ORCs is chosen as N-butane (R600)
- The overall heat transfer coefficients are assumed as 150 $W/(m^2 \cdot ℃)$ and 300 $W/(m^2 \cdot ℃)$ for transferring the sensible heat and latent heat of ORC working fluid
- The fixed charge is assumed as $2.5 \cdot 10^4$ \$ for implementing each of the ORC parallels

5.1. Case study 1

This case study is taken from Yu et al. (2017a), aiming to: 1. validate the proposed method of this study; 2. compare the economic/thermodynamic performances of a single-ORC and multi-parallel ORCs. The background information adopted by Yu et al. (2017a) are given in Table 2. As the waste heat streams are not directly provided, a heat integration should be first carried out to identify the waste heat streams. The modified IBMS superstructure-based model is chosen as the tool for the heat integration. The results of the heat integration are presented in Table 3, and the identified waste heat streams are listed in Table 4.

Table 2. Background information of case study 1 (Yu et al., 2017a)

stream	supply temperature (℃)	target temperature (℃)	heat capacity flowrate (kw/℃)
HS1	300	40	40
HS2	170	80	70
HS3	350	100	70
HS4	120	40	65
HS5	70	40	220
HS6	120	70	160
CS1	70	300	30
CS2	40	120	50
CS3	90	300	70
CS4	160	185	270
CS5	30	50	315
CS6	123	124	1100

Table 3. The result of the heat integration of the background processes

hot utility usage (kW)	1509.3
hot utility annual cost ($/year)	150930.4
number of heat exchanger units	19
total heat exchanger area (m^2)	25175.6
total annualized cost of heat exchangers ($/year)	175199.7

Table 4. Identified waste heat streams

waste heat stream	supply temperature (℃)	target temperature (℃)	heat capacity flowrate (kW/℃)	Heat load (kW)
WS1	109.6	40	40	2784
WS2	91	80	70	770
WS3	70.2	40	65	1963
WS4	70	40	220	6600
WS5	92.8	70	160	3648

Table 5. The conclusive optimization results of case study 1

parallel configuration	Single	Double	Tripple	Literature
total annual cost ($/year)	500110	**499270**	501160.4	565950
hot utility (kW)	1509.3	1509.3	1509.3	2410.0
cold utility (kW) (processes cold utility + ORC cooling water)	15274.7	15258.5	15234.4	15671.1
heat exchanger area (m^2) (background HEN + heat extraction network)	35879.7	36289.6	36910.8	72044
power generation (kW)	477.9	493.6	517.0	947.0

Once the waste heat streams are identified, the next step is to determine the optimum parallel number, in which the iterative method illustrated in Figure 7 is applied. Within each iteration,

a PM model is established and is solved by the General Algebraic Modelling System (GAMS) with the Baron solver (Sahinidis,1996). The hardware used is a desktop PC with Intel(R) Core(TM) i5 CPU 3.33 GHz and 8.00 GB of RAM. The computational time of each iteration is limited within 5 hours.

The searching process is terminated after the third iteration, which implies that the double-parallel configuration is defined as the optimum parallel configuration. During the searching process, the assessment for integrating a single-ORC contains 138 independent equations with 185 continuous variables and 25 discrete variables; the assessment for integrating double-parallels ORCs contains 316 independent equations with 335 continuous variables and 50 discrete variables; the assessment for integrating triple-parallels ORCs contains 447 independent equations with 485 continuous variables and 75 discrete variables. The optimization results, as well as comparison with the literature result (Yu et al., 2017a) are presented in Table 5.

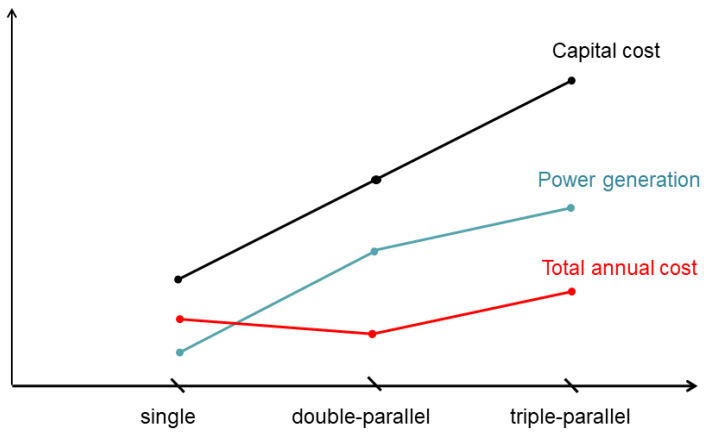

Figure 8. The competition between the power generation and the additional capital cost

The comparison among the different parallel configurations reveals the economic trade-offs in the ORC(s) integration problem. Though the power generation can be increased by implementing more parallel ORC trains, it is inevitable to bring in additional capital costs. As long as the bonus brought up by the increased power output can overcome the extra capital cost, the multi-parallel ORCs should be more profitable (i.e., less total annualized cost) than

a single one. With the increase of the parallel trains, the capital cost continuously increases, but the increasing rate of the power generation is faded. As illustrated in Figure 8, there is always a competition between the power generation and the additional capital cost. In this case study, the best trade-off is found at the double-parallel configuration.

Table 6. The results for sensitivity analysis

parallel configuration	Single	Double	Single	Double
electricity price ($\$/(kW \cdot year)$)	0.09	0.09	0.1	0.1
ORC fixed charge ($)	$2.5 \cdot 10^4$	$2.5 \cdot 10^4$	$3.0 \cdot 10^4$	$3.0 \cdot 10^4$
total annual cost ($/year)	**537261**	538513	**501010**	501070
power generation (kW)	449.5	451.7	477.9	493.6
profit brought up by power generation ($/year)	323630	325190	382320	394880
overall capital cost ($/year)	403881	406743	426906	439850
overall utility cost ($/year)	457010	456960	456424	456100

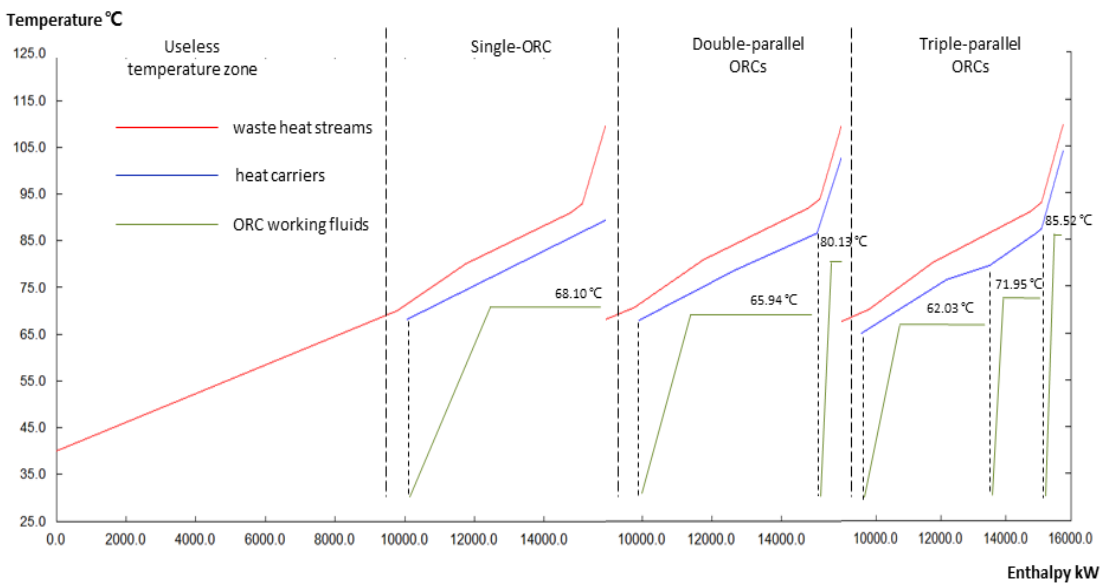

Figure 9. The composite curves of case study 1

Table 7. The optimal operations for various parallel configurations

	single-ORC	**double-parallel**		**triple-parallel**		
Optimization Variable	first parallel	first parallel	second parallel	first parallel	second parallel	third parallel
Power generation section						
working fluid mass flowrate (kg/s)	13.68	11.53	2.51	8.09	5.24	1.56
evaporation temperature (℃)	68.10	65.94	80.13	62.03	71.95	85.52
condensation temperature (℃)	26.85	26.85	26.85	26.85	26.85	26.85
turbine power output (kW)	490.28	393.25	113.28	250.26	203.93	76.43
evaporator heating duty (kW)	5700.91	4769.78	1086.33	3304.45	2213.22	684.67
condenser cooling duty (kW)	5210.63	4376.52	973.05	3054.19	2009.30	608.23
thermal efficiency	8.38%	8.04%	10.12%	7.40%	8.97%	10.81%
Heat extraction section						
heat carrier supply temperature (℃)	68.22	67.30	77.90	65.01	76.47	86.63
heat carrier target temperature (℃)	89.45	85.63	102.87	79.54	87.15	103.78
heat capacity flowrate of heat carrier (kW/℃)	268.62	260.22	43.50	227.42	207.34	39.911

It is worth mentioning that the applications of multi-parallel ORCs may not be suitable for all cases. In the sensitivity analysis, two sets of scenarios are carried out. In the first scenario, the electricity price is slightly adjusted from 0.1 $\$/(\mathrm{kW}\cdot\mathrm{year})$ to 0.09 $\$/(\mathrm{kW}\cdot\mathrm{year})$. Whilst in the second scenario, the fixed charge of implementing an ORC parallel is increased to $3.0\cdot10^{4}$ \$. Results of the sensitivity analysis are presented in Table 6. It can be seen that both of the scenarios lead to the single-ORC as the most profitable configuration rather than the multi-parallel ones.

A common phenomenon we have noticed is that the application of the multi-parallel ORCs can always increase power generation. The amount of power generation is affected by not only the rate of energy recovery but also the ORC thermo-efficiency (Yu et al., 2015). For the same rates of energy recovery, a higher thermo-efficiency can lead to more power generation. In this case study, though the rates of energy recovery of the various parallel configurations are close, the overall thermal efficiency of the double-parallel ORC system of 8.43% is higher than that (8.38%) of the single ORC system. Figure 9 presents the composite curves of the waste heat streams together with the heat carrier streams and the ORC working fluids for each of the parallel configurations. It can be seen that the multi-parallel configurations can result in a better thermal match between the heat sinks and sources, which improves the overall thermal efficiency.

The optimal operations of each of the parallel configurations are organized in Table 7, and the optimal network structure of the double-parallel configuration selected as the most profitable is presented in Figure 10.

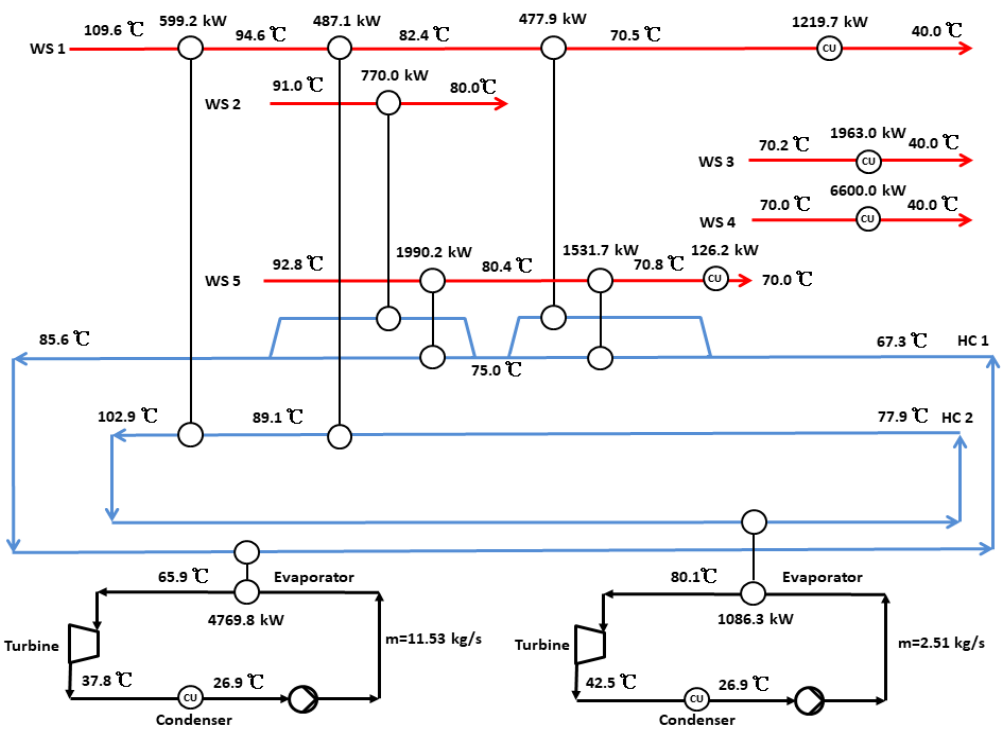

Figure 10. The optimized double-parallel structure of case study 1

5.2. Case study 2

In the first case study, the proposed method has been validated. However, it is noticed that the improvement of applying multi-parallel ORCs instead of a single ORC is unobvious (the total annualized cost is decreased from 500110 to 499270 $/year). With the same marketing conditions, other different background heat source profiles may show more obvious improvement when using multi-parallel ORCs.

It is assumed that the waste heat stream data are pre-identified in this case study, as listed in Table 8. The solving processes are identical to that of the first case study. The assessment for integrating a single-ORC creates 191 independent equations with 210 continuous variables and 13 discrete variables; the assessment for integrating double-parallels ORCs performs 319 independent equations with 375 continuous variables and 21 discrete variables; the assessment for integrating triple-parallels ORCs exhibits 445 independent equations with 538 continuous variables and 29 discrete variables.

The optimization results are presented in Table 9. It can be seen that the double-parallel configuration achieves the minimum annual cost, which is 314132 $/year, about 15.8% less than that of the single-ORC configuration. Among the three configurations, the triple-parallel one can generate the most electricity, which is 1021 kW, about 70.7% and 4.1% higher than that of the single-parallel and double-parallel ones. Though the triple-parallel configuration has the most power generation, it also needs the most capital cost, which is 628370 $/year. The increased power generation of the triple-parallel ORCs cannot compensate the extra capital cost, leading to a higher total annualized cost than the double-parallel one.

Table 8. The waste heat stream data for case study 2

Stream	Supply Temperature (℃)	Target Temperature (℃)	Heat capacity flowrate (kW/℃)	Heat duty (kW)
WS 1	130	100	40	1200

WS 2	125	90	70	2450
WS 3	90	40	160	8000
WS 4	90	35	120	6600
WS 5	80	37	220	9460

Table 9. The optimization results for case study 2

Parallel configuration	Single-ORC	Double-parallel ORCs	Triple-parallel ORCs
Total annual cost ($/year)	373262	**314132**	321031
Total capital cost ($/year)	323165	586582	628370
Total operating cost ($/year)	541904	534038	533187
Power generating profit ($/year)	491807	806488	840526
Cold utility (kW)	27095	26702	26659
Heat extraction area (m^2)	6151	17722	19238
Power generation (kW)	598	980	1021
Overall thermal efficiency	8.63%	8.82%	8.95%

Figure 11 shows the composite curve diagram of this case study. It can be seen that the double-parallel and triple-parallel configurations can exploit additional 4500 kW and 5000 kW waste heat. Due to the pinch limitation caused by the isothermal boiling process of the working fluid, the single-ORC exhibits a poor thermal match with the heat sources, leaving lots of waste heat unexploited. In this case, one can improve the rate of waste heat recovery by increasing the heat capacity flow rate of the ORC working fluid. However, with the increase of the flow rate, the evaporation temperature of the ORC should be synchronously decreased to ensure the feasibility of heat transfer (as shown in Figure 12), leading to a decrease in thermal efficiency, and the amount of power generation could be even lower. Yu et al. (2018) proposed a concept of ‘pinch limitation’ to describe this dilemma. The ‘pinch limitation’ can be debottlenecked by the multi-parallel ORCs. For example, in the double-parallel ORCs system,

the waste heat with different temperatures is assigned to different ORC parallels. The high-temperature parallel (with an 88.1 ℃ evaporation temperature) can guarantee high thermal efficiency, while the low-temperature parallel (with an 61.7 ℃ evaporation temperature) can increase the energy recovery rate. The synergy of the two parallels results in a better thermal match with the heat sources. The detailed results of the optimum operations and the optimum network synthesis are separately presented in Table 10 and Figure 13.

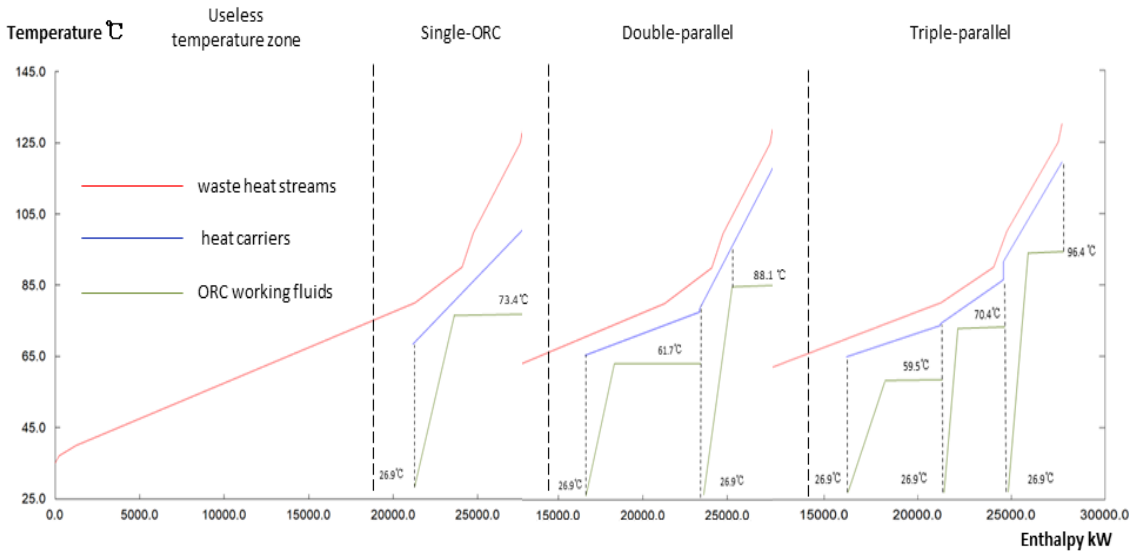

Figure 11. The composite curves of case study 2

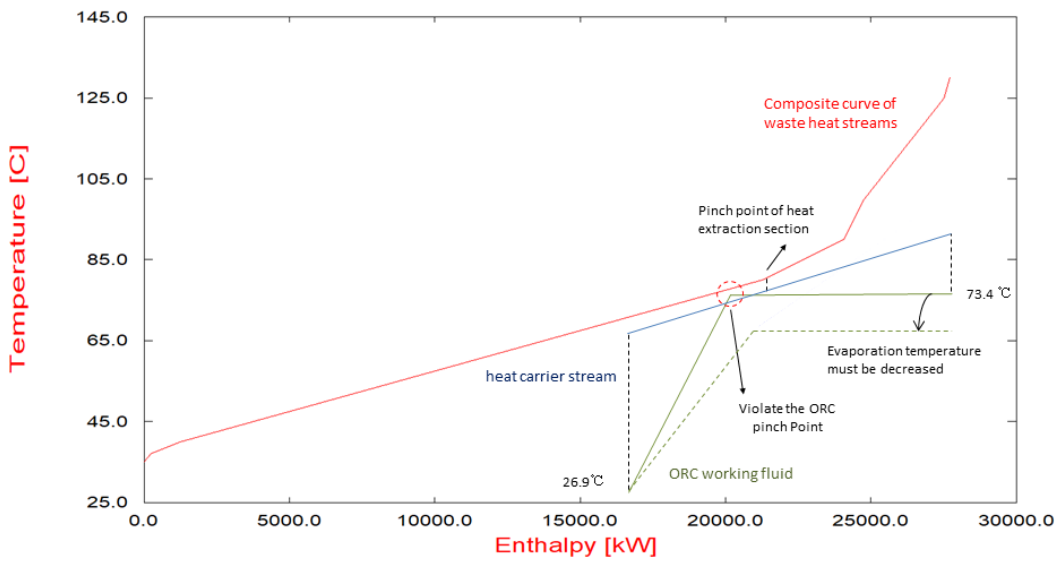

Figure 12. The decrease in the ORC evaporation temperature when trying to recover more waste heat

Table 10. The optimization results in Case Study 2

Optimization Variable	Single ORC	Double-parallel		Triple-parallel		
	first parallel	first parallel	second parallel	first parallel	second parallel	third parallel
Power generation section						
working fluid mass flowrate (kg/s)	15.5	16.6	9.8	12.4	8.0	6.9
evaporation temperature (℃)	73.4	61.7	88.1	59.5	70.4	96.4
Condensation temperature (℃)	26.9	26.9	26.9	26.9	26.9	26.9
Net power generation (kW)	598.0	496.3	483.7	350.4	294.8	375.8
evaporator heating duty (kW)	6566.4	6768.5	4348.2	5033.6	3375.8	3115.7
condenser cooling duty (kW)	5951.7	6260.2	3848.3	4675.3	3073.2	2725.9
thermal efficiency	9.1%	7.3%	11.1%	6.9%	8.7%	12.1%
Heat extraction section						
heat carrier supply temperature (℃)	100.9	77.7	118.4	73.7	86.4	119.3
heat carrier target temperature (℃)	68.5	65.6	78.6	64.9	74.1	91.5
heat capacity flowrat of heat carrier (kW/℃)	202.5	558.3	109.4	567.4	274.6	112.2

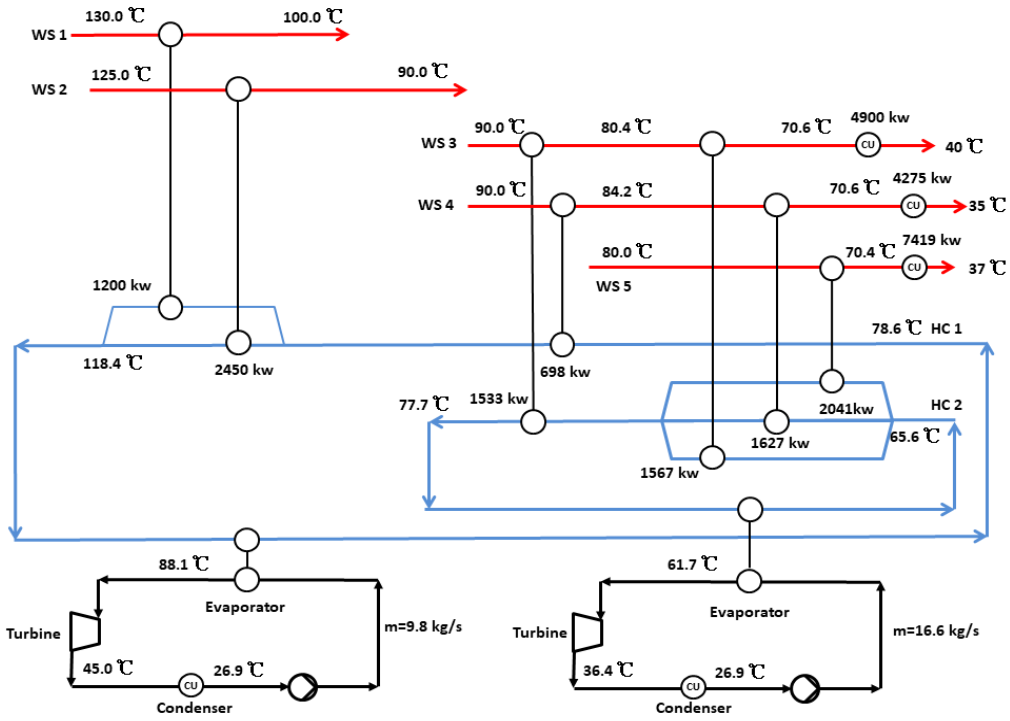

Figure 13. The optimized HEN of the double-parallel ORCs

6. Conclusions

In the research field of ORC integration, the strategic option of adopting multi-parallel ORCs and indirect heat extraction is rarely discussed. To fill the gap, this study proposes a mathematical programming method for indirectly integrating multi-parallel ORCs. An iterative approach is developed to determine the optimum number of ORC parallels. The heat integration with waste heat sources and the optimum operations of the ORCs can be simultaneously determined. Two case studies are presented to illustrate the application of the proposed method. In the first case study, comparisons with the literature result show that the total annual cost is decreased by about 11.7% when applying the proposed method. In the second case study, the total annual cost of the double-parallel ORCs is 15.8% less than that of the single-ORC. Both of the case studies have proved the applicability of the proposed method, indicating that multi-parallel ORCs may be more profitable than a single-ORC in some cases.

Appendix A: Equations of the modified IBMS

Equations of the modified IBMS model are described as follows, including heat balance, temperature assignment, thermodynamic feasibility, logical constrains and heat exchanger area calculations.

- ***Energy balance***

The overall energy balances for each waste heat stream and each heat carrier stream are separately presented in Equation (A1) and (A2) below:

$$(T_{ws}^{s} - T_{ws}^{t})FC_{ws} = \sum_{ti \in TI} \sum_{hc \in HC} q_{ws,hc,ti} + qc_{ws}, \quad ws \in WS \tag{A1}$$

$$(T_{hc}^{t} - T_{hc}^{s})FC_{hc} = \sum_{ti \in TI} \sum_{ws \in WS} q_{ws,hc,ti}, \quad hc \in HC \tag{A2}$$

Equation (A3) and (A4) describe the energy balance in each interval for each waste heat stream and each heat carrier stream. In Equation (A3), the set '[begin, end]' indicate the intervals that a waste heat stream participated.

$$\left(T_{ws,ti} - T_{ws,ti+1}\right)FC_{ws} = \sum_{hc \in HC} q_{ws,hc,ti}, \quad ws \in WS,\ ti \in [begin, end] \tag{A3}$$

$$\left(T_{hc,ti} - T_{hc,ti+1}\right)FC_{hc} = \sum_{ws \in WS} q_{ws,hc,ti}, \quad hc \in HC,\ ti \in TI \tag{A4}$$

The cold utility usage of each waste heat stream is calculated by Equation (A5), where $T_{ws,ti=end+1}$ indicates the outlet temperature of a waste heat stream at its final participated interval.

$$(T_{ws,ti=end+1} - T_{ws}^{t})FC_{ws} = qc_{ws}, \quad ws \in WS \tag{A5}$$

- ***Temperature assignment***

The inlet temperature of each stream in the superstructure can be assigned as follows. In Equation (A6), $T_{ws,ti=begin}$ refers to the inlet temperature of a waste heat stream at its beginning participated interval.

$$T_{ws,ti=begin} = T^{s}_{ws}, \quad ws \in WS \tag{A6}$$

$$T_{hc,ti=1} = T^{t}_{hc}, \quad hc \in HC \tag{A7}$$

$$T_{hc,ti=TI+1} = T^{s}_{hc}, \quad hc \in HC \tag{A8}$$

- ***Thermodynamic feasibility***

Descending trends of temperatures should be fulfilled for any streams in any of the participated intervals. The equations are presented below:

$$T_{ws,ti} \geq T_{ws,ti+1}, \quad ws \in WS, \quad ti \in [begin, end] \tag{A9}$$

$$T_{ws,ti=end+1} \geq T^{t}_{ws}, \quad ws \in WS \tag{A10}$$

$$T_{hc,ti} \geq T_{hc,ti+1}, \quad hc \in HC, ti \in TI \tag{A11}$$

- ***Logical constrains***

The existence of heat exchangers can be denoted by binary variables:

$$q_{ws,hc,ti} - \Omega \cdot Z_{ws,hc,ti} \leq 0, \quad ws \in WS, hc \in HC, ti \in [begin, end] \tag{A12}$$

$$qc_{ws} - \Omega \cdot Zc_{ws} \leq 0, \quad ws \in WS \tag{A13}$$

- ***Heat exchanger area calculations***

The feasibilities of the heat transfers between the waste heat streams and the heat carrier streams are ensured by Equation (A14) and (A15).

$$dT_{ws,hc,ti} \leq T_{ws,ti} - T_{hc,ti} + L(1 - Z_{ws,hc,ti}), \quad ws \in WS, hc \in HC, ti \in [begin, end] \tag{A14}$$

$$dT_{ws,hc,ti+1} \leq T_{ws,ti+1} - T_{hc,ti+1} + L(1 - Z_{ws,hc,ti}), \quad ws \in WS, hc \in HC, ti \in [begin, end] \tag{A15}$$

The logarithm mean temperature differences are calculated as follow (Chen, 1987):

$$LMDT_{ws,hc,ti} = \left[\frac{(dt_{ws,hc,ti})(dt_{ws,hc,ti+1})(dt_{ws,hc,ti} + dt_{ws,hc,ti+1})}{2} \right]^{1/3}, \quad ws \in WS, \ hc \in HC, \ ti \in [begin, end]$$

(A16)

The heat exchanger area can be calculated as:

$$A_{ws,hc,ti} = \frac{q_{ws,hc,ti}}{U_{ws,hc} \cdot LMDT_{ws,hc,ti}}, \quad ws \in WS,\ hc \in HC,\ ti \in [begin, end] \tag{A17}$$

Appendix B: The Peng-Robinson EoS

The Peng-Robinson Equation of State used in the power generation module is presented as below.

$$P = \frac{RT}{\nu - b} - \frac{a(T)}{\nu^2 + 2b\nu - b^2} \tag{B1}$$

Where：

$$a(T) = 0.45274 \frac{R^2 T_c^{\,2}}{P_c} \alpha(T, \omega)$$

$$b = 0.45724 \frac{R^2 T_c^{\,2}}{P_c}$$

$$\alpha(T, \omega) = \left[1 + \kappa(1 - (T / T_c)^{0.5})\right]^2$$

$$\kappa = 0.37464 + 1.54226\omega - 0.26992\omega^2$$

T_c and P_c are the critical temperature and pressure, ω is the acentric factor.

For computational convenience, the P-R EoS can be transformed to:

$$Z^3 + (B-1)Z^2 + (A - 3B^2 - 2B)Z + (B^3 + B^2 - AB) = 0 \tag{B2}$$

Where

$$A = \frac{a(T)P}{(RT)^2}$$

$$B = \frac{bP}{RT}$$

$$Z = \frac{P\nu}{RT}$$

Note that the unit of pressure is used as **Mpa** in the P-R EoS, which is different with the **kpa** unit used in this paper. The enthalpy and entropy of a substance at given temperature and pressure (T_1, P_1) can be calculated as:

$$H(T_1, P_1) - H(T_{ref}, P_{ref}) = H^*(T_{ref}, P_{ref}) + \int_{T_{ref}}^{T_1} C_p^{id} dT - H^*(T_1, P_1) \tag{B3}$$

$$S(T_1,P_1)-S(T_{ref},P_{ref})=S^*(T_{ref},P_{ref})+\int_{T_{ref}}^{T_1}\frac{C_p^{id}}{T}dT-R\ln\frac{P_1}{P_{ref}}-S^*(T_1,P_1) \quad \text{(B4)}$$

Where：

$$\frac{H^*(T,P)}{RT_c}=2.078(1+\kappa)[1+\kappa(1-T_r^{1/2})]\ln[\frac{Z+(1+\sqrt{2})B}{Z+(1-\sqrt{2})B}]-T_r(Z-1)$$

$$\frac{S^*(T,P)}{R}=2.078\kappa[\frac{1+\kappa}{T_r^{1/2}}-\kappa)]\ln[\frac{Z+(1+\sqrt{2})B}{Z+(1-\sqrt{2})B}]-\ln(Z-B)$$

$$T_r=\frac{T}{T_c}$$

Note that the unit of the enthalpy and entropy calculated by the P-R EoS is configured as **molar basis** which is different from the **mass basis** unit used in this paper. T_{ref} and P_{ref} are the given reference temperature and pressure, $H(T_{ref},P_{ref})$ and $S(T_{ref},P_{ref})$ are the enthalpy and entropy at the given reference state. C_p^{id} is the ideal gas heat capacity which can be calculated by the DIPPR107 equation (Aly and Lee, 1981), as presented in Equation (B5).

$$C_p^{id}=C_1+C_2\left[\frac{C_3/T}{\sinh(C_3/T)}\right]^2+C_4\left[\frac{C_5/T}{\cosh(C_5/T)}\right]^2 \quad \text{(B5)}$$

Where C_1, C_2, C_3, C_4, and C_5 are regression parameters, the value of them for N-Butane are listed in the table below.

Table B1. Parameters in DIPPR107 for N-Butane

DIPPR107 Parameter	C_1	C_2	C_2	C_4	C_5
Butane	71340	243000	1630	150330	730.42

The Extended Antonie Equation is used in this paper to formulate the relationship between the saturated vapor pressures and the corresponding temperatures, as presented in Equation (B6).

$$\ln P_{sat}=A_1+\frac{A_2}{(T_{sat}+A_3)}+A_4T_{sat}+A_5\ln T_{sat}+A_6T_{sat}^{A_7} \quad \text{(B6)}$$

Where $A_{1\sim6}$ are regression parameters, the value of them for N-Butane are listed in Table B2 below.

Table B2. Parameters in Extended Antonie Function for N-Butane

Parameter	A_1	A_2	A_2	A_4	A_5	A_6	A_7
N-Butane	59.44	-4363.20	0	0	-7.05	9.45e-06	2

References

Aly, F. and Lee, L., 1981. Self-consistent equations for calculating the ideal gas heat capacity, enthalpy, and entropy. *Fluid Phase Equilibria*, 6(3-4), pp.169-179.

Chen, C., Chang, F., Chao, T., Chen, H. and Lee, J. (2014). Heat-Exchanger Network Synthesis Involving Organic Rankine Cycle for Waste Heat Recovery. Industrial & Engineering Chemistry Research, 53(44), pp.16924-16936.

Desai, N. and Bandyopadhyay, S. (2009). Process integration of organic Rankine cycle. *Energy*, 34(10), pp.1674-1686.

Dong, X., Liao, Z., Sun, J., Huang, Z., Jiang, B., Wang, J. and Yang, Y., 2020. Simultaneous Optimization for Organic Rankine Cycle Design and Heat Integration. *Industrial & Engineering Chemistry Research*, 59(46), pp.20455-20471.

Duran, M.A., Grossmann, I.E., 1986. Simultaneous optimization and heat integration of chemical processes. AIChE J. 32, 123–138.

Floudas, C.A., Ciric, A.R., Grossmann, I.E., Automatic synthesis of optimum heat exchanger network configurations, *AIChE Journal*, 32 (2) (1986) 276.

Hipólito-Valencia, B., Rubio-Castro, E., Ponce-Ortega, J., Serna-González, M., Nápoles-Rivera, F. and El-Halwagi, M., 2013. Optimal integration of organic Rankine cycles with industrial processes. Energy Conversion and Management, 73, pp.285-302.

Huang, X., Lu, P., Luo, X., Chen, J., Yang, Z., Liang, Y., Wang, C. and Chen, Y., 2020. Synthesis and simultaneous MINLP optimization of heat exchanger network, steam Rankine cycle, and organic Rankine cycle. Energy, 195, p.116922.

Isafiade, A. and Fraser, D., 2008. Interval-based MINLP superstructure synthesis of heat exchange networks. Chemical Engineering Research and Design, 86(3), pp.245-257.

Kermani, M., Wallerand, A., Kantor, I. and Maréchal, F., 2018. Generic superstructure synthesis of organic Rankine cycles for waste heat recovery in industrial processes. *Applied Energy*, 212, pp.1203-1225.

Kyle, B., 1992. *Chemical and process thermodynamics*. Englewood Cliffs, N.J.: Prentice Hall.

Martelli, E., Elsido, C., Mian, A. and Marechal, F., 2017. MINLP model and two-stage algorithm for the simultaneous synthesis of heat exchanger networks, utility systems and heat recovery cycles. *Computers & Chemical Engineering*, 106, pp.663-689.

Papoulias, S.A., Grossmann, I.E., 1983. A structural optimization approach in process synthesisdII: heat recovery networks. Comput. Chem. Eng. 7 (6), 15.

Poling, B.E., Prausnitz, J.M., O'Connell, J.P., *The properties of gases & liquids (5th ed.)*, McGraw-Hill, New York (2001)

Sahinidis, N.V., BARON: a general purpose global optimization software package, *Journal of Global Optimization*, 8 (2) (1996) 201e205.

Stijepovic, M., Papadopoulos, A., Linke, P., Stijepovic, V., Grujic, A., Kijevčanin, M. and Seferlis, P., 2017. Organic Rankine Cycle system performance targeting and design for multiple heat sources with simultaneous working fluid selection. Journal of Cleaner Production, 142, pp.1950-1970.

Wang, S., Liu, C., Li, Q., Liu, L., Huo, E. and Zhang, C., 2020. Selection principle of working fluid for organic Rankine cycle based on environmental benefits and economic performance. Applied Thermal Engineering, 178, p.115598.

Yee, T. and Grossmann, I., 1990. Simultaneous optimization models for heat integration—II. Heat exchanger network synthesis. *Computers & Chemical Engineering*, 14(10), pp.1165-1184.

Yu, H., Feng, X. and Wang, Y., 2015. A new pinch based method for simultaneous selection of working fluid and operating conditions in an ORC (Organic Rankine Cycle) recovering waste heat. *Energy*, 90, pp.36-46.

Yu, H., Eason, J., Biegler, L. and Feng, X., 2017a. Simultaneous heat integration and techno-economic optimization of Organic Rankine Cycle (ORC) for multiple waste heat stream recovery. Energy, 119, pp.322-333.

Yu, H., Eason, J., Biegler, L. and Feng, X., 2017b. Process integration and superstructure optimization of Organic Rankine Cycles (ORCs) with heat exchanger network synthesis. Computers & Chemical Engineering, 107, pp.257-270.

Yu, H., Gundersen, T. and Feng, X., 2018. Process integration of organic Rankine cycle (ORC) and heat pump for low temperature waste heat recovery. *Energy*, 160, pp.330-340.

Zhu, X., 1997. Automated design method for heat exchanger network using block decomposition and heuristic rules. *Computers & Chemical Engineering*, 21(10), pp.1095-1104.

Supplementary material: The validations of Modified-IBMS

To validate the proposed modified IBMS, two case studies are carried out. In each case study, given several hot and cold process streams, the corresponding HEN synthesis problems are to be solved by different superstructure-based methodologies (the SWS, the IBMS, and the modified IBMS), and the solving results are compared. The General Algebraic Modelling System (GAMS) with the Baron solver is applied as the mathematical programming platform.

Case study 1

In this case, a small-scale HEN synthesis problem with 3 hot process streams and 4 cold process streams are imported. This case is taken from the third Example of Isafiade and Fraser (2008). The problem data is presented in Table S1.

Table S1. The problem data for case study 1 (Isafiade and Fraser, 2008)

Stream	Ts (℃)	Tt (℃)	FC (kW/℃)	h (kW/m^2 ℃)
H1	626	586	9.802	1.25
H2	620	519	2.931	0.05
H3	528	353	6.161	3.20
C1	497	613	7.179	0.65
C2	389	576	0.641	0.25
C3	326	386	7.627	0.33
C4	313	566	1.690	3.20
HU	650	650		3.50
CU	293	308		3.50

For each heat exchanger: Annulized cost = 8600 +670 * (Area)^0.83

Cold utility: 20$ kW^{-1}year^{-1}

Hot utility: 110$ kW^{-1}year^{-1}

The optimum solutions provided by the different methodologies are summarized in Table S2. It can be seen that all of the three methodologies can bring up similar optimization results,

which are around **169631 $ year^{-1}.** The optimization result of the modified-IBMS model exhibits a deviation less than **0.5%** with the literature result offered by Isafiade and Fraser (2008). The results show that the modified IBMS has the highest calculation efficiency as its CPU time usage is only **37.48s**.

Table S2. The optimization results for case study 1

Solver: Baron (this study)	SWS (this study)	IBMS (this study)	Modified IBMS (this study)	Literature result (Isafiade and Fraser, 2008)
No. of stages	4	7	3	7
Single variables	336	379	190	/
Discrete variables	55	40	27	/
CPU time (s)	73.95	1750.78	37.48	/
Objective ($ year^{-1})	169631	169631	169631	168700
Relative deviation	0.55%	0.55%	0.55%	0
No. of units	7	7	7	10
Cold utiliy (kW)	369.149	369.149	369.149	172.6
Hot utility (kW)	440.684	440.684	400.684	244.2

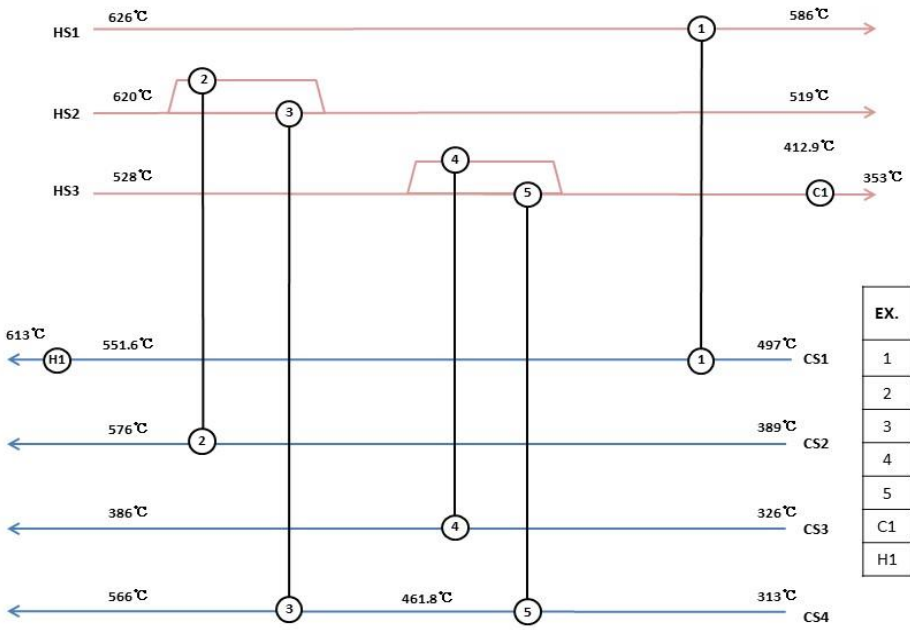

EX.	Q_L (kW)	Area (m2)
1	392.1	11.3
2	119.9	36.3
3	176.2	64.4
4	457.6	13.6
5	251.4	1.9
C1	369.1	2.7
H1	440.7	12.8

Figure S1. SWS network for case study 1 with seven heat exchanger units

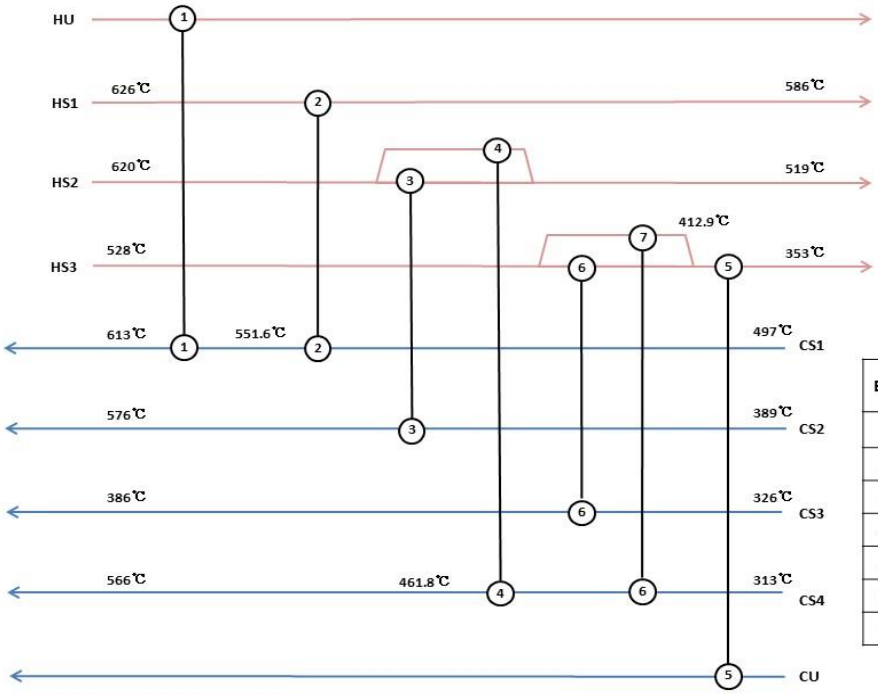

EX.	Q_L (kW)	Area (m2)
1	440.7	12.8
2	392.1	11.3
3	119.9	36.3
4	176.2	64.4
5	369.1	2.7
6	457.6	13.6
7	251.4	1.9

Figure S2. IBMS network for case study 1 with seven heat exchanger units

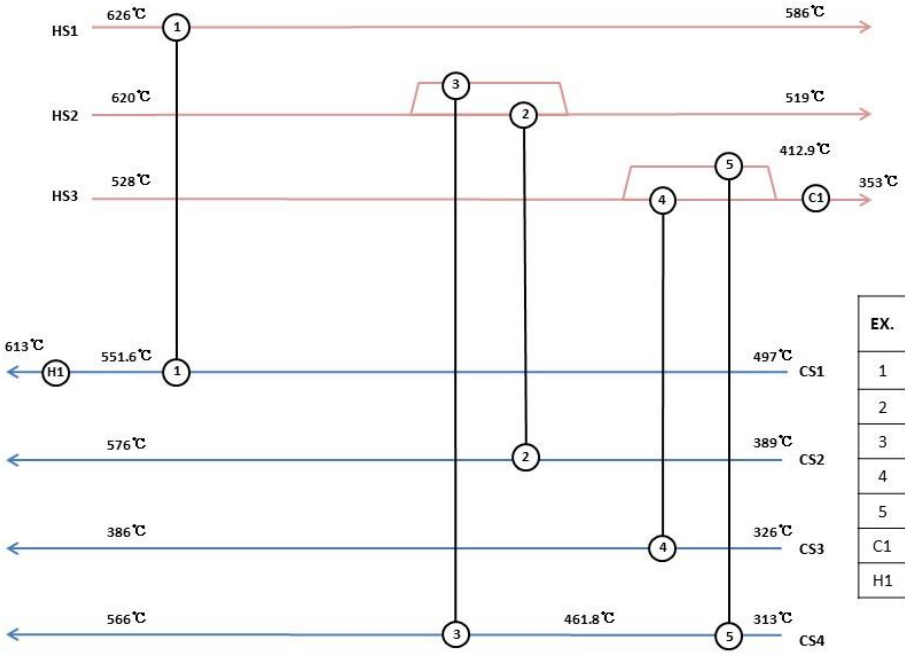

EX.	Q_L (kW)	Area (m2)
1	392.1	11.3
2	119.9	36.3
3	176.2	64.4
4	457.6	13.6
5	251.4	1.9
C1	369.1	2.7
H1	440.7	12.8

Figure S3. Modified IBMS network for case study 1 with seven heat exchanger units

Case study 2

This case study comes up with a medium-sized HEN synthesis problem. The problem data (listed in Table S3) is taken from Papoulias and Grossmann (1983), which is also adopted by Escobar and Trierweiler (2013).

In this case, we set 1800 seconds of CPU time as the maximum computational time for the Baron solver. Within the limited time, the optimum solutions provided by the different methodologies are summarized in Table S4. Compared with the SWS, the modified IBMS can come up with a better solution **(43610.6 \$ year^{-1})** occupying much less CPU time **(68.6 s)**.

Table S3. The problem data for case study 2 (Papoulias and Grossmann, 1983)

Stream	Ts (℃)	Tt (℃)	FC (kW/℃)	h (kW/m^2 ℃)
H1	433	366	8.79	1.7

H2	522	411	10.55	1.7
H3	544	422	12.56	1.7
H4	500	339	14.77	1.7
H5	472	339	17.73	1.7
C1	355	450	17.28	1.7
C2	366	478	13.9	1.7
C3	311	494	8.44	1.7
C4	333	433	7.62	1.7
C5	389	495	6.08	1.7
CU	311	355		1.7
HU	509	509		3.41

For each heat exchanger: Annulized cost = 145.63 * (Area)^0.6

Cold utility: 18.12 $ kW-1year−1

Hot utility: 37.64 $ kW-1year−1

Table S4. The optimization results for case study 2

Solver: Baron (this study)	SWS (this study)	Modified IBMS (this study)	Literature result (Escobar and Trierweiler, 2013).
No. of stages	5	5	/
Single variables	815	601	/
Discrete variables	160	160	/
A feasible solution found at (s)	1051.5 (max. 1800)	68.6 (max. 1800)	/
Objective ($ year^{-1})	43703.9	43610.6	43570.3
Relative deviation	0.31%	0.09%	0
No. of units	10	10	10

Cold utiliy (kW)	1878.96	1878.96	1879
Hot utility (kW)	0	0	0

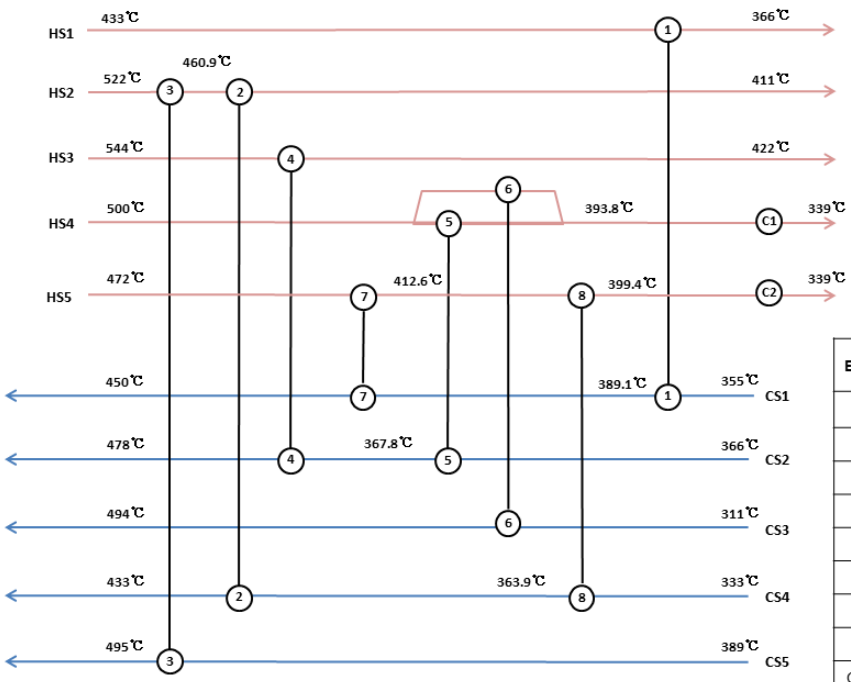

EX.	Q_L (kW)	Area (m2)
1	588.9	29.3
2	526.6	16.9
3	644.5	16.6
4	1532.3	30.1
5	24.5	0.4
6	1544.5	64.8
7	1052.7	54.4
8	235.4	4.9
C1	809.0	22.1
C2	1070.0	27.9

Figure S4. SWS network for case study 2 with ten heat exchanger units

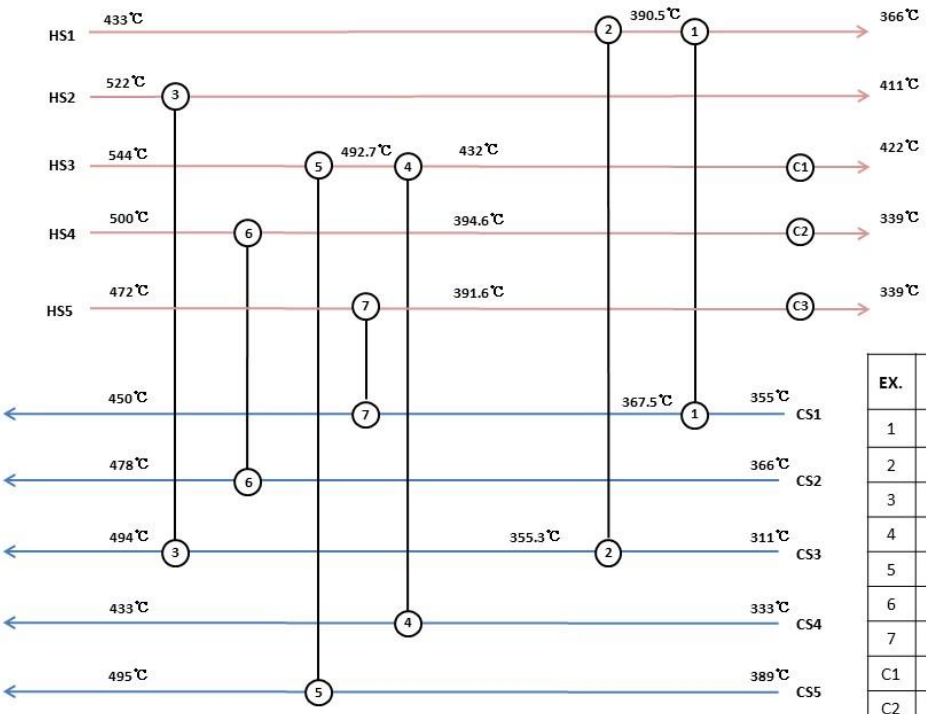

EX.	Q_L (kW)	Area (m2)
1	215.5	15.6
2	373.5	5.6
3	1171.1	34.2
4	762.0	11.5
5	644.5	10.4
6	1556.8	72.8
7	1426.1	72.8
C1	125.8	1.4
C2	821.2	22.3
C3	931.9	26.0

Figure S5. Modified IBMS network for case study 2 with ten heat exchanger units

References

Isafiade, A. and Fraser, D., 2008. Interval-based MINLP superstructure synthesis of heat exchange networks. *Chemical Engineering Research and Design*, 86(3), pp.245-257.

Papoulias, S. and Grossmann, I., 1983. A structural optimization approach in process synthesis—II. *Computers & Chemical Engineering*, 7(6), pp.707-721.

Escobar, M. and Trierweiler, J., 2013. Optimal heat exchanger network synthesis: A case study comparison. *Applied Thermal Engineering*, 51(1-2), pp.801-826.

Chapter 4: Direct Integration of ORCs

This chapter contains one journal-format paper, providing a mathematical programming-based method that adopts the direct-heat-transfer strategic option for ORC integration problems. The method also allows for integrating more than one ORC unit, leading to an arrangement of multi-parallel ORCs

4.1 Introduction to Publication 2

The paper presented in this chapter contributed a mathematical programming-based method for solving the direct integration of ORCs. For the model establishment, first, a novel stage-wise superstructure is specifically developed to represent the direct integration of ORCs. The superstructure can separate an evaporating ORC working fluid into a preheating sub-flow and a two-phase sub-flow so that the difficulties in calculating the heat transfer area of evaporators can be avoided; second, the Peng-Robinson Equation of State is adopted to formulate the thermodynamic properties of ORC working fluids, which can improve the accuracy on calculating the net power output of an ORC system. The established mathematical model leads to an MINLP optimization problem.

For optimization, first, this work adopts a Pinch Analysis-based NLP model as the initialization model, through solving which good starting points can be provided for the MINLP master model. Note that the applicability of the NLP model has been verified by Dong et al (2020a). Second, an iterative solution procedure is developed, which can simultaneously determine the optimal unit number of ORCs, the optimal working conditions of each ORC, and the optimal HEN synthesis.

The case study compares the integration results given by the proposed method and the previous literature. The results indicate the progressiveness of the proposed method.

4.2 Publication 2

Chu Z., Nan Z., Smith R., The Opportunities of Integrating Multi-Parallel ORCs into Total Site for Waste Heat Recovery (ready for submission)

The Opportunities of Integrating Multi-Parallel ORCs into Total Site for Waste Heat Recovery

Zheng Chu, Nan Zhang*, Robin Smith

Centre for Process Integration, Department of Chemical Engineering and Analytical Science, the University of Manchester, M13 9PL, Manchester, United Kingdom

nan.zhang@manchester.ac.uk

Abstract

Organic Rankine Cycle (ORC), which can convert low-grade heat into electricity, has been regarded as a promising technology for waste heat recovery. In industrial applications, the integration of ORCs with background manufacturing processes is a crucial matter that should be considered. Lots of analysis methods have been developed for dealing with ORC integration. It is observed that most of the existing analysis methods are for integrating a single ORC, while the integration of multi-parallel ORCs is rarely discussed. As such, this work aims to propose a mathematical programming-based method for integrating multi-parallel ORCs. For modelling, a stage-wise superstructure is proposed, which is extended from the SYNHEAT superstructure (Yee and Grossmann, 1990). The superstructure allows one to implement any number of ORCs. Besides, rigorous thermodynamic correlations are imported (i.e., the Peng-Robinson Equation of State and the Extended Antonie Equations) to formulate the thermodynamic properties of ORC working fluids. The established model leads to a mixed-integer non-linear programming (MINLP) problem. Through solving the model, the optimal operations of ORCs and the corresponding HEN synthesis can be simultaneously determined. For optimization, an initialization model is imported, which can offer starting points for the MINLP model, guaranteeing the quality of optimization results. The applicability of the proposed method is validated by a case study. Results of the case study show that multi-parallel ORCs can achieve a lower total annualized cost than a single ORC.

Nomenclature

Variables			
Cap	total capital cost ($)	Obj	objective variable
dT	temperature difference (K)	q (Q)	heat duty (kJ)
FC	heat capacity flowrate (kW/K)	T	temperature (K)
HA	heat exchanger area (m^2)	V	volume flowrate (m^3/s)
h (H)	enthalpy (kJ/kg)	W	shaft work output (kW)
LMDT	logarithm approach temperature	Z	binary variable
m	mass flowrate (kg/s)	ρ	density (kg/m^3)
Parameters			
AF	annualized factor	U	heat transfer coefficient
AOH	annual operating hours	η	Isentropic efficiency
L	a constant value	Ω	a constant value
Subscripts			
cu	cold utility	out	outlet
cw	cooling water	pre	pre-heating
de-sup	de-superheating	pump	pump
elec	electricity	s	supply
eva	evaporating/evaporator	re	recovered heat
in	inlet	t	target
int	intermediate	tb	turbine
liq	liquifying	wf	ORC working fluid
latent	latent heat	1, 2, 3, …6	state points
min	the minimum value	2is	isentropic state point
Sets			
cs	solid nodes of cold side	cs_ord	sorted solid nodes of cold side
ct_ord	sorted total nodes of cold side	hs	solid nodes of hot side
hs_ord	sorted solid nodes of hot side	ht_orc	sorted total nodes of hot side
orc	elements in the set of ORCs ORC= {orc|1, 2 ... n}	ws	elements in the set of waste heat streams WS= {ws|1, 2 ... n}
st	elements in the set of stages ST= {st|1, 2 ... ST}		

1. Introduction

Organic Rankine Cycle (ORC), which can convert low-grade heat into electricity, is a promising technology for recovering industrial waste heat. ORCs have a similar working principle with the conventional steam-based Rankine Cycles but use organic compounds instead of water as working fluids. At the same pressure with water, the organic compounds usually have lower saturated temperatures, guarantee the operability of ORCs when coping with low-grade heat sources. An ORC is typically configured with an evaporator, an expander, a condenser, and a pump. When operating, a strand of working fluid is evaporated in the evaporator, absorbing waste heat. The vaporised stream is then sent to the expander to generate electricity. The exhausted gas of the expander is condensed by the condenser and is recycled by the pump.

When applying ORCs in industrial sites, there are usually multiple waste heat sources with various temperatures and heat duties. To achieve the maximum profit, how to extract the waste heat effectively and generate electricity efficiently are crucial questions that should be answered. Lots of systematic analysis methodologies dealing with the questions has been proposed in the last decades.

Desai and Bandyopadhyay (2009) developed a graphical-aided method for integrating a single ORC. Based on the grand composite curve of given background processes, the method can help to estimate the near-maximum electricity generation of an ORC. Once the electricity generation is estimated, the operation of the ORC can be correspondingly determined. Though the graphical-aided method has advantages of intuitiveness, simplicity and clarity (Liu et al., 2014), the optimization results are sub-optimum, and the solving process could consume lots of manual works. Hipólito-Valencia et al. (2013) developed a mathematical programming-based method for integrating a single ORC with multiple waste heat sources, of which the objective is to minimize the total annual cost. The method can automatically carry out HEN synthesis. However, the optimal operation of the ORC is manually determined by trial and error. Chen et al. (2014) contributed to the ORC integration problem by developing a two-

step sequential method. The first step is to identify the heat surplus zone of the given background process streams. Then, a model for integrating a single ORC with the heat surplus zone is established in the next step. The model adopts the Synheat superstructure (Yee and Grossman, 1990) to carry out the HEN synthesis and the Peng-Robinson Equation of State to calculate the relevant thermodynamic properties, leading to a mixed-integer non-linear programming (MINLP) problem. By solving the MINLP, the optimal HEN structure and the optimal operation of the ORC can be simultaneously determined. However, the economic performances of the integrated ORC are not evaluated. Yu et al. (2017b) proposed another sequential method for solving ORC integration problems. In the first step, an NLP model is established to maximize the power generation of ORC without importing extra utility costs. In the second step, a MILP model is formulated to carry out the corresponding HEN synthesis.

Kermani et al. (2018) upgraded the ORC integration problem by considering multiple choices of ORC working fluids and architectures. For modelling, they proposed a novel superstructure to represent the multiple architecture selections of an ORC. For optimization, they applied a bi-level solution strategy, which adopts the Genetic Algorithm (GA) as a master level and mixed-integer linear programming (MILP) as the slave level. The master level is responsible for determining the optimum working fluid, ORC operating pressures and temperatures. The slave level can offer the best choice of ORC architecture. Dong et al. (2020) integrated a single ORC with background processes taking into account various selections of ORC working fluid. In terms of modelling, they developed an NLP model based on the interval heat transfer concept (Linnhoff and Ahmad, 1990), which can consider the trade-off between the capital costs, operating costs and the profit brought up by power generation. In terms of optimization, they developed a bi-level solution strategy, which uses the developed NLP model as a slave level and the GA algorithm as the master level to determine the optimal working fluid selection.

Elsido et al. (2019) and Huang et al. (2020) integrated an ORC with manufacturing processes and utility systems. Elsido et al. (2019) came up with a novel superstructure, namely *p*-

h superstructure, to tackle the synthesis and designs of utility systems. As for the synthesis of manufacturing processes, the Synheat superstructure (Yee and Grossman, 1990) is adopted. The overall model is established by combining the p-h superstructure and the Synheat superstructure, leading to an MINLP problem. Huang et al. (2020) established an MINLP model, which can simultaneously carry out the synthesis of utility systems, the heat integration of process streams, and the optimization of an ORC.

A brief conclusion of the literature review can be given. Desai and Bandyopadhyay (2009) developed a graphical-aided analysis method for integrating a single ORC, which could be regarded as the beginning of the investigation of ORC integration problems. Hipólito-Valencia et al. (2013) and Chen et al. (2014) laid the foundation of the mathematical programming-based methods for integrating a single ORC. Chen et al. (2016) and Yu et al. (2017b) provided different ways of model establishment for the mathematical programming-based methods. Kermani et al. (2018) and Dong et al. (2020) highlighted the necessity of considering the multiple choices of ORC working fluids and architectures. Elsido et al. (2019) and Huang et al. (2020) extended the ORC integration problem by considering the cooperation with utility systems. Table 1 provides a summarization of the previous work dealing with ORC integration problems. It can be seen that the research on ORC integration problems has gained significant improvements. However, we have observed that most of the developed methodologies are for integrating a single ORC, while few studies discuss the integration of multiple ORCs (i.e., multi-parallel ORCs).

We conceived that it is worth discussing the integration of multi-parallel ORCs. Yu et al. (2018) pointed out that a single ORC (subcritical) could have a weak thermal match with background heat sources. As illustrated in Figure 1, due to the isothermal boiling process of the ORC working fluid, a pinch point is formed between the evaporating working fluid and the waste heat stream. Limited by the pinch point, if one tends to increase the evaporation temperature to improve thermal efficiency, the heat recovery should be decreased (represented by the

green line), vice versa (represented by the purple line). In this case, to obtain the optimum design (represented by the blue line), the maximum heat recovery should be given up to ensure a proper evaporation temperature. The applying of multi-parallel ORCs could avoid the pinch limitation, through which the thermal match with heat sources can be improved, and more electricity can be generated (Stijepovic et al., 2017). For example, as shown in Figure 2, there are two parallels of ORCs with different evaporation temperatures. The parallel with higher evaporation temperature can achieve higher thermal efficiency, while another parallel can guarantee maximum heat recovery. The cooperation of the two parallels performs a better thermal match than a single ORC, leading to more electricity generation. Though applying multi-parallel ORCs could generate more electricity, it will also bring up more capital costs. In applications, the trade-off between more electricity generation and the extra capital cost should be considered to determine whether to use multi-parallel ORCs or not. It is logical to deduce that, with proper integration, the multi-parallel ORCs can have better economic performances than a single ORC for some cases. Therefore, it is necessary to develop a systematic analysis method for integrating multi-parallel ORCs.

This study aims to address the integration of multi-parallel ORCs with industrial sites for waste heat recovery by proposing a systematic analysis method. In the method, a mathematical programming-based model will be established, leading to an MINLP problem. To guarantee the quality of the optimization results, this study also proposes an NLP initialization model based on the Pinch Analysis concepts. Through sequentially solving the NLP and MINLP problems, the following questions for integrating multi-parallel ORCs are expected to be solved:

1). The synthesis of HEN for extracting waste heat

2). The optimum parallel numbers

3). The optimum operations of each ORC parallel

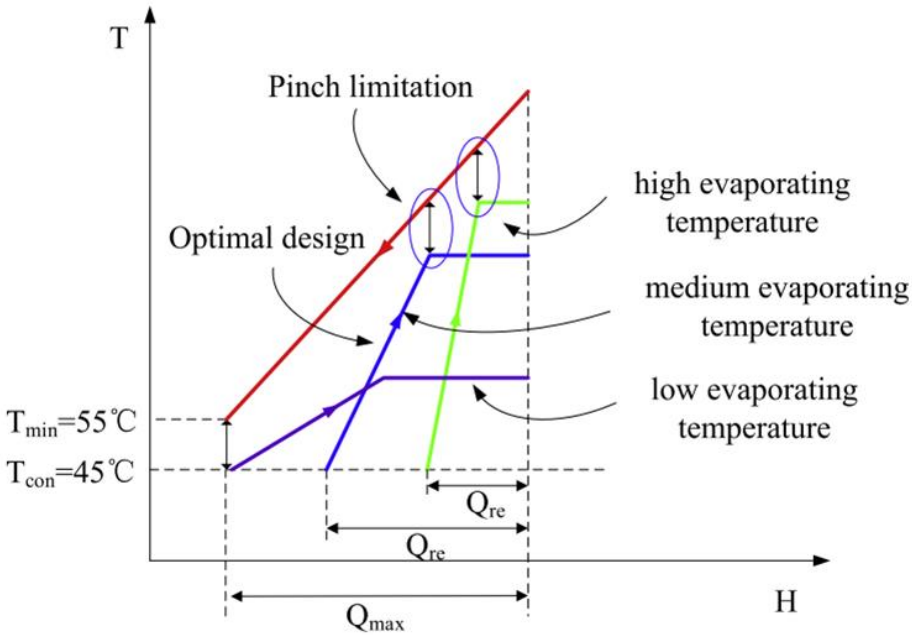

Figure 1. The weak thermal match caused by pinch limitation (Yu et al., 2018)

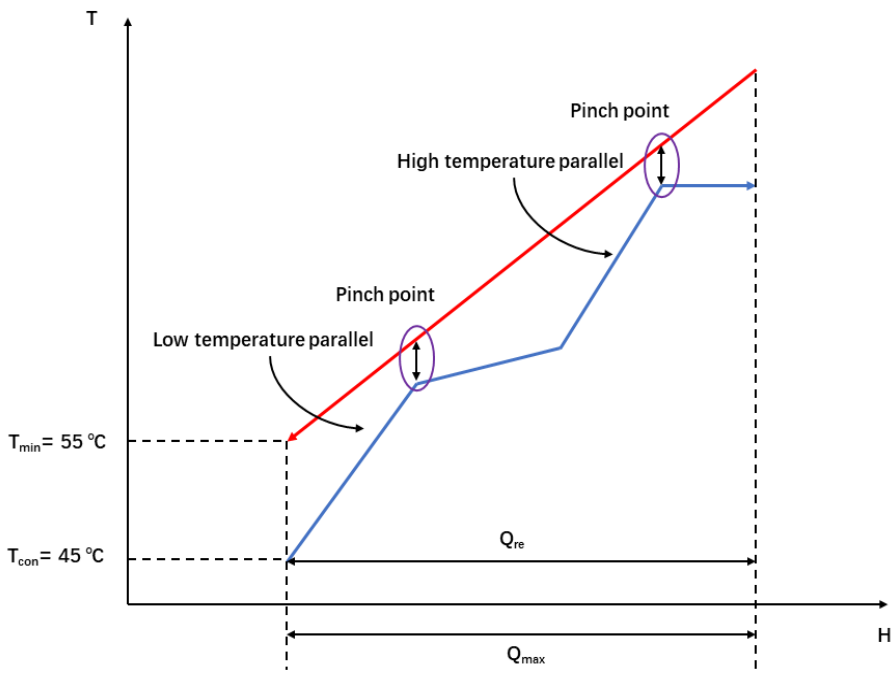

Figure 2. The improved thermal match by applying double-parallel ORCs

Table 1. An overview of the previous work in the field of ORC integration

Articles	Objective(s)	Modelling/ optimization strategy	HEN synthesis	Multi-parallel ORCs	Automatically working fluid selection	Automatically architecture selection
Desai and Bandyopadhyay (2009)	Max. power output	/	N	N	N	N
Hipólito-Valencia et al. (2013)	Min. total cost	MINLP	Y	N	N	N
Chen et al. (2014)	Max. power output	MINLP	Y	N	N	N
Song et al. (2014)	Max. power output	/	N	N	N	N
Yu et al. (2017a)	Min. total cost	NLP+MILP	Y	N	N	N
Yu et al. (2017b)	Min. total cost	NLP	Y	N	N	N
Kermani et al. (2018)	Min. total cost	GA+MILP	Y	N	Y	Y
Elsido et al. (2019)	Min. total cost	MILP+NLP	Y	N	N	Y
Dong et al. (2020)	Min. total cost	NLP	N	N	Y	N
Huang et al. (2020)	Min. total cost	MINLP	Y	N	N	N
This study	Min. total cost	NLP+MINLP	Y	Y	N	N

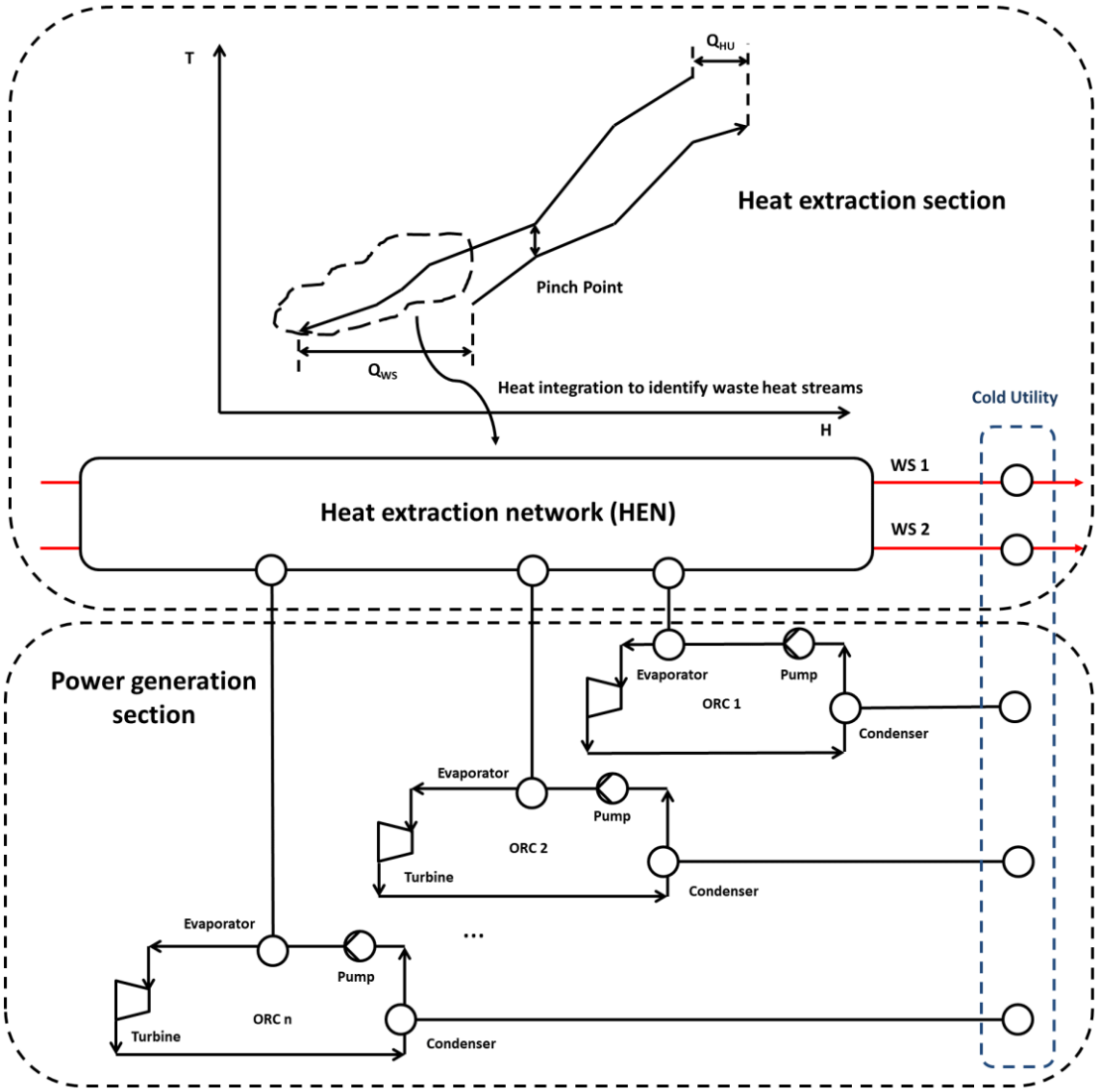

Figure 3. The schematic diagram of the multi-parallel arrangement

2. Problem Statement

Figure 3 depicts the illustration diagram of a multi-parallel ORCs system. The whole system can be geographically separated into a heat extraction section and a power generation section. In the heat extraction section, the waste heat streams can be directly provided or identified by the heat integration of background processes. In this study, we can assume that the waste heat streams have been already identified, given as WS= {ws|1, 2 ... n}. The heat capacity flow rates, supply and target temperatures, and heat transfer coefficients of the waste heat streams are known. The waste heat streams transfer their heat to the downstream ORCs in

parallel and discharge the residual heat to a cold utility. In the power generation section, there is a series of ORCs in parallel, ORC = {orc|1, 2 ... n}, and each ORC train is operated independently. The evaporators are the connections between the ORCs and the waste heat streams, in which waste heat is transferred to ORC working fluids. The exhausting heat of the turbines is discharged to the cold utility through the condensers. The operating temperatures/pressures of the evaporators and the condenser, and the mass flow rate of ORC working fluids, are variables to be determined. The isentropic efficiencies of the turbines are assumed as constant. In addition, the relevant economic data (e.g., the prices of electricity and utilities, the cost models of the working components, etc.) is provided.

The following simplifying assumptions are made:

1) The heat capacity flowrates of the ORC working fluids (preheating and evaporating) are assumed as constants
2) The heat transfer coefficients of the two-phase (evaporating or condensing) ORC working fluids are regarded as constants
3) The pressure drops in heat exchangers and pipelines are neglected
4) All heat exchangers adopt a counter-flow arrangement
5) The heat losses are ignored
6) The cost of pipelines is not considered
7) The changes in kinetic and potential energy are neglected
8) The working conditions of the system component are in steady-state
9) There are no working fluid consumptions during operations

3. Model Description

In this study, a superstructure for the synthesises and designs of the overall multi-parallel system is proposed in advance. Once the superstructure is established, the corresponding mathematical model can be formulated. The construction of the superstructure will be introduced in the first section of this chapter, and the model formulation will be shown in the

second section.

3.1. Superstructure representation

An illustration diagram of the superstructure is shown in Figure 4. Corresponding to the section division in the problem statement, the overall superstructure can be also divided into a heat extraction section (circled by the yellow dashed lines) and a power generation section (circled by the green dashed lines).

3.1.1. Heat extraction section

The heat extraction section is a stage-wise superstructure, constructing the HEN between waste heat streams and ORC working fluids. The superstructure can be viewed as an extension of the one (i.e., the SYNHEAT superstructure) proposed by Yee and Grossman (1990). In this section, the waste heat streams and ORC working fluids are regarded as hot and cold streams, respectively. For the hot side, this superstructure uses the same way as the SYNHEAT superstructure to divide stages and split/mix the streams. For the cold side, due to the isothermal boiling processes of the ORC working fluids, using the same way to divide stages and split/mix the streams could cause difficulties in the calculations of heat transfer coefficients and heat capacity flowrates, as it is hard to tell when and where the evaporation processes occur. To avoid such difficulties, in this superstructure, each of the ORC working fluids is divided into a pre-heating stream and an evaporating stream. The pre-heating stream corresponds to the pre-heating process in an evaporator, the thermo-state of which is changing from sub-cooling liquid state to saturated liquid state. While the evaporating stream corresponds to the evaporation process in the evaporator, the thermo-state of which is changing from saturated liquid state to saturated vapor state. The same principles of stage division and stream splitting/mixing as the hot side are also suitable for the pre-heating streams. As for the evaporating streams, there is no stage divided. Each evaporating stream is split into several sub-streams in parallel. Each paralleled sub-stream is directed to a heat exchanger, representing one possible match with the waste heat streams. The number of the sub-streams

to be split is determined by the following equation.

$$N_{split} = N_{stage} \cdot N_{ws}$$

Where N_{split} is the spilt sub-streams of an evaporating stream; N_{stage} is the total number of the divided stages; N_{ws} is the total number of the waste heat streams.

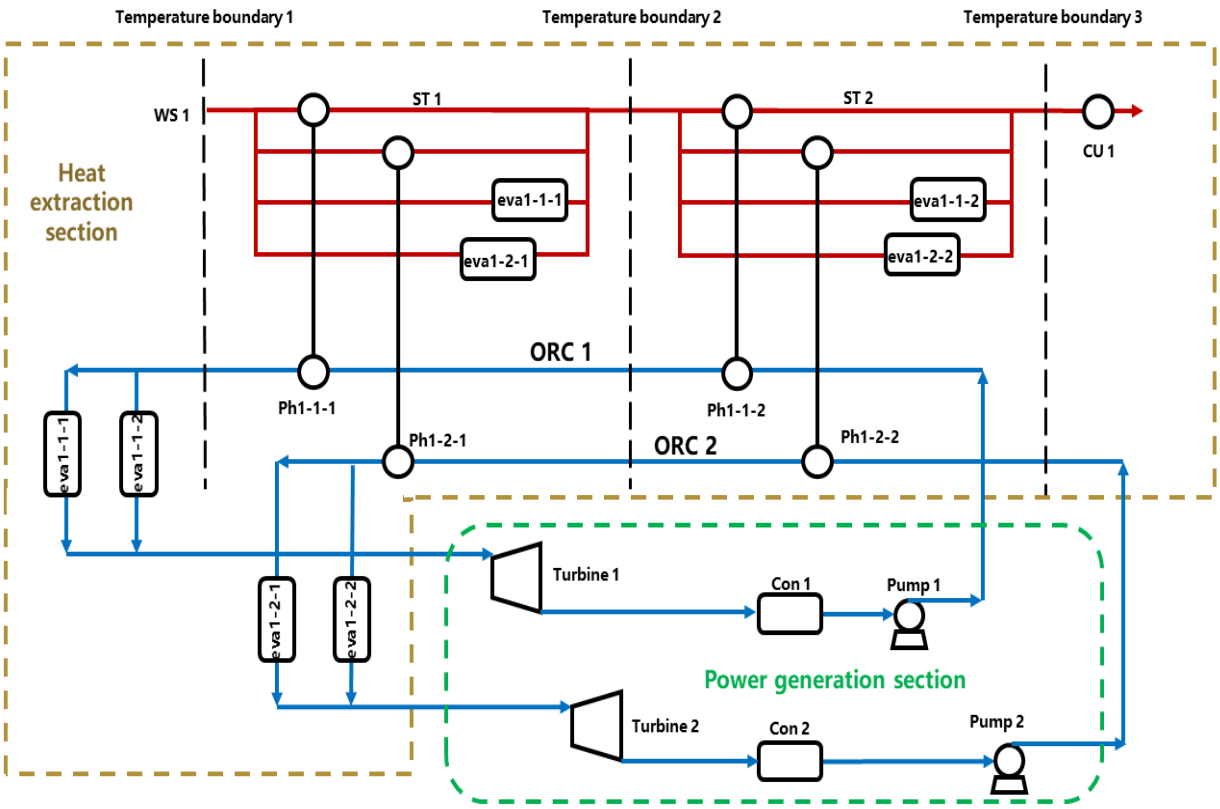

Figure 4. The schematic diagram of the multi-parallel ORCs superstructure

For a more precise understanding, we can take Figure 4 as an example to illustrate the construction of the heat extraction section. In Figure 4, there are one strand of waste heat stream (WS1) and two ORC parallels (ORC1 and ORC2). According to the SYNHEAT superstructure, two stages (ST1 and ST2) are divided. At each stage, the waste heat stream is split into four paralleled sub-streams, while the pre-heating ORC working fluid is not split, as there is only one strand of waste heat stream. As for the evaporating ORC working fluids, they are not divided by any stages, but each is split into two paralleled sub-streams. Once the stage

division and stream splitting procedures are finished, each split stream in each stage will be directed to a heat exchanger, exclusively matching a corresponding sub-stream on the opposite side. For instance, the heat exchanger marked as 'ph1-1-1' represents the match between 'WS1' and the pre-heating working fluid of 'ORC1' at the first stage; the heat exchanger marked as 'eva1-1-2' represents the match between 'WS1' and the evaporating working fluid of 'ORC1' at the second stage.

3.1.2. Power generation section

The power generation section consists of the turbines, pumps and condensers of the multi-parallel ORCs. The inlet working fluids of this section are received from the heat extraction section and are sent to the turbines to generate power. In the condensers, the exhausted gases of the turbines are condensed by cold utilities. The condensed working fluids are then pumped back to the heat extraction section.

3.2. Model establishment

Corresponding with the superstructure described above, the overall model can be divided into two modules, i.e., a heat extraction module and a power generation module. In the following content, the formulations of the two modules are separately introduced. The overall model can be built up by combining the two modules.

3.2.1. Heat extraction module

Equations of the module consist of temperature assignments, energy balances, utility usages, logical constrains, thermodynamic feasibilities and heat exchanger area calculations.

- **Temperature assignments**

It can be seen from figure 4 that there are three temperature boundaries (including the beginning boundary of the first stage, the intermediate boundary between the stages, and the ending boundary of the second stage) created by the two stages. It can be deduced that for a

superstructure with *ST* stages, *ST+1* temperature boundaries are created. This paper uses the same index 'st' to represent the sets of stages and temperature boundaries. If the set of stages has a total number of *ST* elements, the set of temperature boundaries will have *ST+1* elements.

According to the superstructure, the temperatures of waste heat streams at the first boundary can be directly assigned, as shown in Equation (1). Note that the waste heat stream temperatures at intermediate boundaries are variables to be determined.

$$T^{ws,st=1} = T_s^{\mathrm{ws}}, \quad \mathrm{ws} \in \mathrm{WS} \tag{1}$$

As for the preheating ORC working fluids, the temperatures at the first boundary should equal the evaporating temperatures, and the temperatures at the last boundary should equal the condensing temperatures (ignore the temperature raised by the pumps).

$$T_{pre}^{orc,st=1} = T_{eva}^{orc}, \quad \mathrm{orc} \in \mathrm{ORC} \tag{2}$$

$$T_{pre}^{orc,st=ST+1} = T_{con}^{orc}, \quad \mathrm{orc} \in \mathrm{ORC}, \mathrm{st} \in \mathrm{ST} \tag{3}$$

- **Energy balances**

The cooling demands of each waste heat stream should equal the sum of the energy transferred to ORC working fluids (preheating fluids and evaporating fluids) and cold utility, as presented by Equation (4).

$$(T_s^{ws} - T_t^{ws})FC^{ws} = \sum_{st \in ST} \sum_{orc \in ORC} q_{pre}^{ws,orc,st} + \sum_{st \in ST} \sum_{orc \in ORC} q_{eva}^{ws,orc,st} + q_{cu}^{ws}, \quad \mathrm{ws} \in \mathrm{WS} \tag{4}$$

All of the heating energy of either the preheating or evaporating working fluids should come from the waste heat streams:

$$(T_{t,pre}^{orc} - T_{s,pre}^{orc})FC_{pre}^{orc} = \sum_{st \in ST} \sum_{ws \in WS} q_{pre}^{ws,orc,st}, \quad \mathrm{orc} \in \mathrm{ORC} \tag{5}$$

$$Q_{eva}^{orc} = \sum_{st \in ST} \sum_{ws \in WS} q_{eva}^{ws,orc,st}, \quad \mathrm{orc} \in \mathrm{ORC} \tag{6}$$

In order to determine the intermediate boundary temperatures of participated streams, the

energy balances at each stage need to be formulated. The energy balances for each waste heat stream and each ORC preheating fluid at each stage are described by Equations (7) and (8).

$$(T^{ws,st} - T^{ws,st+1})FC^{ws} = \sum_{orc \in ORC} q_{pre}^{ws,orc,st} + \sum_{orc \in ORC} q_{eva}^{ws,orc,st}, \quad \mathrm{ws} \in \mathrm{WS}, \mathrm{st} \in \mathrm{ST} \tag{7}$$

$$(T_{pre}^{orc,st} - T_{pre}^{orc,st+1})FC_{pre}^{orc} = \sum_{ws \in WS} q_{pre}^{ws,orc,st}, \quad \mathrm{orc} \in \mathrm{ORC}, \mathrm{st} \in \mathrm{ST} \tag{8}$$

- **Utility usages**

The cold utility usage of heat extraction section can be calculated as:

$$q_{cu}^{ws} = (T^{ws,ST+1} - T_t^{ws})FC^{ws}, \quad \mathrm{ws} \in \mathrm{WS} \tag{9}$$

- **Logical constraints**

The logical constraints can represent whether the heat transfer between a hot and a cold participated stream is matched successfully or not, where 0-1 binary variables are adopted.

$$q_{pre}^{ws,orc,st} - \Omega Z_{pre}^{ws,orc,st} \le 0, \quad \mathrm{ws} \in \mathrm{WS}, \mathrm{orc} \in \mathrm{ORC}, \mathrm{st} \in \mathrm{ST} \tag{10}$$

$$q_{eva}^{ws,orc,st} - \Omega Z_{eva}^{ws,orc,st} \le 0, \quad \mathrm{ws} \in \mathrm{WS}, \mathrm{orc} \in \mathrm{ORC}, \mathrm{st} \in \mathrm{ST} \tag{11}$$

- **Thermodynamic feasibility**

A monotonic temperature decrease at each successive stage should be regulated for each participated stream to fulfil the second law of thermodynamic.

$$T^{ws,st} \ge T^{ws,st+1}, \quad \mathrm{ws} \in \mathrm{WS}, \mathrm{st} \in \mathrm{ST} \tag{12}$$

$$T^{ws,ST+1} \ge T_t^{ws}, \quad \mathrm{ws} \in \mathrm{WS} \tag{13}$$

$$T_{pre}^{orc,st} \ge T_{pre}^{orc,st+1}, \quad \mathrm{orc} \in \mathrm{ORC}, \mathrm{st} \in \mathrm{ST} \tag{14}$$

Besides, to assure feasible heat transfers of the matched heat exchangers, the approach temperatures at both ends of each of the heat exchangers should be greater than zero.

$$0 < dT_{pre}^{ws,orc,st} \le T^{ws,st} - T_{pre}^{orc,st} + L(1 - Z_{pre}^{ws,orc,st}), \quad \mathrm{ws} \in \mathrm{WS}, \mathrm{orc} \in \mathrm{ORC}, \mathrm{st} \in \mathrm{ST} \tag{15}$$

$$0 < dT_{pre}^{ws,orc,st+1} \le T^{ws,st+1} - T_{pre}^{orc,st+1} + L(1 - Z_{pre}^{ws,orc,st}), \quad \text{ws} \in \text{WS, orc} \in \text{ORC, st} \in \text{ST} \quad (16)$$

$$0 < dT_{eva}^{ws,orc,st} \le T^{ws,st} - T_{\text{eva}}^{orc} + L(1 - Z_{eva}^{ws,orc,st}), \quad \text{ws} \in \text{WS, orc} \in \text{ORC, st} \in \text{ST} \quad (17)$$

$$0 < dT_{eva}^{ws,orc,st+1} \le T^{ws,st+1} - T_{\text{eva}}^{orc} + L(1 - Z_{eva}^{ws,orc,st}), \quad \text{ws} \in \text{WS, orc} \in \text{ORC, st} \in \text{ST} \quad (18)$$

- **Heat exchanger area calculation**

The heat exchanger area can be calculated by Equations (19) & (20). Note that the 'LMDT' terms (logarithm mean approach temperature) are approximated by applying the equation proposed by Chen (1987), as shown in Equations (21) & (22).

$$HA_{pre}^{ws,orc,st} = \frac{q_{pre}^{ws,orc,st}}{U_{pre}^{ws,orc} \cdot LMDT_{pre}^{ws,orc,st}}, \quad \text{ws} \in \text{WS, orc} \in \text{ORC, st} \in \text{ST} \quad (19)$$

$$HA_{eva}^{ws,orc,st} = \frac{q_{eva}^{ws,orc,st}}{U_{eva}^{ws,orc} \cdot LMDT_{eva}^{ws,orc,st}}, \quad \text{ws} \in \text{WS, orc} \in \text{ORC, st} \in \text{ST} \quad (20)$$

$$LMDT_{pre}^{ws,orc,st} = \left[\frac{(dT_{pre}^{ws,orc,st})(dT_{pre}^{ws,orc,st+1})(dT_{pre}^{ws,orc,st} + dT_{pre}^{ws,orc,st+1})}{2} \right]^{1/3} \quad (21)$$

$$, \quad \text{ws} \in \text{WS, orc} \in \text{ORC, st} \in \text{ST}$$

$$LMDT_{eva}^{ws,orc,st} = \left[\frac{(dT_{eva}^{ws,orc,st})(dT_{eva}^{ws,orc,st+1})(dT_{eva}^{ws,orc,st} + dT_{eva}^{ws,orc,st+1})}{2} \right]^{1/3} \quad (22)$$

$$, \quad \text{ws} \in \text{WS, orc} \in \text{ORC, st} \in \text{ST}$$

3.2.2. Power generation module

In the power generation module, the power generated by each turbine, the power consumed by each pump, the cold utility usage of each ORC train, and the heat exchanger area of each condenser will be calculated. In this module, a thermodynamic state-points method is applied, which is also adopted by Yu et al. (2017). As depicted in Figure 5, The thermodynamic state points are marked on the T-S diagram of an ORC. By calculating the thermodynamic properties (mass flowrates, pressures, temperatures, enthalpies, entropies, etc.) of the state-points, the performance of each working component of an ORC train can be evaluated. In this paper, the Peng-Robinson Equation of State is adopted to calculate the thermodynamic properties, of

which the detailed formulations are listed in Supplement Materials.

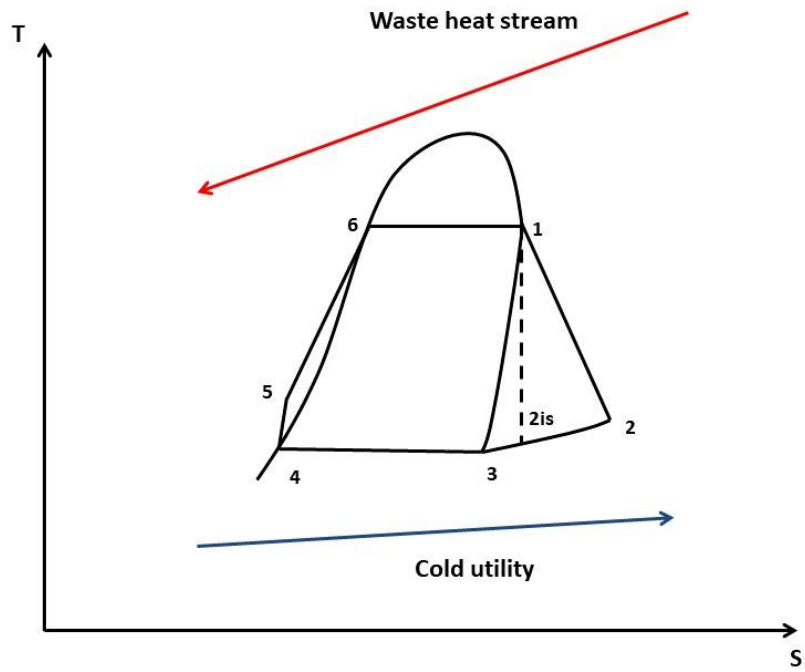

Figure 5. The T-S diagram of a single ORC train

- **Power generated by each turbine**

Ignoring the mechanical energy losses, the amount of the power generated by each turbine can be approximated as:

$$W_{tb}^{orc} \approx m_{wf}^{orc} \cdot (h_1^{orc} - h_2^{orc}) = m_{wf}^{orc} \cdot \eta_{tb}^{orc} (h_1^{orc} - h_{2is}^{orc}), \ \text{orc} \in \text{ORC} \tag{23}$$

- **Power consumed by each pump**

$$W_{pump}^{orc} = \frac{m_{wf}^{orc}}{\eta_{\text{pump}}^{orc} \cdot \rho_{wf}^{orc}} (P_5^{orc} - P_4^{orc}), \ \text{orc} \in \text{ORC} \tag{24}$$

Note that the density of each ORC working fluid ($\rho_{\text{wf}}^{\text{orc}}$) can be calculated by the Extended Rackeet Equation (Spencer and Danner, 1972), the formulation of which can be found in Appendix.

- **Cold utility usage in each condenser**

$$q_{con}^{orc} = m_{wf}^{orc} \cdot \left(h_2^{orc} - h_4^{orc}\right), \ \text{orc} \in \text{ORC} \tag{25}$$

- **Heat transfer area of each condenser**

It can be regarded that there are two different thermodynamic processes that occurred in the condenser, i.e., a de-superheating process (from state-points 2 to 3) and a liquifying process (from state-points 3 to 4). As for the de-superheating process, the heat transfer area can be calculated as follows:

$$HA_{con,de-\text{sup}}^{orc} = \frac{q_{con,de-\text{sup}}^{orc}}{U_{de-\text{sup}}^{orc} \cdot LMDT_{con,de-\text{sup}}^{orc}}, \ \text{orc} \in \text{ORC} \tag{26}$$

$$q_{con,de-\text{sup}}^{orc} = m_{wf}^{orc} \cdot (h_2^{orc} - h_3^{orc}), \ \text{orc} \in \text{ORC} \tag{27}$$

$$LMDT_{con,de-\text{sup}}^{orc} = \left[\frac{(T_2^{orc} - T_{cu,out}^{\text{orc}})(T_3^{orc} - T_{cu,\text{int}}^{orc})(T_2^{orc} - T_{cu,out}^{orc} + T_3^{orc} - T_{cu,\text{int}}^{orc})}{2}\right]^{1/3}, \ \text{orc} \in \text{ORC}$$

(28)

Note that the term $T_{\text{cw,int}}^{\text{orc}}$ means the temperature of cold utility at the beginning of the liquifying process of ORC working fluid, which can be calculated by Equation (29).

$$\frac{(T_{cu,\text{int}}^{orc} - T_{cu,in}^{orc})}{(T_{cu,out}^{orc} - T_{cu,\text{int}}^{orc})} = \frac{q_{con,liq}^{orc}}{q_{con,de\text{-sup}}^{orc}}, \ \text{orc} \in \text{ORC} \tag{29}$$

The heat transfer area of the liquifying process is calculated by the following equations:

$$HA_{con,liq}^{orc} = \frac{q_{con,liq}^{orc}}{U_{liq}^{orc} \times LMDT_{con,liq}^{orc}}, \ \text{orc} \in \text{ORC} \tag{30}$$

$$q_{con,liq}^{orc} = m_{wf}^{orc} \cdot (h_3^{orc} - h_4^{orc}), \ \text{orc} \in \text{ORC} \tag{31}$$

$$LMDT_{con,liq}^{orc} = \left[\frac{(T_3^{orc} - T_{cu,\text{int}}^{\text{orc}})(T_4^{orc} - T_{cu,in}^{orc})(T_3^{orc} - T_{cu,\text{int}}^{orc} + T_4^{orc} - T_{cu,\text{in}}^{orc})}{2}\right]^{1/3}, \ \text{orc} \in \text{ORC}$$

(32)

3.2.3. Correlations of the two modules

So far, the heat extraction module (Equation (1) ~ (22)) and the power generation module (Equation (23) ~ (32)) are established. To complete the overall model, the correlations of the two separate modules should be given. It can be noticed that the supply and target conditions of the pre-heating ORC working fluids in the heat extraction network should correspond to the state-points 5 and 6 in the ORC T-S diagram.

$$T_{s,pre}^{orc} = T_5^{orc}, \ \text{orc} \in \text{ORC} \tag{33}$$

$$T_{t,pre}^{orc} = T_6^{orc}, \ \text{orc} \in \text{ORC} \tag{34}$$

$$(T_{t,pre}^{orc} - T_{s,pre}^{orc}) FC_{pre}^{orc} = m_{wf}^{orc} \cdot (h_6^{orc} - h_5^{orc}), \ \text{orc} \in \text{ORC} \tag{35}$$

Similar, for the evaporating working fluids, the supply and target conditions in the network should match the state-points 6 and 1.

$$T_{s,eva}^{orc} = T_{t,eva}^{orc} = T_6^{orc} = T_1^{\text{orc}}, \ \text{orc} \in \text{ORC} \tag{36}$$

$$Q_{eva}^{orc} = m_{wf}^{orc} \cdot (h_1^{orc} - h_6^{orc}), \ \text{orc} \in \text{ORC} \tag{37}$$

3.2.4. Objective function

As this integration problem aims to minimize the annual cost, the relevant capital costs, operating costs, and the gained profits should be taken into account. A generic formulation of the objective function is shown in Equation (38).

$$\text{Obj} = AF \cdot (Cap_{extration} + Cap_{generation}) + Operating - profit \tag{38}$$

Where AF is the annualized factor, which is a constant number; the $Cap_{extration}$ and $Cap_{generation}$ terms indicate the capital cost of the heat extraction section and power generation section respectively; the $Operating$ term accounts for the overall operating cost; the $profit$ term calculates the profit brought up by power generation. In the following part, the detailed representations of these terms will be introduced separately.

- **Capital cost of the heat extraction section**

The capital cost of the heat extraction section can be regarded as the investment cost of the heat exchangers. The calculation equation is taken from Yu et al. (2017a), as shown below:

$$Cap_{extraction} = 10000 + 800 \cdot [\sum_{ws \in WS} \sum_{orc \in ORC} \sum_{st \in ST} (HA_{pre}^{ws,orc,st} + HA_{eva}^{ws,orc,st})]^{0.7} \quad (39)$$

, $ws \in WS, orc \in ORC, st \in ST$

- **Capital cost of the power generation section**

The power generation section consists of series of turbines, working fluid pumps, and condensers. For each turbine, the capital cost is calculated by Equation (40); for each pump, the capital cost is calculated by Equation (41), which is also adopted by Yu et al. (2017a); and the capital cost of each condenser is calculated by Equation (42).

$$Cap_{tb} = \sum_{orc \in ORC} [1.5 \cdot (225 + 170 \cdot V_2^{orc})] \quad (40)$$

$$Cap_{pump} = \sum_{orc \in ORC} 900 \cdot (\frac{W_{pump}^{orc} \cdot 1000}{300})^{0.25} \quad (41)$$

$$Cap_{con} = \sum_{orc \in ORC} [190 + 310 \cdot (HA_{con,de-\sup}^{orc} + HA_{con,liq}^{orc})] \quad (42)$$

$$Cap_{generation} = Cap_{turbine} + Cap_{pump} + Cap_{con} \quad (43)$$

- **Operating cost**

The operating cost is mainly considered as the cold utility cost, and is calculated by Equation (44). Note that the cold utility could be used by not only waste heat streams but also the condensers of ORCs.

$$Operating = price_{cu} \cdot (\sum_{ws \in WS} q_{cu}^{ws} + \sum_{orc \in ORC} q_{con}^{orc}) \quad (44)$$

- **Profit**

The profit gained by power generation can be calculated as:

$$profit = AOH \cdot price_{elec} \cdot \sum_{orc \in ORC} (W_{tb}^{orc} - W_{pump}^{orc}) \tag{45}$$

4. Optimization

The overall model is established by Equations (1) ~ (45). The corresponding optimization problem (named **PM**) is exhibited as follows. By solving the **PM** problem, the optimal HEN synthesis for extracting waste heat as well as the optimal operations of the relevant working components can be determined. However, it can be realized that the number of the ORC trains to be integrated is still unknown, which is key information for implementing the **PM**. Furthermore, due to the binary variables and non-convex terms created in the **PM** problem, the resulting MINLP optimization problem could be challenging. To assure a high-quality solution of the MINLP problem, it is necessary to offer good starting points. To these perspectives, first, this study provides an NLP initialization model, by solving which a starting point for the **PM** problem is expected to be provided; second, this study also proposes an iteration method for determining the optimal number of ORC trains in parallel.

$$\text{Min: obj}=AF \cdot (Cap_{\text{extraction}} + Cap_{generation}) + Operating - profit$$

(PM)

$$s.t.\ \ \chi(x) = \left\{ x \left| \begin{array}{l} \text{heat extraction module Eqs. (1~22)} \\ \text{power generation module Eqs. (23)} \square \text{ (32)} \\ \text{correlations of the tow modules Eqs. (33)~(37)} \\ \text{Onjective fuction Eqs. (38)~(45)} \end{array} \right. \right\}$$

4.1. Initialization model

The initialization model can be separated into a heat extraction module and a power generation module. The heat extraction module can estimate the minimum heat transfer area and the minimum cold utility usage without considering HEN synthesis. The power generation module is no different from that of the master model, which estimates the power output of the multi-parallel ORCs. Free variables in this model are the evaporating temperatures/pressures, the condensing temperatures/pressures, and the mass flowrates of the ORC trains.

1) Heat extraction module

According to the Pinch Analysis (Linnhoff and Ahmad, 1990), the near-minimum heat exchanger area for a HEN can be approximated by regulating vertical heat transfer (VHT) without considering the unit number of heat exchangers, as shown in Figure 5. The heat extraction module is established based on the VHT concept, of which the mathematical formulas are taken from Dong et al. (2020). Note that the applicability of the VHT-based mathematical model has been verified by the case study 1 of Dong et al. (2020). The following content briefly introduces the derivation of the module formulas. If interested, more details can be found in Dong et al. (2020).

In Figure 5, there are several vertical intervals bounded by the solid and hollow nodes marked on the hot and cold composite curves. Suppose the temperatures and enthalpies of all the nodes are known. In that case, the heat transfer area of the vertical intervals can then be calculated, and further, the overall heat transfer area can be estimated.

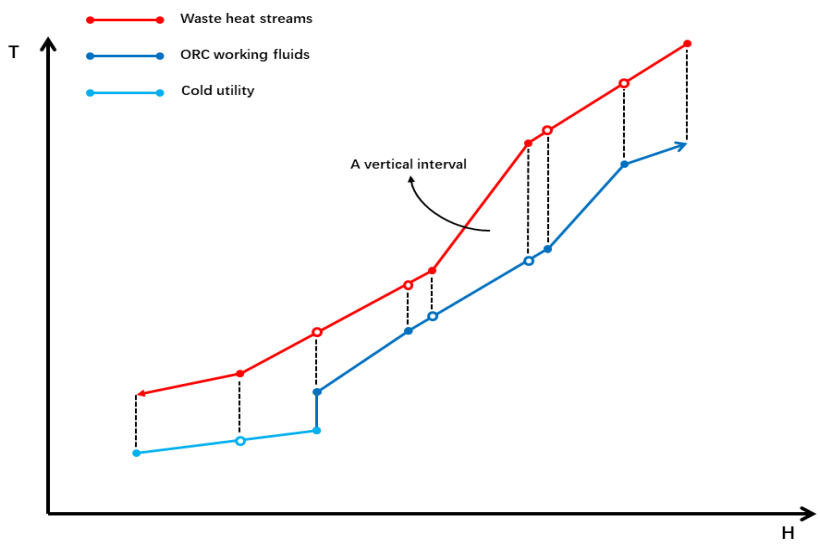

Figure 5. The illustration diagram of VHT

- **Calculate the temperatures and enthalpies of the solid nodes**

At the hot side, the solid-nodes temperatures (T^{hs}) consists of the target and supply temperatures of the waste heat streams.

$T^{hs} \in \left\{ T_s^{ws} \text{and } T_t^{ws}, \forall ws \in WS \right\}$.

T^{hs} can be automatically ordered by Equation (46).

$$T^{hs\_ord} = F(T^{hs}, \forall hs \in HS), hs\_ord \in HS\_ORD \tag{46}$$

Where the functions ***F*** represent the equations of the odd-even sort method. The detailed formulation of the method is omitted, which can be found in Dong et al. (2020).

On the cold side, each ORC in parallel can generate three solid nodes on the composite curve. The temperatures of these nodes correspond to the supply temperatures of preheating working fluids, the target (supply) temperatures of preheating (evaporating) working fluids, and the outlet temperatures of evaporating working fluids. As an evaporation process is isothermal, the inlet temperature of an evaporating working fluid is equal to the outlet temperature, which could lead to difficulties on calculating the heat capacity flowrate. Therefore, this study assumes that the outlet temperature of an evaporating fluid is 1℃ higher than the inlet temperature. Besides the ORC trains, the cold composite curve also includes a cold utility stream, which generates two solid nodes. Temperatures of the nodes correspond to the inlet and outlet temperatures of the cold utility. On the cold side, all the solid-node temperatures are:

$T^{cs} \in \left\{ T_{cu,in}, T_{cu,out}, T_{con}^{orc}, T_{eva}^{orc} \text{ and } T_{eva}^{orc} + 1, \forall orc \in ORC \right\}$.

The solid-node temperatures are ordered by Equation (47):

$$T^{cs\_ord} = F(T^{cs}, \forall cs \in CS), cs\_ord \in CS\_ORD \tag{47}$$

The enthalpies of the ordered hot and cold solid nodes are calculated by the Equations (48) and (49) separately.

$$H^{hs\_ord} = \sum_{ws \in WS} FC_{ws} \left[\left(\max(0, T^{hs\_ord} - T_{ws,t} \right) - \max\left(0, T^{hs\_ord} - T_{ws,s}\right) \right] \quad hs\_ord \in HS\_ORD \tag{48}$$

$$\begin{aligned} H^{cs\_ord} &= FC_{cu}\left[\max\left(0, T^{cs\_ord} - T_{cu,in}\right) - \max\left(0, T^{cs\_ord} - T_{cu,out}\right)\right] + \\ &\sum_{orc \in ORC} FC_{pre}^{orc}\left[\left(\max(0, T^{cs\_ord} - T_{con}^{orc}\right) - \max\left(0, T^{cs\_ord} - T_{eva}^{orc}\right)\right] + \\ &\sum_{orc \in ORC} FC_{eva}^{orc}\left[\left(\max(0, T^{cs\_ord} - T_{eva}^{orc}\right) - \max\left(0, T^{cs\_ord} - T_{eva}^{orc} - 1\right)\right] \\ & cs\_ord \in CS\_ORD \end{aligned} \tag{49}$$

To assure the overall energy balance, the starting and ending nodes of the hot and cold composite curves should be vertically aligned.

$$H^{hs\_ord} = H^{cs\_ord},\ |hs\_ord| = |cs\_ord| = 1 \tag{50}$$

$$H^{hs\_ord} = H^{cs\_ord},\ hs\_ord = |HS\_ORD|,\ cs\_ord = |CS\_ORD| \tag{51}$$

- **Calculate the temperatures and enthalpies of the hollow nodes**

To calculate the hollow-node temperatures, we can firstly determine the enthalpy of each hollow node. It can be noticed that the enthalpy of each hollow node is equivalent to that of the corresponding solid node at the opposite side.

$$\begin{aligned} & H^{hh\_ord} = H^{cs\_ord},\ |hh\_ord| = |cs\_ord| \\ & hh\_ord \in HH\_ORD, cs\_ord \in CS\_ORD \end{aligned} \tag{52}$$

$$\begin{aligned} & H^{ch\_ord} = H^{hs\_ord},\ |ch\_ord| = |hs\_ord| \\ & ch\_ord \in CH\_ORD, hs\_ord \in HS\_ORD \end{aligned} \tag{53}$$

Then, the temperatures of the hollow nodes can be calculated by Equation (54) (for the hot side) and Equation (55) (for the cold side).

$$\begin{aligned} & T^{hh\_ord} = T^{hs\_ord=1} + \\ & \sum_{\substack{hs\_ord \in HS\_ORD \\ hs\_ord < |HS\_ORD|}} \left\{ \frac{(T^{hs\_ord+1} - T^{hs\_ord})}{(H^{hs\_ord+1} - H^{hs\_ord})} \left[\max\left(0, H^{hh\_ord} - H^{hs\_ord}\right) - \max\left(0,\ H^{hh\_ord} - H^{hs\_ord+1}\right)\right] \right\} \\ & hh\_ord \in HH\_ORD \end{aligned}$$

(54)

$$T^{ch\_ord} = T^{cs\_ord=1} + \sum_{\substack{cs\_ord \in CS\_ORD \\ cs\_ord < |CS\_ORD|}} \left\{ \frac{(T^{cs\_ord+1} - T^{cs\_ord})}{(H^{cs\_ord+1} - H^{cs\_ord})} \left[\max\left(0, H^{ch\_ord} - H^{cs\_ord}\right) - \max\left(0, \ H^{ch\_ord} - H^{cs\_ord+1}\right) \right] \right\}$$
$$ch\_ord \in CH\_ORD$$

(55)

Besides, the second law of thermodynamics should be ensured:

$$T^{hh\_ord} - T^{cs\_ord} \geq \Delta T_{\min}, hh\_ord \in HH\_ORD, cs\_ord \in CS\_ORD \quad (56)$$

$$T^{hs\_ord} - T^{ch\_ord} \geq \Delta T_{\min}, hs\_ord \in HS\_ORD, ch\_ord \in CH\_ORD \quad (57)$$

- **Rearrange the total nodes**

The total (solid and hollow) nodes of both the hot and cold sides can be re-ordered as:

$$H^{ht\_ord} = F(H^{hs\_ord}, H^{hh\_ord}), hs\_ord \in HS\_ORD, \ hh\_ord \in HH\_ORD \quad (58)$$

$$T^{ht\_ord} = F(T^{hs\_ord}, T^{hh\_ord}), hs\_ord \in HS\_ORD, \ hh\_ord \in HH\_ORD \quad (59)$$

$$T^{ct\_ord} = F(T^{cs\_ord}, T^{ch\_ord}), cs\_ord \in CS\_ORD, \ ch\_ord \in CH\_ORD \quad (60)$$

Where functions F represent the equations of the odd-even-method.

- **Calculate the heat transfer area of each interval**

Once all the enthalpies and temperatures of the marked nodes are calculated, the heat exchanger area of each vertical interval can then be calculated. For simplicity purposes, the formulas are omitted in this chapter. Readers can refer to Dong et al. (2020).

$$HA^{vi} = HA^{vi}(H^{ht\_ord}, T^{ht\_ord}, T^{ct\_ord})$$
$$vi \in VI, ht\_ord \in HT\_ORD, ct\_ord \in CT\_ORD \quad (61)$$

2) Power generation module

The power generation module of the initialization model is the same as that of the master model. Therefore, equations (23) ~ (32) can be directly transplanted.

3) Objective function

The objective function of the initialization model consists of the capital costs of heat extraction section and power generation section, the operating cost, and the profit generated by the multi-parallel ORCs, as shown by equation (62).

$$Obj = AF \cdot (Cap_{extration} + Cap_{generation}) + Operating - profit \tag{62}$$

In which, the term $Cap_{extration}$ is calculated by equation (63), which is given below; the term $Cap_{generation}$ can be calculated by equations (40) ~(43); the term $Operating$ and $profit$ can be calculated by equations (44) and (45) respectively.

$$Cap_{extration} = 10000 + 800 \cdot (\sum_{vi \in VI} HA^{vi})^{0.7} \tag{63}$$

4.2. Optimization strategy

Based on the established initialization model, an NLP problem, namely '**PI**', is formulated, of which the objective is to minimize total annualized cost. As shown below, the symbol 'i' denotes a set of free variables to be optimized, $\mathrm{I(i)}$ represents the feasible search space defined by the constraints.

$$\text{Min: obj=AF} \cdot (\text{Capital}_{\text{extraction}} + \text{Capital}_{\text{generation}}) + \text{Operating} - \text{Profit}$$

(PI)

$$\text{s.t. } \mathrm{I(i)} = \left\{ \mathrm{i} \left| \begin{array}{l} \text{heat extraction module, Eqs. (46) ~ (61)} \\ \text{power generation module, Eqs. (23) ~ (32)} \\ \text{objective function, Eqs. (62) ~ (63), (40) ~ (43), (44) ~ (45)} \end{array} \right. \right\}$$

To implement the **PI**, the number of ORC trains in parallel should be given in advance. It can be realized that with a different number of ORC trains, the heat exchanger area, power generation, and utility usage could be different, leading to diverse optimization results. There should be an optimal number of ORC trains that can lead to the minimum total annual cost. To find it out, an iterative method is proposed by this study, of which the flowsheet is shown in Figure 6.

At the first iteration, a base case is set, in which a single ORC is integrated. The second iteration will create a comparative case with a double-parallel ORCs system by adding one more parallel into the base case. If the optimization result of the second iteration is better than that of the first iteration (i.e., has a lower annual cost), then the double-parallel configuration is set as the new base case, and the third iteration will create a new comparative case by adding one more ORC in parallel; if not, the searching process will be terminated, outputting the base case as the optimum configuration. The search process can be repeated until the optimal number of the parallels is identified. With the identifying of the number of ORC trains in parallel, the corresponding optimization result given by the iteration process is also output as the starting point of the **PM** problem.

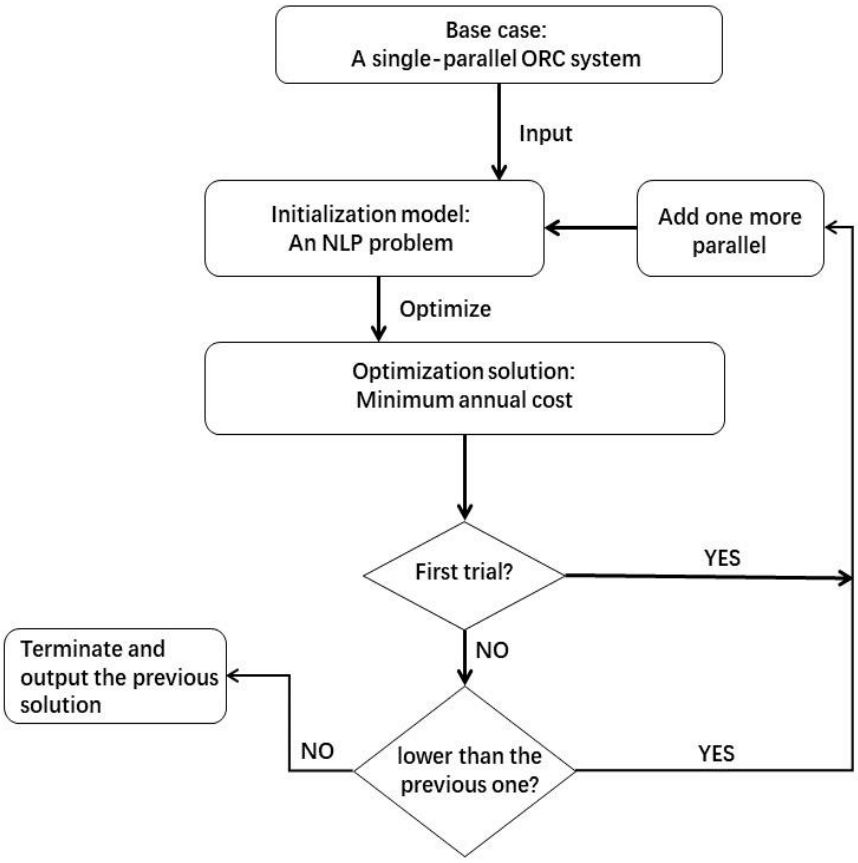

Figure 6. The flowsheet of the trial-and-error method

5. Case Study

5.1. Background information

To illustrate the application of the proposed method for integrating multi-parallel ORCs, a case study is exhibited in this chapter. The case is taken from Yu et al. (2017a), of which the pre-configured parameters and the relevant marketing prices are represented below.

- The cold utility cost for the heat extraction section and the hot utility cost for the background HEN are 20 $\$/(\mathrm{kW}\cdot\mathrm{year})$ and 100 $\$/(\mathrm{kW}\cdot\mathrm{year})$
- The electricity price is set as 0.10 $\$/(\mathrm{kW}\cdot\mathrm{year})$
- The AOH (annual operating hours) is assumed to be 8000 hours per year
- The isentropic efficiency $\eta_{\mathrm{tb}}^{\mathrm{orc}}$ of each turbine is assumed as 80%
- The isentropic efficiency $\eta_{\mathrm{pump}}^{\mathrm{orc}}$ of each pump is assumed as 95%
- The AF (annualized factor) is assumed as 0.18
- The overall heat transfer coefficients are assumed as 150 $\mathrm{W}/(\mathrm{m}^2\cdot℃)$ and 300 $\mathrm{W}/(\mathrm{m}^2\cdot℃)$ for transferring the sensible heat and latent heat respectively of the working fluid
- The fixed charge is assumed as $2.5\cdot10^4$ \$ for implementing each of the ORC parallels
- The working fluid of the multi-parallels ORCs is chosen as N-butane (R600)

Table 2. Background process stream data for the case study

process stream	supply temperature (℃)	target temperature (℃)	heat capacity flowrate (kw/℃)
HS1	300	40	40
HS2	170	80	70
HS3	350	100	70
HS4	120	40	65
HS5	70	40	220

HS6	120	70	160
CS1	70	300	30
CS2	40	120	50
CS3	90	300	70
CS4	160	185	270
CS5	30	50	315
CS6	123	124	1100

The background process stream data (with six hot streams and six cold streams) are listed in Table 2. As the waste heat stream data are not directly given, the heat integration of the background processes should be carried out in advance to identify the waste heat streams. In this case study, the Synheat method is chosen as the tool for the background heat integration. The result of the background heat integration is shown in Table 3, and the detailed data of the identified waste heat streams are listed in Table 4.

Table 3. The conclusive results of the background heat integration

Hot utility usage (kW)	1509.3
Hot utility annual cost ($/year)	150930.4
Heat exchanger unit number	19
Total heat exchanger area (m^2)	25175.6
Heat exchangers total annualized cost ($/year)	175199.7

Table 4. The identified waste heat stream data

waste heat stream	supply temperature (℃)	target temperature (℃)	heat capacity flowrate (kW/℃)	Heat load (kW)
WS1	109.6	40	40	2784
WS2	91	80	70	770

WS3	70.2	40	65	1963
WS4	70	40	220	6600
WS5	92.8	70	160	3648

5.2. Optimization results

Once the waste heat streams are identified, the corresponding mathematical model of the **PM** and **PI** problem can be established. To solve the problems, the iterative process illustrated in Figure 4 is carried out. Within each iteration, given the number of ORCs in parallel, the corresponding **PI** problem is established, and is solved by the General Algebraic Modeling System (GAMS) platform with the Conopt solver (Drud, 1994). The solving results of the iteration, including the optimal number of the ORCs in parallel and the corresponding optimized operative variables, are output as the starting point of the **PM** problem. The **PM** problem leads to MINLP, and is solved by the GAMS platform with the Baron solver (Sahinidis, 1996). The hardware used is a desktop PC with Intel(R) Core (TM) i5 CPU 3.33 GHz and 8.00 GB of RAM.

Table 5. The solver information and model statistics of the initialization process

Trial	Number of ORCs in parallel	Number of equations	Number of continues variables	Solver	CPU time
1	Single	661	651	Conopt	0.203
2	Double	899	885	Conopt	0.265
3	Tripple	1165	1148	Conopt	0.579

Results of the iteration are shown in Table 6. It can be seen that the iterative process is terminated after the third iteration, indicating that the double-parallel is selected as the optimal configuration of the ORC trains, which has the minimum total annualized cost (50345 $/year). The relevant operative variables of the double-parallel configuration consist of cold utility usage, total heat exchanger area, power generation of each ORC train, mass flowrates of

ORC working fluids, evaporation temperatures, turbine outlet temperatures, and condensation temperatures, of which the optimized values are output as the starting point of the **PM** problem, as shown by the italics printing terms in Table 6.

The mathematical model of the **PM** problem exhibits 624 independent equations with 595 continuous variables and 100 binary variables. The optimization result of the **PM** problem is shown in Table 7. By solving the **PM** problem, the total annualized cost decreases from the 50345 $/year given by the **PI** problem to 21576 $/year, and the total heat exchanger area of the HEN decreases from 4070 m^2 to 3320 m^2. The total power generation given by the **PM** problem is 812 kW which is close to that (837 kW) given by the **PI** problem. The PM problem also carries out the corresponding HEN synthesis. The optimized network structure is shown in Figure 7. By combining the solving result of the **PM** problem and the integration result of the background processes, the whole picture of the integration problem can be viewed, as shown in Table 8.

Table 6. The solving results of the iterative process

Number of ORCs in parallel	**Single (1st iteration)**	**Double (2nd iteration)**		**Tripple (3rd iteration)**		
	ORC 1	**ORC 1**	**ORC 2**	**ORC 1**	**ORC 2**	**ORC 3**
Conclusive results						
Total annualized cost ($/year)	125370	*50345*			105180	
Cold utility (kW)	15123.81	*14969.85*			14916.64	
The heat exchanger area for extracting Waste heat (m^2)	3202.09	*4070.96*			4245.97	
Power generation (kW)	654.49	*297.03*	*540.65*	217.58	244.68	408.19
Total annualized capital cost ($/year)	346485	*421092*			503207	
ORC operations						
ORC working fluid mass	19.55	*11.50*	*13.67*	9.04	7.26	9.71

flowrate (kg/s)						
Evaporation temperature (℃)	66.19	*56.59*	*74.19*	54.44	66.51	77.59
Turbine outlet temperature (℃)	37.89	*34.73*	*40.57*	34.04	37.99	41.69
Condensation temperature (℃)	26.85	*26.85*	*26.85*	26.85	26.85	26.85

Table 7. Optimization result of the master problem

	First parallel	Second parallel
Conclusive result		
Total annualized cost ($/year)	21576	
Cold utility (kW)	14931.57	
The heat exchanger area for extracting waste heat (m^2)	3302.45	
Power generation (kW)	284.86	527.54
Thermal efficiency (%)	6.43%	9.28%
Detailed operation		
ORC working fluid mass flowrate (kg/s)	11.06	13.37
Evaporation temperature (℃)	56.51	74.06
Turbine outlet temperature (℃)	34.71	40.52
Condensation temperature (℃)	26.85	26.85

Table 8. Whole picture of the solved ORC integration problem

Variable	Optimal value	Variable	Optimal value
Total annual cost ($/year)	347706	Area of waste heat extraction network (m^2)	3302
Hot utility (kW)	1509	Area of condensers (m^2)	3197
Cold utility (kW)	14932	Net power output (kW)	812

Area of background HEN (m^2)	25176	Overall thermal efficiency (%)	8.05%

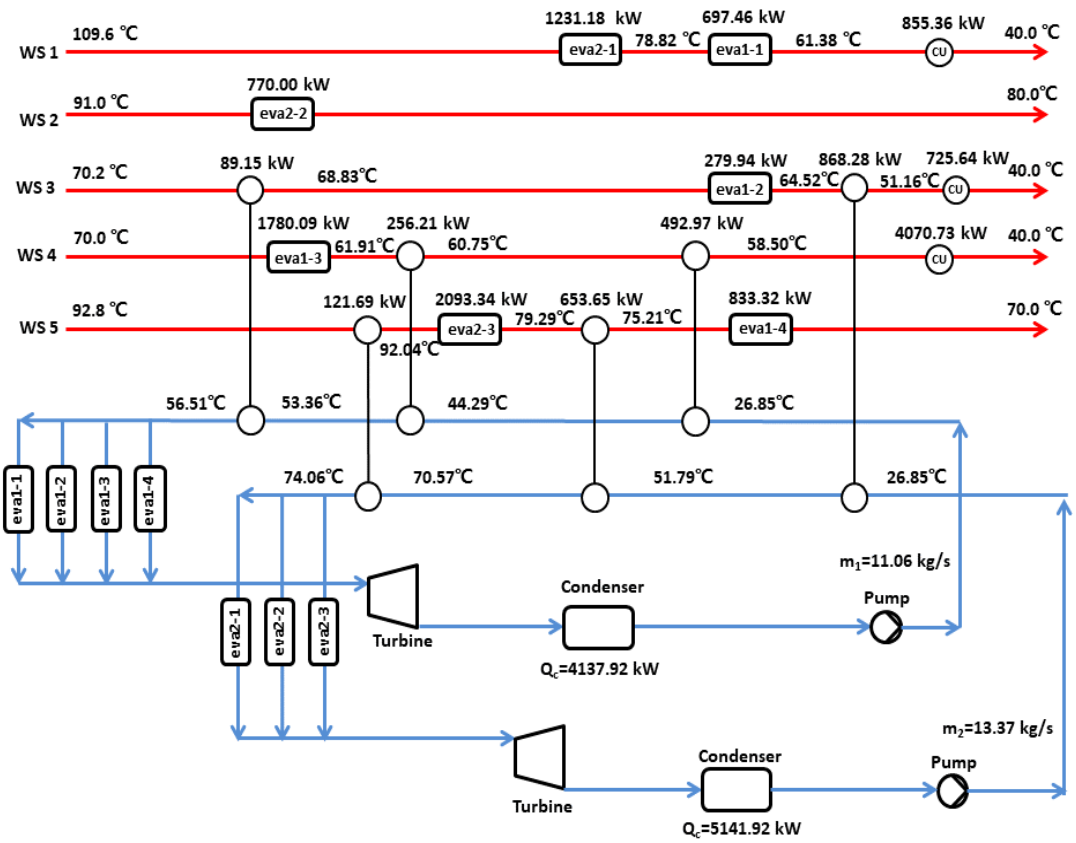

Figure 7. The structure of the integrated double-parallel ORCs

5.3. Result discussion

In the iterative process, the configuration of double-parallel ORCs is calculated to have the minimum total annualized cost as 50345 $/year, which is much lower than that of the single or triple-parallel configuration. The disparity in the total annualized cost between the different configurations is caused by the trade-offs between the profits brought up by power generation and the relevant capital costs. Though implementing multi-parallel ORCs can increase power generation, the additional ORC working components, increased heat exchanger area, and relevant auxiliary facilities could bring up extra capital costs.

It can be seen from Table 6 that the total power generation of the double-parallel configuration

is 837.68 kW, 183.19 kW more than that of the single ORC. The 183.19 kW extra power generation is equivalent to a 146552 $ bonus per year (the electricity price is set as 0.1 $/kWh). The total annualized capital cost of the double-parallel configuration is 421092 $/year, 74607 $/year more than that of the single ORC. The 146552 $ bonus can overcome the 74607 $/year extra capital costs, leading to a decrease in the total annualized cost of the double-parallel configuration (from 125370 $/year to 50345 $/year). As for the triple-parallel configuration, the total power generation is 870.45 kW, 32.77 kW more than that of the double-parallel configuration. The 32.77 kW extra power generation is equivalent to 26216 $ bonus per year, which cannot compete with the corresponding extra capital costs, resulting in an increase in the total annualized cost.

It is declared by Yu et al. (2015) that two main factors affect the power generation of an integrated ORC(s) system, which are: 1. the rate of heat recovery; 2. the thermal efficiency of the ORC(s) system. To the perspective of energy recovery, the composite curve (Figure 8) shows that the amount of the unrecovered waste heat is 7696.76 kW, 5407.15 kW and 5032.08 kW for the single, double and triple-parallel configurations, respectively. Based on energy balance, we know that the double and triple-parallel configurations can have 2289.61kW and 2664.68 kW more waste heat recovered than the single ORC. To the perspective of thermal efficiency, the calculation results of Equation (62) show no significant differences in the overall thermal efficiencies among those configurations. For the single, double, and triple-parallel

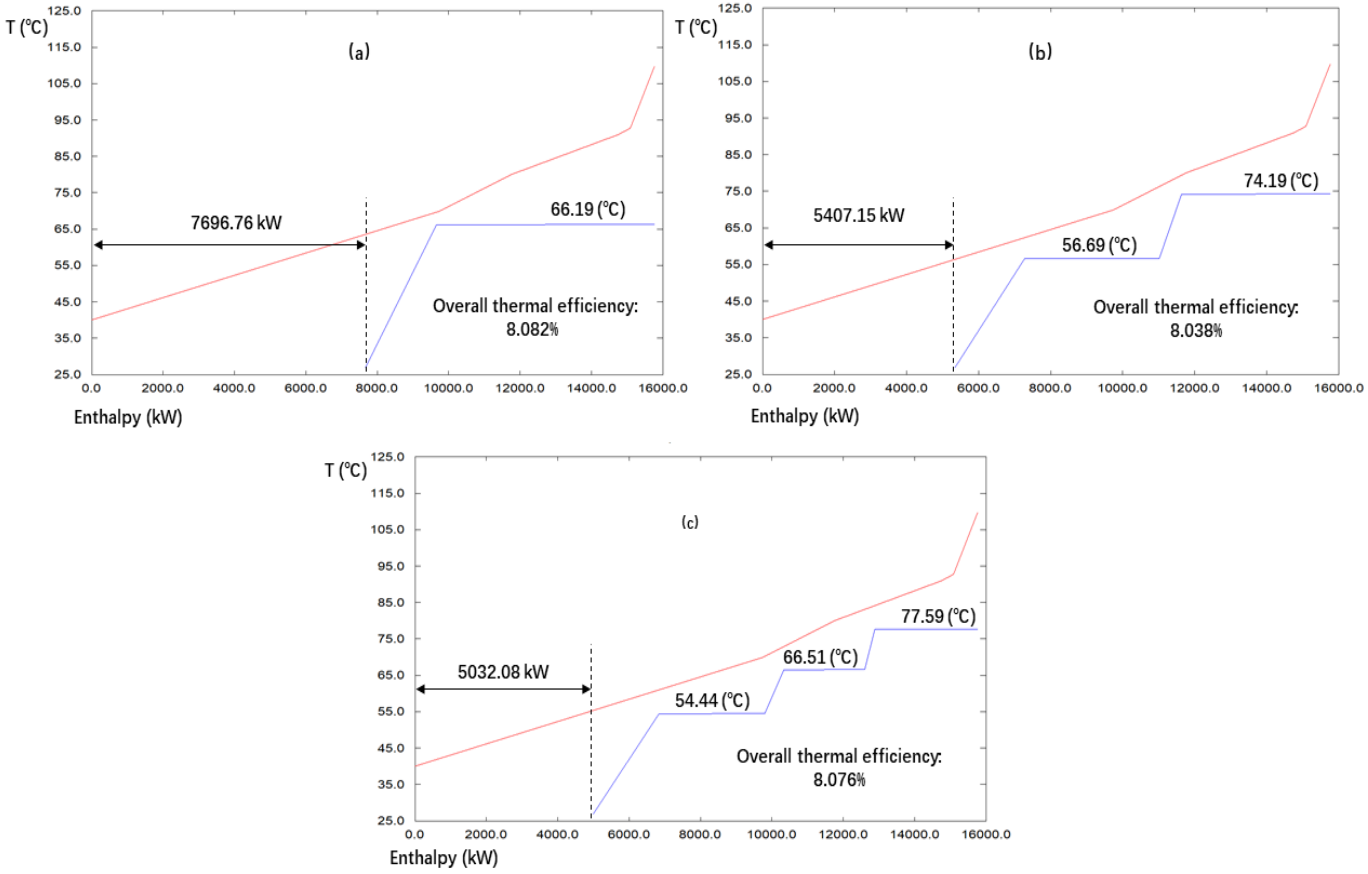

Figure 8. The composite curves of the different configurations of ORCs in parallel.

(a) single-parallel; (b) double-parallel; (c) triple-parallel

configurations, the corresponding overall thermal efficiencies are 8.072%, 8.038%, and 8.076%, respectively. With similar thermal efficiency, the increased rate of heat recovery can lead to an increase in power generation.

$$\text{overall thermall efficiency}=\frac{\text{total net power generation}}{\text{total heat absorbed}} \tag{62}$$

The **PI** problem estimates the total heat exchanger area for extracting waste heat by assuming vertical heat transfers, whereas the possibilities of arranging criss-cross heat transfers are neglected. In this case study, the estimated heat exchanger area given by the **PI** problem is 4071 m^2. In contrast, the optimal value provided by the **PM** problem is 3302 m^2, 769 m^2 smaller than the estimated value. As the criss-cross heat transfer is considered, the **PM** problem can obtain a smaller value of heat exchanger area, leading to a better optimization consequence.

Combining the optimization result of the **PM** problem (shown in Table 7) and the heat integration result (shown in Table 3) of the background processes, a final result can be obtained, as shown in Table 8. The total annualized cost is 347706 $/year, which accounts for the hot and cold utility costs, capital cost of the background HEN, capital cost of the waste heat extraction network, capital cost for implementing the ORCs, and the profit gained by power generation. In contrast, without implementing any ORCs, the total annualized cost is about 641349 $/year.

For comparison, the optimizing results with Yu et al. (2017a) are exhibited in Table 9. As shown in Tabe 8, the net power output given by Yu et al. (2017a) is 947 kW, 135 kW more than that offered by this study. While the total heat exchanger area (accounts for both the background HEN and the waste heat extraction network) given by the previous study is 72044 m^2, 43566 m^2 larger than this study. Though the previous study achieves more power output, it also brings up a much larger heat exchanger area than this study, leading to a higher total annualized cost. The minimum annualized cost obtained by Yu et al. (2017a) is 565950 $/year, 218244 $/year higher than that given by this study. Such a discrepancy could be caused by the

different heat extraction strategy and different optimizing methodologies. For extracting waste heat, the previous study configures an intermediate heat carrier to transport heat from waste heat sources to the integrated ORC (i.e., indirect heat transfers), while this study regulates direct heat transfers. It is found that the indirect heat transfer strategy could result in a larger heat exchanger area, as the heat should be first transferred to a heat carrier(s) before being transferred to ORC working fluid(s). However, Yu et al. (2017a) declared that the indirect heat extraction strategy might be favorable in practice due to controllability and operability considerations. For optimization, Yu et al. (2017a) adopted a sequential methodology rather than a simultaneous one. They firstly maximize the net power output of the ORC and then calculate the corresponding capital cost. Though the amount of power output is maximized, the corresponding capital cost could be even higher, leading to a worsen optimization result.

Table 9. The comparison with Yu et al. (2017a)

Variable	Optimal value of this study	Optimal value of Yu et al. (2017)
Total annual cost ($/year)	347706	565950
Hot utility (kW)	1509	2410
Cold utility (kW)	14932	15691
Total power generation (kW)	812	947
Total heat exchanger area (m^2)	28478	72044

6. Conclusions

This study focuses on the integration of multi-parallel ORCs, which is rarely discussed in the previous work. A mathematical programming-based method is developed for integrating multi-parallel ORCs. The method consists of a master problem, namely **PM,** and an initialization problem, namely **PI**. For modelling, in the **PM** problem, this study proposes a superstructure, especially for synthesizing and designing a multi-parallel ORCs system, as shown by Figure 4. The corresponding model leads to MINLP. While in the **PI** problem, referred from Dong et al. (2020), and based on the vertical heat transfer concept of the Pinch Analysis (Linnhoff and

Ahmad, 1990), an NLP model is established, which can estimate the total heat transfer area for extracting waste heat without considering HEN synthesis. For optimization, this study proposes an iterative approach. The iteration can determine the optimal number of ORC in parallel as well as the optimal value of the corresponding operative variables, offering good starting points for the **PM** problem. A case study is presented to illustrate the application of the proposed method. Results show that double-parallel ORCs can generate more power than a single ORC, leading to a decrease in total annualized cost.

Supplement materials: The Peng-Robinson EoS

The Peng-Robinson Equation of State used in the power generation module is presented as below.

$$P = \frac{RT}{v - b} - \frac{a(T)}{v^2 + 2bv - b^2} \tag{S1}$$

Where:

$$a(T) = 0.45274 \frac{R^2 T_c^{\,2}}{P_c} \alpha(T, \omega)$$

$$b = 0.45724 \frac{R^2 T_c^{\,2}}{P_c}$$

$$\alpha(T, \omega) = \left[1 + \kappa(1 - (T / T_c)^{0.5})\right]^2$$

$$\kappa = 0.37464 + 1.54226\omega - 0.26992\omega^2$$

T_c and P_c are the critical temperature and pressure, ω is the acentric factor.

For computational convenience, the P-R EoS can be transformed to:

$$Z^3 + (B - 1)Z^2 + (A - 3B^2 - 2B)Z + (B^3 + B^2 - AB) = 0 \tag{S2}$$

Where:

$$A = \frac{a(T)P}{(RT)^2}$$

$$B = \frac{bP}{RT}$$

$$Z = \frac{Pv}{RT}$$

Note that the unit of pressure is used as **Mpa** in the P-R EoS, which is different with the **kpa** unit used in this paper.

The enthalpy and entropy of a substance at given temperature and pressure (T_1, P_1) can be calculated as:

$$H(T_1,P_1)-H(T_{ref},P_{ref})=H^*(T_{ref},P_{ref})+\int_{T_{ref}}^{T_1}C_p^{id}dT-H^*(T_1,P_1) \quad \text{(S3)}$$

$$S(T_1,P_1)-S(T_{ref},P_{ref})=S^*(T_{ref},P_{ref})+\int_{T_{ref}}^{T_1}\frac{C_p^{id}}{T}dT-R\ln\frac{P_1}{P_{ref}}-S^*(T_1,P_1) \quad \text{(S4)}$$

Where:

$$\frac{H^*(T,P)}{RT_c}=2.078(1+\kappa)[1+\kappa(1-T_r^{1/2})]\ln[\frac{Z+(1+\sqrt{2})B}{Z+(1-\sqrt{2})B}]-T_r(Z-1)$$

$$\frac{S^*(T,P)}{R}=2.078\kappa[\frac{1+\kappa}{T_r^{1/2}}-\kappa)]\ln[\frac{Z+(1+\sqrt{2})B}{Z+(1-\sqrt{2})B}]-\ln(Z-B)$$

$$T_r=\frac{T}{T_c}$$

Note that the unit of the enthalpy and entropy calculated by the P-R EoS is configured as **molar basis** which is different from the **mass basis** unit used in this paper. T_{ref} and P_{ref} are the given reference temperature and pressure, $H(T_{ref},P_{ref})$ and $S(T_{ref},P_{ref})$ are the enthalpy and entropy at the given reference state. C_p^{id} is the ideal gas heat capacity which can be calculated by the DIPPR107 equation (Aly and Lee, 1981), as presented in Equation (S5).

$$C_p^{id}=C_1+C_2\left[\frac{C_3/T}{\sinh(C_3/T)}\right]^2+C_4\left[\frac{C_5/T}{\cosh(C_5/T)}\right]^2 \quad \text{(S5)}$$

Where C_1, C_2, C_3, C_4, and C_5 are regression parameters, the value of them for N-Butane are listed in the table below.

Table S1. Parameters in DIPPR107 for N-Butane

DIPPR107 Parameter	C_1	C_2	C_2	C_4	C_5
Butane	71340	243000	1630	150330	730.42

References

Desai, N. and Bandyopadhyay, S. (2009). Process integration of organic Rankine cycle. *Energy*, 34(10), pp.1674-1686.

Liu, G., Zhou, H., Shen, R. and Feng, X., 2014. A graphical method for integrating work exchange network. *Applied Energy*, 114, pp.588-599.

Hipólito-Valencia, B., Rubio-Castro, E., Ponce-Ortega, J., Serna-González, M., Nápoles-Rivera, F. and El-Halwagi, M., 2013. Optimal integration of organic Rankine cycles with industrial processes. Energy Conversion and Management, 73, pp.285-302.

Chen, C., Chang, F., Chao, T., Chen, H. and Lee, J. (2014). Heat-Exchanger Network Synthesis Involving Organic Rankine Cycle for Waste Heat Recovery. Industrial & Engineering Chemistry Research, 53(44), pp.16924-16936.

Kermani, M., Wallerand, A., Kantor, I. and Maréchal, F., 2018. Generic superstructure synthesis of organic Rankine cycles for waste heat recovery in industrial processes. *Applied Energy*, 212, pp.1203-1225.

Dong, X., Liao, Z., Sun, J., Huang, Z., Jiang, B., Wang, J. and Yang, Y., 2020. Simultaneous Optimization for Organic Rankine Cycle Design and Heat Integration. *Industrial & Engineering Chemistry Research*, 59(46), pp.20455-20471.

Yee, T. and Grossmann, I., 1990. Simultaneous optimization models for heat integration—II. Heat exchanger network synthesis. *Computers & Chemical Engineering*, 14(10), pp.1165-1184.

Linnhoff, B. and Ahmad, S., 1990. Cost optimum heat exchanger networks—1. Minimum energy and capital using simple models for capital cost. *Computers & Chemical Engineering*, 14(7), pp.729-750.

Yu, H., Gundersen, T. and Feng, X., 2018. Process integration of organic Rankine cycle (ORC) and heat pump for low temperature waste heat recovery. *Energy*, 160, pp.330-340.

Stijepovic, M., Papadopoulos, A., Linke, P., Stijepovic, V., Grujic, A., Kijevčanin, M. and Seferlis, P., 2017. Organic Rankine Cycle system performance targeting and design for multiple heat sources with simultaneous working fluid selection. Journal of Cleaner Production, 142, pp.1950-1970.

Huang, X., Lu, P., Luo, X., Chen, J., Yang, Z., Liang, Y., Wang, C. and Chen, Y., 2020. Synthesis and simultaneous MINLP optimization of heat exchanger network, steam Rankine cycle, and organic Rankine cycle. Energy, 195, p.116922.

Elsido, C., Martelli, E. and Grossmann, I., 2019. A bilevel decomposition method for the simultaneous heat integration and synthesis of steam/organic Rankine cycles. *Computers & Chemical Engineering*, 128, pp.228-245.

Song, J., Li, Y., Gu, C. and Zhang, L., 2014. Thermodynamic analysis and performance optimization of an ORC (Organic Rankine Cycle) system for multi-strand waste heat sources in petroleum refining industry. *Energy*, 71, pp.673-680.

Yu, H., Eason, J., Biegler, L. and Feng, X., 2017a. Simultaneous heat integration and techno-economic optimization of Organic Rankine Cycle (ORC) for multiple waste heat stream recovery. Energy, 119, pp.322-333.

Yu, H., Eason, J., Biegler, L. and Feng, X., 2017b. Process integration and superstructure optimization of Organic Rankine Cycles (ORCs) with heat exchanger network synthesis. Computers & Chemical Engineering, 107, pp.257-270.

Chen, J., 1987. Comments on improvements on a replacement for the logarithmic mean. *Chemical Engineering Science*, 42(10), pp.2488-2489.

Sahinidis, N., 1996. BARON: A general purpose global optimization software package. *Journal of Global Optimization*, 8(2), pp.201-205.

Drud, A., 1994. CONOPT—A Large-Scale GRG Code. *ORSA Journal on Computing*, 6(2), pp.207-216.

Aly, F. and Lee, L., 1981. Self-consistent equations for calculating the ideal gas heat capacity, enthalpy, and entropy. *Fluid Phase Equilibria*, 6(3-4), pp.169-179.

Chapter 5: Working Fluid Selections for Integrating ORCs

The appended papers in the preceding chapters address the simultaneous optimization of HEN synthesis and the operations of ORCs. However, it can be noticed that the optimal working fluid selection of each of the integrated ORCs are not addressed. This chapter contains a journal-format paper, providing a mathematical programming-based method for automatically selecting the optimal working fluid of each integrated ORC.

5.1 Introduction to Publication 3

The paper presented in this chapter contributed a mathematical programming-based method for solving the integration of ORCs considering the optimal working fluid selections.

For the model establishment, this paper adopts an identical approach with that of the second paper to establish its mathematical model (MINLP). The novelty of this paper comes from the optimization strategy, i.e., a bi-level decomposition method is adopted for optimizing the established model. The outer level uses a genetic algorithm, which can determine the optimal number of ORCs to be integrated and the optimal working fluid selection of each ORC. In the inner level, the established MINLP model is incorporated and is solved by a deterministic algorithm (e.g., the Baron solver). If necessary, the MINLP model can be transformed into an NLP model so that the computational efficiency can be improved. By implementing the bi-level procedure, the optimal HEN synthesis, unit number of ORCs, operation of each ORC, and working fluid selection of each ORC can be simultaneously determined.

In the case study, through comparing the solving result of the proposed method with that of previous literature, the feasibility of the proposed method is proved. It is also shown that, when integrating ORCs, the optimal working fluid selection of each ORC could be different.

4.2 Publication 3

Chu Z., Nan Z., Smith R., The Automatic Working Fluid Selection for Integrating Multi-parallel ORCs into Total Sites (ready for submission)

The Automatic Working Fluid Selection for Integrating Multi-parallel ORCs into Total Sites

Zheng Chu, Nan Zhang*, Robin Smith

Centre for Process Integration, Department of Chemical Engineering and Analytical Science, the University of Manchester, M13 9PL, Manchester, United Kingdom
nan.zhang@manchester.ac.uk

Abstract

When trying to integrate ORC(s) into industrial sites, the working fluid selection(s) could exert influences on system performances, which is an essential matter that should be considered. In the last few decades, lots of research efforts have focused on selecting a proper working fluid for integrating a single ORC, while the working fluid selections for integrating multi-parallel ORCs are rarely investigated. This study aims to fill this blank by proposing a bi-level decomposition method. For modelling, a superstructure-based technology is adopted to represent the heat exchanger network (HEN) for extracting waste heat; a concept of state-point is implemented for evaluating the performances of ORCs. For optimization, the method proposes a bi-level optimization strategy. The outer level adopts a genetic algorithm (GA) to identify the optimal number of ORC parallels, the optimal operation of each ORC train, and the corresponding working fluid selections. While in the inner level, the established MINLP model is incorporated, through solving which the HEN synthesis and the corresponding minimum total annualized cost can be determined. An alternative version of the optimization strategy is also provided, which can improve the calculation efficiency by using a non-linear programming (NLP) problem to substitute the MINLP problem in the inner level. Two case studies are carried out to validate the proposed method. The comparison results show that the multi-parallel ORCs with working fluid selections can achieve more power generation than those that use a monotonous type of working fluid, leading to a decrease in total annualized cost.

Nomenclature

Variables			
Cap	annualized capital cost ($/year)	P	pressure (kPa)
dT	temperature difference (K)	q (Q)	heat duty (kJ)
FC	heat capacity flowrate (kW/K)	S	entropy (kJ/mol·K)
HA	heat exchanger area (m^2)	T	temperature (K)
h (H)	enthalpy (kJ/kg)	U	heat transfer coefficient ($kW/m^2℃$)
LMDT	logarithm approach temperature	W	power output/consumption (kW)
m	mass flowrate (kg/s)	Z	binary variable
Obj	objective variable	ρ	density (kg/m^3)
Parameters			
L	a constant value: 10^4	U	heat transfer coefficient
MF	multiplication factor	η	Isentropic efficiency
M	relative molecular mass	Ω	a constant value: 10^6
Price	marketing price	x	dryness fraction
Subscripts			
bp	boiling point	pre-heat	pre-heating section
c	critical state	prestr	preheating streams
cu	cold utility	re	recovered heat
de-sup	de-superheating	s	supply
elec	electricity	two-phase	two-phase section
eva	evaporators	t	target
evastr	evaporating streams	tb	turbine
hu	hot utility	wf	ORC working fluid
in	inlet	1, 2, 3, …6	state points
int	intermediate	2is	isentropic state point
out	outlet		
Sets			
ORC	the set of ORCs ORC= {orc|1, 2 ... n}	WS	set of waste heat streams WS= {ws|1, 2 ... n}
ST	the set of stages ST= {st|1, 2 ... ST}		

1. Introduction

Organic Rankine Cycles (ORCs) are commonly used to convert low-temperature heat (less than 200 ℃) into electricity. ORCs have a similar working principle to the conventional steam-based Rankine Cycles but using organic compounds to substitute water as working fluids. A typical ORC consists of four main components, i.e., an evaporator, a condenser, an expander, and a working fluid pump, as shown in Figure 1. When operating, a strand of working fluid is vaporized in an evaporator, absorbing heat from heat sources. Then the vaporized stream is sent to a generator-connected expander, where electricity is generated. The exhaust gas of the expander is condensed by a condenser and recycled by a pump.

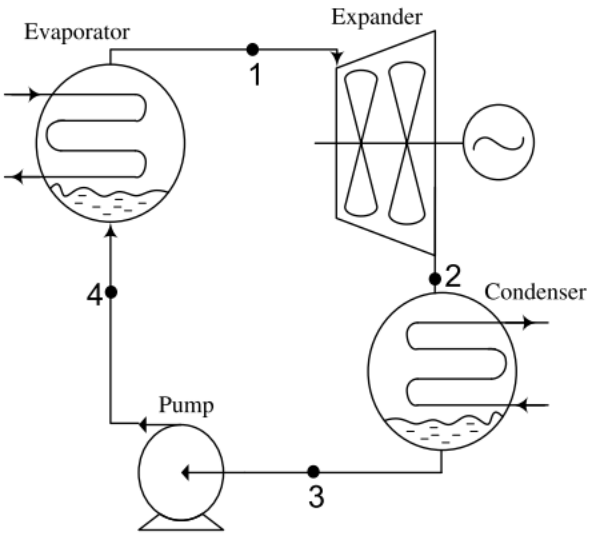

Figure 1. An illustration diagram of a typical Organic Rankine Cycle (Xi et al., 2013)

When integrating ORC(s) into industrial sites for waste heat recovery, how to design the heat exchanger network (HEN) for extracting waste heat, how to determine the optimal operations of ORCs, and how to choose the optimal working fluid for each ORC are the three main problems to be tackled. Lots of relevant methods have been developed in the last few decades. Desai and Bandyopadhyay (2009) proposed a graphical-based method. The method can address the optimal operation of a single ORC system considering various modified architectures, but cannot automatically design the corresponding HEN nor select the optimal working fluid. Hipólito-Valencia et al. (2013) highlighted the necessity of developing

mathematical programming-based methods to deal with ORC integration problems. They proposed a mixed-integer non-linear programming (MINLP) model for integrating a single ORC, through solving which the optimal operation of an ORC and the corresponding HEN synthesis can be simultaneously determined. Chen et al. (2014) proposed another mathematical programming-based method. The method consists of sequential steps. In the first step, a heat integration of background processes is carried out, through which a surplus zone is identified. Then a single ORC is incorporated into the heat surplus zone to recover waste heat. The corresponding model is established by a superstructure-based technology, using rigorous Equation of States (EoS) to correlate the relevant thermodynamic properties, leading to an MINLP optimization problem. Yu et al. (2017b) adopted the Duran-Grossman model (Duran and Grossman, 1986) to target the optimal duty of power generation of a single ORC, leading to a non-linear programming (NLP) problem. Once the duty is given, the corresponding ORC operation and HEN synthesis can then be determined.

Song et al. (2014), Stijepovic et al. (2017) and Dong et al. (2020a) observed that applying multi-parallel ORCs instead of a single ORC could achieve more power generation in some cases. Song et al. (2014) may be the first ones who propose a dual-parallel ORCs system. They divided background waste heat sources into a high-temperature level and a low-temperature level and made each of them exclusively cooperate with a stand-alone ORC, forming a dual-parallel ORCs system. A case study has shown that the dual-parallel system can generate more power than a single ORC system. Stijepovic et al. (2017) proposed an MINLP model for integrating multi-parallel ORCs. The model is established based on the Pinch Analysis technology (Linhoff and Flower, 1978) and the transhipment model (Papoulias and Grossmann,1983). Dong et al. (2020a) developed a method to simultaneously optimize the integrated multi-parallel ORCs and the corresponding HEN. They compared the integration results of a single ORC and dual-parallel ORCs and found that the dual-parallel ORCs can achieve higher net power output than the single ORC.

The studies mentioned above offer methods for integrating single or multi-parallel ORCs. By

using the methods, one can sequentially or simultaneously determine the optimal operation(s) of ORC(s) and the corresponding HEN synthesis. However, it is observed that the methods failed to provide an efficient way to select the optimal working fluid(s) for the integrated ORC(s).

To this perspective, some researchers proposed heuristical principles, aiming to select the optimal working fluids of ORCs without mathematical calculations. SALEH et al. (2007) screened 31 pure organic substances as ORC working fluids. It was regulated that the ORCs are operated between 100 ℃ (evaporation temperature) and 30 ℃ (condensation temperature) with a maximum pressure of 20 bar. Results show that different working fluids can exhibit significant discrepancies in thermal efficiency even with the same evaporation temperature. Amongst the 31 investigated substances, n-hexane is conceived to have the highest thermal efficacy (13.00%), followed by n-pentane (12.91%) and iso-pentane (12.75%). Xu and Yu (2014) correlated the ORC performances with the critical temperatures of working fluids. They declared that the working fluids with critical temperatures close to the inlet temperatures of heat sources could achieve maximum thermal efficiency. They recommended selecting the organic compounds with critical temperatures 20 K to 100 K higher than the inlet temperatures of heat sources as ORC working fluids. Wang et al. (2020) screened the environmental and economic performances of 14 different working fluids that cooperate with a heat source with a temperature range from 90℃ to 230℃. They declared that, with different heat source temperatures, different working fluids could lead to diverse economic performances and environmental benefits. They carried out a series of parametric analyses, through which the promising working fluids and the corresponding optimal heat source temperatures are advised.

The heuristical principles provide an efficient way to select the optimal (or near-optimal) ORC working fluid for the cases with a single heat source. However, when integrating ORCs into practical industrial sites, for most cases, there could be multiple heat sources with different temperatures and heat duties, leading to more complex thermal matches. In such

circumstances, the applicability of the heuristical principles is limited. In another aspect, the trade-off between power generation and the related capital and operating costs increases the difficulties of applying the heuristical principles. In summary, it is pointed out that the selections of optimal working fluids are case-sensitive, which should be carried out by rigorous calculations (Dong et al., 2020b). Therefore, it is necessary to develop mathematical programming-based methods to help select the optimal ORC working fluids.

There are a few developed mathematical programming-based methods extended ORC integration problems by considering working fluid selections. Kermani et al. (2018) proposed a bi-level optimization strategy. The outer level adopts a genetic algorithm (GA) to determine the optimal working fluid and the corresponding operation of an ORC. The inner level consists of a mixed-integer linear programming (MILP) problem, which can carry out the heat integration with background processes. Dong et al. (2020b) not only included the operating temperature, pressure, and flowrate of an ORC as decision variables but also considered the different selections of working fluids. They pre-selected 43 pure organic components and 36 binary mixtures as the working fluid candidates. For modelling, they adopted the Pinch Location method (Duran and Grossman, 1986), leading to an NLP model. For optimization, a bi-level decomposition strategy was applied.

However, it can be observed that the previous studies only considered to select the optimal working fluid for integrating a single ORC, while the working fluid selections for integrating multi-parallel ORCs are still left as blank. Compared with the integration of a single ORC, the integration of multi-parallel ORCs could be more challenging. The challenges are: 1. the optimal number of ORC parallels is variable; 2. each ORC in parallel could have different operating conditions, leading to different optimal working fluid; 3. the heat integration with background heat sources could become more complex. As such, this study aims to fill the blank by proposing a mathematical programming-based method, which can automatically select the optimal working fluids for the integrated multi-parallel ORCs. The challenges

mentioned above are to be addressed. For modelling, the method adopts a superstructure-based technology and a concept of thermodynamic state-points, of which the details will be introduced in Chapter 4. For optimizing, the method proposes a bi-level optimization strategy, which will be introduced in Chapter 5 and 6. By applying the method, the operating conditions of multi-parallel ORCs, the optimal working fluids, and the heat integration with background heat sources can be simultaneously determined, leading to a minimum total annualized cost.

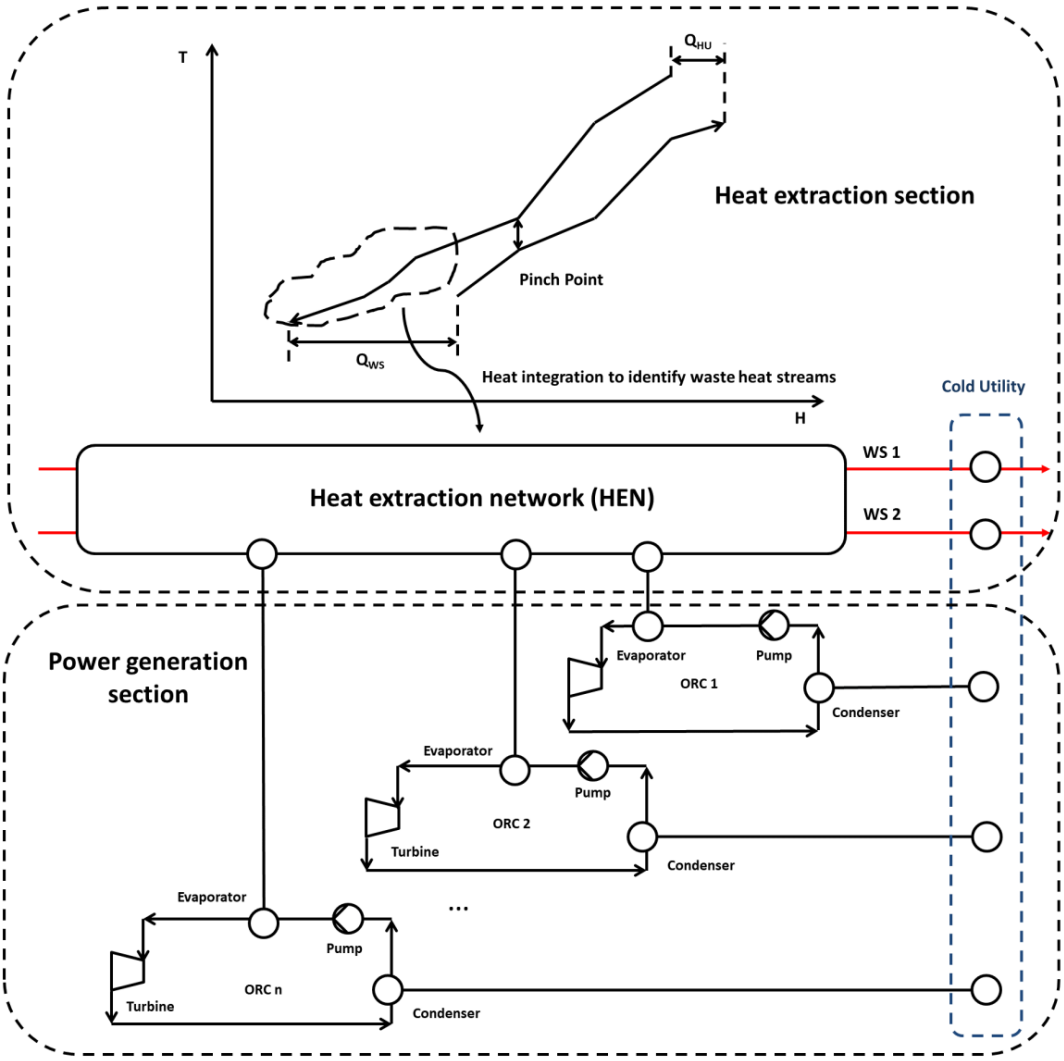

Figure 2. The illustration diagram of a multi-parallel ORCs system

2. Problem Statement

The illustrative diagram of a multi-parallel ORCs system is shown in Figure 2. It can be

assumed that a set of waste heat streams, WS= {ws|1, 2 ... n}, have been identified, of which the inlet/outlet temperatures, the heat capacity flowrates, and the heat transfer coefficients are specified. There are multi-parallel ORCs, ORC = {orc|1, 2 ... n}, implemented to exploit the waste heat. Note that each ORC in parallel operates independently. The residual heat that the ORCs cannot exploit is discharged to cold utilities. The goal is to minimize the total annualized cost via integrating the multi-parallel ORCs with the waste heat streams. The decision variables include the number of ORC parallels, the operating condition (evaporating temperature/pressure, condensing temperature/pressure, and working fluid mass flowrate) of each ORC, the working fluid selection of each ORC, the utility consumption, and the related variables of HEN synthesis.

3. Working fluid Pre-Screening

There are three main aspects that should be considered for pre-screening ORC working fluids, which are thermodynamic performance, safety, and the impacts on the environment.

- **Thermodynamic performance**

According to the slopes of saturated vapour curves in T-S diagrams, Huang et al. (1997) classified the ORC working fluids into three categories: wet, dry, and isentropic. The dry working fluids present positive slopes; the wet working fluids exhibit negative slopes; the isentropic ones typically have infinite large slopes. An illustrative diagram of the three types of working fluid is shown in Figure 3. It is argued that dry or isentropic working fluids are more favourable in practical applications, as wet working fluids could form droplets at the exits of turbines, resulting in a series of operative issues (Yu et al., 2015).

On the other hand, the critical temperatures of the pre-selected working fluids have to be higher than the evaporating temperatures of ORCs to avoid supercritical operating conditions. In the application scenarios of waste heat recovery, the evaporating temperatures are normally ranged from 50℃ to 200℃. So, the pre-selected working fluids should have critical

temperatures higher than 50℃ in general. In addition, this study regulates that the saturated pressures of the pre-selected working fluids at 35℃ should be higher than the atmospheric pressure to avoid the creation of vacuum during condensation (the lower limit of condensation temperatures are assumed as 35℃).

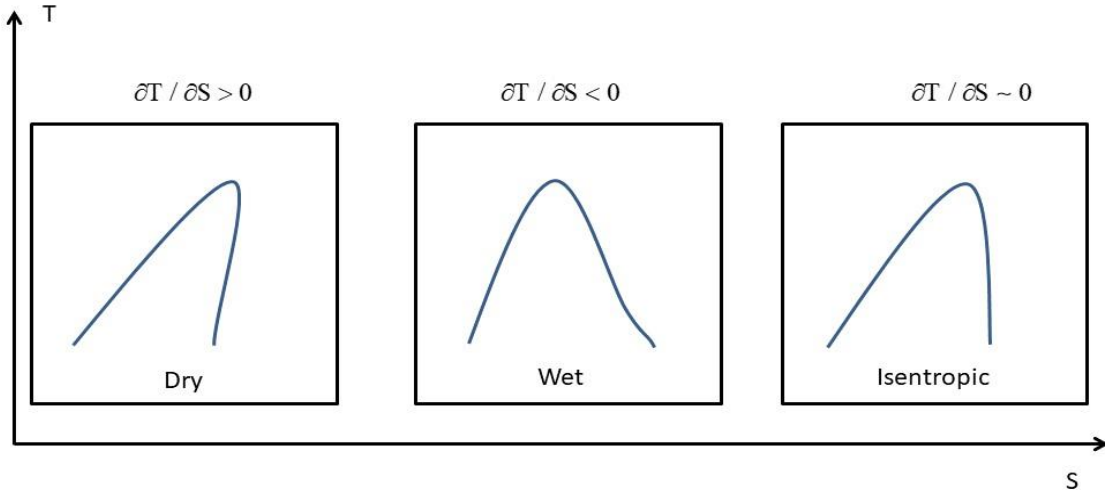

Figure 3. The T-S diagram of different types of working fluid

- **Safety**

An appropriate ORC working fluid is expected to be non-flammable, non-corrosive, and non-toxic (Chen et al., 2010). As for the toxicity, this study references the assessments proposed by ASHRAE (2009). According to ASHRAE (2009), the toxicity of working fluids is graded into A and B levels. The ones with B-level grades are more toxic than the A-level ones. In this study, it is regulated that all the pre-selected working fluids should have A-level grades. As for the corrosive and flammability, it is inevitable for organic working fluids to be flammable and corrosive to some extent. However, recommendation lists of working fluids that have relatively low flammability and corrosiveness can be found in the previous literature (Bao and Zhao, 2013; Yu et al., 2015; Scaccabarozzi et al., 2018), and the lists are referenced by this study.

- **Impacts on the environment**

A basic environmental requirement for ORC working fluids is zero ozone depletion potential

(ODP) (Wang et al., 2020). Therefore, this study regulates that all the pre-selected working fluid should have zero ODP.

Considering all the above factors, 9 working fluids are pre-screened, of which the details are listed in Table 1

Table 1. The pre-screened working fluids

Substance	Formula	M	T_{bp} (K)	T_c (K)	P_c (Mpa)	Toxicity (ASHRAE)	ODP
R245ca	$C_3F_5H_3$	134.05	298.28	447.57	3.940	A	0
R236fa	C3F6H2-D1	152.04	271.71	398.07	3.200	A	0
R227ea	C3F7H	170.03	256.70	374.80	2.912	A	0
R218	C3F8	188.02	236.32	345.10	2.640	A	0
R601	C5H12-1	72.14	309.26	469.70	3.368	A	0
R601a	C5H12-2	72.14	301.10	460.35	3.378	A	0
R600	C4H10-1	58.12	272.60	425.13	3.796	A	0
R600a	C4H10-2	58.12	261.48	407.80	3.640	A	0
Cyclopentane	C5H10	70.13	322.45	556.75	4.52	A	0

4. Model Description

In this section, an MINLP model is established. The overall model is separated into three sub-modules, which are a heat extraction module, a power generation module, and an objective function. The heat extraction module represents the heat integration with background waste heat sources, while the power generation module formulates the thermodynamic performances of ORCs. These two modules are correlated by energy balances. The objective function evaluates the economic performance of the integration of ORCs.

4.1. Heat extraction sub-module

This module is established by a superstructure-based technology, which is derived from the Synheat superstructure-based model (Yee and Grossman, 1990). The illustrative diagram of

the superstructure is shown in Figure 4, where the hot streams (waste heat streams) and cold streams (ORC working fluids) are represented by the red and blue lines, respectively.

For the hot side, there are several stages divided. In each stage, each participated hot stream is split into several sub-streams in parallel, and each sub-stream is directed to a heat exchanger, representing a potential match of heat transfer with the opposite side. The principles of dividing stages and splitting/mixing sub-streams are in correspondence with the Synheat superstructure (Yee and Grossman, 1990).

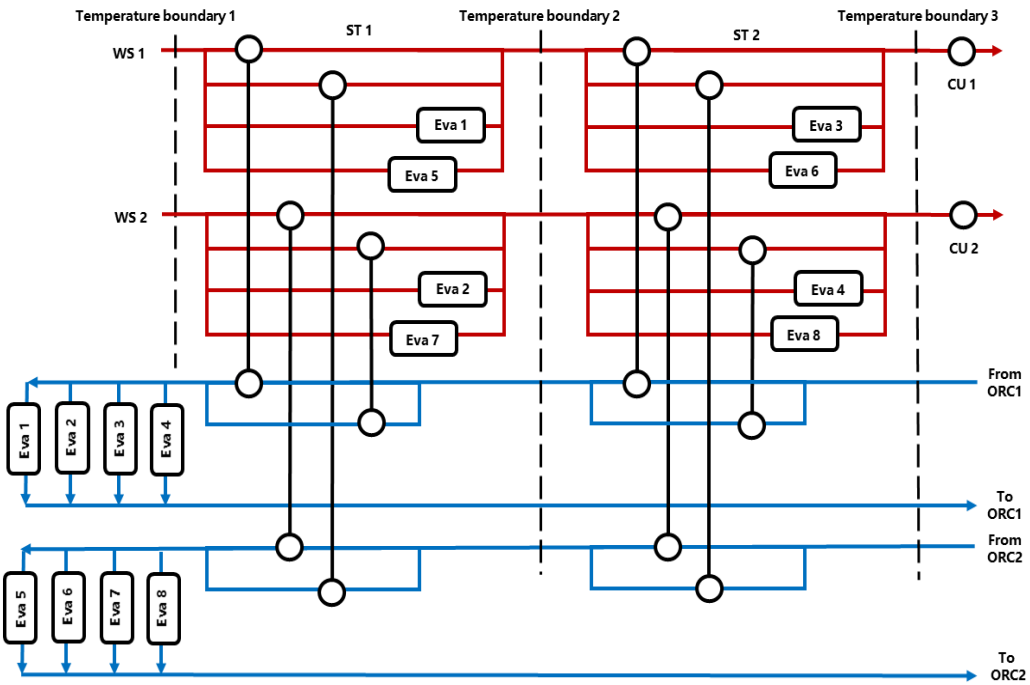

Figure 4. The illustrative diagram of the stage-wise superstructure

For the cold side, to avoid difficulties in the calculations of heat transfer coefficients and heat transfer area, each strand of ORC working fluid is separated into a pre-heating stream and an evaporating stream. The theoretical basis of doing this is referred from Wei et al. (2008) and Imran et al. (2020). It can be seen from Figure 4 that the pre-heating streams are divided into the same number of stages as that of the hot side. In contrast, the evaporating streams are split in parallel without any stage divisions. For each evaporating stream, the number of sub-streams to be split is determined by the following equation：

$$N_{split} = N_{stage} \cdot N_{ws}$$

Where N_{split} is the spilt sub-streams of an evaporating stream; N_{stage} is the total number of the divided stages; N_{ws} is the total number of the waste heat streams.

Once the superstructure has been determined, the corresponding mathematical formulation, including temperature assignments, energy balances, utility usages, logical constrains, thermodynamic feasibilities and heat exchanger area calculations, can be established. The relevant equations are similar to those of the Synheat model, which are omitted in this section. Readers can find them in Appendix A.

4.2. Power generation sub-module

A method of thermodynamic state-points is imported for establishing this sub-module. The main idea of the method is to calculate the thermodynamic properties of the state-points mapped on the T-S diagram of an ORC (as shown in Figure 5), through which the operating conditions of ORC working components can be correlated, and the performance of the whole ORC system can be evaluated.

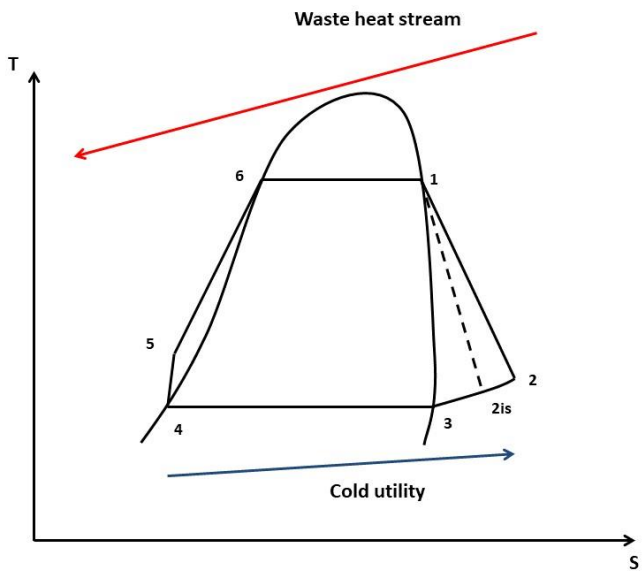

Figure 5. The T-S diagram of an ORC

- **Turbines**

Turbines are operated between state points 1 (turbine inlet) and 2 (turbine outlet). State point 2_{is} represents an ideal situation without any irreversible losses (i.e., the isentropic efficiency is 100%). If ignoring mechanical losses, the power output of a turbine can be given as:

$$W_{tb}^{orc} = m_{wf}^{orc} \cdot (h_1^{orc} - h_2^{orc}) = m_{wf}^{orc} \cdot \eta_{tb}^{orc} (h_1^{orc} - h_{2is}^{orc}), \ \text{orc} \in \text{ORC} \tag{1}$$

As for multi-parallel ORCs, the total power output is:

$$W_{tb,total} = \sum_{orc \in ORC} W_{tb}^{orc} \tag{2}$$

- **Condensers**

In condensers, working fluids go through state points 2, 3 and 4. From state points 2 to 3, the thermodynamic states of working fluids are transformed from superheated gas to saturated vapour. Then from state points 3 to 4, the thermodynamic states are transformed to saturated liquid. Corresponding with these thermodynamic processes, we can divide a condenser into two sections, i.e., a de-superheating section (point 2 to point 3) and a two-phase section (point 3 to point 4). The energy balance of the de-superheating section is:

$$q_{con,de-\sup}^{orc} = m_{wf}^{orc} \cdot (h_2^{orc} - h_3^{orc}), \ \text{orc} \in \text{ORC} \tag{3}$$

The energy balance of the two-phase section is:

$$q_{con,two-phase}^{orc} = m_{wf}^{orc} \cdot (h_3^{orc} - h_4^{orc}), \ \text{orc} \in \text{ORC} \tag{4}$$

The cooling demand of a condenser is:

$$q_{con,total}^{orc} = q_{con,de-\sup}^{orc} + q_{con,two-phase}^{orc} \ , \ \text{orc} \in \text{ORC} \tag{5}$$

As for multi-parallel ORCs, the total cooling demand is:

$$q_{con,total} = \sum_{orc \in ORC} q_{con,total}^{orc} \tag{6}$$

- **Working fluid pumps**

A working fluid pump is operated between state points 4 (a saturated liquid state) and 5 (a sub-cooling liquid state). The power consumption of a working fluid pump can be calculated by Equation (7), as shown below:

$$W_{pump}^{orc} = \frac{m_{wf}^{orc}}{\eta_{\text{pump}}^{orc} \cdot \rho_{wf}^{orc}} (P_5^{orc} - P_4^{orc}), \ \text{orc} \in \text{ORC} \tag{7}$$

Where η_{pump}^{orc} is the isentropic efficiency of each pump; ρ_{wf}^{orc} is the density of the working fluid flowing through.

The total power consumed by the pumps of multi-parallel ORCs is:

$$W_{pump,total} = \sum_{orc \in ORC} W_{pump}^{orc} \tag{8}$$

- **Evaporators**

As depicted in Figure 5, there are two thermodynamic processes occurring in an evaporator. From state points 5 to 6, the thermodynamic state of working fluid is transformed from sub-cooling liquid to saturated liquid. From state points 6 to 1, the thermodynamic state is transformed from saturated liquid to saturated vapour. Corresponding to the thermodynamic processes, two sections (i.e., a pre-heating section and a two-phase section) can be divided, of which the energy balances are given below:

$$q_{eva,pre-heat}^{orc} = m_{wf}^{orc} \cdot (h_6^{orc} - h_5^{orc}), \ \text{orc} \in \text{ORC} \tag{9}$$

$$q_{eva,two-phase}^{orc} = m_{wf}^{orc} \cdot (h_1^{orc} - h_6^{orc}), \ \text{orc} \in \text{ORC} \tag{10}$$

- **Thermodynamic properties of state points**

The decision variables are evaporating and condensing temperatures (T_1 and T_4) of each ORC. The thermodynamic properties of each state point can be correlated with the decision variables, shown by the following equations.

1) For state point 1:

$$P_1^{orc} = \boldsymbol{P}(T_1^{orc}, x = 1), \ \text{orc} \in \text{ORC} \tag{11}$$

$$h_1^{orc} = \boldsymbol{H}(T_1^{orc}, x = 1), \ \text{orc} \in \text{ORC} \tag{12}$$

$$s_1^{orc} = \boldsymbol{S}(T_1^{orc}, x = 1), \ \text{orc} \in \text{ORC} \tag{13}$$

2) For state points 2 and 2is:

$$P_{2is}^{orc} = P_2^{orc} = P_3^{orc} \tag{14}$$

$$s_{2is}^{orc} = s_1^{orc} \tag{15}$$

$$h_{2is}^{orc} = \boldsymbol{H}(P_{2is}^{orc}, s_{2is}^{orc}),\ \text{orc} \in \text{ORC} \tag{16}$$

$$h_2^{orc} = h_1^{orc} - \eta_{tb}^{orc} \cdot (h_1^{orc} - h_{2is}^{orc}) \tag{17}$$

$$T_2^{orc} = \boldsymbol{T}(P_2^{orc}, h_2^{orc}),\ \text{orc} \in \text{ORC} \tag{18}$$

3) For state point 3:

$$T_3^{orc} = T_4^{orc} \tag{19}$$

$$P_3^{orc} = \boldsymbol{P}(T_3^{orc}, x = 1),\ \text{orc} \in \text{ORC} \tag{20}$$

$$h_3^{orc} = \boldsymbol{H}(T_3^{orc}, x = 1),\ \text{orc} \in \text{ORC} \tag{21}$$

4) For state point 4:

$$P_4^{orc} = \boldsymbol{P}(T_4^{orc}, x = 0),\ \text{orc} \in \text{ORC} \tag{22}$$

$$h_4^{orc} = \boldsymbol{H}(T_4^{orc}, x = 0),\ \text{orc} \in \text{ORC} \tag{23}$$

$$s_4^{orc} = \boldsymbol{S}(T_4^{orc}, x = 0),\ \text{orc} \in \text{ORC} \tag{24}$$

5) For state point 5:

$$P_5^{orc} = P_1^{orc} \tag{25}$$

$$h_5^{orc} = h_4^{orc} + \frac{W_{pump}^{orc}}{m_{wf}^{orc}},\ \text{orc} \in \text{ORC} \tag{26}$$

$$T_5^{orc} = \boldsymbol{T}(P_5^{orc}, h_5^{orc}),\ \text{orc} \in \text{ORC} \tag{27}$$

6) For state point 6:

$$T_6^{orc} = T_1^{orc} \tag{28}$$

$$h_6^{orc} = \boldsymbol{H}(T_6^{orc}, x = 0),\ \text{orc} \in \text{ORC} \tag{29}$$

In this study, we did not adopt any Equation of States to establish the explicit formulations of the functions $y = \boldsymbol{P}(x)$, $y = \boldsymbol{T}(x)$, $y = \boldsymbol{H}(x)$, $y = \boldsymbol{S}(x)$. As to correlate the thermodynamic performances of different working fluids, we may need to adopt different types of Equations of State to guarantee the calculation accuracy, which could increase the complexity of the model. Therefore, to simplify the modelling and coding process, the corresponding function values are calculated by the NIST REFPROP® software.

4.3. Correlation of the two sub-modules

The common part of the two sub-modules are evaporators. The pre-heating streams defined in the heat extraction sub-module correspond to the pre-heating sections in evaporators, while the evaporating streams in the heat extraction sub-module correspond to the two-phase sections in evaporators. According to this correspondence, the energy balance of the two sub-modules can be given as:

$$q_{eva,pre-heat}^{orc} = q_{prestr,total}^{orc} = (T_{t,prestr}^{orc} - T_{s,prestr}^{orc}) \cdot FC_{prestr}^{orc} \tag{30}$$

$$T_{t,prestr}^{orc} = T_{6}^{orc} \tag{31}$$

$$T_{s,prestr}^{orc} = T_{5}^{orc} \tag{32}$$

$$q_{eva,two-phase}^{orc} = q_{evastr,total}^{orc} \tag{33}$$

4.4. Objective function

The objective function calculates the total annualized cost of integrating multi-parallel ORCs, in which the relevant capital cost, operating cost, and the profit brought up by power generation are taken into account. A general formulation of the objective function is shown in Equation (34).

$$\mathrm{Obj} = (Cap_{extration} + Cap_{generation}) + Operating - Profit \tag{34}$$

Where the $Cap_{extration}$ and $Cap_{generation}$ terms are the annualized capital costs for extracting waste heat and generating power respectively; the $Operating$ term is the relevant operating cost; the $Profit$ term is the total profit brought up by power generation.

This study assumes that the annualized capital cost for extracting waste heat ($Cap_{extration}$) is mainly contributed by heat exchangers, which can be calculated by Equation (35). This equation is original from Couper et al. (2012), and is also adopted by Dong et al. (2020b).

$$Cap_{extraction} = \frac{MF}{PB_{\mathrm{yr}}}[16620 + 575 \cdot \sum_{ws \in WS} \sum_{orc \in ORC} \sum_{st \in ST} (HA_{prestr}^{ws,orc,st} + HA_{evastr}^{ws,orc,st})] \tag{35}$$

The annualized capital cost of power generation ($Cap_{generation}$) mainly comes from the annualized costs of ORC working components (turbines, pumps, and condensers), which can be calculated by the following equations. Note that equations (38) and (39) are taken from Dong et al. (2020b).

$$Cap_{generation} = Cap_{tb} + Cap_{pump} + Cap_{con} \tag{36}$$

$$Cap_{tb} = \sum_{orc \in ORC} \frac{MF}{PB_{yr}} (2050 \cdot W_{tb}^{orc\ 0.83}) \tag{37}$$

$$Cap_{pump} = \sum_{orc \in ORC} \frac{MF}{PB_{yr}} 3540 \cdot W_{pump}^{orc\ 0.71} \tag{38}$$

$$Cap_{con} = \sum_{orc \in ORC} \frac{MF}{PB_{yr}} [16620 + 575 \cdot (HA_{con,de-\sup}^{orc} + HA_{con,two-phase}^{orc})] \tag{39}$$

In Equation (39), the $HA_{con,de-\sup}^{orc}$ and $HA_{con,two-phase}^{orc}$ terms are still unknown, which can be calculated by the following equations.

$$HA_{con,de-\sup}^{orc} = \frac{q_{con,de-\sup}^{orc}}{U_{de-\sup}^{orc} \cdot LMDT_{con,de-\sup}^{orc}}, \ \mathrm{orc} \in \mathrm{ORC} \tag{40}$$

$$LMDT_{con,de-\sup}^{orc} = \left[\frac{(T_2^{orc} - T_{cu,out}^{\mathrm{orc}})(T_3^{orc} - T_{cu,\mathrm{int}}^{orc})(T_2^{orc} - T_{cu,out}^{orc} + T_3^{orc} - T_{cu,\mathrm{int}}^{orc})}{2} \right]^{1/3}, \ \mathrm{orc} \in \mathrm{ORC} \tag{41}$$

The $\mathrm{T}_{\mathrm{cw,int}}^{\mathrm{orc}}$ term in Equation (41) represents an intermediate temperature of cold utility stream, which can be calculated by Equation (42).

$$\frac{(T_{cu,\text{int}}^{orc} - T_{cu,in}^{orc})}{(T_{cu,out}^{orc} - T_{cu,\text{int}}^{orc})} = \frac{q_{con,two-phase}^{orc}}{q_{con,de\text{-sup}}^{orc}}, \ \text{orc} \in \text{ORC} \tag{42}$$

$$HA_{con,two-phase}^{orc} = \frac{q_{con,two-phase}^{orc}}{U_{two-phase}^{orc} \times LMDT_{con,two-phase}^{orc}}, \ \text{orc} \in \text{ORC} \tag{43}$$

$$LMDT_{con,two-phase}^{orc} = \left[\frac{(T_3^{orc} - T_{cu,\text{int}}^{\text{orc}})(T_4^{orc} - T_{cu,in}^{orc})(T_3^{orc} - T_{cu,\text{int}}^{orc} + T_4^{orc} - T_{cu,\text{in}}^{orc})}{2} \right]^{1/3}, \ \text{orc} \in \text{ORC} \tag{44}$$

It is assumed that the operating cost are mainly contributed by utility usage, which can be calculated by Equation (45).

$$Operating = price_{cu} \cdot (\sum_{ws \in WS} q_{cu}^{ws} + \sum_{orc \in ORC} q_{con,total}^{orc}) \tag{45}$$

The profit from the sale of generated power is calculated as:

$$Profit = AOH \cdot price_{elec} \cdot \sum_{orc \in ORC} (W_{tb}^{orc} - W_{pump}^{orc}) \tag{46}$$

5. Optimization Strategy

In the last chapter, the established model leads to an MINLP problem, namely **MP**, which is presented as following:

$$\text{Min: obj}=AF \cdot (Cap_{\text{extraction}} + Cap_{generation}) + Operating - profit$$

$$s.t. \ \ \chi(x) = \left\{ x \left| \begin{array}{l} \text{heat extraction sub-module Eqs. (A1)~(A25)} \\ \text{power generation sub-module Eqs. (1)□ (29)} \\ \text{correlations of the tow modules Eqs. (30)~(33)} \\ \text{Onjective fuction Eqs. (34)~(46)} \end{array} \right. \right\} \tag{MP}$$

By solving the **MP,** the power output of ORCs, as well as the HEN synthesis between the ORCs and background heat sources, can be determined. However, there are problems left: 1. the optimal number of ORCs to be implemented is still unknown; 2. the model cannot select

the optimal working fluids for the integrated ORCs. To address these problems, this study proposes a bi-level optimization strategy, of which the block-flow diagram is illustrated in Figure 6.

In the outer level, decision variables include the number of ORCs to be implemented, the operating condition (evaporating temperature, condensing temperature, and mass flowrate of working fluid) of each ORC, and the working fluid selection of each ORC. A genetic algorithm (GA) implemented in the MATLAB® platform is adopted to determine the optimal values of these variables. During optimizing, first, the GA generates an initial population by randomly assigning sets of different values to the decision variables. Each set of values is regarded as an individual of population. Note that the values assigned to the variables should be within their bounds. Then, for each individual, the MATLAB® calls the NIST REFPROP® software to calculate the related thermodynamic properties. The calculated thermodynamic properties and the decision variables are introduced as parameters to the inner level.

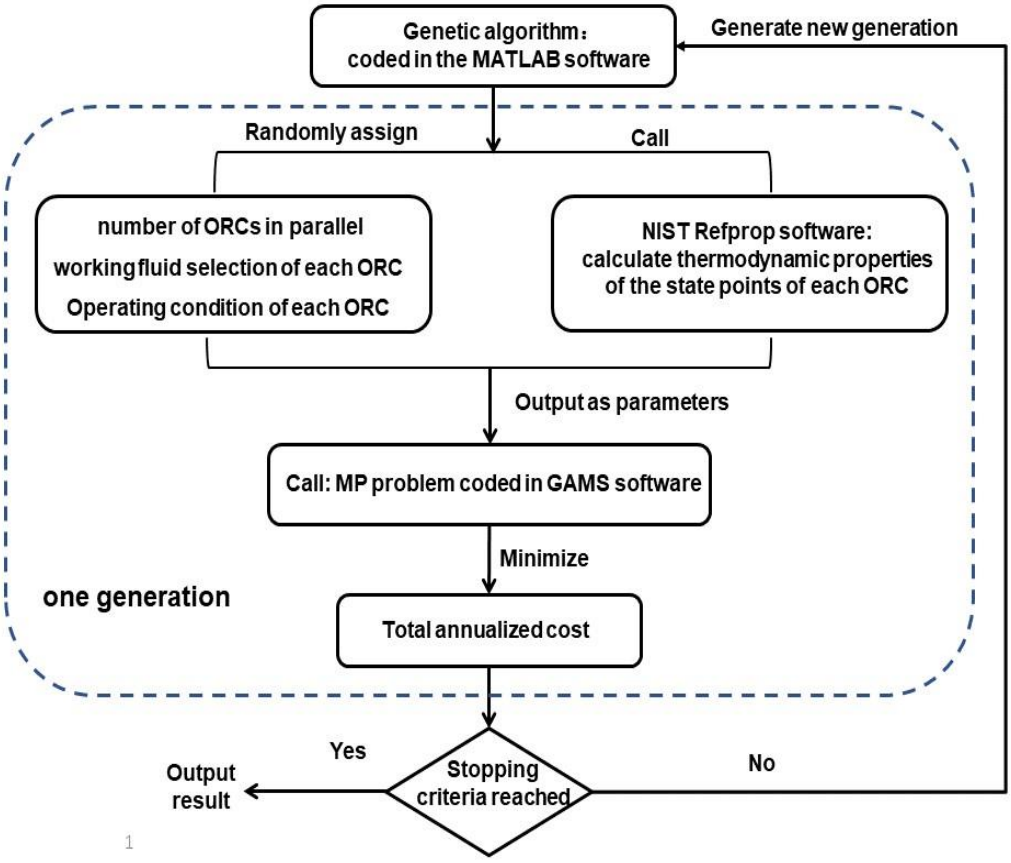

Figure 6. The block-flow diagram of the optimization strategy

In the inner level, receiving the outputs from the outer level, **MP** problems are solved by the GAMS® software with the Baron MINLP solver (Sahinidis, 1996). For different individuals, the corresponding solving result could be different, leading to various HEN synthesises and total annualized costs. The solving results are then sent back to the outer level, where the GA selects the individuals that behave well (i.e., with less total annualized costs), using them to generate a new generation.

Such an optimizing process will be repeated again and again until one of the following convergence criteria is reached. The convergence criteria are:

a) the maximum generation is set as 200

b) the maximum computational time is set as 10 hours

c) the best individual does not change in 10 successive generations

6. An Alternative Optimization Strategy

Several case studies have proven that the Baron solver, which is based on the Branch and Bound technique, could be relatively computational expensive for solving HEN synthesis problems. For instance, for a HEN synthesis problem with three hot streams and two cold streams, it is tested that the Baron solver requires about 100 seconds of CPU time to get convergence (Escobar and Trierweiler, 2013). In this study, the Baron solver is integrated with a GA, which even increases the overall computational effort. It is logical to deduce that the time consumption could be unacceptable for some cases.

To this perspective, this study offers an alternative optimization strategy improved from the original one, of which the block-flow diagram is shown in Figure 7. In the inner level of the alternative strategy, an NLP problem, namely **MP-alt**, is proposed to substitute the previous **MP** problem, of which the details are introduced in Appendix B. The Conopt NLP solver (Drud, 1985) is adopted to solve the **MP-alt** problem. As illustrated in Figure 7, the optimization result of the bi-level algorithm, including the optimal parallel number, the optimal working fluid selection of each ORC in parallel, the operating conditions of ORCs, and the relevant thermodynamic properties, are further output to an **MP** problem. By solving the **MP** problem, the HEN synthesis can then be carried out, and the corresponding minimum total annualized cost is output as the final solution.

Compared to the original optimization strategy, the alternative strategy adopts an NLP problem solved by the Conopt solver instead of an MINLP problem solved by the Baron solver as its inner level. The NLP problem can still consider the trade-off between costs and profits, providing enough information for the GA to optimize the relevant decision variables. Based on the comparison results of previous case studies (Escobar and Trierweiler, 2013), it is reasonable to expect that the solving process of the NLP problem can lead to less computational time. It should be noted that the nonconvex nature of the **MP-alt** problem may lead to more than one local optimal solution. To increase the likelihood of obtaining the global

optimal solution, the initialization procedure proposed by Yee and Grossmann (1990) is taken.

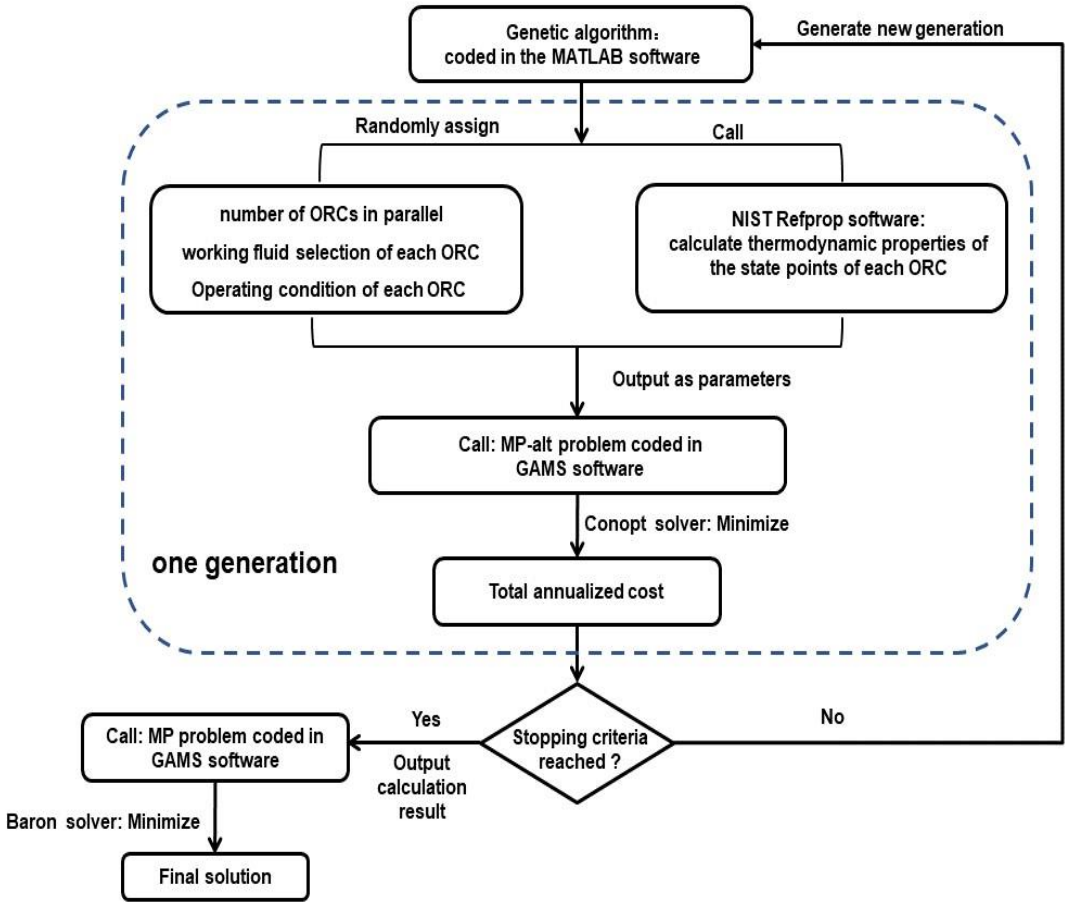

Figure 7. The block-flow diagram of the alternative optimization strategy

7. Case Study

7.1. Case study 1

This case study is taken from Elsido et al. (2017), which is also analyzed by Done et al. (2020a). We use this case study to validate the applicability of the proposed method. The background information is shown in Table 2. Note that the previous literature adopted different equations from those of this study (Equations (35) ~ (39)) to evaluate the economic performances of working components, leading to a different objective function. As such, for ease of comparison, it is regulated that the objective function applied in this case study should be identical to that of the previous literature.

Table 2. The background information of case study 1

streams	supply temperature (℃)	target temperature (℃)	heat capacity flowrate (kW/℃)	heat transfer coefficient (kW/m^2 ℃)
WS1	150	70	12.5	0.5
WS2	100	60	62.5	0.5
WS3	130	70	50	0.5
cold utility	15	20		1.5
ORC heat transfer coefficient				
pre-heating working fluids				1.0
evaporating working fluids				10.0
de-superheating working fluids				0.6
condensing working fluids				2.0
Economic data				
parameters			**value**	
annualized factor			0.2	
multiplication factor			2.5	
operating hours			7000 h	
cold utility cost			20 $/kW • year	
electricity price			0.14 $/kW • h	

More details of the objective function can be found in Elsido et al. (2017) and Done et al. (2020a). Other necessary information is provided below:

1. the isentropic efficiencies of turbines and pumps are 82% and 70%, respectively;
2. according to Done et al. (2020a), the fixed charge for implementing a heat exchanger is considered, which is 100$;

The proposed method is applied to integrate ORCs with the waste heat streams. We first tried to integrate a single ORC using the original optimization strategy introduced in Chapter 5. The population of each generation of GA is configured as 200 individuals. The time limitation for running the Baron solver is set as 80 seconds. A desktop PC with Intel® Core (TM) i5 CPU

3.33 GHz and 8.00 GB of RAM is used for processing the program. Based on such configuration, it is found that the original optimization strategy takes about 3 hours to finish one generation of GA. In this case, it can be deduced that the time consumption for getting convergence is unacceptable. As such, in order to improve solving efficiency, the alternative optimization strategy introduced in Chapter 6 is adopted instead of the original one.

First, the integration of a single ORC is carried out as the reference case. During optimization, the bi-level algorithm terminates at the 57th generation, occupying about 420 seconds of CPU time. The solving result of the bi-level algorithm is then output to the corresponding **MP** problem, which is solved by the Baron solver to obtain the global optimum. The solving process of the **MP** problem takes about 150 seconds of CPU time.

After integrating a single ORC, the integration of multi-parallel ORCs is considered. We set the maximum number of ORC parallels as four. The optimization strategy can automatically determine the optimal number of the ORCs in parallel to be implemented, as well as the corresponding optimal working fluid for each ORC train. During optimization, the bi-level algorithm terminates at the 88th generation, taking about 610 seconds of CPU time. The sequenced **MP** problem occupies about 330 seconds of CPU time to be solved, leading to an overall 940 seconds CPU time for completing the optimization process.

Table 3. The comparison results for Case 1

	Elsido et al. (2017)	**Dong et al. (2020a)**		**current paper**	
Number of ORCs	dual-parallel	single	dual-parallel	single (Ref. case)	dual-parallel
working fluid	n-pentane	n-pentane		R600a (iso-butane)	cyclopentane& R600a
mass flowrate of 1st ORC (kg/s)	14.63	33.94	18.90	37.62	17.17
mass flowrate of 2nd ORC (kg/s)	19.31	/	13.41	/	16.91

evaporating temperature of 1st ORC (℃)	115.70	82.1	107.1	93.19	108.67
evaporating temperature of 2nd ORC (℃)	84.30	/	80.2	/	81.52
condensing temperature of 1st ORC (℃)	30.00	25.00	25.00	25.00	25.00
condensing temperature of 2nd ORC (℃)	30.00	/	25.00	/	25.00
net power output (MW)	1.85	1.74	1.98	1.86	2.06
overall thermal efficiency	11.93%	11.23%	12.77%	12.09%	13.32%
number of heat exchangers	12	8	13	7	14
total heat exchanger area (m^2)	4994	4081.5	4682	4773.5	5226.8
total cold utility usage (kW)	13536.7	13935.8	13612.1	13542.7	13399.1

The optimization results given by the proposed method are shown in Table 3 and Figure 8, in which the comparisons with the previous research are also presented. As shown in Figure 8, the integration of a single ORC (reference case) obtains a total annualized cost of -0.623 M$/year by using the proposed method, which is 8.7% lower than that given by Dong et al. (2020a). The corresponding optimal working fluid selection is iso-butane instead of n-pentane. Compared with Dong et al. (2020a), even though the proposed method introduces a 692 m^2 extra heat exchanger area, it also increases the net power output from 1.74 MW to 1.86 MW, leading to an increase of 0.118 M$/year in power generation revenue. The improvement in optimization result validates the applicability of the proposed method.

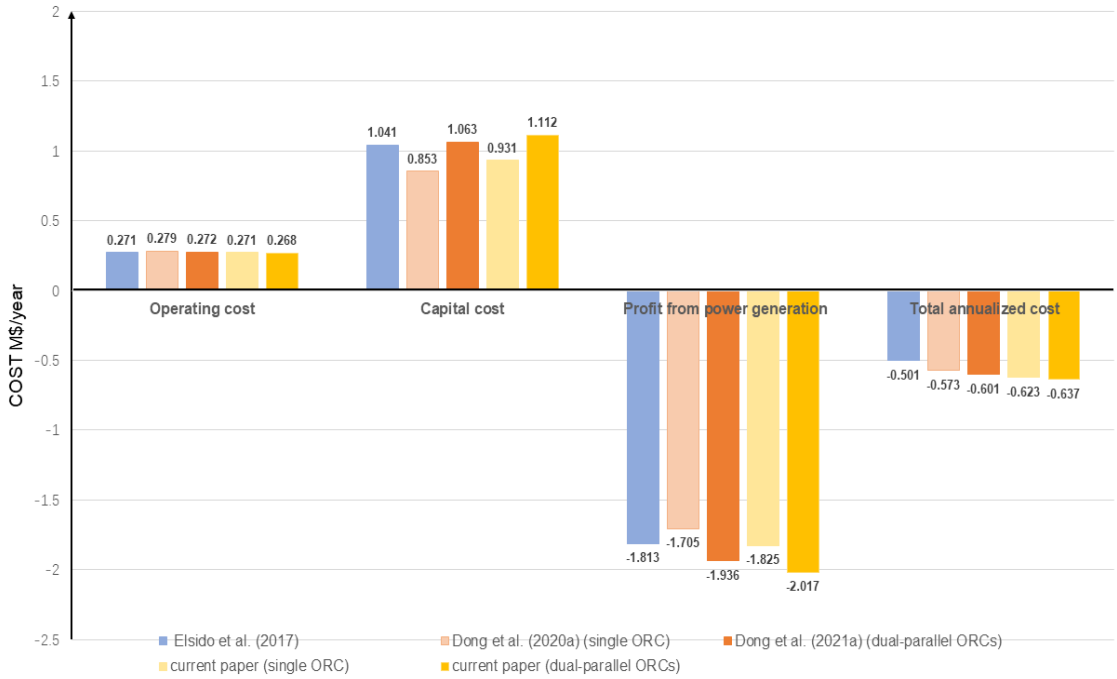

Figure 8. The comparison results for case 1

As for the integration of multi-parallel ORCs, the proposed method automatically configured dual-parallel ORCs as the best solution, of which the total annualized cost is -0.638 M$/year, 6.2% and 27.3% lower than that given by Dong et al. (2020a) and Elsido et al. (2017). The net power output given by this paper is 2.06 MW, 0.08 MW higher than that of Dong et al. (2020a), which is equivalent to about 0.078 M$/year extra revenue. The corresponding capital cost is 1.112 M$/year, 0.049 M$/year more than that of Dong et al. (2020a). It is obvious that the increased power output can overcome the increased heat exchanger area, leading to a decrease in total annualized cost. The optimal working fluids are respectively selected as cyclopentane and iso-butane for the different ORC trains with high and low evaporating temperatures.

Figure 9 presents the optimal HEN for integrating dual-parallel ORCs. There is a total of twelve heat exchangers configured in the HEN for extracting waste heat. Nine of them are for preheating ORC working fluids, while the others are for vaporizing the working fluids. The optimal evaporation temperatures of the dual-parallel ORCs are 108.67℃ and 81.52℃, and

the corresponding working fluid mass flowrates are 17.17 kg/s and 16.91 kg/s. Both the two parallels have condensation temperatures of 25℃.

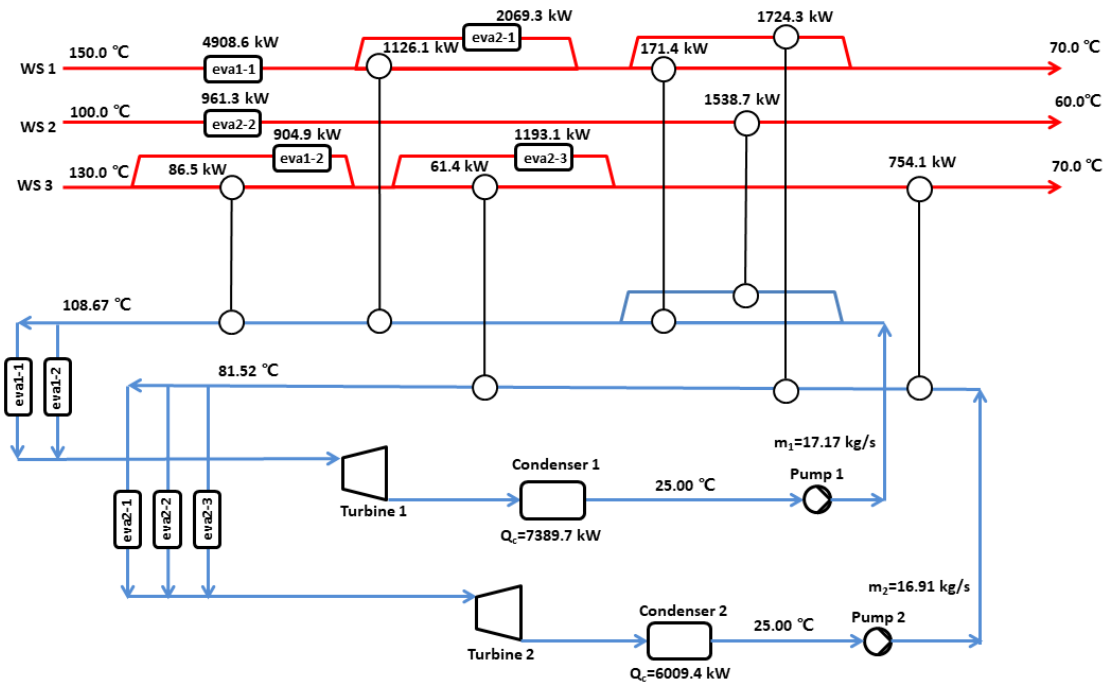

Figure 9. The optimal HEN for case 1 with dual-parallel ORCs integrated

7.2 Case study 2

For this case, the waste heat streams are not directly provided, instead of which are the inlet/outlet temperatures, heat capacity flowrates, and heat transfer coefficients of hot and cold process streams. The relevant information is given in Table 4. Other necessary information is provided below:

1. the isentropic efficiencies of turbines and pumps are 82% and 75%, respectively.

2. the fixed charges for implementing a heat exchanger and a stand-alone ORC are considered, which are 1000$ and 25000$, respectively.

Table 4. The background information of case study 2

streams	supply temperature (℃)	target temperature (℃)	heat capacity flowrate (kW/℃)	heat transfer coefficient (kW/m^2 ℃)

HS1	128	65	105	1
HS2	205	175	17	1
HS3	315	185	25	1
HS4	299	80	14	1
CS1	60	123	15	1
CS2	89	160	13	1
CS3	105	235	10	1
CS4	133	215	8	1
cold utility	20	30		2
hot utility	350	330		5

ORC heat transfer coefficient	
pre-heating working fluids	1.50
evaporating working fluids	4.00
de-superheating working fluids	0.25
condensing working fluids	4.00

Economic data	
parameters	**value**
multiplication factor	0.15
payback year	5
operating hours	8000 h/year
cold utility cost	10.19 $/kW • year
hot utility cost	192.1 $/kW • year
electricity price	0.12 $/kW • h

As waste heat stream data is not directly provided, a heat integration of the background process streams should be first carried out to identify the waste heat streams. In this case study, the Synheat superstructure-based model (Yee and Grossmann, 1990) is applied for heat integration. The identified waste heat streams are listed in Table 5, and the conclusive result of the background heat integration is shown in Table 6.

Once the waste heat streams are identified, the proposed method can be applied to integrate ORCs. For saving computational time, the alternative optimization strategy introduced in Chapter 6 is used. The corresponding optimization program is processed by the same desktop

PC used in case study 1.

Table 5. Identified waste heat streams

waste heat stream	supply temperature (℃)	target temperature (℃)	heat capacity flowrate (kW/℃)	Heat load (kW)
WS1	128.00	65	105	6615.0
WS2	205.00	175	17	510.0
WS3	236.76	185	25	1294.0
WS4	165.57	80.0	14	1198.0

Table 6. Conclusive result of the background heat integration

hot utility usage (kW)	0
number of heat exchangers between process streams	4
heat exchanger area between process streams (m^2)	76.66
annualized capital cost ($/year)	60700

The bi-level algorithm automatically selects dual-parallel ORCs as the optimal configuration to generate power, of which the solving process is terminated at the 86th generations, consuming 1590 seconds of CPU time. The calculation results of the bi-level algorithm are then sent to the sequencing **MP** problem for further optimization. The MP problem is solved by the Baron solver, consuming about 485 seconds of CPU time.

The economic performance of the integrated dual-parallel ORCs is listed in Table 7. For comparison, the table also includes the economic assessment of integrating a single-ORC. Note that the relevant costs of the heat integration of background process streams should be taken into account. It can be seen that the dual-parallel configuration achieves the minimum total annualized cost of -372,200 $/year. The net power output of the dual-parallel ORCs is 1208 kW, 177 kW more than that of the single ORC. Based on the regulated electricity price (0.12 $/kWh), the 117kW extra power generation can bring up 112,320 $/year extra revenue, overcoming the increased capital cost. Besides, as the dual-parallel configuration can

transform more waste heat into power, the corresponding cold utility usage decreases, leading to a less annualized operating cost than the single ORC.

Table 6. The economic profile of case study 2

parallel configuration	Single	dual-parallel	Without any ORCs
total annualized cost ($/year)	-266,180	-372,200	155,310
annualized capital cost ($/year)	636,466	702,167	57,313
annualized operating cost ($/year)	87114	85,313	97,997
profit from power generation ($/year)	-989,760	-1,159,680	0
hot utility usage (kW)	0	0	0
cold utility usage (kW)	8549	8372	9617
heat exchanger area (m^2)	1882	1993	257
number of heat exchangers	13	18	8
power generation (kW)	1031	1208	0

The composite curves of the single and dual-parallel ORCs are depicted in Figures 10(a) and (b). As shown in Figure 10(a), about 18.7% (1795.3 kW) waste heat cannot be extracted by the single ORC due to temperature limitation. While the residual waste heat that the dual-parallel ORCs cannot use (shown in Figure 10(b)) takes part only about 8.4% (807.2 kW) of the total amount. It is obvious that the dual-parallel ORC can achieve a higher rate of heat recovery. To the term of thermal efficiency, the single ORC transforms 7821.7 kW recovered heat into 1031 kW electricity, achieving a 13.18% overall thermal efficiency; while the dual-parallel ORCs can use 8809.9 kW recovered heat to generate 1208 kW electricity, leading to a 13.71% overall thermal efficiency, higher than that of the single ORC.

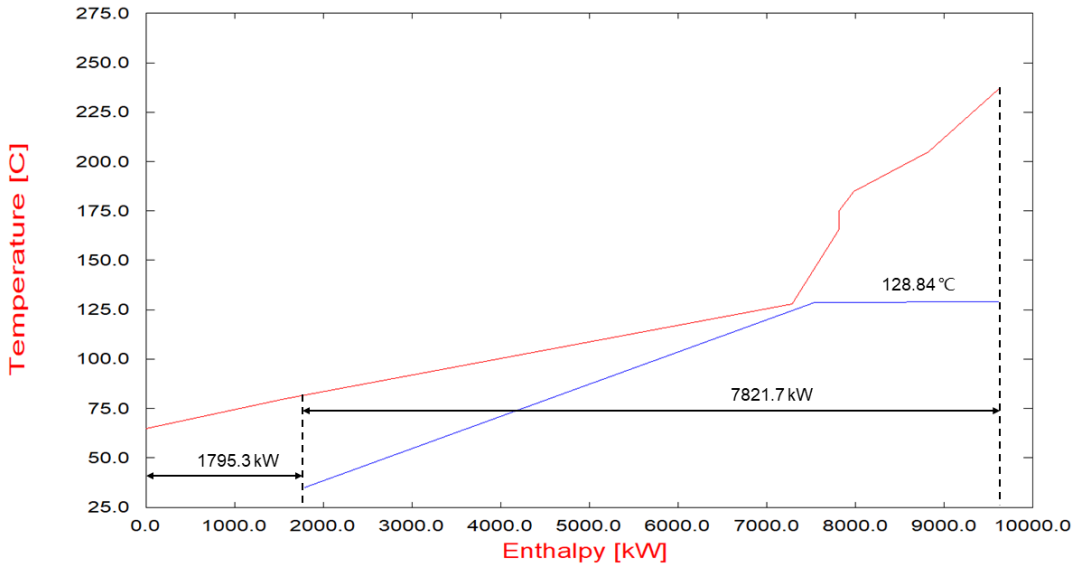

Figure 10(a). The composite curve of integrating a single ORC for case 2

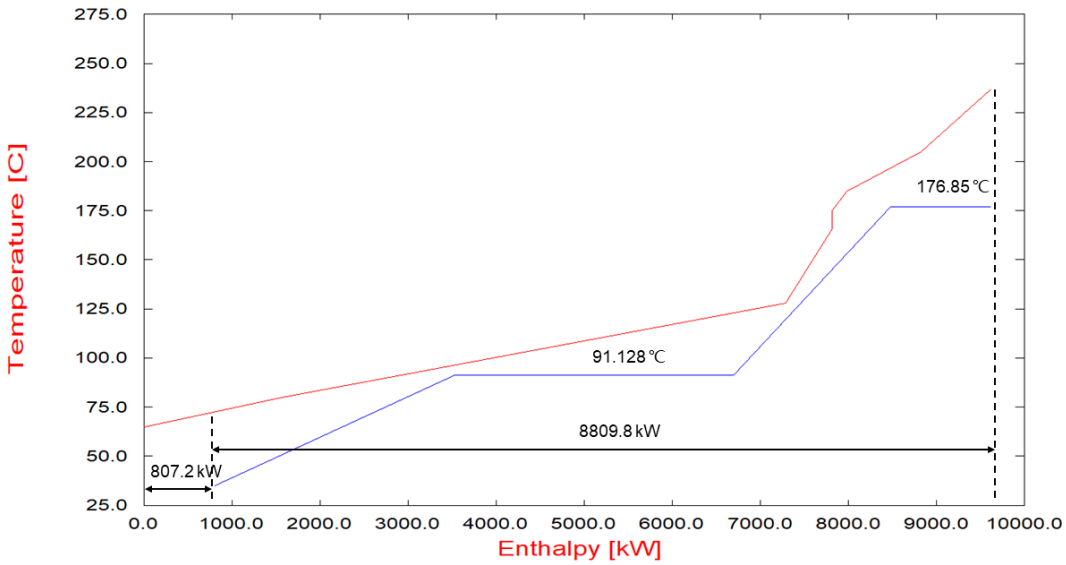

Figure 10(b). The composite curve of integrating dual-parallel ORCs for case 2

Figure 11 presents the optimal operations of the integrated dual-parallel ORCs as well as the corresponding HEN synthesis. We can classify the two individual ORCs in parallel into a high-temperature parallel (with a 176.85℃evaporation temperature) and a low-temperature parallel (with a 91.13℃ evaporation temperature). For the high-temperature parallel, the optimal working fluid is pentane, of which the mass flowrate is 7.23 kg/s, whereas the low-temperature

parallel has chosen iso-pentane as the optimal working fluid, the corresponding optimal mass flowrate is 11.12 kg/s. To generate more power, the optimal condensation temperatures of both the high and low-temperature parallels are bound to the lowest limit of 35℃.

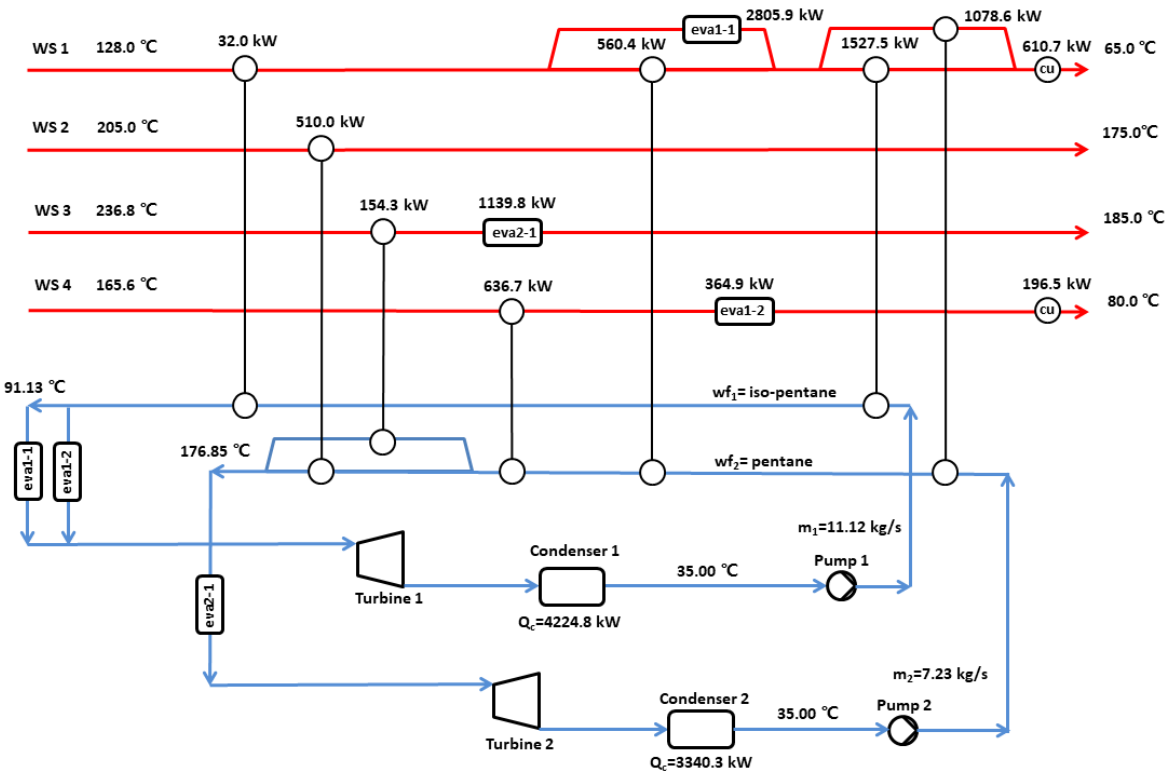

Figure 11. The optimal operations of the integrated dual-parallel ORCs with HEN synthesis

8. Conclusions

This paper proposes a simultaneous optimization method to address the working fluid selection problem for integrating multi-parallel ORCs. For modelling, the method establishes a superstructure-based model, leading to an MINLP problem, namely **MP**. By solving the **MP** problem, the optimal operations of the integrated ORCs, as well as the corresponding HEN synthesis, can be simultaneously determined. For optimization, the method proposes a bi-level optimization strategy. The outer level uses a GA, which can determine the optimal number of ORCs to be integrated and the working fluid selection of each ORC in parallel. In the inner level, the **MP** problem is incorporated and is solved by a deterministic algorithm (e.g., the Baron solver). It is also mentioned that, if necessary, the **MP** problem can be transformed

into an NLP problem so that the computational efficiency can be improved.

This paper presents two case studies. The first case study compares the optimization consequence of the proposed method with those of previous literature. Results show that, with proper working fluid selections, the integrated ORCs can gain lower total annualized costs than those without working fluid selections. The second case study illustrates the application of the method in the situations that waste heat streams are not directly provided.

Appendix A: Equations of heat extraction sub-module

It can be seen from figure 3 that there are three temperature boundaries (including the beginning boundary of the first stage, the intermediate boundary between the stages, and the ending boundary of the second stage) created by the two stages. It can be deduced that for a superstructure with *ST* stages, *ST+1* temperature boundaries are created. This paper uses the same index 'st' to represent the sets of stages and temperature boundaries. If the set of stages has a total number of *ST* elements, the set of temperature boundaries will have *ST+1* elements.

- **Temperature assignment**

$$T^{ws,st=1} = T_s^{ws}, ws \in WS \tag{A1}$$

$$T_{prestr}^{orc,st=1} = T_{t,prestr}^{orc}, orc \in ORC \tag{A2}$$

$$T_{prestr}^{orc,st=ST+1} = T_{s,prestr}^{orc}, orc \in ORC \tag{A3}$$

- **Energy balance**

$$(T_s^{ws} - T_t^{ws}) \cdot FC^{ws} = \sum_{st \in ST} \sum_{orc \in ORC} q_{prestr}^{ws,orc,st} + \sum_{st \in ST} \sum_{orc \in ORC} q_{evastr}^{ws,orc,st} + q_{cu}^{ws}, ws \in WS \tag{A4}$$

$$(T_{t,prestr}^{orc} - T_{s,prestr}^{orc}) \cdot FC_{prestr}^{orc} = \sum_{st \in ST} \sum_{ws \in WS} q_{prestr}^{ws,orc,st}, orc \in ORC \tag{A5}$$

$$q_{eva,two-phase}^{orc} = \sum_{st \in ST} \sum_{ws \in WS} q_{evastr}^{ws,orc,st}, orc \in ORC \tag{A6}$$

$$(T^{ws,st} - T^{ws,st+1}) \cdot FC^{ws} = \sum_{orc \in ORC} q_{prestr}^{ws,orc,st} + \sum_{orc \in ORC} q_{evastr}^{ws,orc,st}, ws \in WS, st \in ST \quad \text{(A7)}$$

$$(T_{prestr}^{orc,st} - T_{prestr}^{orc,st+1}) \cdot FC_{prestr}^{orc} = \sum_{ws \in WS} q_{prestr}^{ws,orc,st}, orc \in ORC, st \in ST \quad \text{(A8)}$$

- **Utility usage**

$$q_{cu}^{ws} = (T^{ws,st=ST+1} - T_t^{ws}) \cdot FC^{ws}, ws \in WS \quad \text{(A9)}$$

- **Logical constraints**

$$q_{prestr}^{ws,orc,st} - \Omega \cdot Z_{prestr}^{ws,orc,st} \le 0, ws \in WS, orc \in ORC, st \in ST \quad \text{(A10)}$$

$$q_{evastr}^{ws,orc,st} - \Omega \cdot Z_{evastr}^{ws,orc,st} \le 0, ws \in WS, orc \in ORC, st \in ST \quad \text{(A11)}$$

$$q_{cu}^{ws} - \Omega \cdot Z_{cu}^{ws} \le 0, ws \in WS \quad \text{(A12)}$$

- **Thermodynamic feasibility**

$$T^{ws,st} \ge T^{ws,st+1}, ws \in WS, st \in ST \quad \text{(A13)}$$

$$T^{ws,st=ST+1} \ge T_t^{ws}, ws \in WS \quad \text{(A14)}$$

$$T_{prestr}^{orc,st} \ge T_{prestr}^{orc,st+1}, orc \in ORC, st \in ST \quad \text{(A15)}$$

$$0 < dT_{prestr}^{ws,orc,st} \le T^{ws,st} - T_{prestr}^{orc,st} + L \cdot (1 - Z_{prestr}^{ws,orc,st}), ws \in WS, orc \in ORC, st \in ST \quad \text{(A16)}$$

$$0 < dT_{prestr}^{ws,orc,st+1} \le T^{ws,st+1} - T_{prestr}^{orc,st+1} + L \cdot (1 - Z_{prestr}^{ws,orc,st}), ws \in WS, orc \in ORC, st \in ST \quad \text{(A17)}$$

$$0 < dT_{evastr}^{ws,orc,st} \le T^{ws,st} - T_{evastr}^{orc} + L \cdot (1 - Z_{evastr}^{ws,orc,st}), ws \in WS, orc \in ORC, st \in ST \quad \text{(A18)}$$

$$0 < dT_{evastr}^{ws,orc,st+1} \le T^{ws,st+1} - T_{evastr}^{orc} + L \cdot (1 - Z_{evastr}^{ws,orc,st}), ws \in WS, orc \in ORC, st \in ST \quad \text{(A19)}$$

- **Heat exchanger area calculation**

$$HA_{prestr}^{ws,orc,st} = \frac{q_{prestr}^{ws,orc,st}}{U_{prestr}^{ws,orc} \cdot LMDT_{prestr}^{ws,orc,st}}, ws \in WS, orc \in ORC, st \in ST \quad \text{(A20)}$$

$$HA_{evastr}^{ws,orc,st} = \frac{q_{evastr}^{ws,orc,st}}{U_{evastr}^{ws,orc} \cdot LMDT_{evastr}^{ws,orc,st}}, ws \in WS, orc \in ORC, st \in ST \quad \text{(A21)}$$

$$HA_{cu}^{ws} = \frac{q_{cu}^{ws}}{U_{cu}^{ws} \cdot LMDT_{cu}^{ws}}, ws \in WS \tag{A22}$$

Where:

$$LMDT_{prestr}^{ws,orc,st} = \left[\frac{(dT_{prestr}^{ws,orc,st})(dT_{prestr}^{ws,orc,st+1})(dT_{prestr}^{ws,orc,st} + dT_{prestr}^{ws,orc,st+1})}{2} \right]^{1/3} \tag{A23}$$

$$, ws \in WS, orc \in ORC, st \in ST$$

$$LMDT_{evastr}^{ws,orc,st} = \left[\frac{(dT_{evastr}^{ws,orc,st})(dT_{evastr}^{ws,orc,st+1})(dT_{evastr}^{ws,orc,st} + dT_{evastr}^{ws,orc,st+1})}{2} \right]^{1/3} \tag{A24}$$

$$, ws \in WS, orc \in ORC, st \in ST$$

$$LMDT_{cu}^{ws} = \left[\frac{(T_t^{ws} - T_{cu,in})(T^{ws,st=ST+1} - T_{cu,out})(T_t^{ws} - T_{cu,in} + T^{ws,st=ST+1} - T_{cu,out})}{2} \right]^{1/3} \tag{A25}$$

$$, ws \in WS$$

Appendix B: The MP-alt problem

The **MP-alt** problem can be regarded as an NLP version of the **MP** problem. In the heat extraction sub-module of an **MP-alt** problem, the discrete variables that are used to indicate the successful matches between hot and cold streams are eliminated, as well as the corresponding equations (Equations (A10) ~ (A12)). Besides, Equations (A16) ~ (A19) are substituted by the following equations:

$$dT_{prestr}^{ws,orc,st} = \max\{0, (T^{ws,st} - T_{prestr}^{orc,st})\}, ws \in WS, orc \in ORC, st \in ST \tag{B1}$$

$$dT_{prestr}^{ws,orc,st=ST+1} = \max\{0, (T^{ws,st=ST+1} - T_{prestr}^{orc,st=ST+1})\}, ws \in WS, orc \in ORC \tag{B2}$$

$$dT_{evastr}^{ws,orc,st} = \max\{0, (T^{ws,st} - T_{evastr}^{orc})\}, ws \in WS, orc \in ORC, st \in ST \tag{B3}$$

$$dT_{evastr}^{ws,orc,st=ST+1} = \max\{0, (T^{ws,st=ST+1} - T_{evastr}^{orc})\}, ws \in WS, orc \in ORC \tag{B4}$$

In this paper, the *max* operator is smoothed by the following function (Balakrishna and Biegler, 1992):

$$\max\{0, x\} \approx \frac{1}{2}(x + \sqrt{x^2 + \varepsilon}) \tag{B5}$$

Where ε is a very small constant parameter, typically valued as 10^{-3}.

The formulated **MP-alt** problem can be presented as:

$$\text{Min: obj}=AF \cdot (Cap_{\text{extraction}} + Cap_{generation}) + Operating - profit$$

$$s.t.\ \ \chi(x) = \left\{ x \left| \begin{array}{l} \text{heat extraction sub-module Eqs. (A1)~(A9), (A13)~(A15),} \\ \qquad\qquad\qquad\qquad\qquad\qquad\text{(B1)~(B5), (A20)~(A25)} \\ \text{power generation sub-module Eqs. (1)□ (29)} \\ \text{correlations of the tow modules Eqs. (30)~(33)} \\ \text{Onjective fuction Eqs. (34)~(46)} \end{array} \right. \right\} \tag{MP-alt}$$

Reference list

Ashrae. (2009). *2009 ASHRAE handbook*. Atlanta, GA.: ASHRAE.

Bao, J. and Zhao, L., 2013. A review of working fluid and expander selections for organic Rankine cycle. *Renewable and Sustainable Energy Reviews*, 24, pp.325-342.

Balakrishna, S. and Biegler, L., 1992. Targeting strategies for the synthesis and energy integration of nonisothermal reactor networks. *Industrial & Engineering Chemistry Research*, 31(9), pp.2152-2164.

Chen, C., Chang, F., Chao, T., Chen, H. and Lee, J. (2014). Heat-Exchanger Network Synthesis Involving Organic Rankine Cycle for Waste Heat Recovery. *Industrial & Engineering Chemistry Research*, 53(44), pp.16924-16936.

Chen, H., Goswami, D. and Stefanakos, E., 2010. A review of thermodynamic cycles and working fluids for the conversion of low-grade heat. *Renewable and Sustainable Energy Reviews*, 14(9), pp.3059-3067.

Couper, J. R.; Penney, W. R.; Fair, J. R.; Walas, S. M. 21-Costs of Individual Equipment. *Chemical Process Equipment*, 3rd ed.; Butterworth-Heinemann: Boston, 2012; pp 731−741.

Desai, N. and Bandyopadhyay, S. (2009). Process integration of organic Rankine cycle. *Energy*, 34(10), pp.1674-1686.

Dong, X., Liao, Z., Sun, J., Huang, Z., Jiang, B., Wang, J. and Yang, Y., 2020a. Simultaneous Optimization of a Heat Exchanger Network and Operating Conditions of Organic Rankine Cycle. *Industrial & Engineering Chemistry Research*, 59(25), pp.11596-11609.

Dong, X., Liao, Z., Sun, J., Huang, Z., Jiang, B., Wang, J. and Yang, Y., 2020b. Simultaneous Optimization for Organic Rankine Cycle Design and Heat Integration. *Industrial & Engineering Chemistry Research*, 59(46), pp.20455-20471.

Drud, A., 1985. CONOPT: A GRG code for large sparse dynamic nonlinear optimization problems. *Mathematical Programming*, 31(2), pp.153-191.

Duran, M.A., Grossmann, I.E., 1986. Simultaneous optimization and heat integration of chemical processes. *AIChE J*. 32, 123–138.

Elsido, C., Mian, A. and Martelli, E., 2017. A systematic methodology for the techno-economic optimization of Organic Rankine Cycles. *Energy Procedia*, 129, pp.26-33.

Escobar, M. and Trierweiler, J., 2013. Optimal heat exchanger network synthesis: A case study comparison. *Applied Thermal Engineering*, 51(1-2), pp.801-826.

Hipólito-Valencia, B., Rubio-Castro, E., Ponce-Ortega, J., Serna-González, M., Nápoles-Rivera, F. and El-Halwagi, M., 2013. Optimal integration of organic Rankine cycles with industrial processes. *Energy Conversion and Management*, 73, pp.285-302.

Hung, T., Shai, T. and Wang, S., 1997. A review of organic rankine cycles (ORCs) for the recovery of low-grade waste heat. *Energy*, 22(7), pp.661-667.

Imran, M., Pili, R., Usman, M. and Haglind, F., 2020. Dynamic modeling and control strategies of organic Rankine cycle systems: Methods and challenges. *Applied Energy*, 276, p.115537.

Kermani, M., Wallerand, A., Kantor, I. and Maréchal, F., 2018. Generic superstructure synthesis of organic Rankine cycles for waste heat recovery in industrial processes. *Applied Energy*, 212, pp.1203-1225.

Linnhoff, B. and Flower, J., 1978. Synthesis of heat exchanger networks: I. Systematic generation of energy optimal networks. *AIChE Journal*, 24(4), pp.633-642.

Papoulias, S. and Grossmann, I., 1983. A structural optimization approach in process synthesis—II. *Computers & Chemical Engineering*, 7(6), pp.707-721.

Sahinidis, N.V., BARON: a general purpose global optimization software package, *Journal of Global Optimization*, 8 (2) (1996) 201e205.

Saleh, B., Koglbauer, G., Wendland, M. and Fischer, J., 2007. Working fluids for low-temperature organic Rankine cycles. *Energy*, 32(7), pp.1210-1221.

Scaccabarozzi, R., Tavano, M., Invernizzi, C. and Martelli, E., 2018. Comparison of working fluids and cycle optimization for heat recovery ORCs from large internal combustion engines. *Energy*, 158, pp.396-416.

Song, J., Li, Y., Gu, C. and Zhang, L., 2014. Thermodynamic analysis and performance optimization of an ORC (Organic Rankine Cycle) system for multi-strand waste heat sources in petroleum refining industry. *Energy*, 71, pp.673-680.

Stijepovic, M., Papadopoulos, A., Linke, P., Stijepovic, V., Grujic, A., Kijevčanin, M. and Seferlis, P., 2017. Organic Rankine Cycle system performance targeting and design for multiple heat sources with simultaneous working fluid selection. *Journal of Cleaner Production*, 142, pp.1950-1970.

Wang, S., Liu, C., Li, Q., Liu, L., Huo, E. and Zhang, C., 2020. Selection principle of working fluid for organic Rankine cycle based on environmental benefits and economic performance. *Applied Thermal Engineering*, 178, p.115598.

Wei, D., Lu, X., Lu, Z. and Gu, J., 2008. Dynamic modeling and simulation of an Organic Rankine Cycle (ORC) system for waste heat recovery. *Applied Thermal Engineering*, 28(10), pp.1216-1224.

Xi, H., Li, M., Xu, C. and He, Y., 2013. Parametric optimization of regenerative organic Rankine cycle (ORC) for low grade waste heat recovery using genetic algorithm. *Energy*, 58, pp.473-482.

Xu, J. and Yu, C., 2014. Critical temperature criterion for selection of working fluids for subcritical pressure Organic Rankine cycles. *Energy*, 74, pp.719-733.

Yee, T. and Grossmann, I., 1990. Simultaneous optimization models for heat integration—II. Heat exchanger network synthesis. *Computers & Chemical Engineering*, 14(10), pp.1165-1184.

Yu, H., Eason, J., Biegler, L. and Feng, X., 2017b. Process integration and superstructure optimization of Organic Rankine Cycles (ORCs) with heat exchanger network synthesis. *Computers & Chemical Engineering*, 107, pp.257-270.

Yu, H., Feng, X. and Wang, Y., 2015. A new pinch based method for simultaneous selection of working fluid and operating conditions in an ORC (Organic Rankine Cycle) recovering waste heat. *Energy*, 90, pp.36-46.

Chapter 6: Conclusions and Future Work

6.1 Conclusions

Adequate research works have been carried out for dealing with ORC integration problems. However, we observed that most of the previous works only considered integration of a single unit of ORC, while the opportunities of implementing multiple ORCs were rarely discussed. Besides, we also found that most of the relevant studies focused on integrating the ORC(s) in a direct way (i.e., the recovered heat is designed to be transferred directly between waste heat streams and ORC working fluids), while the strategic option of utilizing intermediate heat carriers (i.e., an indirectly way of heat extraction) was neglected. As such, this work proposes several methodologies for integrating ORCs, considering different strategic options of extracting waste heat and generating power, aiming to supplement the deficiencies of the previous research.

The final thesis consists of six main chapters. First, the research background and research motivation are fully introduced in Chapter 1. Then, a comprehensive literature review was undertaken in Chapter 2 to provide the state of art in ORC integration for industrial waste heat recovery. In Chapter 3 and 4, different strategic options of integrating ORCs are taken into account, leading to different developments of methodologies. Publication 3 addresses the optimal working fluid selections for integrating ORCs.

The main contributions achieved by this work can be concluded as follows:

(1) This work proposed two mathematical programming-based methodologies for the indirect and direct integrations of ORCs. By applying the methods, subjected to the minimum total annualized cost, the optimal heat exchanger network configuration, the optimal operating conditions of intermediate heat carriers (if indirect heat transfer is adopted), the optimal

number of ORCs to be implemented, and the optimal operation of each ORC can be simultaneously determined.

(2) This work proposed a bi-level decomposition method, which can automatically determine the optimal working fluid selections for integrating ORCs.

Several novel technologies are developed or adopted to accomplish the achievements, which are summarised below.

For model establishment:

- Two superstructure-based frameworks for representing waste heat extraction

In Publication 1, a superstructure, namely 'Modified-IBMS', is developed, which is an improved version of the interval-based superstructure proposed by Isafiade and Fraser (2008). Compared to the previous superstructure developed by Yee and Grossman (1990), it is proved that Modified-IBMS can create fewer continuous and discrete variables for representing the feasible network configurations of ORC integration, leading to less computational time.

In Publication 2, a novel superstructure, which can represent the direct integration of ORCs, is proposed. In the superstructure, the ORC working fluid in an evaporator is separated into two sub-flows, i.e., a pre-heating flow and a two-phase flow. By such configuration, the difficulties of determining when and where a two-phase evaporation process occurs are avoided, offering conveniences on calculating the heat transfer coefficient and heat transfer area of an evaporator.

- Rigorous thermodynamic equations

The Peng-Robinson Equation of State is adopted to formulate the thermodynamic equations for calculating the thermodynamic states of ORC working fluids, increasing the accuracy of estimating the thermodynamic performances of different ORC components (evaporator,

condenser, pump, expander).

For optimization:

- An initialization model for offering starting points

In Publication 2, the master model performs an MINLP optimization problem. In order to enhance the solution quality of the master model, an initialization model is developed, performing an NLP problem. The initialization model is established based on the Pinch Analysis technique, which can consider the capital-energy trade-off without synthesizing the HEN.

- Iterative optimizing procedure for determining the optimal unit number of ORCs

In Publication 1 and 2, integrative optimizing procedures are developed, through which the optimal unit number of ORCs can be simultaneously determined with the other decision variables.

- A bi-level decomposition optimization strategy

In Publication 3, a bi-level decomposition optimization strategy is adopted, which allows for the simultaneous optimization of the working fluid of each integrated ORC. In the strategy, the outer level adopts a genetic algorithm, which is responsible for determining the optimal number of ORCs to be implemented and the optimal working fluid selection of each ORC. While the inner level consists of an MINLP problem, by solving which the HEN synthesis and the optimal operating condition of each ORC can be determined.

Through case studies, the main finding of this work can be concluded as:

1. Compared with a single ORC, the implementation of multiple ORCs could gain a better thermal match with background heat sources, leading to an increase in power generation. However, the extra ORC units could also bring up more capital costs, which could partially or totally overcome the bonus brought up by the increased power generation. Therefore,

whether to implement single or multiple ORCs is case-dependent, which should be determined by systematic analysis.

2. Compared with the strategic option of indirect heat transfer, the direct heat transfer strategy could have less approach temperature difference, leading to a better thermal match with background heat sources. Besides, in Publication 2, it is found that the indirect heat transfer strategy could result in a larger heat exchanger area, as the heat should be first transferred to a heat carrier(s) before being transferred to ORC working fluid(s). However, it is pointed out that indirect heat transfer may be preferred in practice due to safety and controllability considerations (Yu et al., 2017b).

3. Compared with the multi-ORCs systems that adopt a monotonous type of working fluid, the systems adopting different working fluids on each ORC could gain more power generation. In a multi-ORCs system, each of the ORC could have different operating conditions, leading to different optimal working fluid selections. To another hand, different working fluids could exhibit different temperature-enthalpy profile, leading to different thermal match with background heat sources. The best thermal match could be gained by the combination of multiple working fluids rather than a monotonous one. To this point, allowing for selecting different working fluids for different ORCs can increase the searching space of the problem.

6.2 Future Work

When integrating ORCs, different architecture selections could lead to different thermal efficiency of the ORC systems and thermal matches with background heat sources. How to automatically select the most suitable architecture for each of the integrated ORCs, simultaneously with the optimal working fluid selection, the optimal operation, and the optimal HEN synthesis could be an interesting topic. However, due to time limitations, this work failed

to address this topic, which has to be left as future work.

Another limitation of this work is that the techno-economic feasibility of adopting mixtures as ORC working fluids is not discussed. Compared with pure components, the boiling processes of mixtures are usually temperature-changing processes, which may lead to better thermal matches with background heat sources in some cases. Therefore, it is necessary to develop a methodology to determine whether to adopt pure components or mixtures as the optimal working fluids of ORCs. Furthermore, it should be realized that the thermodynamic properties of mixtures could be different by the change of composition. As such, when considering adopting mixtures as ORC working fluids, it should be an essential matter for one to determine the proper compositions of mixtures.

It is also mentioned that, to consider waste heat extraction, one can both adopt the strategic options of direct and indirect heat transfer. It is logical to assume that, for a total site, there could be some waste heat sources that are more suitable to be extracted directly, while some others could be better transferring their heat through intermediate heat carriers. It could be an interesting topic to develop a pre-screening method for classifying and selecting the waste heat sources to determine adopting which kind of strategic option of heat transfer. Further, based on the pre-screening method, a holistic framework could be proposed to represent the integration of ORCs, considering both of the strategic options.

Reference List

Agathokleous, R., Bianchi, G., Panayiotou, G., Aresti, L., Argyrou, M., Georgiou, G., Tassou, S., Jouhara, H., Kalogirou, S., Florides, G. and Christodoulides, P., 2019. Waste Heat Recovery in the EU industry and proposed new technologies. *Energy Procedia*, 161, pp.489-496.

Ahmad, S., 1985. Heat exchanger networks: cost trade-offs in energy and capital, *PhD Thesis UMIST,* UK.

Ahmad, S., Linnhoff, B. and Smith, R., 1988. Design of multipass heat exchangers: An alternative approach. *Journal of Heat Transfer*, 110(2), pp.304-309.

Ammar Y, Joyce S, Norman R, Wang Y, Roskilly AP., 2012. Low grade thermal energy sources and uses from the process industry in the UK, *Applied Energy*, 89, pp. 3–20.

Andreasen, J., Larsen, U., Knudsen, T., Pierobon, L. and Haglind, F., 2014. Selection and optimization of pure and mixed working fluids for low grade heat utilization using organic Rankine cycles. *Energy*, 73, pp.204-213.

Andres, R., Gregg, J., Losey, L., Marland, G. and Boden, T., 2011. Monthly, global emissions of carbon dioxide from fossil fuel consumption. *Tellus B*, 63(3).

Bendig M, Marechal F, Favrat D., 2013. Defining “Waste heat” for industrial processes, *Applied Thermal Engineering*, 61(1), pp. 134–42.

Best, R. and Rivera, W., 2015. A review of thermal cooling systems. *Applied Thermal*

Engineering, 75, pp.1162-1175.

Bianchi, G., Panayiotou, G., Aresti, L., Kalogirou, S., Florides, G., Tsamos, K., Tassou, S. and Christodoulides, P., 2019. Estimating the waste heat recovery in the European Union Industry. *Energy, Ecology and Environment*, 4(5), pp.211-221.

Bruckner, S., Liu, S., Miró, L., Radspieler, M., Cabeza, L. F. and Lävemann, E., 2015. Industrial waste heat recovery technologies: An economic analysis of heat transformation technologies, *Applied Energy*, 151, pp. 157–167.

Carmo, C., Detlefsen, N. and Nielsen, M., 2014. Smart Grid Enabled Heat Pumps: An Empirical Platform for Investigating how Residential Heat Pumps can Support Large-scale Integration of Intermittent Renewables. *Energy Procedia*, 61, pp.1695-1698.

Cena V., Mustacchi, C., and Natali, F., 1977. Synthesis of heat exchange networks: a non-iterative approach. *Chemical Engineering Science*, 32, pp.1227-1231.

Cerda, J. and Westerburg, A., 1983. Synthesizing heat exchanger networks having restricted stream/stream matches using transportation problem formulations. *Chemical Engineering Science*, 38(10), pp.1723-1740.

Chan, C., Ling-Chin, J. and Roskilly, A., 2013. Reprint of “A review of chemical heat pumps, thermodynamic cycles and thermal energy storage technologies for low grade heat utilisation”. *Applied Thermal Engineering*, 53(2), pp.160-176.

Chen, C., Chang, F., Chao, T., Chen, H. and Lee, J., 2014. Heat-Exchanger Network Synthesis Involving Organic Rankine Cycle for Waste Heat Recovery. *Industrial & Engineering Chemistry Research*, 53(44), pp.16924-16936.

Chen, C., Li, P. and Le, S., 2016. Organic Rankine Cycle for Waste Heat Recovery in a Refinery. *Industrial & Engineering Chemistry Research*, 55(12), pp.3262-3275.

Chen, H., Goswami, D. Y. and Stefanakos, E. K., 2010. A review of thermodynamic cycles and working fluids for the conversion of low-grade heat, *Renewable and Sustainable Energy Reviews*, 14(9), pp. 3059–3067.

Ciric, A. and Floudas, C., 1991. Heat exchanger network synthesis without decomposition. *Computers & Chemical Engineering*, 15(6), pp.385-396.

Cortés, E. and Rivera, W., 2010. Exergetic and exergoeconomic optimization of a cogeneration pulp and paper mill plant including the use of a heat transformer. *Energy*, 35(3), pp.1289-1299.

Dai, Y., Wang, J. and Gao, L., 2009. Parametric optimization and comparative study of organic Rankine cycle (ORC) for low grade waste heat recovery. *Energy Conversion and Management*, 50(3), pp.576-582.

Desai, N. and Bandyopadhyay, S., 2009. Process integration of organic Rankine cycle. *Energy*, 34(10), pp.1674-1686.

Dhole, V. and Linnhoff, B., 1993. Total site targets for fuel, co-generation, emissions, and cooling. *Computers & Chemical Engineering*, 17, pp.S101-S109.

DiGenova, K., Botros, B. and Brisson, J., 2013. Method for customizing an organic Rankine cycle to a complex heat source for efficient energy conversion, demonstrated on a Fischer Tropsch plant. *Applied Energy*, 102, pp.746-754.

Dong, X., Liao, Z., Sun, J., Huang, Z., Jiang, B., Wang, J. and Yang, Y., 2020a. Simultaneous Optimization of a Heat Exchanger Network and Operating Conditions of Organic Rankine Cycle. *Industrial & Engineering Chemistry Research*, 59(25), pp.11596-11609.

Dong, X., Liao, Z., Sun, J., Huang, Z., Jiang, B., Wang, J. and Yang, Y., 2020b. Simultaneous Optimization for Organic Rankine Cycle Design and Heat Integration. *Industrial & Engineering Chemistry Research*, 59(46), pp.20455-20471.

Duran, M. and Grossmann, I., 1986. Simultaneous optimization and heat integration of chemical processes. *AIChE Journal*, 32(1), pp.123-138.

Elsido, C., Martelli, E. and Grossmann, I., 2019. A bilevel decomposition method for the simultaneous heat integration and synthesis of steam/organic Rankine cycles. *Computers & Chemical Engineering*, 128, pp.228-245.

Escobar, M. and Trierweiler, J., 2013. Optimal heat exchanger network synthesis: A case study comparison. *Applied Thermal Engineering*, 51(1-2), pp.801-826.

Floudas, C. and Ciric, A., 1989. Strategies for overcoming uncertainties in heat exchanger network synthesis. *Computers & Chemical Engineering*, 13(10), pp.1133-1152.

Floudas, C., Ciric, A. and Grossmann, I., 1986. Automatic synthesis of optimum heat exchanger network configurations. *AIChE Journal*, 32(2), pp.276-290.

Furman, K. and Sahinidis, N., 2002. A Critical Review and Annotated Bibliography for Heat Exchanger Network Synthesis in the 20th Century. *Industrial & Engineering Chemistry Research*, 41(10), pp.2335-2370.

Garimella, S., 2012. Low-grade waste heat recovery for simultaneous chilled and hot water generation, *Applied Thermal Engineering*, 42, pp. 191–198.

Grassi, W., 2018. HEAT PUMPS. *SPRINGER INTERNATIONAL PU*, US.

Gundepsen, T. and Naess, L., 1988. The synthesis of cost optimal heat exchanger networks. *Computers & Chemical Engineering*, 12(6), pp.503-530.

Guo, C., Du, X., Yang, L. and Yang, Y., 2014. Performance analysis of organic Rankine cycle based on location of heat transfer pinch point in evaporator. *Applied Thermal Engineering*, 62(1), pp.176-186.

He, C., Liu, C., Gao, H., Xie, H., Li, Y., Wu, S. and Xu, J., 2012. The optimal evaporation temperature and working fluids for subcritical organic Rankine cycle. *Energy*, 38(1), pp.136-143.

Hemadri, V. and Subbarao, P., 2021. Thermal integration of reheated organic Rankine cycle (RH-ORC) with gas turbine exhaust for maximum power recovery. *Thermal Science and Engineering Progress*, 23, p.100876.

Hickenbottom, K., Miller-Robbie, L., Vanneste, J., Marr, J., Heeley, M. and Cath, T., 2018. Comparative life-cycle assessment of a novel osmotic heat engine and an organic Rankine cycle for energy production from low-grade heat. *Journal of Cleaner Production*, 191, pp.490-501.

Hipólito-Valencia, B., Rubio-Castro, E., Ponce-Ortega, J., Serna-González, M., Nápoles-Rivera, F. and El-Halwagi, M., 2013. Optimal integration of organic Rankine cycles with

industrial processes. Energy Conversion and Management, 73, pp.285-302

Hohmann, E. C., 1971. Optimum networks for heat exchange. *Ph.D. Thetis, University of Southern California*, US

Hu, K., Zhu, J., Zhang, W., Liu, K. and Lu, X., 2017. Effects of evaporator superheat on system operation stability of an organic Rankine cycle. *Applied Thermal Engineering*, 111, pp.793-801.

Huang, F. and Elshout, G. V., 1976. Optimizing the heat recovery of crude units. *Chemical Engineering Progress*. 72, pp.68-74.

Huang, X., Lu, P., Luo, X., Chen, J., Yang, Z., Liang, Y., Wang, C. and Chen, Y., 2020. Synthesis and simultaneous MINLP optimization of heat exchanger network, steam Rankine cycle, and organic Rankine cycle. *Energy*, 195, p.116922.

Hung, T., Shai, T. and Wang, S., 1997. A review of organic rankine cycles (ORCs) for the recovery of low-grade waste heat. *Energy*, 22(7), pp.661-667.

Hung, T., Wang, S., Kuo, C., Pei, B. and Tsai, K., 2010. A study of organic working fluids on system efficiency of an ORC using low-grade energy sources. *Energy*, 35(3), pp.1403-1411.

IEA. 2022. *World Energy Outlook 2018 – Analysis - IEA*. [online] Available at: <https://www.iea.org/reports/world-energy-outlook-2018> [Accessed 07 October 2021].

IEA. 2022. *World Energy Outlook 2019 – Analysis - IEA*. [online] Available at: <https://www.iea.org/reports/world-energy-outlook-2019> [Accessed 07 October 2021].

IEA. 2022. *World Energy Outlook 2020 – Analysis - IEA*. [online] Available at:

<https://www.iea.org/reports/world-energy-outlook-2020> [Accessed 07 October 2021].

IEA. 2022. *World Energy Outlook 2021 – Analysis - IEA*. [online] Available at: <https://www.iea.org/reports/world-energy-outlook-2021> [Accessed 07 October 2021].

Isafiade, A. and Fraser, D., 2008. Interval-based MINLP superstructure synthesis of heat exchange networks. Chemical Engineering Research and Design, 86(3), pp.245-257.

Johnson I, Choate WT, Davidson A. Waste heat recovery. Technology and opportunities in US industry. Laurel, MD (United States): BCS, Inc.; 2008.

Jouhara, H. and Olabi, A., 2018. Editorial: Industrial waste heat recovery. *Energy*, 160, pp.1-2.

Kalina, A., 1984. Combined-cycle system with novel bottoming cycle. *Journal of Engineering for Gas Turbines and Power*, 106(4), pp.737-742.

Kapil, A., Bulatov, I., Smith, R. and Kim, J.-K., 2011. Site-wide process integration for low grade heat recovery, *Computer Aided Chemical Engineering*, pp. 1859–1863.

Kermani, M., Wallerand, A., Kantor, I. and Maréchal, F., 2018. Generic superstructure synthesis of organic Rankine cycles for waste heat recovery in industrial processes. *Applied Energy*, 212, pp.1203-1225.

Kesicki, F. and Yanagisawa, A., 2014. Modelling the potential for industrial energy efficiency in IEA's World Energy Outlook. *Energy Efficiency*, 8(1), pp.155-169.

Kesler, M. G. and Parker,R. O., 1969. Optimal networks of heat exchange. *Chem. Engng Prog.*

Syrup. Ser., 65, pp.110-120.

Klemeš, J. and Kravanja, Z., 2013. Forty years of Heat Integration: Pinch Analysis (PA) and Mathematical Programming (MP). *Current Opinion in Chemical Engineering*, 2(4), pp.461-474.

Klemeš, J., Dhole, V. R., Raissi, K., Perry, S. J. and Puigjaner, L., 1997. Targeting and design methodology for reduction of fuel, power and CO on total sites, *Applied Thermal Engineering*, 17(s 8–10), pp. 993–1003.

Klemeš, J., Varbanov, P., and Kravanja, Z., 2013. Recent developments in Process Integration. *Chemical Engineering Research and Design*, 91(10), pp.2037-2053.

Kobayashi, S., Umeda, T., and Ichikawa, A., 1971. Synthesis of optimal heat exchange systema--an approach by the optimal assignment problem in linear programming. *Chemical Engineering Science*, 26, pp.1367-1380 (1971).

Law, R., Harvey, A. and Reay, D., 2013. Opportunities for low-grade heat recovery in the UK food processing industry. *Applied Thermal Engineering*, 53(2), pp.188-196.

Lecompte, S., Huisseune, H., van den Broek, M., Vanslambrouck, B. and De Paepe, M., 2015. Review of organic Rankine cycle (ORC) architectures for waste heat recovery. *Renewable and Sustainable Energy Reviews*, 47, pp.448-461.

Li, T., Wang, Q., Zhu, J., Hu, K. and Fu, W., 2015. Thermodynamic optimization of organic Rankine cycle using two-stage evaporation. *Renewable Energy*, 75, pp.654-664.

Li, X., Li, X. and Zhang, Q., 2013. The first and second law analysis on an organic Rankine cycle with ejector. *Solar Energy*, 93, pp.100-108.

Linnhoff, B. and Ahmad, S., 1990. Cost optimum heat exchanger networks—1. Minimum energy and capital using simple models for capital cost. *Computers & Chemical Engineering*, 14(7), pp.729-750.

Linnhoff, B. and Eastwood, A., 1997. Overall site optimisation by Pinch Technology. *Chemical Engineering Research and Design*, 75, pp.S138-S144.

Linnhoff, B. and Flower, J., 1978. Synthesis of heat exchanger networks: I. Systematic generation of energy optimal networks. *AIChE Journal*, 24(4), pp.633-642.

Linnhoff, B. and Hindmarsh, E., 1983. The pinch design method for heat exchanger networks. *Chemical Engineering Science*, 38(5), pp.745-763.

Linnhoff, B. and Turner, J. A., 1981. Heat-recovery networks: new insights yield big savings. *Chemical Engineering Journal*, 88, pp.56-70.

Linnhoff, B., Mason, D. and Wardle, I., 1979. Understanding heat exchanger networks. *Computers & Chemical Engineering*, 3(1-4), pp.295-302.

Linnhoff, B., Townsend, D.W., Boland, D., Hewitt, G.F., Thomas, B.E.A., Guy, A.R. and Marsland, R.H., 1982. A User Guide on Process Integration for the Efficient Use of Energy, *IChemE*, UK.

Long, R., Bao, Y., Huang, X. and Liu, W., 2014. Exergy analysis and working fluid selection of organic Rankine cycle for low grade waste heat recovery. *Energy*, 73, pp.475-483.

Lu, H., Price, L. and Zhang, Q., 2016. Capturing the invisible resource: Analysis of waste heat

potential in Chinese industry. *Applied Energy*, 161, pp.497-511.

Luo, X., Zhang, B., Chen, Y. and Mo, S., 2011. Modeling and optimization of a utility system containing multiple extractions steam turbines, *Energy*, 36(5), pp. 3501–3512.

Mahmoudi, A., Fazli, M. and Morad, M., 2018. A recent review of waste heat recovery by Organic Rankine Cycle. *Applied Thermal Engineering*, 143, pp.660-675.

Market, W., 2022. *Waste Heat Recovery System Market by Application & End-Use Industry - Global Forecast 2021 | MarketsandMarkets | Last Updated on January-2022*. [online] Marketsandmarkets.com. Available at: <https://www.marketsandmarkets.com/Market-Reports/waste-heat-recovery-system-market-202657867.html> [Accessed 01 January 2022].

Martelli, E., Elsido, C., Mian, A. and Marechal, F., 2017. MINLP model and two-stage algorithm for the simultaneous synthesis of heat exchanger networks, utility systems and heat recovery cycles. *Computers & Chemical Engineering*, 106, pp.663-689.

Matsuda, K., 2014. Low heat power generation system. *Applied Thermal Engineering*, 70(2), pp.1056-1061.

Meinel, D., Wieland, C. and Spliethoff, H., 2014. Economic comparison of ORC (Organic Rankine cycle) processes at different scales. *Energy*, 74, pp.694-706.

Micheletto, S. R., Carvalho, M. C. A. and Pinto, J. M., 2008. Operational optimization of the utility system of an oil refinery, *Computers & Chemical Engineering*, 32(s 1–2), pp. 170–185.

Miró, L., Brückner, S. and Cabeza, L. F., 2015. Mapping and discussing industrial waste heat (IWH) potentials for different countries, *Renewable and Sustainable Energy Reviews*, 51, pp.

847–855.

Mizutani, F., Pessoa, F., Queiroz, E., Hauan, S. and Grossmann, I., 2003. Mathematical Programming Model for Heat-Exchanger Network Synthesis Including Detailed Heat-Exchanger Designs. 1. Shell-and-Tube Heat-Exchanger Design. *Industrial & Engineering Chemistry Research*, 42(17), pp.4009-4018.

Morandin, M., Hackl, R. and Harvey, S., 2014. Economic feasibility of district heating delivery from industrial excess heat: A case study of a Swedish petrochemical cluster, *Energy*, 65, pp. 209–220.

Nemet, A., Klemeš, J. and Kravanja, Z., 2012. Minimisation of a heat exchanger networks' cost over its lifetime. *Energy*, 45(1), pp.264-276.

Nishida, N., Stephanopoulos, G. and Westerberg, A., 1981. A review of process synthesis. *AIChE Journal*, 27(3), pp.321-351.

Oluleye, G., Jobson, M., Smith, R. and Perry, S., 2016. Evaluating the potential of process sites for waste heat recovery. *Applied Energy*, 161, pp.627-646.

Oluleye, O., 2016. Integration of waste heat recovery in process sites, *PhD Thesis UMIST,* UK.

Papapetrou, M., Kosmadakis, G., Cipollina, A., La Commare, U. and Micale, G., 2018. Industrial waste heat: Estimation of the technically available resource in the EU per industrial sector, temperature level and country. *Applied Thermal Engineering*, 138, pp.207-216.

Papoulias, S. and Grossmann, I., 1983a. A structural optimization approach in process

synthesis—I. *Computers & Chemical Engineering*, 7(6), pp.695-706.

Papoulias, S. and Grossmann, I., 1983b. A structural optimization approach in process synthesis—II. *Computers & Chemical Engineering*, 7(6), pp.707-721.

Ponton, J. W. and Donaldson, R. A. B., 1974. A fast method for the synthesis of optimal heat exchanger networks. *Chemical Engineering Science*, pp. 29, 2375-2377.

Quoilin, S., Declaye, S., Tchanche, B. and Lemort, V., 2011. Thermo-economic optimization of waste heat recovery Organic Rankine Cycles. *Applied Thermal Engineering*, 31(14-15), pp.2885-2893.

Raissi, K., 1994. Total site integration, *PhD Thesis UMIST,* UK.

Saleh, B., Koglbauer, G., Wendland, M. and Fischer, J., 2007. Working fluids for low temperature organic Rankine cycles, *Energy*, 32(7), pp. 1210–1221.

Schuster, A., Karellas, S. and Aumann, R., 2010. Efficiency optimization potential in supercritical Organic Rankine Cycles. *Energy*, 35(2), pp.1033-1039.

Shang, Z. and Kokossis, A., 2004. A transhipment model for the optimization of steam levels of total site utility system for multiperiod operation, *Computers & Chemical Engineering*, 28(9), pp. 1673–1688.

Smith, R., 2005. Chemical Process Design and Integration, 1st Edition. *John Wiley & Sons*, UK.

Song, J., Li, Y., Gu, C. and Zhang, L., 2014. Thermodynamic analysis and performance

optimization of an ORC (Organic Rankine Cycle) system for multi-strand waste heat sources in petroleum refining industry. *Energy*, 71, pp.673-680.

Soršak, A. and Kravanja, Z., 1999. Simultaneous MINLP synthesis of heat and power integrated heat exchanger networks. *Computers & Chemical Engineering*, 23, pp.S143-S147.

Steinmetz, F. J. and Chaney, M. O., 1985. Total plant process energy integration. *Chemical Engineering Progress*. 81, pp.27-32.

Stijepovic, M., Papadopoulos, A., Linke, P., Stijepovic, V., Grujic, A., Kijevčanin, M. and Seferlis, P., 2017. Organic Rankine Cycle system performance targeting and design for multiple heat sources with simultaneous working fluid selection. *Journal of Cleaner Production*, 142, pp.1950-1970.

Tartière, T. and Astolfi, M., 2017. A World Overview of the Organic Rankine Cycle Market. *Energy Procedia*, 129, pp.2-9.

Tjoe, T. N. and Linnhoff, B., 1986. Using pinch technology for process retrofit. *Chemical Engineering Journal*, 93, pp.47--60.

Toffolo, A., 2014. A synthesis/design optimization algorithm for Rankine cycle based energy systems. *Energy*, 66, pp.115-127.

Townsend, D. W. and Linnhoff, B., 1983. Heat and power networks in process design. Ⅱ: design procedures for equipment selection and process matching. *AIChE Journal*, 29, pp. 748-771.

Umeda, T., Harada, T. and Shiroko, K., 1979. A thermodynamic approach to the synthesis of

heat integration systems in chemical processes. *Computers & Chemical Engineering*, 3(1-4), pp.273-282.

Varbanov, P. S., Doyle, S. and Smith, R., 2004. Modelling and optimization of utility systems, *Chemical Engineering Research and Design*, 82(5), pp. 561–578

Varbanov, P., Perry, S., Makwana, Y., Zhu, X. X. and Smith, R., 2004. Top-level analysis of site utility systems, *Chemical Engineering Research and Design*, 82(6), pp. 784–795.

Victor, R., Kim, J. and Smith, R., 2013. Composition optimisation of working fluids for Organic Rankine Cycles and Kalina cycles. *Energy*, 55, pp.114-126.

Viklund, S. B. and Johansson, M., 2014. Technologies for utilization of industrial excess heat: Potentials for energy recovery and CO2 emission reduction. *Energy Conversion and Management*, 77, pp.369-379.

Viklund, S. B. and Karlsson, M., 2015. Industrial excess heat use: Systems analysis and CO emissions reduction, *Applied Energy*, 152, pp. 189–197.

Wang, S., Liu, C., Li, Q., Liu, L., Huo, E. and Zhang, C., 2020. Selection principle of working fluid for organic Rankine cycle based on environmental benefits and economic performance. *Applied Thermal Engineering*, 178, p.115598.

Wang, Y. and Lior, N., 2011. Proposal and analysis of a high-efficiency combined desalination and refrigeration system based on the LiBr–H2O absorption cycle—Part 2: Thermal performance analysis and discussions, *Energy Conversion and Management*, 52(1), pp. 228–235.

Wells, O. and Hodgkinson, M., 1977. The heat content diagram way to heat exchanger networks. *Process Engineering Journal*, August, pp. 59-63.

Westerberg, A. W., 1983. The heat path diagram for energy management. *AICIHE Diamond Jubilee Mtg*, Washington D.C.

Wieland, K. and Christoph, T., 2021. Market report on Organic Rankine Cycle power systems: recent developments and outlook. *Proceedings of the 6th International Seminar on ORC Power Systems*.

Wood, R., Wilcox, R. and Grossmann, I., 1985. A note on the minimum number of units for heat exchanger network synthesis. *Chemical Engineering Communications*, 39(1-6), pp.371-380.

Woolley, E., Luo, Y. and Simeone, A., 2018. Industrial waste heat recovery: A systematic approach. *Sustainable Energy Technologies and Assessments*, 29, pp.50-59.

Wu, W., Wang, B., Shi, W. and Li, X., 2014. Absorption heating technologies: A review and perspective. *Applied Energy*, 130, pp.51-71.

Xi, H., Li, M., Xu, C. and He, Y., 2013. Parametric optimization of regenerative organic Rankine cycle (ORC) for low grade waste heat recovery using genetic algorithm. *Energy*, 58, pp.473-482.

Xu, H., Gao, N. and Zhu, T., 2016. Investigation on the fluid selection and evaporation parametric optimization for sub- and supercritical organic Rankine cycle. *Energy*, 96, pp.59-68.

Xu, J. and Yu, C., 2014. Critical temperature criterion for selection of working fluids for subcritical pressure Organic Rankine cycles. *Energy*, 74, pp.719-733.

Yee, T. and Grossmann, I., 1990. Simultaneous optimization models for heat integration—II. Heat exchanger network synthesis. *Computers & Chemical Engineering*, 14(10), pp.1165-1184.

Yu, H., Eason, J., Biegler, L. and Feng, X., 2017a. Process integration and superstructure optimization of Organic Rankine Cycles (ORCs) with heat exchanger network synthesis. *Computers & Chemical Engineering*, 107, pp.257-270.

Yu, H., Eason, J., Biegler, L. and Feng, X., 2017b. Simultaneous heat integration and techno-economic optimization of Organic Rankine Cycle (ORC) for multiple waste heat stream recovery. *Energy*, 119, pp.322-333.

Yu, H., Feng, X. and Wang, Y., 2015. A new pinch based method for simultaneous selection of working fluid and operating conditions in an ORC (Organic Rankine Cycle) recovering waste heat. *Energy*, 90, pp.36-46.

Yu, H., Gundersen, T. and Feng, X., 2018. Process integration of organic Rankine cycle (ORC) and heat pump for low temperature waste heat recovery. *Energy*, 160, pp.330-340.

Zhang, C., Liu, C., Xu, X., Li, Q., Wang, S. and Chen, X., 2018. Effects of superheat and internal heat exchanger on thermo-economic performance of organic Rankine cycle based on fluid type and heat sources. *Energy*, 159, pp.482-495.

Zhang, X., He, M. and Zhang, Y., 2012. A review of research on the Kalina cycle. *Renewable and Sustainable Energy Reviews*, 16(7), pp.5309-5318.

Zhao, H., Feng, Y. and Rong, G., 2015. Effective solution approach for integrated optimization models of refinery production and utility system, *Industrial and Engineering Chemistry Research*, 54(37), pp. 9238–9250.